Understanding the role of E2F7 in the regulation of cellular proliferation and DNA damage responses

Jon Vallejo Rodríguez

Leioa, 2018

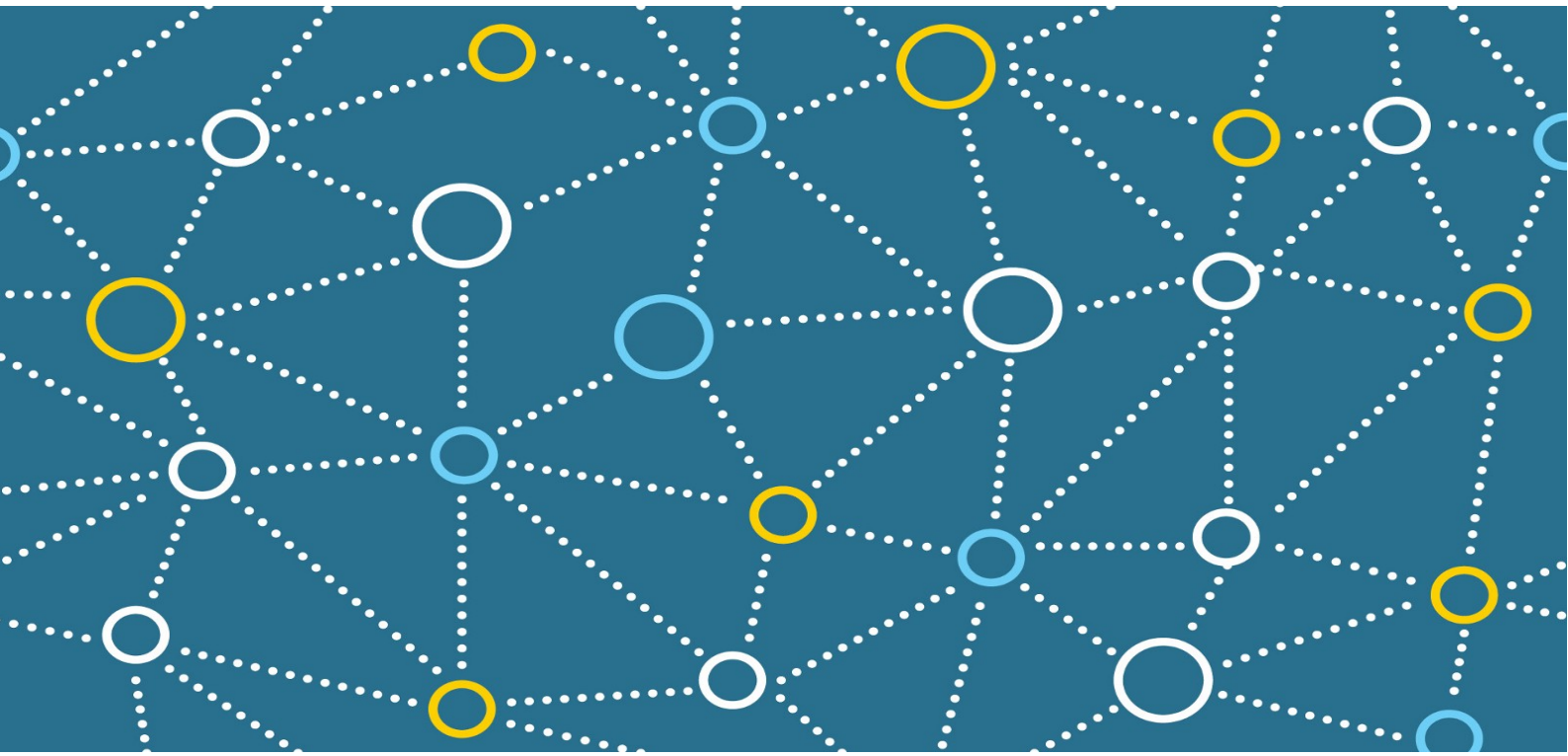

eman ta zabal zazu

Universidad del País Vasco

Euskal Herriko Unibertsitatea

Understanding the role of E2F7 in the regulation of cellular proliferation and DNA damage responses

PhD Thesis

Jon Vallejo Rodríguez

Leioa, 2018

Supervisors: Ana María Zubiaga Elordieta and Asier Fullaondo Elordui-Zapaterieche

Jon Vallejo Rodríguez was recipient of a research training fellowship from the University of the Basque Country UPV/EHU (PIF2013). This thesis work has been funded by the Spanish Ministry of Economy and Competitiveness (SAF2012-33551 and SAF2015-67562-R), the Basque Government (IT634-13) and the University of the Basque Country UPV/EHU (UFI11/20).

Table of contents

ABBREVIATIONS

AP-1	Activator protein 1
APAF1	Apoptotic protease activating factor 1
APC/C	Anaphase-promoting complex/cyclosome
APE1	Apurinic/apyrimidinic Endonuclease 1
ATM	Ataxia-Telangiectasia Mutated
ATR	Ataxia-Telangiectasia Related
BARD1	BRCA1-associated RING domain protein 1
BER	Base Excision Repair
BIM	Bcl-2-like protein 11
BRCA2	Breast cancer type 2 susceptibility protein
BRCT	BRCA1 C Terminus
BrDU	Bromodeoxyuridine
BRIP1	BRCA1-interacting protein 1
CDK	Cyclin Dependent Kinase
cDNA	Complementary DNA
CDC6	Cell division control protein 6
CDT1	Chromatin licensing and DNA replication factor 1
CFSE	Carboxyfluorescein succinimidyl ester
CSP	Cisplatin
ChIP	Chromatin immunoprecipitation
CHK1	Checkpoint Kinase 1
CHK2	Checkpoint Kinase 2
CTIP	CtBP-interacting protein
DBD	DNA Binding Domain
DD	Dimerization Domain
DDR	DNA Damage Response
DHFR	Dihydrofolate reductase
DMEM	Dulbecco's Modified Eagle Medium
DNA	Deoxyribonucleic acid
DP	Dimerization protein
DSB	Double Strand Break
E2F	E2 factor

EDTA	Ethylenediaminetetraacetic acid
FA	Fanconi Anemia
FANCD2	Fanconi Anemia group D2 protein
FANCE	Fanconi Anemia group E protein
FANCI	Fanconi Anemia group I protein
FBS	Fetal Bovine Serum
γ-H2AX	Gamma H2A histone family member X
GFP	Green Fluorescent Protein
H2A	Histone 2A
HDAC	Histone deacetylases
HR	Homologous Recombination
HRP	Horseradish Peroxidase
HU	Hydroxyurea
ICL	Interstrand Crosslink
IF	Immunofluorescence
IR	Ionizing radiation
LIG3	DNA Ligase III
LIG4	DNA Ligase IV
MCM2	Minichromosome Maintenance Complex 2
MMC	Mitomycin C
MMS	Methyl methanesulfonate
NCS	Neocarzinostatin
NES	Nuclear Export Signal
NHEJ	Non-Homologous End Joining
NLS	Nuclear Localization Signal
NT	Non-target
OLA	Olaparib
PARP1	Poly [ADP-ribose] polymerase 1
PBS	Phosphate Buffered Saline
PCR	Polymerase Chain Reaction
PI	Propidium Iodide
PMSF	Phenylmethanesulfonyl Fluoride
PRC1	Polycomb repressive complex 1
PRC2	Polycomb repressive complex 2
PTM	Posttranslational Modification
PUMA	p53 upregulated modulator of apoptosis

ROS	Reactive Oxygen Species
RT-qPCR	Reverse transcription- Quantitative PCR
RNA	Ribonucleic acid
RPA	Replication protein A
RRM2	Ribonucleoside-diphosphate reductase subunit M2
SCF/SKP2	Skp, Cullin, F-box and SKP2 containing complex
SDS-PAGE	Sodium Dodecyl Sulfate-PolyAcrylamide Gel Electrophoresis
siRNA	Small Interfering Ribonucleic Acid
SSB	Single Strand Break
SV40LT	Simian Virus 40 Large T antigen
TAE	Tris/Acetic acid/EDTA
TBS-T	Tris Buffered Saline-Tween 20
TLS	Translesion Synthesis
UT	Untreated
UV	Ultraviolet
WT	Wild Type
XPO1	Exportin 1
XRCC1	X-Ray Repair Cross Complementing 1
XRCC4	X-Ray Repair Cross Complementing 4

ABSTRACT

E2F transcription factors control diverse biological processes through regulation of target gene expression. The identification of a large set of genes regulated by each individual E2F, including those coding for microRNAs, has led to a better understanding of the functions performed by the different members of the family. Many studies have detailed the role of classical E2Fs in cell cycle control and DNA damage response. By contrast, the contribution of the atypical members of the family, E2F7 and E2F8, to these processes has not been clearly defined. A recent study from our group identified a set of novel microRNAs and protein-coding genes regulated by E2F7. These genes are involved in processes such as cell cycle regulation or DNA damage response. In this work, we have examined the role that E2F7 plays in the regulation of these processes through the transcriptional regulation of its target genes.

We have identified E2F7 as a transcription factor required for the repression of a set of microRNAs that promote cellular proliferation. We show that miR-25, miR-92 and miR-7 expression is controlled at the transcriptional level by the antagonistic activity of E2F7 and E2F1-3. Interestingly, we find that several E2F7-repressed microRNAs downregulate the expression of cell cycle progression inhibitors and promote cellular proliferation, suggesting that E2F7 restrains cell cycle progression through repression of proliferation-promoting microRNAs.

Importantly, we show that E2F7 plays a key role in the maintenance of genomic stability. We present evidence of E2F7-dependent transcriptional and non-transcriptional mechanisms for modulating cellular responses to genotoxic exposure. We identify an E2F7-dependent transcriptional regulation program that restricts homologous recombination-mediated DNA repair and cellular recovery upon induction of DNA lesions that interfere with replication fork progression (DNA interstrand cross-links and PARP1 inhibition).Additionally, we present evidence of a non-transcriptional mechanism by which E2F7 modulates cellular responses to alkylating DNA damage, possibly involving interaction with the repair protein XRRC1. Loss of E2F7 confers an increased resistance to chemotherapy in homologous recombination-deficient cells, a potentially harmful outcome for cancer treatment.

Altogether, results in this work reveal a key role for E2F7 in limiting cellular proliferation and promoting genomic stability by ensuring the timely expression of protein-coding and microRNA genes that are required for cell cycle progression and DNA damage repair.

1. - INTRODUCTION

1.1. E2F family of transcription factors

The E2 factor (E2F) was originally identified more than three decades ago as the cellular factor required for the activation of the adenoviral E2 promoter (Kovesdi, Reichel and Nevins, 1986). Subsequent studies revealed that the term "E2F" encompasses a large family of transcription factors present in all multicellular organisms, which can bind target consensus sequences present in the promoters of many cellular genes and thereby regulate their expression (Reviewed in Dimova & Dyson 2005). Presently, it is well established that E2F transcription factors are essential for cell cycle regulation and cell fate decisions, and that their deregulation results in severe pathological consequences including cancer or autoimmunity (Reviewed in Dimova & Dyson 2005; Chen et al 2009; Iglesias-Ara & Zubiaga 2015; Julien &Blais, 2017).

E2F factor activity is primarily regulated by the so-called pocket protein (PP) family members (pRB, p107 and p130), with which they interact on the promoters of target genes in a reversible manner: when is bound to a PP, E2F represses transcription, whereas free E2F activates transcription (Hauck and von Harsdorf, 2005; Fischer and Müller, 2017). To carry out transcriptional regulation, E2Fs are recruited to a consensus DNA binding motif (*TTTXXCGC* in mammals, where *X* may be *C* or *G*). This motif is usually present in a region near the transcription start site (between -1000bp and +500bp from the transcription start site) called the proximal promoter region (Rabinovich *et al.*, 2008; Lee, Bhinge and Iyer, 2011; Laresgoiti *et al.*, 2013), which is critical for the regulation of gene expression. There is also evidence that E2Fs can bind sequences that are not the consensus sites (Weinmann *et al.*, 2002; Bieda *et al.*, 2006; Xu *et al.*, 2007), although little is still known on this differential binding.

In mammals, the E2F family comprises eight genes (E2F1–8), which give rise to ten distinct proteins: E2F1, 2, 3a, 3b, 4, 5, 6, 7a, 7b and 8 (Figure 1). These proteins exhibit a relatively conserved sequence structure, particularly in the DNA binding domain (DBD), which is present in all family members. While the first described members of the family (E2F1-6), also known as "classical E2Fs" show a single DBD, the more recently added E2F family members (E2F7-8), also known as "atypical E2Fs" show two DBDs arranged in tandem (Figure 1).

Classical E2F family members bind DNA as heterodimers with one of the three dimerization partner proteins (DP1, DP2 and DP3) through their DP interaction domain (Figure 1). This dimerization enables E2Fs to bind DNA with high affinity, and to function as transcriptional regulators (Helin, 1998; Chen, Tsai and Leone, 2009). By contrast, atypical members of the family, E2F7 and E2F8, do not heterodimerize with DP family members. Instead, they harbor two DBDs with which they bind to the DNA molecule and mediate homo and heterodimerization among themselves to regulate transcription (Logan *et al.*, 2004; Maiti *et al.*, 2005).

E2F1-5 have a transactivation domain in their protein carboxy-terminus (Figure 1) that enables activation of gene expression. Within the transactivation domain, a short amino-acid stretch that mediates binding of pocket proteins is embedded. E2F1-3 have been shown to interact exclusively with pRB, whereas E2F4 and E2F5 preferentially bind p107 and p130, and with less affinity to pRB (Liban *et al.*, 2016). The interaction with PPs masks the transactivation domain, and allows E2F1-5 to carry out their repressive activity over target genes. E2F6-8 do not harbor a transactivation domain, and are thought to function mainly as transcriptional repressors, independently of pocket proteins.

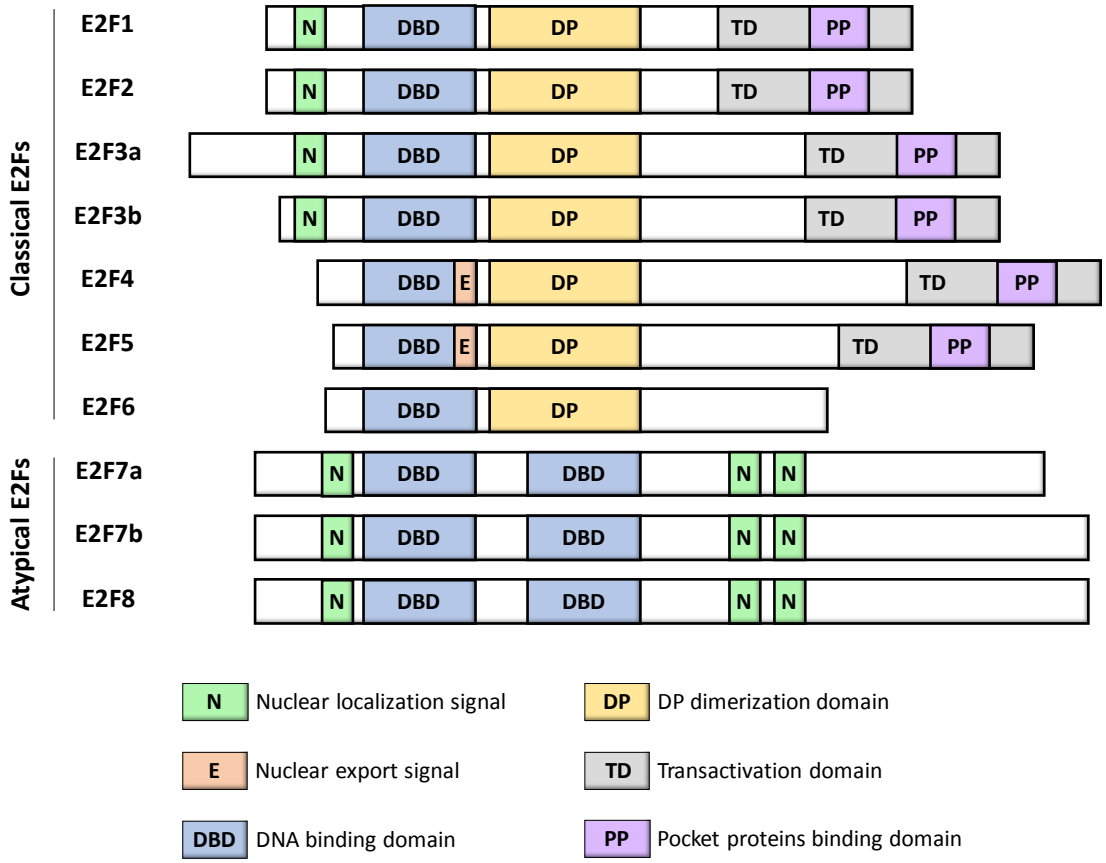

Figure 1: Schematic representation of the mammalian E2F family of transcription factors. The most representative domains identified in E2F proteins are shown (Modified from Lv et al. 2017).

Most E2F proteins are localized in the nucleus owing to nuclear localization signals (NLS) present in their sequence, with the exception of E2F4 and E2F5, which lack this signal. These factors rely on binding to pocket proteins to be transported to the nucleus in order to carry out their regulatory function.

1.1.1. Mechanisms of transcriptional regulation by E2F family members

Traditionally, and mostly based on the findings gathered after ectopic expression of E2F factors *in vitro*, E2F members have been subdivided into transcriptional activators (E2F1-3a), and transcriptional repressors (E2F3b-8) (Chen, Tsai and Leone, 2009). To achieve these functions, E2Fs form complexes with a variety of proteins involved mainly in chromatin remodeling (Fischer and Müller, 2017).

Transcriptional activation is carried out by E2F1-3a together with DP proteins, bound to target gene promoters through E2F consensus elements. These E2Fs can recruit, through their transactivation domain, protein complexes carrying histone acetyl transferase (HAT) activity, including the GCN5 complex (Lang *et al.*, 2001) and the TIP60 complex (Taubert *et al.*, 2004). This allows for the recruitment of Pol II and the subsequent induction of E2F target gene expression (Figure 2).

E2F-dependent transcriptional repression can be achieved through a variety of protein complexes. The best characterized complexes involve pocket proteins. As mentioned above, binding of pRB to activator E2Fs masks their transactivation domain and blocks their activity (Figure 2). Moreover, pRB has been found to interact with a variety of chromatin modifiers, including the histone deacetylases HDAC1/2 and the SIN3B/ HDAC complex, or histone methyltransferases (HMTs) such as HP1 and SUV39H (Talluri and Dick, 2012; Uchida, 2016) (Figure 2). The deacetylation and methylation of the chromatin carried out by these interacting proteins ensures chromatin condensation and target gene repression.

Binding of p107/p130 to E2F4/5 at the promoter region of its target genes triggers the assembly of the DREAM complex (dimerization partner, RB-like, E2F and multi-vulval class B) (Reviewed in Fischer and Müller, 2017), which includes the MuvB core complex (comprised of LIN9, LIN37, LIN52, LIN54, and RBBP4). The DREAM complex is responsible for the repression of gene expression at G0, but, unlike the pRB-HDAC/HMT complex, is unlikely to interact with histone modifiers. Instead, this complex has been described to promote the recruitment of H2A.Z, a variant of histone H2A, to the promoters (Latorre *et al.*, 2015), and consequently reduce the access of the RNA polymerase and repress gene expression through the compaction of nucleosomes (Marques *et al.*, 2010).

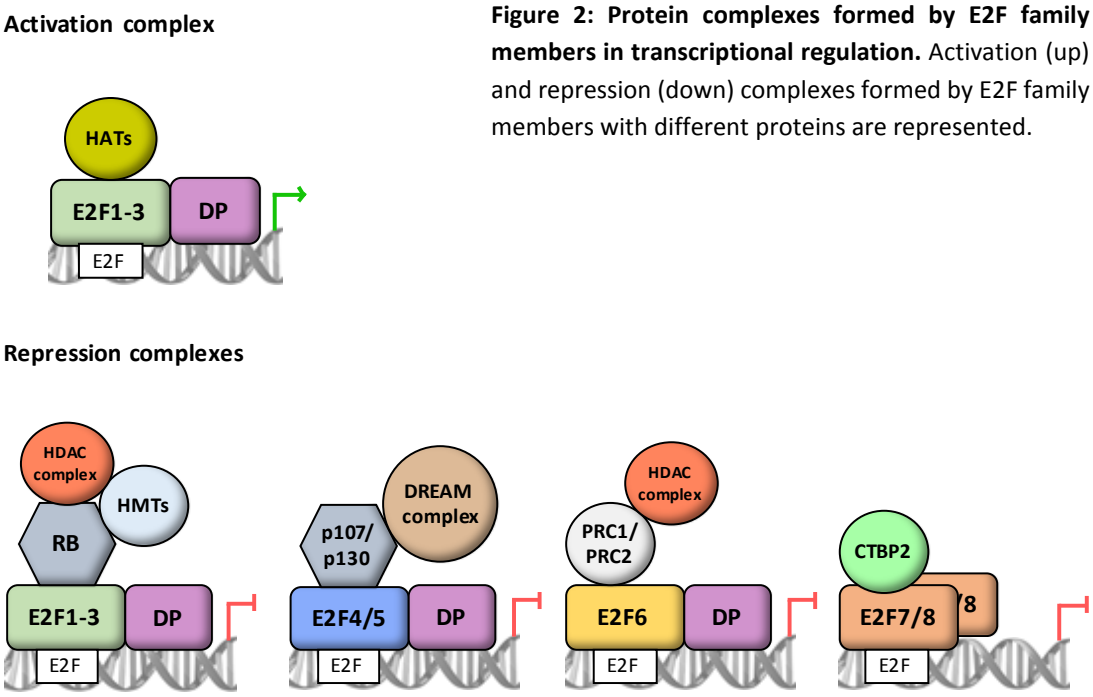

Figure 2: Protein complexes formed by E2F family members in transcriptional regulation. Activation (up) and repression (down) complexes formed by E2F family members with different proteins are represented.

E2F6 does not exhibit a transactivation domain or a PP-binding domain. It is thought to regulate transcription through interaction with a different set of protein complexes, including Polycomb Repressive Complex 1 (PRC1) and Polycomb Repressive Complex 2 (PRC2) (Trimarchi *et al.*, 2001; Attwooll *et al.*, 2005; Leung and Nevins, 2012) (Figure 2). More specifically, E2F6 has been described to interact with the PRC2-complex protein EZH2 (Attwooll *et al.*, 2005), a key protein for the histone methyltransferase activity of the PRC2 complex. This methylating activity, together with the additional interaction of PRC with HDAC1/2 proteins are responsible for the repressive activity of E2F6-PRC complex on target promoters (Morey and Helin, 2010).

Atypical E2F7-8 bind DNA as homodimers or heterodimers formed among themselves. They are thought to carry out their transcriptional regulation through interaction with co-repressor proteins in a pocket protein-independent manner. Yeast two-hybrid assays and proteomic screenings have identified co-repressors CTBP1 and CTBP2 as E2F7-interactor proteins (Liu *et al.*, 2013; Zalmas *et al.*, 2013), which could be involved in the recruitment of deacetylases such as HDAC2 (Figure 2), and subsequent gene repression (Zhao *et al.*, 2014). However, the repressor complex involving E2F7 and E2F8 remains to be fully characterized, and the mechanism of repression has not been addressed.

This variety of protein complexes recruited by E2F family members points to a high level of complexity in the mechanisms of transcriptional regulation involving E2Fs. Furthermore, an additional level of complexity stems from the fact that the traditional classification of E2Fs into activators and repressors of transcription is clearly oversimplified. Data gathered by our group and others has shown that although individual overexpression of E2F1-3 *in vitro* activates the expression of numerous responsive genes, the critical function of these E2Fs *in vivo* is to repress gene expression in quiescence (G0) and early G1 phase of the cell cycle, in complex with pRB protein (Murga *et al.*, 2001; Infante *et al.*, 2008; Chong *et al.*, 2009; Zhang *et al.*, 2017). In fact, these studies have shown that E2F1-3 proteins are mostly dispensable for transcriptional activation of their target genes in proliferating cells. Regarding the repressor arm of the E2F family, E2F4-5 and atypical E2F7-8 are not always transcriptional repressors. Numerous reports have shown that they are also able to activate gene transcription of many target genes under certain conditions (Lee, Bhinge and Iyer, 2011; Weijts *et al.*, 2012; Arbi *et al.*, 2016). Differences in cellular contexts may be responsible for this duality in functional activity of E2F factors, which hinders a clear understanding of their mechanisms of action.

1.1.2. Regulation of E2F factor expression

The expression of E2F family members can be regulated at several levels, of which transcriptional regulation has been described as the most important one. Additionally, there is evidence for non-transcriptional regulation, including post-translational modifications on E2F factors, which affect protein stability, and, more recently, microRNA-mediated regulation of E2F mRNA expression (Woods et al. 2007; Emmrich & Pützer 2010).

Regarding transcriptional regulation, most E2F factors are controlled through a cell cycle-dependent regulation. As part as this regulation, E2F factors themselves are able to regulate the expression of members of the family, forming both positive as well as negative feedback loops that ensure balanced levels of activators and repressors in each phase of the cell cycle.

In quiescent cells (G0), the protein complexes formed by E2F1-3 or E2F4-5, together with pocket proteins, bind the promoters of *E2F1-3* and *E2F6-8* genes, as well as many of their downstream target genes, concomitant with their transcriptional silencing (Figure 3) (Takahashi, Rayman and Dynlacht, 2000; Balciunaite *et al.*, 2005; Infante *et al.*, 2008). These complexes maintain low transcription levels of *E2F1-3* and *E2F6-8* during G0 and early G1. E2F4 and E2F5 are not regulated by E2F, and their levels are maintained constant throughout the cell cycle (Dimova and Dyson, 2005).

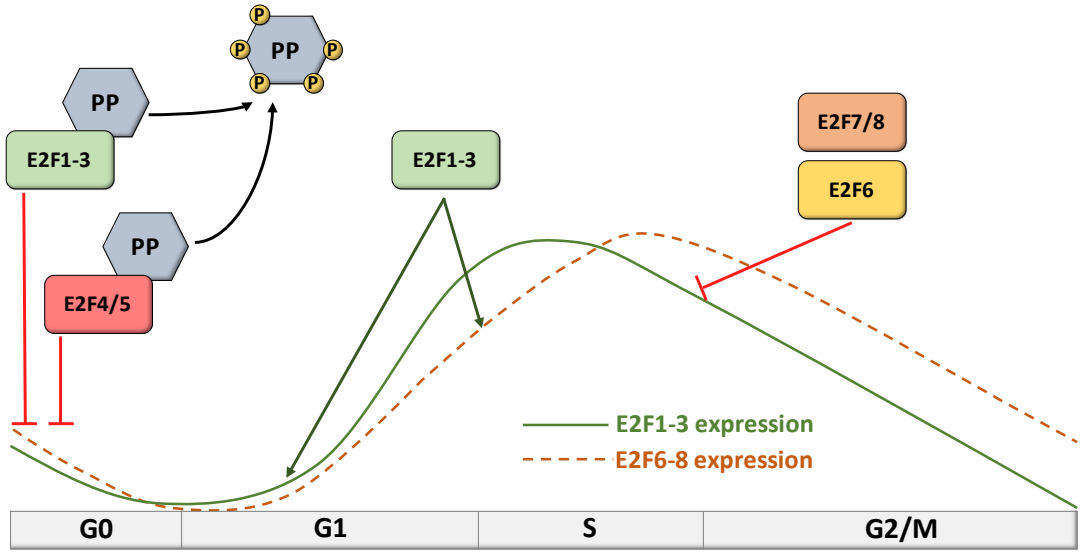

Figure 3: Expression and regulation of mammalian E2Fs by other family members. In quiescent (G0) cells, the constitutively expressed E2F4 and E2F5, as well as E2F1-E2F3, repress the expression of E2F1-3 and E26-8. Mitogenic stimulation signals induce E2F1-3 expression late in G1 phase; thereby activating the G1/S transcriptional program. E2F6, E2F7 and E2F8 have been suggested to accumulate during G1/S. In turn, E2F6-8 mediate the repression of E2F1-3.

Upon mitogenic stimulation and progression through G1, pocket proteins undergo sequential phosphorylation by cyclin-dependent kinases, which reduce their affinity for E2Fs. Consequently, repression complexes turn into activation complexes and *E2F1-3* genes are transcriptionally induced. E2F1 was first shown to induce its own expression through binding to canonical E2F motifs present in its promoter, resulting in a positive autoregulation (Johnson, Ohtani and Nevins, 1994). The promoters of E2F2 and E2F3 also display E2F motifs (Sears, Ohtani and Nevins, 1997; Adams *et al.*, 2000) and they are thought to employ autoregulatory mechanisms similar to that of E2F1 to modulate their expression. This positive transcriptional feedback loop creates an “all-or-none switch” that results in the commitment of cells to progress through the cell cycle once the restriction point is reached (Skotheim *et al.*, 2008).

In G1, E2F1-3 initiate a transcriptional program driving cells into S phase. Concurrent with the entry into S phase, E2F1-3 expression and E2F-driven G1/S-specific transcriptome is attenuated. It has become increasingly clear that the mechanism of this transcriptional inactivation relies on negative feedback loops, which involve, among others, E2F6-8 proteins, whose expression is induced in late G1 by E2F1-3 (Figure 3). E2F7 and E2F8 directly repress E2F1-3 expression (Moon and Dyson, 2008; Endo-Munoz *et al.*, 2009; Mitxelena, 2014) resulting in a negative regulation of E2F1-3 by atypical repressor E2F proteins, thus ensuring that activator E2Fs are transcriptionally silent when cells enter mitosis.

In addition to transcriptional regulation, an important regulatory process that finely tunes E2F levels takes place post-translationally. Post-translational modifications identified in E2F members include acetylation, phosphorylation and ubiquitination. These modifications can change E2F levels and exert either activating or inhibitory effects on E2F transcriptional activity (Dagnino, Kaur and Judah, 2011).

E2F1 has been the most studied member of the E2F family referring to post-translational regulation, although E2F2 and E2F3 are thought to undergo similar post-translational modifications (Gong *et al.*, 2016). Acetylation of lysine residues adjacent to DBDs allow for stabilization and significant increase in E2F1 protein levels (Martínez-Balbás *et al.*, 2000; Ianari *et al.*, 2004). Additionally, these acetylations increase DNA-binding activity of E2F1, leading to an elevation in the transcriptional induction of its target genes (Martínez-Balbás et al. 2000). Phosphorylation of E2F1 can also affect its stability, along with its ability to interact with other proteins. For example, it has been described that CDK8 protein phosphorylates E2F1 on serine 375, both *in vitro* and *in vivo*, thereby modulating its ability to bind pRB and repress target genes (Zhao, Ramos and Demma, 2013).

An ubiquitin/proteasomal system whereby the stability of E2F1 is controlled by ubiquitination throughout the cell cycle was described initially by Krek and collaborators (Marti *et al.*, 1999), and its components have been subsequently identified by several groups. In early S phase, E2F1 is conjugated with K63-linked ubiquitin chains in a cIAP1-dependent manner, contributing to its stabilization (Glorian *et al.*, 2017). At the end of the S phase, the SCF/SKP2 complex mediates E2F1 ubiquitination and subsequent proteasomal degradation (Lu *et al.*, 2014). The low levels of E2F1 in G2 and M are further guaranteed by APC/C-mediated ubiquitination and proteasomal degradation of this E2F (Peart *et al.*, 2010; Budhavarapu *et al.*, 2012).

Over the last decade, microRNAs have been described to modulate E2F transcription factor expression, adding a new layer of complexity to their non-transcriptional regulation (Emmrich and Pützer, 2010; Bueno and Malumbres, 2011; Chafin *et al.*, 2014; Teplyuk *et al.*, 2015; Luo *et al.*, 2016; Xu *et al.*, 2017). One of the first studies relating E2F factors with microRNAs showed that E2F1 expression is negatively regulated by *miR-17*-92, whose expression is induced by c-MYC and E2F1-3, thus ensuring the correct turn off of E2F1 during the progression of cell cycle (O'Donnell *et al.*, 2005; Woods, Thomson and Hammond, 2007). Since the discovery of this novel level of regulation of E2F factors, more than 50 microRNAs have been described to control E2F mRNA expression (only within last year, close to 20 new microRNAs were described to target E2F family members).

The cellular consequences of microRNA-targeted E2F mRNA degradation are diverse, ranging from effects on proliferation, apoptosis, differentiation, migration or angiogenesis. However, in general, increased levels of these microRNAs result in a reduction of proliferation, by direct binding to individual activator E2F mRNA and its consequent degradation. For example, overexpression of miR-93 in primary leiomyoma cells result in a reduction of E2F1 levels and a consequent time-dependent inhibition of cell proliferation and cell motility (Chuang and Khorram, 2018). Conversely, overexpression of miR-26a led to a reduction of E2F7 sustaining cell proliferation in acute myeloid leukemia cells (Salvatori *et al.*, 2012). Despite the recent identification of these microRNAs, little is known about the microRNA-dependent regulatory networks operating in cells that impact E2F mRNA stability, and to what extent these networks are relevant for E2F expression and function.

1.1.3. Functions of E2F protein family

1.1.3.1. Cell cycle regulation by E2F factors

E2F factors are best known for their role in cell cycle control through the regulation of the transcriptional machinery required for the expression of genes involved in cell cycle entry and DNA synthesis (Bertoli, Skotheim and de Bruin, 2013). According to the currently accepted model of cell cycle regulation, in quiescent cells, the transcription of genes required for cell cycle entry and progression is repressed by complexes formed by hypophosphorylated pocket proteins bound to E2F factors (Weinberg, 1995; Trimarchi and Lees, 2002), together with a large number of chromatin modifying components. The main repressor complex present in some cells, such as fibroblasts, appears to be formed by E2F4-5 proteins (Li *et al.*, 1997; Gaubatz *et al.*, 2000). By contrast, our group has shown that in resting lymphocytes the repressor complexes formed by E2F1-3 are as prevalent as those formed by E2F4-5 (Infante *et al.*, 2008; Laresgoiti *et al.*, 2013).

Growth factor-mediated stimulation of quiescent cells triggers several signaling cascades leading to the activation of Cyclin/CDK complexes, thus allowing entry into the cell cycle (Santamaria and Ortega, 2006). The RAS-MAPK signaling pathway is well-known for its role in Cyclin/CDK activation, whereby activated MAP kinases phosphorylate the transcription factors MYC and AP-1, and lead to the transcriptional activation of Cyclin D1, CDK4 and CDK6 (Coleman, Marshall and Olson, 2004; Bretones, Delgado and León, 2015). Newly generated CyclinD1/CDK4-6 complexes are capable of mono-phosphorylating pocket proteins (Narasimha *et al.*, 2014) (Figure 4). The phosphorylation of PPs is thought to be sufficient to release a few repressor complexes, thereby leading to the expression of some E2F target genes, including Cyclin E.

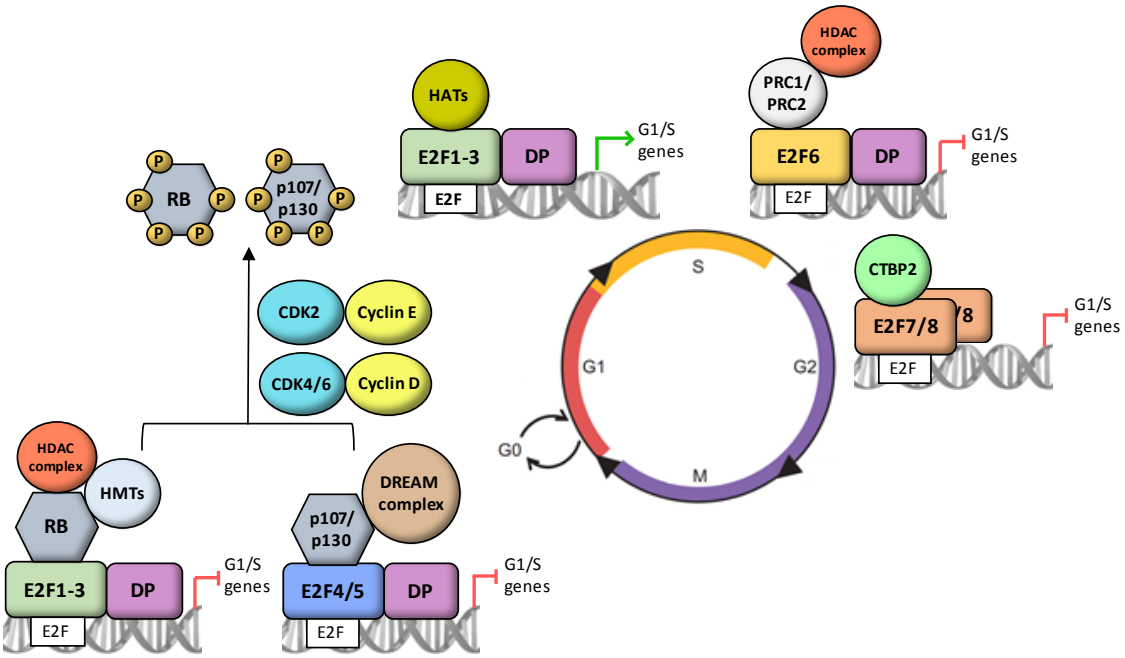

Figure 4: Mammalian cell cycle-dependent transcriptional regulation by E2F and pocket proteins. In G0 (quiescence) and G1, the constitutively expressed E2F4 and E2F5, as well as E2F1-E2F3, associate with pocket proteins and maintain repression of E2F-responsive genes. Upon mitogenic stimulation, the sequential phosphorylation of PPs by activated CDKs results in the loss of PPs function, and release of E2Fs. These events initiate a transcriptional program driven by E2F1, E2F2 and E2F3 that leads cells into S phase. This G1/S-specific transcriptome is then attenuated on completion of S phase and G2 by the action of E2F6 and E2F7/8.

In late G1 phase, the newly transcribed Cyclin E complexes with CDK2 to multiphosphorylate the mono-phosphorylated PPs, leading to the full release of the activating E2F1–3 (Narasimha *et al.*, 2014), an event that is critical for cells to proceed through the restriction point (Yao *et al.*, 2008). Cyclin D/CDK4-6 and Cyclin E/CDK2 can also phosphorylate p107 and p130, which enables the disruption of the DREAM complex (Guiley *et al.*, 2015). Subsequently, free E2F4 is exported from the nucleus, and it is not thought to participate in the transcriptional induction of E2F target genes (Gaubatz *et al.*, 2001).

Once released from pRB, E2F1–3 together with DP1 or DP2 and histone acetylases (HATs) activate target gene promoters through E2F promoter elements (Figure 4). These G1/S genes encode many of the factors required for DNA replication (i.e. MCM2-7, CDC6, PCNA), transcriptional regulation (i.e. MYBL2, E2Fs, EZH2), or key proteins for cell cycle progression such as kinases/phosphatases or polymerases (i.e. CCNE1-2, CDC7, CHEK1, POLA1-2) (Figure 5). Notably, genes that encode E2F1, E2F2 and E2F3 themselves are G1/S cell cycle genes and participate in a positive autoregulatory feedback loop that amplifies transactivator function at the G1/S boundary (Figure 5). E2F1-3 transcription factors are not only regulators of protein-

coding genes involved in cell cycle regulation, but are also critical for the timely activation of a set of cell cycle-dependent microRNAs during G1/S. At least four microRNA clusters, *let-7a-d, let-7i, mir-15b-16-2*, and *mir-106b-25*, have been identified as direct targets of E2F1 and E2F3 during G1/S (Bueno *et al.*, 2010).

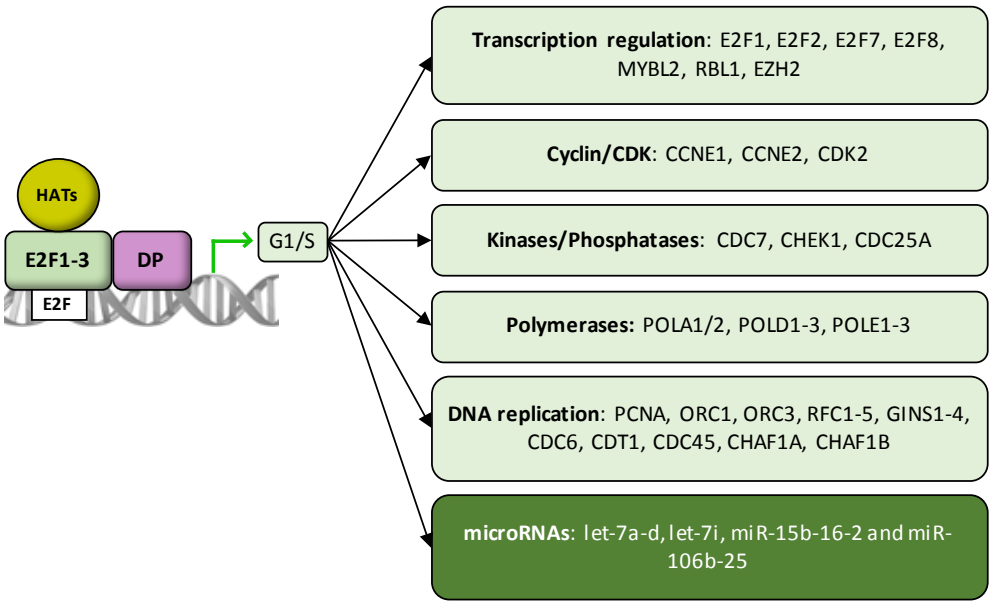

Figure 5: G1/S phase genes and microRNAs regulated by E2Fs. Genes and microRNAs activated by E2F1-3 in the G1-S transition are represented by their different functions.

The classical model arguing that the main role of E2F1-3 factors is to promote cell cycle entry and progression (Nevins, 1992; Weinberg, 1995; C. Lee *et al.*, 2002) has been recently challenged by findings gathered by our group. We have shown that loss of E2F2, or more dramatically, the combined loss of E2F1 and E2F2 leads to overexpression of target genes and to accelerated replication of DNA in multiple cell types, implying a negative role for these proteins in proliferation control (Murga et al. 2001; Infante et al. 2008; Laresgoiti, 2013). This findings have been subsequently confirmed by others (Pusapati *et al.*, 2009; Zhang *et al.*, 2017). Importantly, our group has shown that inappropriate DNA replication upon E2F1/E2F2-loss leads to DNA replication stress and subsequent cell cycle arrest, suggesting that the critical role of activating E2Fs is not to promote cell cycle entry. Instead, they are required to prevent unscheduled DNA replication and replicative stress by repressing target genes involved in these processes, presumably in complex with pRB (Iglesias-Ara et al. 2010; 2015). E2F1-3 induced microRNAs also contribute to limit the cellular responses to E2F activation by dowregulating the expression of G1/S genes necessary to progress through the cell cycle, thus preventing replicative stress and genomic instability (Bueno *et al.*, 2010).

When cells progress through S phase, the repressing E2Fs (E2F6-8) are induced by E2F1-3 (Giangrande et al. 2004; Christensen et al. 2005, Di Stefano et al. 2003). During late S phase, E2F6-8 replace E2F1-3 on target promoters, and serve to repress the expression of the G1/S genes when DNA synthesis is completed (Giangrande et al. 2004; Di Stefano et al. 2003; Christensen et al. 2005; Westendorp et al. 2012) (Figure 4). Regarding E2F7, genome-wide chromatin immunoprecipitation and transcriptomic assays carried out by Alan de Bruin's group has identified a set of E2F7 target genes involved in DNA replication and metabolism, as well as cell cycle regulation, whose expression is repressed by E2F7 in late S-phase (de Bruin *et al.*, 2003). The list of genes includes CDC6, CDT1, MCM2, DHFR and RRM2, all of which have been described as induced by E2F1-3. RNA-Seq experiments carried out recently by our group upon E2F7 mRNA silencing have confirmed the identity of the DNA replication and cell cycle regulation genes reported previously (Mitxelena, 2014), suggesting that E2F7 plays an important role in the attenuation of the transcriptional program that drives cells through G1 and S. The fact that overexpression of E2F7 blocks cell cycle progression (Westendorp *et al.*, 2012), and that depletion of E2F7 accelerates the cell cycle (Mitxelena, 2014) is consistent with this repressor role for E2F7. Interestingly, our transcriptomic analysis also revealed a set of microRNAs that are repressed by E2F7 throughout the cell cycle (Mitxelena, 2014), although their cellular function was not established.

1.1.3.2. Apoptosis regulation by E2F factors

In addition to their role in regulating cell cycle progression, E2F transcription factors can also promote the expression of a set of genes that induces the apoptotic program in certain contexts. Given the seemingly opposite roles of E2Fs as pro-apoptotic and pro-proliferative factors, a considerable effort has been dedicated to elucidate the factors influencing E2F-induced apoptosis, as well as downstream targets of E2F in this process, to try to understand the mechanisms for such disparate roles.

Among the E2F family members, E2F1 is the best characterized apoptosis regulator, owing to its ability to modulate a large number of pro-apoptotic genes (Jiang *et al.*, 2015; Pagliarini *et al.*, 2015; He *et al.*, 2018; Xie *et al.*, 2018). E2F1 overexpression was firstly described as apoptosis inducer by the Adams group in 1994 (Qin *et al.*, 1994). Consistent with this, our lab showed subsequently that E2F1 knockout mice exhibit reduced apoptosis rates in the thymus (Field *et al.*, 1996) and deficient thymic negative selection, giving rise to the accumulation of self-reactive T cells in the peripheral lymphoid organs (García *et al.*, 2000). E2F1 knockout mice develop late-onset tumors (Rounbehler *et al.*, 2002), which has led to propose that E2F1 functions as a tumor surveillance factor, detecting aberrant proliferation and engaging apoptotic pathways to protect the organism from developing tumors.

Mechanistically, E2F1-induced cell death is thought to occur via multiple pathways. E2F1 was first described to induce apoptosis through a p53-dependent pathway by inducing the transcription of E2F1 target gene $p14^{ARF}$, which binds directly to MDM2 and inhibits its ability to degrade p53 (Pomerantz *et al.*, 1998). This regulation results in p53 accumulation and subsequent activation of its downstream target genes required for apoptosis (Kowalik *et al.*, 1998). E2F1 can also induce apoptosis in a p53-independent manner regulating genes that are not directly related to p53 pathway. The main apoptotic gene regulated by E2F1 is the p53 family member p73. Activation of p73 by E2F1 can lead, at least in part, to the transcriptional activation of p53-responsive target genes and apoptosis in cells that are p53 deficient (Stiewe and Pützer, 2000), which might constitute a p53-independent anti-tumorigenic safeguard mechanism. Moreover, E2F1 can also directly activate the expression of several pro-apoptotic genes, including APAF1, which forms a complex with cytochrome c and activates procaspase 9 leading to apoptosis (Bracken *et al.*, 2004; Pützer, 2007; Polager and Ginsberg, 2008).

It has recently been proposed that E2F1-driven regulation of apoptosis is dependent on the cellular levels of E2F1 protein and on the different affinities of E2F1 for its target genes. Low levels of E2F1 were found to only induce cell cycle-promoting genes which bind E2F1 with high affinity, whereas higher levels where necessary to induce the key apoptotic E2F1 targets APAF1, PUMA, HRK and BIM (Shats *et al.*, 2017). Thus, the level of E2F1 expression emerges as a key parameter that determines whether a cell will progress into the cell cycle or whether it will undergo apoptosis.

Other members of the E2F protein family have also been described as apoptosis modulators. The apoptosis elicited by E2F3 overexpression has been associated in some studies with increased E2F1 levels and E2F1-dependent apoptosis (Lazzerini Denchi and Helin, 2005; Martinez *et al.*, 2010), whereas in another study it was described to be E2F1-independent (Hong, Paulson and Johnson, 2008). E2F2 has also been described to induce apoptosis independently of E2F1 levels (Chen *et al.*, 2013).

While E2F1-3 appear to be pro-apoptotic factors when overexpressed, E2F6-8 seem to have an anti-apoptotic role through the downregulation of E2F1 levels. E2F6 represses apoptosis by counteracting E2F1 expression in human hematopoietic cells (Kikuchi *et al.*, 2007) and in human embryonic kidney cells (Yang *et al.*, 2008). Similarly, E2F7 and E2F8 were found to modulate apoptotic responses through the regulation of E2F1 expression (Moon and Dyson, 2008). In keratinocytes, E2F7 was able to antagonize E2F1-induced apoptosis (Endo-Munoz *et al.*, 2009), and the combined inactivation of E2F7-8 triggered apoptosis via induction of E2F1 in response to stress (Thurlings *et al.*, 2016).

All these previous evidences point to E2F1 as a critical E2F family member in apoptosis regulation, which may impact tumor development because of its dual roles as a promoter of cell-cycle progression and as an inducer of apoptosis (Pomerantz *et al.*, 1998; Irwin *et al.*, 2000; Polager *et al.*, 2002). In non-tumor cells expressing physiological levels of E2F1, its contradictory pro-survival and pro-apoptotic activities are thought to be under tight regulation in order to keep the homeostasis of the cell. In the event of a deregulation of the PP/E2F pathway, E2F1 levels increase, thus activating the apoptotic program to eliminate aberrant cells. In cancer cells, in which E2F1 activity is typically increased, its pro-apoptotic activity needs to be restrained in order to achieve neoplastic transformation, either by the inhibition of negative regulators of E2F1 activity (such as p53) or by the activation of counterbalancing pro-survival signals (such as PI3K pathway) (Dynlacht, 2008; Hallstrom, Mori and Nevins, 2008). The number of modulators of E2F1's apoptotic activity is probably more numerous, but their nature remains to be identified.

1.1.3.3. E2F factors and cancer

Genomic aberrations involving PP/E2F pathway have been described in most cancer types during the last decades. Mutation of the pRB gene was first observed in inherited retinoblastoma (Friend *et al.*, 1986). It was later found that loss of pRB function is very common in human cancer, including osteosarcomas, small cell lung carcinomas, breast carcinomas and others (Weinberg, 1995). Besides mutation in pRB gene, other mutations in human cancers that disrupt the regulation of the PP/E2F pathway involve inactivating mutations of the $p16^{INK4a}$ cyclin kinase inhibitor or activating mutations of Cyclin D. In the absence of p16, Cyclin D/CDK4 activity is elevated, leading to abnormal pRB phosphorylation. Loss of $p16^{INK4a}$ function is highly prevalent in sporadic cancers of a variety of types (Romagosa *et al.*, 2011). Cyclin D1, which functions as a mitogenic sensor and allosteric activator of CDK4/6, is one of the more frequently altered cell cycle regulators in cancers, and its overexpression can be attributed to many factors including increased transcription, translation, and protein stability (Witzel, Koh and Perkins, 2010).

Due to the mutations in the PP/E2F pathway described above, virtually all cancers have an increased E2F activity, and for some cancers, such as ovarian carcinoma, it has been demonstrated that elevated E2F activity is the triggering cause for tumor growth (Zhan *et al.*, 2016).

In addition to increased E2F activity due to loss pRB function, E2F amplification has also been described in several cancers. According to the bioinformatics tool cBioportal (http://www.cbioportal.org/index.do) and the recently released The Cancer Genome Atlas (TCGA) data, E2F family genes are amplified in tumoral processes such as prostate cancer, cervical cancer or ovarian cancer (Table 1). More specifically, E2F1 has been described as amplified in a subset of head and neck squamous cell carcinomas (HNSCCs) infected with human papillomavirus (TGCA Network, 2014).

Table 1: Percentage of tumoral processes showing E2F amplification

Amplified E2F	Cancer type	% of the cases
E2F1	Prostate	17
	Ovarian	4.1
	Cervical	2.9
E2F2-3	Bladder	11.7
	Ovarian	8.2
E2F4-5	Breast	6.59
	Prostate	4.87
E2F6	Ovarian	2.31
	Endometrial	1.71
E2F7	Prostate	14
	Soft Tissues	4.15

The amplification of both E2F1 and E2F7 genes in prostate cancer could seemingly result in contradictory outcomes due to the negative-loop regulation that is established between these E2Fs. However, additional mechanisms may be in place in these cancers that counteract some of the effects of these E2Fs. For example, it has been recently described that head and neck squamous cell carcinomas express aberrant levels of XPO1, leading to the nuclear exclusion of E2F7 specifically. As a consequence, the transcription of E2F responsive genes by E2F1 is increased due to lack of E2F7-mediated repression (Saenz-Ponce *et al.*, 2018). These results suggest a mechanism by which a tumor cell can develop in the simultaneous presence of both activator and repressor E2Fs.

In summary, the increased E2F activity as well as the genomic amplification of E2F family members in many types of cancer suggest an important role for these factors in tumor development. However, mechanisms by which E2Fs could be regulating this process remain poorly understood.

1.2. The DNA Damage Response and E2F

Genomic screens carried out to identify the transcriptional program regulated by E2Fs have identified a surprisingly large number of genes with functions in DNA repair and DNA damage checkpoints (Wang *et al.*, 2000; Ren *et al.*, 2002; Iglesias *et al.*, 2004; Stevens and La Thangue, 2004; Infante *et al.*, 2008; Laresgoiti *et al.*, 2013; Collin *et al.*, 2018). These findings suggest that E2F directly links cell cycle progression with the coordinated regulation of genes essential for DNA stability and repair. Because of their interest for this thesis work, the types of DNA lesions and their repair mechanism will be examined in more detail in this section, including the role of E2F in this process.

1.2.1. Sources of DNA damage and types of DNA lesions

The genome of any living cell is constantly exposed to many sources of damage, both endogenous and exogenous, which can generate a great variety of DNA lesions. In order to solve these lesions and overcome the damage, cells are equipped with several systems – together called the DNA damage response (DDR) – to detect DNA damage, signal its existence and facilitate its repair.

1.2.1.1. Endogenous sources of DNA damage

A large proportion of the DNA damage that is relevant to mutagenesis, carcinogenesis and aging is of endogenous origin. Most of endogenous DNA damage metabolites generated as byproducts of cellular metabolic processes, such as reactive oxygen species (ROS), nitrous acid and S-adenosylmethionine, are examples of sources of endogenous DNA damage. Reactive oxygen species are produced during aerobic respiration and can result in base modification and single- or double-strand DNA breaks (Figure 6) (De Bont and van Larebeke, 2004).

Another important example is nitrous acid, which is formed in the stomach during consumption of nitrite-containing foods and certain metabolites of alcohol, cigarette, and high fat diet, such as acetaldehyde and malondialdehyde. These metabolites are endogenous sources of interstrand crosslinks (ICLs) in the DNA molecule (Langevin *et al.*, 2011; Garaycoechea *et al.*, 2012; Huang and Li, 2013). In ICL lesions, two nucleotides on opposite strands are covalently joined and, thus, ICLs prevent the separation of the two DNA strands (Figure 6). DNA ICLs are considered among the most deleterious DNA lesions, since they block DNA replication and transcription.

Finally, S-adenosylmethionine is a reactive methyl group donor contributing to physiological enzymatic DNA methylation. This enzyme plays a role in regulation of gene expression (Holliday and Ho, 1998). However, it can also form mutagenic adducts (Figure 6) in the DNA due to its alkylating role (Stern *et al.*, 2000).

1.2.1.2. Exogenous sources of DNA damage

As regards exogenous sources of DNA damage, they are environmental sources of DNA damage that could mainly come in form of radiation or exogenous genotoxic chemicals.

Radiation is capable of penetrating to the cell nucleus and cause various injuries to the chemical structure of DNA. Ionizing radiation, such as X rays or gamma (γ) radiation, can generate single-strand and double-strand breaks in the DNA (Figure 6) (Roots, Kraft and Gosschalk, 1985). Radiation of ultraviolet (UV) wavelength is the main example of non-ionizing DNA damage. UV-radiation induces covalent bonds between nucleotides, generating dimers of different nature (Jiang *et al.*, 2009).

Regarding exogenous genotoxic chemicals, each agent causes lesions of different nature and toxicity (Hühn, Bolck and Sartori, 2013). Radiomimetic compounds such as neocarzinostatin (NCS), DNA intercalators (e.g. doxorubicin) and topoisomerase I and II inhibitors (e.g. etoposide and camptothecin) form single-strand and double-strand breaks in the DNA. There are also DNA interstrand crosslink-inducing agents (e.g. cisplatin and mitomycin-C) and DNA alkylating agents (e.g. temozolamide and methyl methanesulfonate) that form DNA adducts (Figure 6).

Most anti-cancer therapies are based on the exogenous generation of DNA lesions either through use of radiation or through treatment with chemical compounds. A better understanding of how the various chemical agents damage DNA, and how this damage is repaired, has become a priority towards the design of effective doses and combination therapies for each type of cancer.

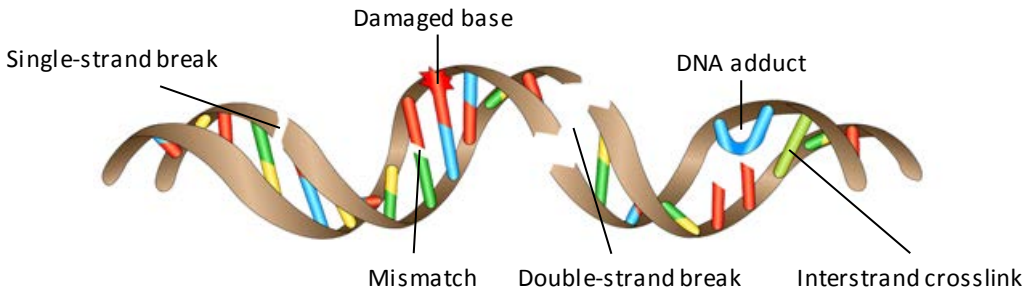

Figure 6: Sources and types of DNA lesions. Exogenous and endogenous DNA damaging agents generate various types of lesions including DNA single- and double-strand breaks (SSBs and DSBs), DNA interstrand crosslinks (ICL), mismatches, DNA adducts and damaged pair bases.

1.2.2. DNA damage response

1.2.2.1. DNA damage sensors and transducers

In order to protect the genome, all types of structural alterations generated in the DNA must be detected by the cell. As a result, a DNA repair response will be activated. The DDR is a hierarchical process that activates several groups of proteins in a certain order and specific manner, depending on the type of damage (Figure 7) (Ciccia and Elledge, 2010). DNA damage signaling starts with the recognition of the lesion by several molecular complexes that sense and signal different types of insults in the DNA. These complexes, known as sensors, are in constant contact with the chromatin and, upon damage; they transmit and amplify the signal through complexes known as transducers.

In the case of DNA adducts created by alkylating agents, those are first recognized by specific DNA glycosylases which remove the damaged base creating an abasic site. Subsequently, the endonuclease APE1 acts as a transducer to promote the recruitment of the SSB repair machinery (Figure 7).

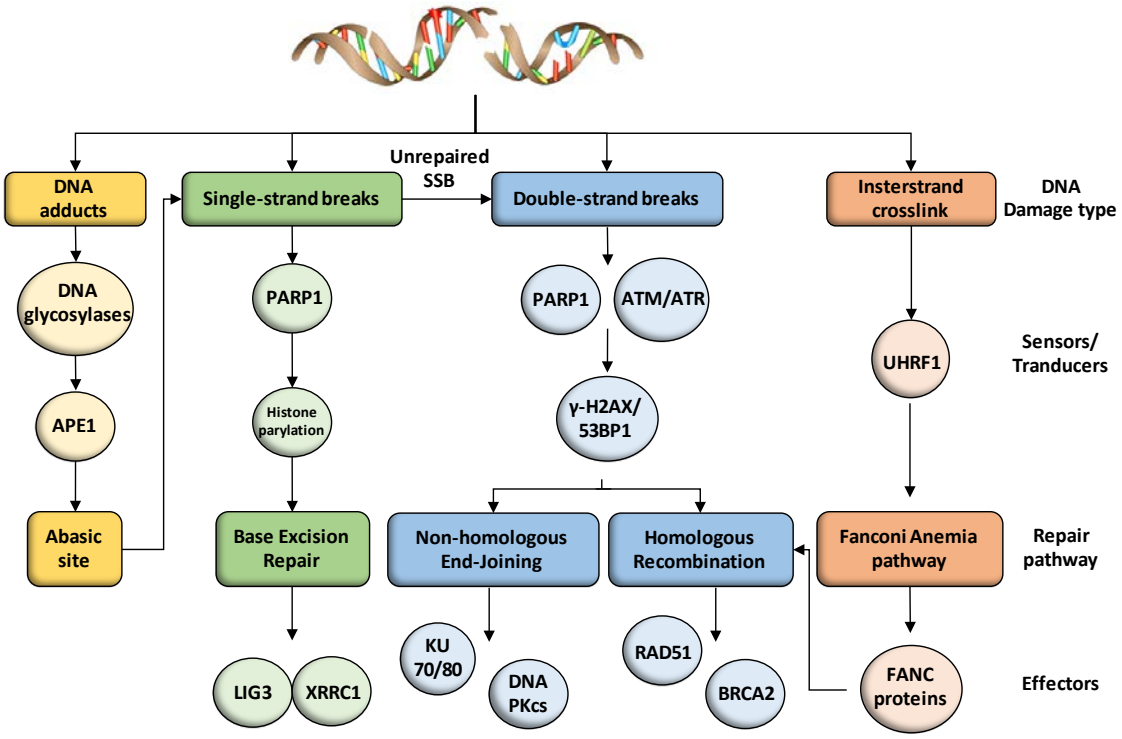

Figure 7: DNA damage responses. Schematic representation of different DNA response pathways depending the damage type. Examples of main sensors, transducers and effectors are indicated.

When a single-strand break (SSB) is generated, usually by γ-IR or ROS, or indirectly during repair of DNA adducts, PARP1 protein acts as molecular sensor (Figure 7). Activated PARP1 carries the synthesis of poly(ADP-ribose) (PAR) chains at damaged sites, and this is one of the earliest events of the DNA damage response to SSBs. Upon binding on sites of damaged DNA PARP1 assembles PAR chains on target proteins, including histones H1 and H2B, and PARP1 itself (Schreiber et al., 2006). This histone parylation leads to the repair of the gap by one of the SSB repair mechanisms.

When a double-strand break (DBS) is generated the most significant transducers of damage in the DNA are the kinases ATM (Ataxia Telangiectasia Mutated) and ATR (ATM and Rad3 related) (Blackford and Jackson, 2017), whereas PARP1 plays a role in its sensing (Ray Chaudhuri and Nussenzweig, 2017). ATR and ATM regulate a global cellular response by phosphorylating a number of target proteins that amplify the signal. Directly downstream of the ATM and ATR kinases, several substrates, also known as mediators of the DDR, regulate the spatio-temporal assembly of protein complexes involved in DNA repair in the chromatin region next to the lesion (Fernandez-Capetillo *et al.*, 2002; Blackford and Jackson, 2017). Among the proteins involved in amplifying the signal, the variant histone H2AX has been the most intensively studied. At the site of DNA damage, H2AX becomes phosphorylated on Ser139 by ATM and ATR (Rogakou *et al.*, 1998). This event facilitates an efficient signaling and repair of the lesion.

UHRF1 acts as a sensor for DNA interstrand crosslinks (ICLs). UHRF1 is an integral part of the Fanconi anemia DNA repair pathway and is recruited to ICLs within seconds of their appearance in the genome. Its recruitment is required for proper assembly of FANC proteins to damaged sites (Liang *et al.*, 2015).

1.2.2.2. DDR signaling pathways

In order to continue being viable, once the damage is identified and the transducers have amplified and transmitted the signal, the DNA lesion must be repaired by the cell. Several main repair mechanisms are used by the cells depending on the type of damage and the sensor involved.

In the case of DNA adducts provoked by alkylating agents, the gap produced in the DNA by DNA glycosylases is repaired by Base Excision Repair (BER), one of the SSB repair mechanisms, through a short or a long-patch (Caldecott, 2008). In the short-patch repair pathway (used to repair single nucleotide gaps) PARP1 recruits the scaffold protein XRCC1 and DNA polymerase β (POLβ) to replace the damaged nucleotide.

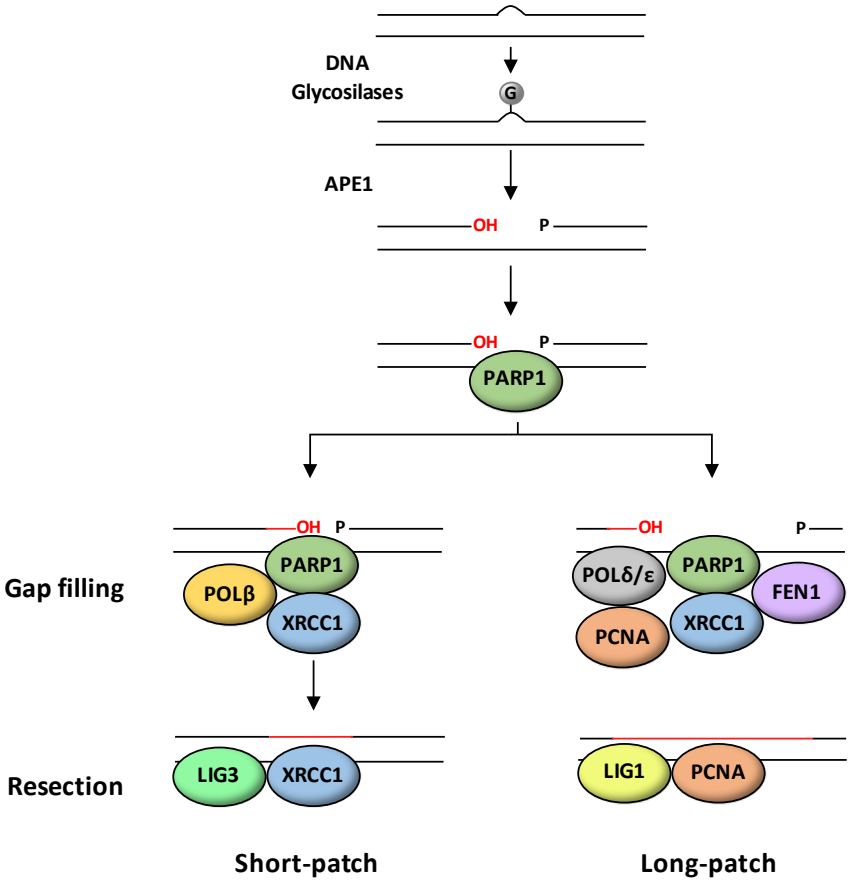

Figure 8: Simplified BER repair pathway. The first step of BER involves recognition, base removal and incision. Then, depending on the incision length, one of the two pathways, short patch repair (left) and long patch repair (right) are chosen in order to carry out the repair.

Finally, DNA ligase III (LIG3) is recruited to ligate the nick, and intact DNA is restored (Figure 8). In the long-patch repair pathway (used to repair 2-15 nucleotide gaps), PARP1 also recruits XRCC1 as before, but now this is followed by the recruitment of PCNA. Subsequently, DNA polymerase δ/ε (POLδ/ε) extends the strand and FEN1 closes the gap. The nick is subsequently ligated by DNA ligase I (LIGI) (Figure 8).

Double-strand breaks are repaired either by non-homologous end-joining (NHEJ) or homologous recombination (HR) mechanisms (Ciccia and Elledge, 2010). During NHEJ, after the break detection by KU70/80, DNA-dependent protein kinase (DNA-PKcs) plays a critical role in stabilizing DSB ends and preventing end resection through a series of phosphorylation reactions providing access to end-processing enzymes, such as ARTEMIS (Meek, Dang and Lees-Miller, 2008). After DNA-PKcs is loaded, scaffold protein XRCC4 is recruited, allowing the subsequent recruitment of the DNA Ligase 4 (LIG4) which promotes the religation of the broken ends (Mahaney, Meek and Lees-Miller, 2009).

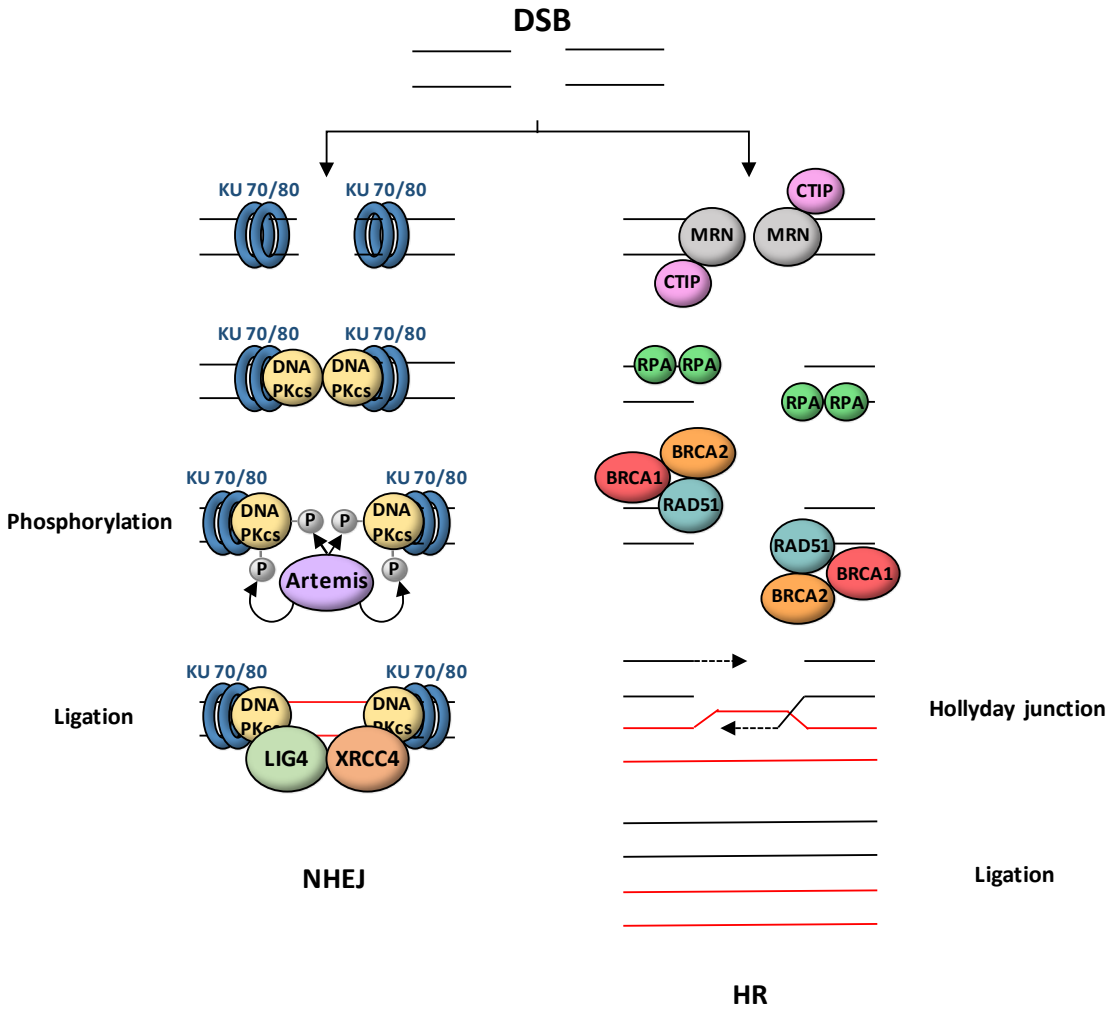

Figure 9: Double-strand break repair pathways. Once the cell recognize the double strand breaks, one of the two main repair mechanisms is selected depending on the cellular context. In NHEJ (left) the action of KU 70/80, DNA-PKcs and Artemis kinase led to the recruitment of XRCC4 and LIG4 in order to repair the break. In HR (right) the recruitment of RAD51 and BRCA1/2 by RPA proteins led to the formation of the Holliday junction and the repair of the break.

HR requires 5´-3´resection of DSBs, a process that depends largely on CTIP (also known as RBBP8) which cooperates with several MRN complex proteins (Ciccia and Elledge, 2010). The resection process generates ssDNA, which is covered by RPA. This initiates BRCA1- and BRCA2- dependent recruitment of RAD51 to the lesion (Ciccia and Elledge, 2010). Next, the replication machinery fills the lacking sequence using ssDNA ends as primers. This structure, known as Holliday junction, will later give rise to two separate sister chromatids by a mechanism that is still under debate.

Interstrand crosslinks present a formidable challenge to the cellular repair machinery. It's repair is thought to involve the coordination of components of several repair systems, including homologous recombination (HR) and translesion synthesis (TLS) (Walden and Deans, 2014).

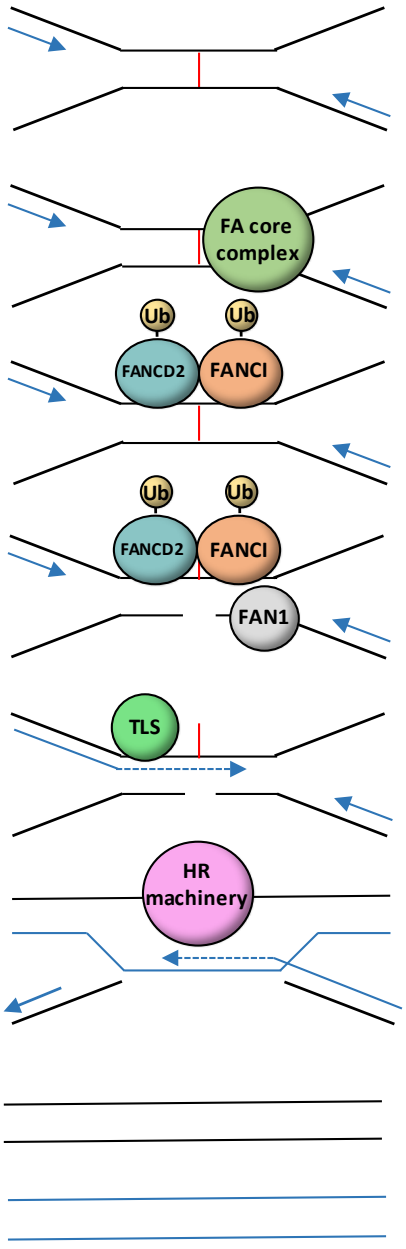

Figure 10: Fanconi Anemia repair pathway Schematic sequential representation of the steps of the Fanconi Anemia pathways are represented.

ICLs are extremely toxic for the cell because they produce stalled replication forks and avoid the progression of the cell cycle (Osawa, Davies and Hartley, 2011). To cope with this life-threatening crisis, cells must invoke the Fanconi anemia (FA) DNA repair pathway. ICLs recruit and activate the FA core complex (FANCA, B, C, E, F, G, L) which is required for monoubiquitination of FANCD2 and FANCI, leading to their retention on chromatin (Figure 10).

Retention of FANCD2–FANCI on chromatin is followed by the recruitment of components of HR and translesion synthesis (TLS), which bypass DNA lesions at the replication fork (Figure 10) (Ciccia and Elledge, 2010). FAN1 nuclease is thought to provoke the incision of ICLs by serial nuclease activity and the resulting gap is subsequently bypassed by TLS polymerases, followed by removal of the unhooked ICL. The resulting DSB is repaired by HR as described above.

1.2.3. DNA damage and cell cycle control

In order to have enough time for the cells to detect the damage in the DNA molecule, repair it and avoid its spreading to next generations, the described DDR pathways are able to pause cell cycle progression in proliferating cells through the activation of DNA damage checkpoints (Ciccia and Elledge, 2010). The DDR curbs the activity of Cyclin-CDK complexes to elicit a cell cycle arrest in G1 or G2 phases, or to slow down replication in S-phase (Mikhailov, Cole and Rieder, 2002). Checkpoint kinases CHK1 and CHK2, direct substrates of ATR and ATM respectively, play important roles in this process through multiple mechanisms (Shaltiel *et al.*, 2015). On the one hand, CHK1 phosphorylates and activates proteins such as WEE1 kinase, which phosphorylates amino acids tyrosine 15 and threonine 14 of CDK1, keeping its kinase activity low and preventing entry into mitosis and contributing to G2/M checkpoint (Harvey *et al.*, 2005). On the other hand, CHK2 phosphorylates the phosphatase CDC25 in serine 123 leading to its inhibition, which also leads to a blocking into mitosis entry and activation of G2/M checkpoint (Falck *et al.*, 2001).

Additionally, ATM, ATR, CHK1 and CHK2 DNA damage response proteins are able to phosphorylate p53 during all phases of the cell cycle, contributing to its stabilization (Canman *et al.*, 1998) and enhancement of its transcriptional activity, both as an inductor and repressor of gene expression (Bieging, Mello and Attardi, 2014). For example, one of the mayor targets of p53 transcriptional activation is $p21^{CIP1}$, a potent cyclin-dependent kinase inhibitor (CKI) that binds and inhibits CDK complexes thereby promoting activation of a checkpoint (Shaltiel *et al.*, 2015).

Besides the more classical G1 or G2/M checkpoints, other checkpoints have been described that are also crucial in order to ensure a proper progression of the cell cycle, including the DNA replication checkpoint (Toledo, Neelsen and Lukas, 2017). Cells activate this checkpoint in response to damage during S phase to protect genomic integrity and ensure replication fidelity. The checkpoint prevents genomic instability mainly by regulating origin firing, fork progression, and transcription of G1/S genes in response to DNA damage. Several studies hint that regulation of forks progression is perhaps the most critical function of the DNA replication checkpoint (Iyer and Rhind, 2017), and despite many years of intensive research into the replication checkpoint, the mechanisms underlying the consequences of its failure remain largely elusive and controversial.

1.2.4. Role of E2F factors in the DNA Damage Response.

Genome-wide studies performed in the absence of an obvious induction of DNA lesions with gain-of-function and loss-of-function cellular models of E2Fs have led to the identification of a large number of genes involved in DNA Damage Response regulated by E2Fs. Included in this group are checkpoint regulators (CHK1, BUB3, TTK or DHFR) or DNA repair factors (BRCA1, UHFR1, BARD1, RAD51 or FEN1) (Wang *et al.*, 2000; Ren *et al.*, 2002; Iglesias *et al.*, 2004; Westendorp *et al.*, 2012; Laresgoiti *et al.*, 2013), suggesting an important role for E2Fs in genome stability. However, the E2F-dependent regulation of these target genes upon exogenous DNA damage, and the role of individual E2Fs in DNA damage responses are still poorly understood.

In response to DNA damage of diverse origins, such as UV radiation or chemotherapeutic agents, the levels of some E2F proteins are increased significantly (Engelmann *et al.*, 2009; Biswas, Mitchell and Johnson, 2014). The induction of E2F1 was described to be primarily due to an increase in the stability of the protein through post-translational modifications such as phosphorylations by ATM/ATR in serine 31 after neocarzinostatin treatment (Lin, Lin and Nevins, 2001) or acetylations on lysines adjacent to DBD domain (Martínez-Balbás *et al.*, 2000). Phosphorylation of E2F3 by ATR/CHK1 axis on serine 124 in response to treatment with the alkylating compound MNNG also leads to protein stabilization (Gong *et al.*, 2016). At the transcriptional level, E2F1 expression can also be induced together with E2F2 in neurons after oxidative damage (Castillo *et al.*, 2015). The atypical E2F protein, E2F7, was also shown to be induced in response to genotoxic damage (Zalmas *et al.*, 2008). Again, E2F7 accumulation was the result of protein stabilization due to a specific phosphorylation by CHK1 in cells treated with etoposide or doxorubicin (Yuan *et al.*, 2018) or by increase in p53-dependent mRNA expression in cells treated with doxorubicin (Carvajal *et al.*, 2012).

Little is known about the role of E2Fs in DNA damage responses. It has been reported that E2F1 protein accumulates at sites of DSBs and UV radiation-induced lesions. In this lesion sites, E2F1 functions to enhance DNA repair by the recruitment of repair factors such as NBS1, leading to the correct formation of DSB repair foci (Liu *et al.*, 2003; Chen *et al.*, 2011; Biswas, Mitchell and Johnson, 2014). Moreover, E2F1 together with E2F2, can be located in DNA damage sites after oxidation and UV-treatment interacting with γH2AX promoting the repairing RAD51 foci formation (Castillo *et al.*, 2015). E2F7 has been described to locate to damaged sites of DNA after treatment with camptothecin and to recruit CTBP and HDAC proteins thus, altering the local chromatin environment of the DNA lesion (Zalmas *et al.*, 2013).

E2F-mediated transcriptional regulation of DDR genes has been described in several examples of genotoxic damage. E2F1 was found to be involved in DNA SSB responses through cell-cycle-dependent upregulation of the repair protein XRCC1 expression leading to the increase of the DNA repair (Jin *et al.*, 2011). E2F1 has also been described as regulator of UV-induced DNA damage response by upregulation of target genes including $p19^{INK4}$ (Carcagno *et al.*, 2012) which improves DNA repair. Regarding the other classical members of the family, E2F3 activates RRM2 expression to maintain genome stability in response to environmental chemical carcinogens (Gong *et al.*, 2016). Atypical E2F7 is thought to act in concert with p53 in the arrest of the cell cycle upon treatment with doxorubicin by repressing the expression of cell cycle genes such as DHFR or RRM2 (Carvajal *et al.*, 2012). However, with the exception of a few reports, the role of E2Fs in DNA damage responses and repair has not been fully addressed.

2.- HYPOTHESIS AND AIMS

E2F transcription factors control the cell cycle and DNA damage responses through regulation of target gene expression. Work from numerous laboratories has led to the identification of a large set of genes regulated by each individual E2F (Dyson, 1998; Nevins, 1998; DeGregori and Johnson, 2006; Xu *et al.*, 2007; Infante *et al.*, 2008; Bueno *et al.*, 2010; Westendorp *et al.*, 2012; Laresgoiti *et al.*, 2013). However, most of these studies have been focused on the classical E2Fs (E2F1-5), whereas the contribution of the newest additions to the family, E2F7 and E2F8, to these processes has not been clearly defined.

E2F7, an atypical member of the family, whose expression is cell-cycle regulated, displays a transcriptional repressor activity capable of suppressing E2F target promoters independently of RB (de Bruin *et al.*, 2003; Di Stefano, Jensen and Helin, 2003; Mitxelena, 2014). Gene expression profiling analyses carried out recently in our group have identified a set of microRNAs and protein-coding genes whose expression is regulated by E2F7 (Mitxelena, 2014).

We hypothesize that E2F7 plays a unique role in the regulation of cell cycle progression and DNA damage response through the transcriptional regulation of its target genes (microRNA and protein-coding genes).

In order to test this hypothesis we established the following aims:

1. To define the regulation and functional role of E2F7-responsive microRNAs.
2. To define the regulation and functional role of E2F7-responsive protein-coding genes, with a particular focus on the DNA damage response and repair processes.

3.- MATERIALS AND METHODS

3.1 Cellular biology methods

3.1.1. Cell lines and culture conditions

The U2OS human osteosarcoma cell line and U2OS-TetOn cell line were purchased from American Type Culture Collection. U2OS-DR-GFP cells were kindly provided by Dr. Jordi Surrallés (Universitat Autònoma de Barcelona). The HeLa human epithelial cervix carcinoma cell line was kindly provided by Dr Jose Antonio Rodriguez (UPV/EHU). The CAPAN-1 human metastatic pancreatic cell line was kindly provided by Dr. David Olmos (CNIO).

U2OS and HeLa cell lines were maintained in *DMEM* medium supplemented with 10% (vol/vol) fetal bovine serum (FBS) at 37°C in a humidified atmosphere containing 5% CO_2. CAPAN-1 cell line was maintained in *DMEM* medium supplemented with 20% (vol/vol) fetal bovine serum (FBS) at 37°C in a humidified atmosphere containing 5% CO_2

Table 2: Cell seeding conditions in each experimental setting.

Procedure	Cell line	Type of plate	Cell density
Western Blot	U2OS	6-well	$0.25x10^6$/well
	U2OS-DR-GFP	6-well	$0.25x10^6$/well
RT-Q-PCR	U2OS	6-well	$0.2x10^6$/well
	HeLa	6-well	$0.2x10^6$/well
pH3+ Mitotic index	U2OS	6-well	$0.2x10^6$/well
	U2OS-E2F7 KO	6-well	$0.2x10^6$/well
	HeLa	6-well	$0.2x10^6$/well
Metaphase spreads	U2OS	100 mm dish	$1.5x10^6$/dish
ChIP	U2OS	150 mm dish	$5x10^6$/dish
Co-Immunoprecipitation	U2OS-TetOn	150 mm dish	$5x10^6$/dish
CFSE	U2OS	6-well	$0.25x10^6$/well
BrDU	U2OS	6-well	$0.25x10^6$/well
Colony formation assay	U2OS-E2F7 KO	6-well	10.000/well
	CAPAN-1	6-well	10.000/well
γ-H2AX staining	U2OS-E2F7 KO	6-well	$0.25x10^6$/well
Homologous Recombination efficiency	U2OS-DR-GFP	6-well	$0.25x10^6$/well
Cell survival assay	U2OS-TRE-E2F1	96-well	10.000/well
High-throughput screening	U2OS-TRE-E2F1	384 well	1.500/well

For each experimental condition, cells were seeded at a specific concentration, as detailed in Table 2. Briefly, cells were detached by incubation with trypsin-EDTA (Sigma) solution for about 3 minutes at 37°C, and resuspended in culture medium containing FBS to inhibit further trypsin activity. The cell density of the suspension was evaluated using a Neubauer cell-counting chamber. In order to count only viable cells, an aliquot of the cell suspension was diluted in the vital dye trypan blue. This dye allows discriminating between live and dead cells, since the latter have their plasma membrane damaged, and thus are stained blue when treated with trypan blue.

3.1.2. Cell lines generated in this thesis

3.1.2.1. U2OS-E2F7-KO cells

E2F7 knockout cells were generated using the CRISPR/Cas9 system with the collaboration of Dr. Iraia García-Santisteban in the laboratory. A CRISPR guide RNA (gRNA) targeting the second coding exon of E2F7 was designed using Benchling, and cloned into the BbsI site of pX330 (42230, Addgene). U2OS cells were co-transfected with this plasmid, together with pDonorPuro plasmid containing a gRNA to the zebrafish TIA gene (5 -GGTATGTCGGGAACCTCTCC3) and a P2A-puromycin resistance cassette flanked by two TIA target sites, kindly provided by Dr. Brummelkamp (Netherlands Cancer Institute) (Figure 11).

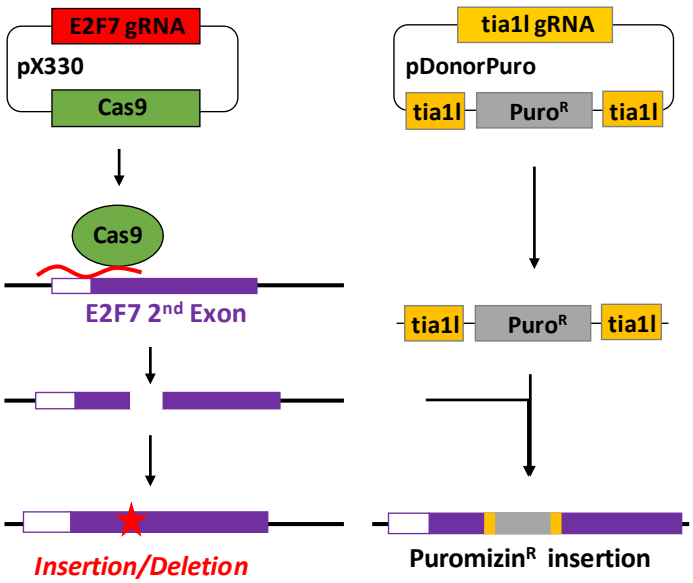

Figure 11: Schematic representation of the generation of U2OS-E2F7-KO using CRISPR-Cas9 system.

Co-transfection resulted in excision of the cassette and subsequent sporadic incorporation at the site of the targeted genomic locus as previously described (Matas-Rico *et al.*, 2016). Successful integration of the cassette into the targeted gene disrupts the allele and renders cells resistant to puromycin (Figure 11). After puromycin selection, resistant clones were expanded and screened for cassette integration and insertions or deletions into the target gene by sequencing the region after PCR amplification (Figure 11). A cell clone carrying an integrated puromycin cassette in one allele of E2F7 gene, and a base-pair insertion in the other allele of E2F7 gene was selected for experiments involving E2F7-knockout studies (Figure 12).

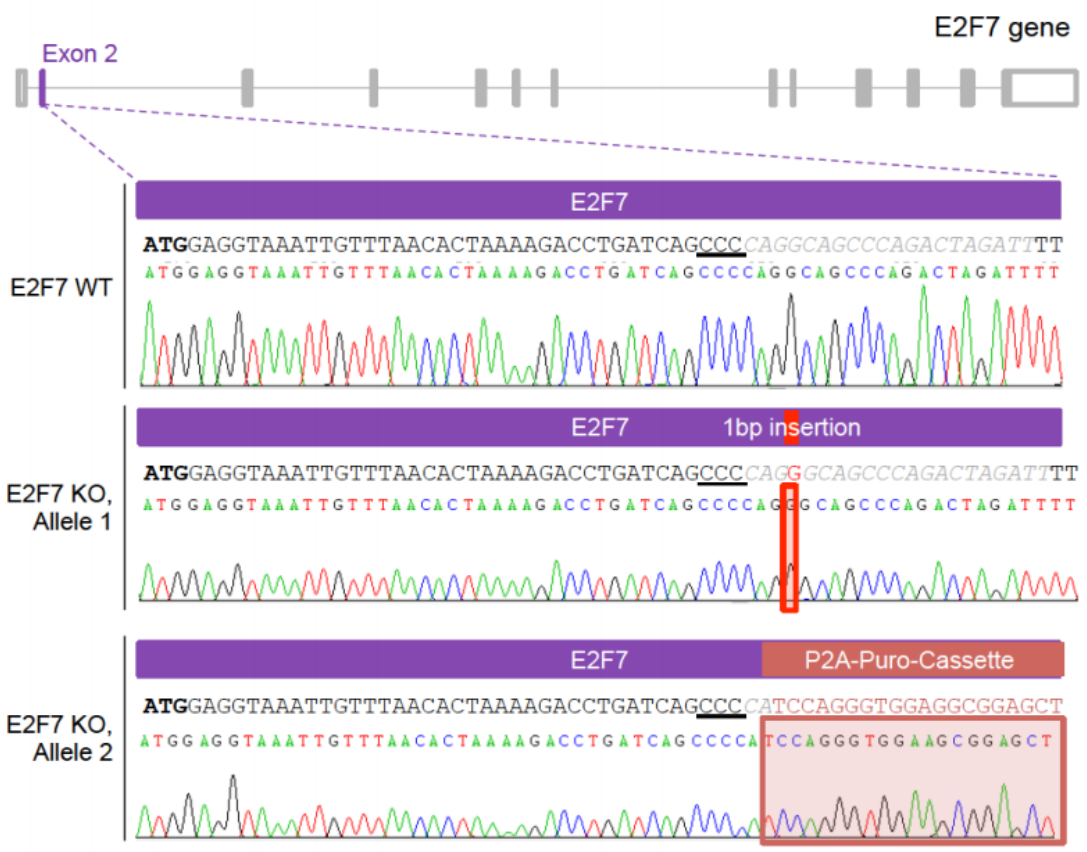

Figure 12: Validation of U2OS E2F7 CRISPR knockout cell clone. Schematic overview of E2F7 gene, including exons (grey boxes) and introns (grey line). CRISPR-targeted exon 2 is highlighted in purple, and its sequence is indicated below. Guide RNA (gRNA) sequence is indicated in italics, and PAM sequence is underlined. Sequences corresponding to the wild type (WT) and knockout (KO) E2F7 cell lines are represented. Regarding to the KO cell line, each allele carries a different mutation after the PAM sequence: allele 1 has a single base pair insertion, and allele 2 has the P2A-Puromycin-cassette insertion.

3.1.2.2. U2OS-TRE-E2F1

U2OS-TRE-E2F1 cells were generated to achieve a regulated overexpression of E2F1 with the addition of doxycycline (Das, Tenenbaum and Berkhout, 2016). Plasmids pTetOn Advanced and pTRE2hyg2-HA were purchased from Clontech (ref.: 631069 and 631051).

In order to generate U2OS-TRE-E2F1 cells, E2F1 gene was inserted in pTRE2hyg2-HA plasmid. Subsequently, both pTetOn and pTRE2hyg2-E2F1-HA plasmids were co-transfected into cells as described in section 3.1.3. Neomycin and hygromycin B resistant cells were selected for experiments.

3.1.3. Transfection

Transfection of protein-coding and microRNA-coding plasmids (Voorhoeve *et al.*, 2006) was performed using *XtremeGENE HD* (Roche) transfection reagent following manufacturer´s recommendations. For 6-well culture plates, the following transfection mixture was prepared: 1 µg of DNA, 200 µl *Optimem* culture medium (GIBCO) and 3 µl of *XtremeGene HD*. The mixture was incubated for 15 minutes at room temperature and added dropwise to cell cultures.

Transfection of small interfering RNAs (siRNAs) and of anti-microRNA oligonucleotides (miRVanas) was performed using *Lipofectamine RNAiMAX* transfection reagent (Lifetechnologies) following manufacturer´s recommendations. Briefly, transfection reagent was mixed with *Optimem* (3 µl transfection reagent + 150 µl *Optimem* per 6-well plate) and incubated for 2 min at room temperature. The transfection reagent/*Optimem* mix was added dropwise into a tube containing 0.3 µl siRNA or miRVanas (50 µM) diluted in 150 µl of *Optimem*. The mixture was incubated for 20 minutes at room temperature and added to the cells whilst rocking the plate.

To knockdown the endogenous expression of E2F7, TP53, RAD51 and BRCA2, we used commercial siRNAs from Ambion (Life Technologies). As a control, an oligonucleotide with no sequence specificity for any human RNA (siNT) was used (Life Technologies) (Table 3). To knockdown the expression of miR-7, miR-92 and let-7f we used commercial miRVana from Ambion (Life Technologies) and pooled them (Table 3). As a control, a scramble miRVana with no specificity (Life Technologies) was used (Table 3).

To achieve E2F7 overexpression, U2OS-TetOn cells were transfected with pTRE2hyg2-HA containing E2F7 coding gene carrying a FLAG tag inserted in the amino terminal end (E2F7-FLAG) the protein generated previously in the lab (Mitxelena, 2014).

Table 3: List of siRNAs and miRVanas used in this study

siRNA/miRVana	Reference
siE2F7	s49665
sip53	106141
siRAD51	s11734
siBRCA2	s2085
siNT	4390843
Scramble miRVana	4464076
miR-7 miRVana	4464084
miR-92 miRVana	4464084
let-7f miRVana	4464084

3.1.4. Cell synchronization

To synchronize cell cultures in early S phase, exponentially growing cells were incubated with 4mM hydroxyurea (HU) for 24 hours (Westendorp *et al.*, 2012). HU is known to inhibit the activity of ribonucleotide reductase (Elford, 1968), the enzyme that catalyzes the conversion of ribonucleotides to deoxyribonucleotides. As a result of such inhibition, treatment with HU generates damage in the DNA and cells are arrested at the beginning of S phase. To induce entry into cell cycle after HU-induced block, cells were washed twice with PBS and incubated in complete medium in the absence of HU.

To collect cells in mitosis and to prevent their progression to the next cell division cycle, the antimitotic drug nocodazole (50ng/ml) was added to the cultures for another 10 hours.

3.1.5. DNA replication assays (BrDU)

The immunofluorescent staining of incorporated bromodeoxyuridine (BrdU) provides a high-resolution technique to determine the number of cells that have newly synthesized DNA. In this method, BrdU (an analog of the DNA precursor thymidine) is incorporated into newly synthesized DNA by cells entering and progressing through the S phase of the cell cycle.

For the assessment of cell replication, we used FITC Mouse Anti-BrdU Set assay (ref.: 556028) supplied by BD Bioscience. Cells were incubated with 10 µM BrDU for 30 minutes at 37ºC and 5% CO_2 to follow its incorporation into the cells. Then, cells were fixed at various time points in

70% ethanol in PBS. Finally, cells were disrupted with an HCl solution (2M HCL/Triton X-100 0.5%) and $1x10^5$ cells were incubated with FITC-anti-BrDU antibody. Samples were analyzed on a FACSCalibur flow cytometer (Becton Dickinson). Data generated by the flow cytometer were processed with the *Summit 4.3* (Beckman Coulter) software.

3.1.6. Proliferation assays

3.1.6.1. Carboxyfluorescein succinimidyl ester (CFSE) assay

The assay based on carboxyfluorescein succinimidyl ester (CFSE) intracellular labelling is an effective technique to monitor cell division. CFSE covalently labels long-lived intracellular molecules with the fluorescent dye, carboxyfluorescein. Thus, when a CFSE-labeled cell divides, its progeny are endowed with half the number of carboxyfluorescein-tagged molecules and thus each cell generation can be assessed by measuring the corresponding decrease in cell fluorescence via flow cytometry. Samples collected at the beginning of the assay represent the parental generation (Figure 13), in which intracellular CFSE is undiluted. Cells in the following generation (Division 1) carry half the amount of CFSE.

We used the CellTrace™ CFSE Cell Proliferation Kit (ref.: C34554) supplied by Invitrogen. Cells were stained with 0.5 µM CFSE for 20 minutes, washed twice with PBS and seeded for the experiment. At various time-points, a sample of the cells were fixed in 70% ethanol in PBS 48h after staining. Samples were analyzed on a FACSCalibur flow cytometer (Becton Dickinson). Data generated by the flow cytometer were processed with the *Summit 4.3* (Beckman Coulter) software.

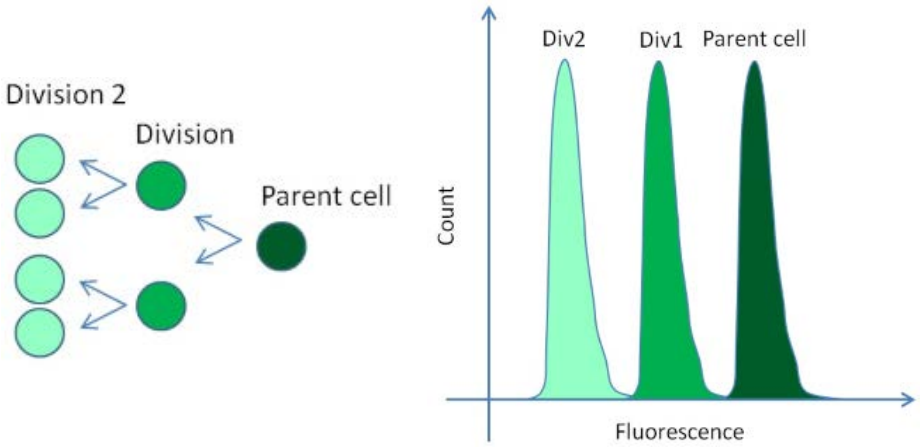

Figure 13: Example of CFSE lost due to first two cell divisions after staining. Each cell generation could be identified due to the lost fluorescent signal after CFSE staining

3.1.6.2. Crystal violet staining

To measure cell proliferation by the crystal violet staining method, cells were seeded in 6-well plates under indicated experimental conditions and then fixed with 3.7% of paraformaldehyde. Then, cells were stained with 0.1% crystal violet (in 70% ethanol/PBS) for 30 minutes and washed twice with PBS. Finally, the stained cells were dissolved in 20% acetic acid in water and the signal was measured at 590 nm.

3.1.6.3. Colony formation assay

The effect of genotoxic compounds on cell survival was assessed by the colony formation assay. First, cells were seeded in low density conditions (10.000 cells/well on a 6-well plate). Subsequently, cells were transfected and treated as indicated in each case. After 14 days in culture, surviving cell colonies were fixed with 3.7% of paraformaldehyde, stained with 0.1% crystal violet (in 70% ethanol/PBS) for 30 minutes and washed twice with PBS. Finally, the number of colonies was counted manually and we took pictures of each well were taken.

3.1.7. Mitotic index analysis and DDR quantification assay

In order to analyze the percentage of cells in mitosis cells were stained with an antibody against the phosphorylated form of Histone H3 on serine 10 (pH3), a specific marker for chromosome condensation occurring in mitosis (Crosio *et al.*, 2002). In order to analyze the percentage of cells undergoing DNA damage repair, cells were stained with an antibody against γ-H2AX protein as a key protein localized on damage sites (Kuo and Yang, 2008).

Cell cultures were fixed in 70% ethanol in PBS, centrifuged for 5 min at 1400 rpm and permeabilized with 0.05% Tween-20 in PBS. Subsequently, cells were incubated for 2 hours at room temperature with a specific antibody against pH3 (06-570, Millipore) to detect mitotic cells or with antibody γ-H2AX to detect DDR. Both antibodies were diluted 1:500 in 0.05% Tween-20/3% BSA solution. Samples were washed twice with permeabilization solution (0.05% Tween-20), followed by incubation with the secondary antibody against rabbit immunoglobulin labeled with a green fluorophore (*Alexa Fluor 488*) during 1 hour at room temperature. After incubation with the secondary antibody three washes were performed with permeabilization solution to finally stain the DNA with Propidium Iodide (PI); cells were resuspended in 300 µl staining solution composed of 140µM PI, 38mM NaCitrate and 0.01% Triton X-100 (vol/vol). Finally samples were incubated for 30 min in darkness at 37°C.

Samples were analyzed on a FACSCalibur flow cytometer (Becton Dickinson). Data generated by the flow cytometer were processed with the *Summit 4.3* (Beckman Coulter) software.

3.1.8. Homologous recombination efficiency assay

Homologous recombination (HR)-dependent DNA double stranded break (DSB) repair was assessed using the DR-GFP/SceI assay described by M. Jasin´s group (Pierce *et al.*, 1999) (Figure 14). For these experiments we used a U2OS cell line that carries a recombination substrate, DR–GFP, inserted in the genome (U2OS DR-GFP cell line). DR–GFP is composed of two inactive *GFP* genes carrying different mutations, and oriented as direct repeats. One of the *GFP* genes, *Sce-GFP*, is mutated to contain the recognition site for the rare-cutting *Sce* I endonuclease. As a result, it will undergo a DSB when the enzyme is expressed ectopically in the cells. The *Sce* I site was incorporated by substituting 11 bp of wild-type GFP sequence with those of the *Sce* I site (Pierce *et al.*, 1999). These substituted base pairs also supply two in-frame stop codons, which terminate translation and inactivate the protein. Downstream of the *Sce-GFP* gene lies an 812-bp inactive *GFP* fragment, which contains the wild-type sequence of the region mutated in the *Sce-GFP* copy, and thus, can be used as a substrate for homologous recombination-mediated repair of the *Sce-GFP* copy. Expression of functionally active GFP protein only occurs after an HR-mediated repair event of Sce I-produced breaks, which can be assessed by flow cytometry as cellular green fluorescence.

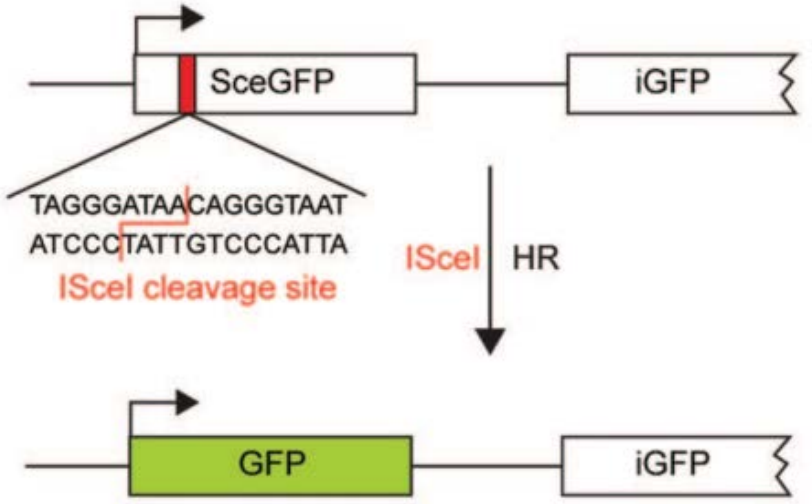

Figure 14: M. Jasin group method to analyze HR-mediated repair efficiency. DR-GFP substrate contains two defective alleles of GFP, one of which harbors an SceI restriction endonuclease site. This DNA substrate is integrated into U2OS DR-GFP cells at a single site in the genome. Active repair of the double-stranded DNA break at the SceI site by homologous recombination produces a functionally active GFP allele.

3.1.9. Analysis of chromosomal aberrations

Chromosomal aberrations were visualized in chromosome spreads following published protocols, with minor modifications (Remeseiro *et al.*, 2012). Cells were arrested in metaphase after treating cell cultures with *Karyomax Colcemid* (Lifetechnologies) for 12 hours at a final concentration of 100 ng/ml. Metaphase-arrested cells were subsequently harvested and resuspended in 9 ml of 75mM KCl at 37°C for 30 mins. 3-4 drops of freshly prepared Carnoy fix solution (3:1 Methanol/Acetic) were added to the suspension. Cells were then centrifuged at 900 rpm and resuspended in 9 ml of fixing solution. After repeating this process three times, an aliquot of the cellular suspension was dropped onto microscopy slides to obtain chromosome spreads, which were stained and mounted with *ProLong Gold Antifade with DAPI* (Lifetechnologies) reagent. Image acquisition was performed on a Leica DMI 6000B fluorescence microscope.

3.1.10. High-throughput apoptosis screening assay

A screening assay using 4216 pharmaceutical compounds approved by the FDA (supplied by Chemical Biology Consortium Sweden) was used to identify mediators of E2F1-driven apoptosis. For these experiments, we used U20S-TRE-E2F1 as shown in Figure 15A. Twenty-four hours after cell seeding in 384-well plates, doxycycline was added to each well to induce E2F1 expression. One day later compounds were added to each corresponding well. Cells were fixed and stained with Propidium Iodide (PI) and Hoechst 24 hours later.

Differences in cell death were detected by high-throughput microscopy with an IN CellAnalyzer 2200 microscope (General Electric). Using Propidium Iodide (PI) and Hoechst double staining; PI positive cells were identified as cells with their membrane compromised, which is one of the first hallmarks of cells in apoptosis, and Hoechst staining provided us the total cell amount of each cell. The number of PI positive cells relative to Hoechst positive cells provided the accurate percentage of cell death.

Individual images of each well were taken for cell analysis. Image analysis was done using Cell Profiler program. To analyze the 4216 compounds in triplicates, 45 384-well plates were used (Figure 15B). As positive controls, we used cells treated with doxycycline (overexpressing E2F1), but without any compound treatment. As negative controls, we used cells without doxycycline or treatments addition. These cells were distributed in several wells in each plate as shown in Figure 15B. After image acquisition, the percentage of cell death (PI positive cells/Hoechst positive cells) was calculated for each well, being the result the average of three triplicates.

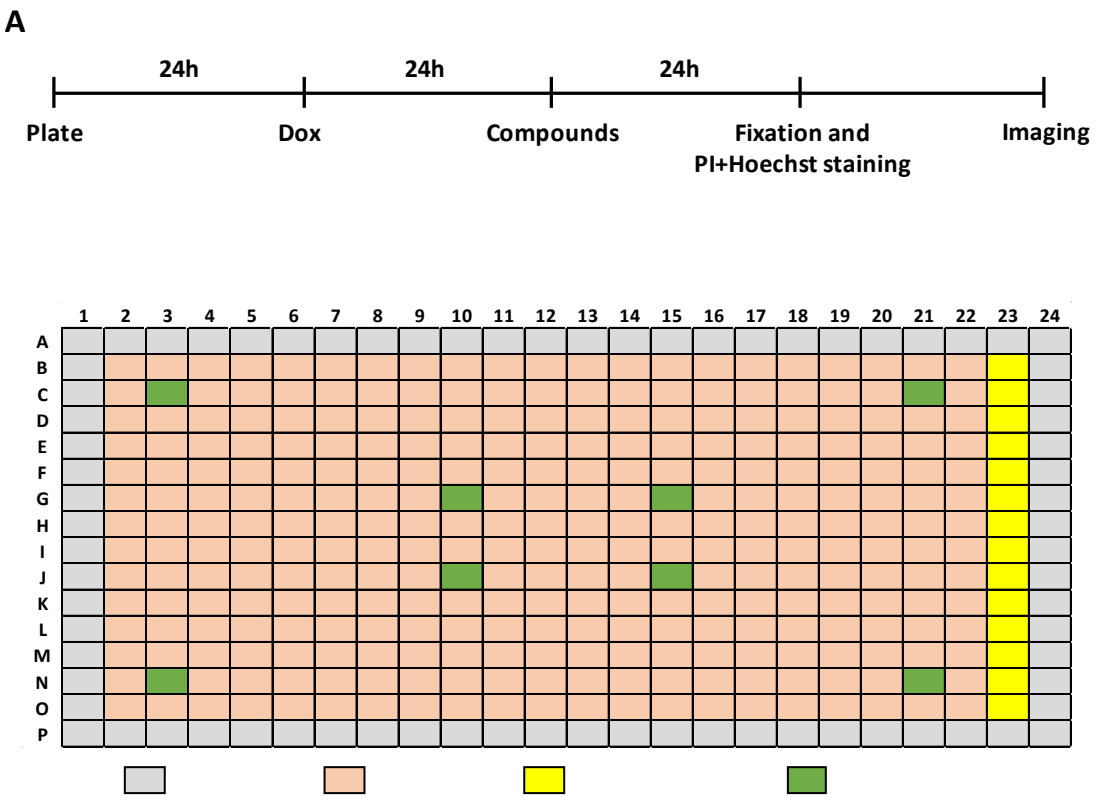

Figure 15: Screening approach. (A) Workflow diagram of the experimental protocol followed (B) Schematic representation of each plate of the screening

3.2. Molecular biology techniques

3.2.1. RNA expression analyses

3.2.1.1.RNA extraction

RNA is a fragile and unstable biological material. To protect RNA from undergoing degradation, all manipulations of RNA samples were performed in RNase-free conditions, as previously indicated (Infante et al., 2008).

Total RNA extraction was performed using *Trizol* reagent (Lifetechnologies). Cells were lysed by adding 1 ml of *Trizol* per well of a 6-well plate well and were subsequently transferred to an eppendorf tube. Next, 400 µl chloroform were added, and tubes were vigorously shaken and incubated for 2-3 minutes at room temperature. Samples were centrifuged at 10000 rpm for 10 minutes at 4°C, and the aqueous phase containing RNA was transferred to a clean microcentrifuge. RNA was purified using the *miRNeasy kit* (Qiagen) following the manufacturer's recommendations. This procedure allows the purification of both mRNA and small RNAs, including microRNAs.

The concentration of purified RNA was determined with a NanoDrop spectrophotometer (Thermo Fisher Scientific), by measuring absorbance at 260 nm. RNA samples were stored at –80°C until use.

3.2.1.2. RT-Q-PCR of mRNA

RNA was reverse-transcribed into cDNA using the *High-Capacity cDNA Reverse Transcription kit* (Lifetechnologies). One µg of previously extracted and purified RNA was reverse-transcribed following the manufacturer's instructions.

To determine the abundance of specific mRNAs, quantitative PCRs (qPCR) were conducted using *SYBR Green* chemistry. This chemistry uses *SYBR Green* dye, which binds to double stranded nucleic acids emitting fluorescence at 580 nm. During the PCR reaction, *SYBR Green* dye binds to each new copy of double-stranded DNA, resulting in a proportional increase in fluorescence as PCR products accumulate during PCR cycles.

Due to the nonspecific nature of *SYBR Green* dye´s detection, primer optimization needs to be performed with caution. The amplicon should span one or more introns to avoid amplification of the target gene in genomic DNA. In our case, primers were designed using the PrimerQuest tool from the *Integrated DNA Technologies* website (https://eu.idtdna.com/site). To identify the optimal primer concentrations that provide optimal assay performance, several optimization reactions were performed by independently varying forward and reverse primer concentrations and using as a template cDNA obtained from control samples.

cDNA samples were mixed with specific primers for each gene in the optimized concentrations (Table 4) together with the Power SYBR Green PCR Master Mix product containing SYBR Green dye, AmpliTaq Gold DNA polymerase, dNTPs with a mixture of dUTP/dTTP and buffer components. Quantitative PCR reactions were performed in a QuantStudio3 thermocycler (Applied Biosystems) as described previously (Infante et al., 2008). The following PCR program was used: a first cycle at 95 ° C for 10 minutes, required for activation of the polymerase and, a second step of 40 repetitions consisting of 15 s at 95°C for DNA denaturation to take place and 1 min at 60°C to allow annealing between primers and target sequence and subsequent polymerization. After completing these cycles samples were subjected to a dissociation protocol to look for the presence of multiple products and nonspecific amplification, to this end the temperature was gradually increased from 60 to 90°C.

The qPCR method allows reactions to be quantified by the point in time during cycling when amplification of a PCR product achieves a fixed level of fluorescence, rather than the amount of PCR product accumulated after a fixed number of cycles, as in semi-quantitative PCR reactions. This fixed fluorescence level, known as the threshold, is set within the exponential phase of the amplification curve, that is, when the amount of amplified product is proportional to the amount of initial cDNA. The amount of cDNA of a particular sequence is estimated from the number of necessary cycles (C_T) for fluorescence to reach the established threshold (T).

Table 4: List of RT-qPCR primers used in this study. Nucleotide sequence and concentrations of each primer are specified.

	Forward (F)		Reverse (R)	
Target Gene	**Sequence (5´-3´)**	**[nM]**	**Sequence (5´-3´)**	**[nM]**
$p21^{CIP1}$	AGCAGAGGAAGACCATGTGGAC	900	TTTCGACCCTGAGAGTCTCCAG	50
p57	CAAGGAGTCTCAGCGTGGTATG	300	TCCTCCTGGAACAGGTCCG	300
PTEN	CCCAGTCAGAGGCGCTATGT	300	CTGAGGATTGCAAGTTCCGC	300
p130	CGCTGGAGGGAAATGACCTT	300	TCCTTCAGCGGTCCCTTTG	300
$p18^{INK4C}$	CTGCGCTGCAGGTTATGAAA	900	TGCTCTGGCAGCATCATGA	300
RAD51	TGCTTATTGTAGACAGTGCCACC	50	CACCAAACTCATCAGCGAGTC	50
BARD1	GCTCGCGTTGTACTAACATTC	50	TTCAAGTCTTGTATCCAGGCC	50
CTIP	ACAGCTGAGGGAACAGCAGAAA	300	TCTGCTGGAGTTGTTCAGAAAGC	300
FANCE	TCTGGATGATGCTAAAGGTCTGG	900	TGAAGAAGCTGTAGCTCAACTG	900
FANCI	CACCACACTTACAGCCCTTG	300	ATTCCTCCGGAGCTCTGAC	300
BRIP1	GCGTATCACCACTGCTACTTT	50	ACTTCTCTTGCCTCCTCTTTAC	300
XRCC1	ACAGCACGCACCTCATC	300	TCCAGCACCCACTCCTTA	300
LIG3	CGCCTCATTTGTCACCAGTA	300	TGCTTGAAGACAGACTTCTCTTAG	300
EIF2C2	GTCCCTTTTGAGACGATCCAG	50	AGCCAAACCACACTTCTCG	50

Relative quantification of gene expression was performed using the comparative C_T ($\Delta\Delta C_T$) method. It has been established that target amplification and endogenous control amplification efficiencies must be approximately equal for the $\Delta\Delta C_T$ to be valid. This requirement is fulfilled by the *SYBR Green* assays used in this work (according to the manufacturer´s specifications), which allowed us to apply the $\Delta\Delta C_T$ method. Relative expression levels were represented as $2^{-\Delta\Delta CT}$. Relative target gene quantity was determined from a standard curve prepared using serial dilutions of a control cDNA sample. In addition, the quantity of an endogenous control (EIF2C2) (Ben Shachar *et al.*, 2010) was determined to normalize the amount of cDNA present in each sample. To determine the fold difference in mRNA expression between control and test samples, $\Delta\Delta C_T$ was calculated (ΔC_T test sample-ΔC_T control sample). Table 4 shows the nucleotide sequence of the primers used for qPCR, and the concentration used for each particular primer.

3.2.1.2. RT-Q-PCR of microRNA

microRNA RT-qPCR analyses were performed using specific *Taqman* assays from Applied Biosystems. *TaqMan microRNA Assays* are preformulated primer and probe sets designed to detect and quantify mature microRNAs, as they can discriminate mature microRNA sequences from their precursors, as well as from highly similar microRNAs. These assays use a stem-looped primer for reverse transcription and a sequence specific *TaqMan* assay to accurately detect mature microRNAs. Each TaqMan Assay includes one tube containing small RNA-specific RT primer and a second tube containing a mix of the following components: a small RNA-specific forward PCR primer, a specific reverse PCR primer and a small RNA-specific *TaqMan* MGB probe. *TaqMan microRNA Assays* used in this study are listed below (Table 5).

For reverse transcription, the *TaqMan MicroRNA Reverse Transcription Kit* (Lifetechnologies) was used. Total RNA (300 ng) was used to synthesize cDNA for each microRNA, using for this purpose the specific primer provided by the *TaqMan* assay kit. Reverse transcription reaction contained 1.5 µl of RT primer, 0.075 µl of dNTP-s, 0.75 µl of buffer, 0.095 µl of RNAse inhibitor and 0.5 µl of reverse transcriptase in a final volume of 5 µl. The reactions were incubated in a thermocycler for 30 minutes at 16°C, 30 minutes at 42°C, 5 minutes at 85°C and stored at 4 ° C.

Quantitative PCR amplification was performed using the *TaqMan Universal PCR Master Mix 2x,* and the specific primers and TaqMan probes for each microRNA. The reaction contained 2 µl of the RT reaction product, 5 µl of the *TaqMan Universal PCR master mix* and 0.5 µl of primer and probe mix provided by the manufacturer, in a final reaction volume of 10 µL. Samples were incubated at 95°C for 10 minutes, followed by 40 cycles of 95°C for 15 seconds and 60°C for 30 seconds in a QuantStudio3 thermocycler (Applied Biosystems).

To correct quantification errors due to variations in either the amount of starting material, sample collection, or RNA quality, microRNA quantities for each sample were normalized to two endogenous small RNAs: RNU6B and RNU19 (Bueno and Malumbres, 2011; Ofir, Hacohen and Ginsberg, 2011).

Table 5: TaqMan microRNA Assays used in this study

Taqman assay	Lifetechnologies reference
hsa-miR-7	1338
hsa-miR-92	2137
hsa-miR-25	2442
RNU6B	1093
RNU19	1003

Relative quantification of microRNA expression was performed using the comparative C_T ($\Delta\Delta C_T$) method. It has been established that target amplification and endogenous control amplification efficiencies must be approximately equal for the $\Delta\Delta C_T$ to be valid. This requirement is fulfilled by the Taqman assays used in this work (according to the manufacturer´s specifications), which allowed us to apply the $\Delta\Delta C_T$ method. To obtain microRNA comparative C_T (ΔC_T) values, the quantity of endogenous small RNAs (calculated by the geometric mean of RNU6B and RNU19 values) was subtracted from the target microRNA quantity in each sample (C_T Target microRNA-C_T Endogenous microRNA). To determine the fold difference in microRNA expression between control and test samples, $\Delta\Delta C_T$ was calculated (ΔC_T test sample-ΔC_T control sample). Relative expression levels were represented as $2^{-\Delta\Delta CT}$.

3.2.2. Protein expression analyses

3.2.2.1. Protein extraction

Cell plates were washed once with ice-cold PBS, lysed by scrapping in protein lysis buffer (supplemented with Na_3VO_4, PMSF and *Complete Protease Inhibitor Cocktail* from Roche), and incubated for 30 min in a rotating platform at 4°C. Samples were centrifuged at 13000 rpm for 10 min at 4°C, and the supernatant was transferred to a clean microcentrifuge tube.

Protein concentration was determined using the colorimetric kit *DC Protein Assay (Bio-Rad),* which is based on the Lowry method. Standards of bovine serum albumin (BSA) prepared at known concentrations were used to determine the concentration of the protein extracts.

Protein samples were diluted with 6X protein loading buffer and boiled for 5 min inmediately before electrophoresis.

3.2.2.1. Western Blotting

Proteins were separated according to their molecular weight by SDS-PAGE (Sodium Dodecyl Sulfate PolyAcrylamide Gel Electrophoresis). Protein samples (10-30 µg per lane) were migrated in a *MiniPROTEAN Tetra Cell Vertical Electrophoresis* system (Bio-Rad) at constant amperage (25 mA per gel) in 1x Running buffer. *BenchMark Pre-Stained Protein Ladder* (Lifetechnologies) was loaded as protein standard to determine the size of the proteins under analysis.

Following electrophoresis, proteins were transferred from the gel to a nitrocellulose membrane (Bio-Rad). Transfer was performed using the *Mini Trans-Blot Cell transfer system* (*Bio-Rad)* in 1x transfer buffer for 2 hours at 100 V. The membrane was then stained with *Ponceau S* (Sigma), in order to confirm the successful transfer of the proteins. Membranes were blocked with 5% (w/v) non-fat dry milk powder in TBS-T (TBS + 0.05 % Tween-20) for 1 hour at room temperature with gentle shaking.

Membranes were incubated with a specific primary antibody diluted in blocking solution overnight at 4°C with gentle shaking (Table 6), washed three times for 5 minutes with TBS-T and subsequently incubated with the corresponding horseradish peroxidase (HRP)-labeled secondary antibody in blocking solution for 1 hour at room temperature. Membranes were again washed as described above.

The detection of the antibodies bound to their target proteins was carried out using *Pierce ECL Western Blotting Substrate* (Thermo Scientific) in a *ChemiDoc Imaging System* (Bio-Rad). Quantifications were performed by densitometry analysis using the *Quantity One* software (Bio-Rad).

Table 6: List of antibodies used in this work. Antibody, provider, reference, host and working dilution for each method are indicated.

Antibody	Provider	Reference	Host	Method	Dilution
E2F1	Santa Cruz	sc-251	Mouse	ChIP	1:50
E2F2	Santa Cruz	sc-633	Rabbit	ChIP	1:50
E2F3	Santa Cruz	sc-878	Rabbit	ChIP	1:400
E2F7	Santa Cruz	sc-32574	Goat	Western blotting	1:400
		sc-66870	Rabbit	ChIP	1:50
p53	Santa Cruz	sc-126	Mouse	Western blotting	1:400
$p21^{CIP1}$	Santa Cruz	sc-6246	Mouse	Western blotting	1:400
RAD51	Santa Cruz	sc-8349	Rabbit	Western blotting	1:400
XRCC1	Abcam	ab1838	Mouse	Western blotting	1:1000
LIG3	BD	611876	Mouse	Western blotting	1:1000
FLAG	Sigma	F1804	Mouse	Immuno-precipitation	1:1000
γH2AX	Millipore	05-636	Mouse	Immuno-stainning	1:1000
pH3 (Ser 10)	Millipore	06570	Rabbit	Immuno-stainning	1:500
α-Tubulin	Sigma	T-9026	Mouse	Western blotting	1:3000
Anti-mouse-HRP	Santa Cruz	sc-3697	Goat	Western blotting	1:3000
Anti-rabbit-HRP	Santa Cruz	sc-2030	Goat	Western blotting	1:3000
Anti-goat-HRP	Santa Cruz	sc-2056	Donkey	Western blotting	1:3000
SV40LT	Santa Cruz	sc-147	Mouse	ChIP	1:50
Rabbit AF488	Invitrogen	A-11008	Goat	Immuno-stainning	1:500
Mouse AF488	Invitrogen	A11001	Goat	Immuno-stainning	1:500

3.2.3. Chromatin Immunoprecipitation (ChIP) analyses

ChIP analyses were performed following previously published protocols with minor modifications (Infante *et al.*, 2008; Laresgoiti *et al.*, 2013), in collaboration with Dr. Jone Mitxelena in the laboratory.

Cell cultures (10-15 x 10^6 cells per ChIP) were fixed for 10 min at room temperature with a solution containing 1.1 % formaldehyde (90% PBS 1X, 7% "formaldehyde dilution buffer" and 3% of formaldehyde 37%). This step produces a reversible crosslink of amino and imino groups between DNA and amino acids at a maximum distance of 2 Å (Orlando, 2000). Cross-linking was stopped by the addition of glycine to a final concentration of 0.125 M and subsequent incubation for 5 min at room temperature.

Fixed cells were harvested by incubation with trypsin and washed twice with PBS. Cells were lysed on ice for 10 min with a hypotonic buffer ("Cell lysis buffer"). Nuclei were collected by centrifugation, resuspended in "Nuclei lysis buffer", and incubated for 10 min on ice. Chromatin was sonicated applying 10 pulses of 15 seconds each, with a rest period of 1 minute between pulses. DNA concentration (A_{260}) was measured using a NanoDrop spectrophotometer (Thermo Scientific).

To verify successful chromatin fragmentation, a small volume of the sonicated sample was subjected to crosslink reversion, protein digestion, and DNA purification steps, as specified below. The fragmented chromatin was visualized in an agarose gel containing ethidium bromide. Only chromatin samples with fragments displaying an average length of 300–400 bp were selected for further analysis.

Fragmented chromatin was diluted in "ChIP dilution buffer" supplemented with 1 mM PMSF and protease inhibitor cocktail. At this point 200 µl of sample were set aside to be used as the "input DNA" sample. In order to reduce possible non-specific antibody binding we performed a pleclearing step with protein A-Sepharose (50% slurry, 50% TE) blocked with salmon sperm DNA and BSA. Twenty µL of protein A-Sepharose per 400 µL of the chromatin sample were added and incubated at 4°C for 3 h with gentle shaking. After incubation, protein A-Sepharose was discarded by two consecutive centrifugations. Fragmented and precleared chromatin (100–120 µg) was incubated overnight at 4°C with 4 µg of test antibody (Table 6).

Antibody-bound samples were incubated with protein A-Sepharose (20 µl per 400µl of sample) at 4°C for 3 h and immune complexes were recovered by centrifugation. Immune complexes were washed once with each of "Low Salt Wash", "High Salt Wash" and "LiCl Wash" buffers, and three times with TE buffer, in order to remove non-specific and low affinity antibody-chromatin binding.

Immunocomplex were eluted with a buffer containing 0.1 M $NaHCO_3$ and 1% SDS. Crosslinking was reversed by addition of NaCl to a final concentration of 200 mM followed by an overnight incubation at 65°C. RNA digestion was simultaneously performed with 10 µg of RNase A. Both immunoprecipitated and "input DNA" samples underwent crosslink reversal and RNA digestion treatments. Before protein digestion, EDTA pH 8.0 (10mM) and Tris-Cl pH 6.5 (36mM) were added to the samples. Subsequently, proteins were digested with 80 µg of proteinase K at 42°C for 2 h.

Table 7: Promoter-specific primer sequences and concentrations for ChIP analysis

	Forward (F)		Reverse (R)	
Target Gene	Sequence (5´-3´)	[nM]	Sequence (5´-3´)	[nM]
RAD51	GCTCAGACGATACTCTCGCCTC	50	CGCTAACCCAAGACGGGAG	50
FANCE	ACACCGCCCACAAACTAAC	300	AAGTCCAGCCGGAGTAGG	300
FANCI	CCCTTCAGTCTTCATGGTACAC	300	TCCGTTACCCGTAACAACAAG	900
CTIP	TGTGTCTGATGAAATAGGCCG	300	AGACCCAGAAGTAGTACTGAGG	300
BARD1	TCCCCTAAGTCCCACACG	900	CCGCAATGCTCCCAAAATAG	900
BRIP1	AGGATTTGGCACTCTGGTG	300	TTCTGAGGCTGTGAAAGGAC	300
miR-7 (HNRNPK)	CGTGAACTAGGCAGTTGTTAGA	900	GCAGCAGAGAAACAGAGGATAA	900
miR-92 (MIR17HG)	GGAGGTCGGAAGTACTTTGTTT	300	AAGGACCATGTGGGTGAATG	300
miR-25 (MCM7)	TAGACAAGAAGACGGCGAAAG	300	GGAGGAGAATCGCTCTTAAAGG	300
ACTB	GTGTGGTCCTGCGACTTCTAAGT	300	CCTGGGCTTGAGAGGTAGAGTGT	300

DNA was purified with the classical phenol-chloroform protocol, precipitated with ethanol and resuspended in 60 µl of H_2O. Immunoprecipitated DNA was quantified by real-time PCR in the QuantStudio3 thermocycler using *Power SYBR Green PCR master mix*. Primers were designed in order to flank promoter regions bound by E2F factors according to ENCODE data obtained from UCSC Genome Browser (http://genome.ucsc.edu/). Quantitative PCRs were performed as previously specified in section 3.2.1.2. Primers and conditions used for qPCR are specified in Table 7. Data were represented as percentages of the input sample.

3.2.4. Co-Immunoprecipitation (CoIP) analyses

CoIP experiments were carried out after transfecting U2OS-TetOn cells with the pE2F7-FLAG plasmid and extracting the protein fraction. Paralelly, cells were transfected with a plasmid expressing the FLAG tag, which served as a negative regulator.

Protein extracts were pre-cleaned with magnetic beads for 3h (Dynabeads, ThermoFischer Scientific) to remove the non-specificities of the protein. A small fraction of each extract was removed at this point in order to be used later as an "Input" sample in the final Western Blot. Following the pre-cleaning step, extracts were incubated with magnetic beads previously crosslinked with a specific antibody against FLAG tag. This crosslinking was achieved by incubating the beads and the antibody for 90 minutes in a rotating platform at 4°C. After the incubation, the mixture was washed twice with trietanolamine 0.2M and incubated with the crosslinking agent DMP (20mM) for 30 minutes in a rotating platform at room temperature and finally washed with 50mM and pH 7.5 TrisHCl.

After incubation of pre-cleaned extracts with antibody-bound magnetic beads, fractions were eluted twice (IP1 and IP2) and analyzed by Western Blot (as described above).

3.3. Bioinformatic analyses

3.3.1. Localization of E2F consensus motifs

Localization analysis of E2F motifs in E2F7-regulated genes was carried out with the MotifLocator tool from TOUCAN program (https://gbiomed.kuleuven.be/english /research/50000622/lcb /tools/toucan) (Aerts *et al.*, 2005). This application allows searching and localizing transcription factor binding motifs (TFBMs) in sequences provided by the user. The sequences introduced by the user are compared with position-weight matrices (PWMs) belonging to the database JASPAR. The comparison is based on the similarity between the sequence and the matrix, as established by the MatInspector program (http://www.genomatix.de/products/ MatInspector/index.html).

The search was restricted to the proximal promoter region (-1000 and +500 bp relative to the transcription start site). Cutoffs of 0.8, 0.85 and 0.9 were applied, and the "Human 1 Kb Proximal 1000 ENSMUSG" was used as background.

3.3.2. Identification of protein motifs

Identification of functional small linear motifs present in the protein E2F7 was carried out with the bioinformatics webtool ELM (http://elm.eu.org/) after uploading the aminoacid sequence of E2F7 protein in the application. This tool identifies by sequence similarity which small sections of a protein could be involved on functional processes such as interactions with other proteins. It also identified post-transcriptional modification sites.

3.4. Statistical analyses

Data are presented as mean ± SD. The significance of the difference between two groups was assessed using the Student two-tailed t-test. A $P<0.05$ was considered statistically significant.

4.- RESULTS

4.0 PREVIOUS FINDINGS GENERATED IN THE LABORATORY

The work presented in this thesis report stems from previous results generated in the laboratory whereby an E2F7-regulated gene expression profile was identified. The study consisted of silencing E2F7 by transient transfection of specific siRNA molecules in cell cycle-synchronized U2OS cells and assessing by RNA-seq the expression profiles of micro-RNA coding and protein coding genes at G1/S, S and G2/M phases (Mitxelena, 2014).

Regarding microRNA expression profile analysis, a total of 18 microRNAs were found to be deregulated upon E2F7 knockdown, 15 of which were upregulated whereas 3 microRNAs were downregulated, suggesting a major role for E2F7 as a negative regulator of microRNA expression through the cell cycle (Figure 16).

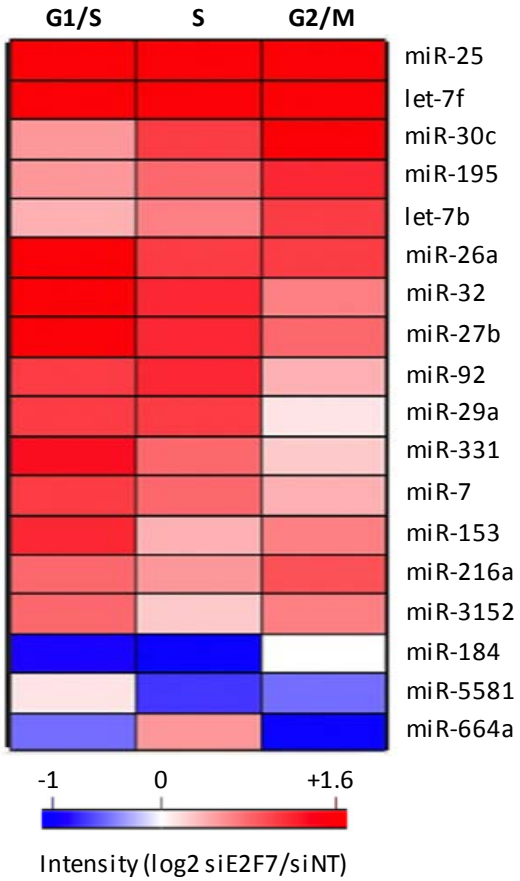

Figure 16: Identification of E2F7-regulated microRNAs. microRNA expression levels under E2F7 knockdown are represented in red (upregulated expression) and blue (downregulated expression).

Using these results as a starting point, in the present thesis work we have carried out an extensive analysis on the regulation and functional characterization of these E2F7-responsive micro-RNAs, in particular those microRNAs repressed by E2F7.

Regarding protein-coding mRNA expression profiles, a Gene Set Enrichment Analysis performed with significantly deregulated genes produced a list of pathways that were enriched in E2F7-depleted cells compared to their corresponding controls (i.e. cells transfected with non-target siRNA) (Table 8).

Table 8: Overrepresented pathways in E2F7-depleted cells throughout the cell cycle (Modified from Mitxelena, 2014). In red pathways important to DNA Damage Response

Gene expression	G1/S	S	G2/M
Upregulated	• E2F Network • RB signaling pathway • Fanconi Anemia pathway • BARD1 signaling events • ATR signaling pathway • Regulation of telomerase	• E2F Network • RB signaling pathway • Fanconi Anemia pathway • BARD1 signaling events • ATR signaling pathway	• E2F Network • RB signaling pathway • Fanconi Anemia pathway • BARD1 signaling events • ATR signaling pathway • FOXM1 network • PLK1 signaling events
Downregulated			• Osteoponin pathway • Integrin 1 pathway • Integrin 3 pathway

As shown in Table 8, E2F and Rb protein pathways were identified as regulated by E2F7, consistent with previous reports (Moon and Dyson, 2008; Westendorp *et al.*, 2012). Included in this last group were E2F1, E2F2 and E2F3 genes, whose expression was significantly increased upon E2F7 silencing, supporting the prevailing view that typical and atypical members of the E2F family cross-regulated each other´s expression (Sears, Ohtani and Nevins, 1997; Adams *et al.*, 2000; Westendorp *et al.*, 2012)

Remarkably, the transcriptomic analysis revealed novel pathways regulated by E2F7, mainly related to DNA damage response and repair pathways, including the categories of Fanconi Anemia (FA), BARD1 signaling and ATR signaling pathway suggesting major role for E2F7 in DDR. The E2F7-mediated repression of some of these genes (FANCE, FANCI, CTIP, RAD51, BARD1 and BRIP1) was subsequently validated by RT-Q-PCR (Mitxelena, 2014). Using these results as a starting point, one aim of the present thesis work, has been to define the mechanisms by which E2F7-mediates DNA damage responses.

4.1 FUNCTIONAL ANALYSIS OF microRNAs REGULATED BY E2F7

In this section, we aimed to analyze the regulation and function of microRNAs that are negatively regulated by E2F7. This work has been performed in collaboration with two members of our group, Dr. Mitxelena and Dr. Apraiz.

4.1.1 Validation of the microRNA profiling

We selected three microRNAs exhibiting different expression levels in the RNA-seq study (miR-25, miR-92 and miR-7). We performed RT-qPCR analyses using *Taqman* assays designed to detect and quantify mature microRNAs in siNT- and siE2F7-transfected cells (Figure 17A). These analyses were carried out with RNA samples extracted from cells in G1/S, S phase and G2/M boundary (0h, 4.5h and 10.5h respectively after exit from HU-induced arrest) following the protocol used for the original RNA-seq analysis.

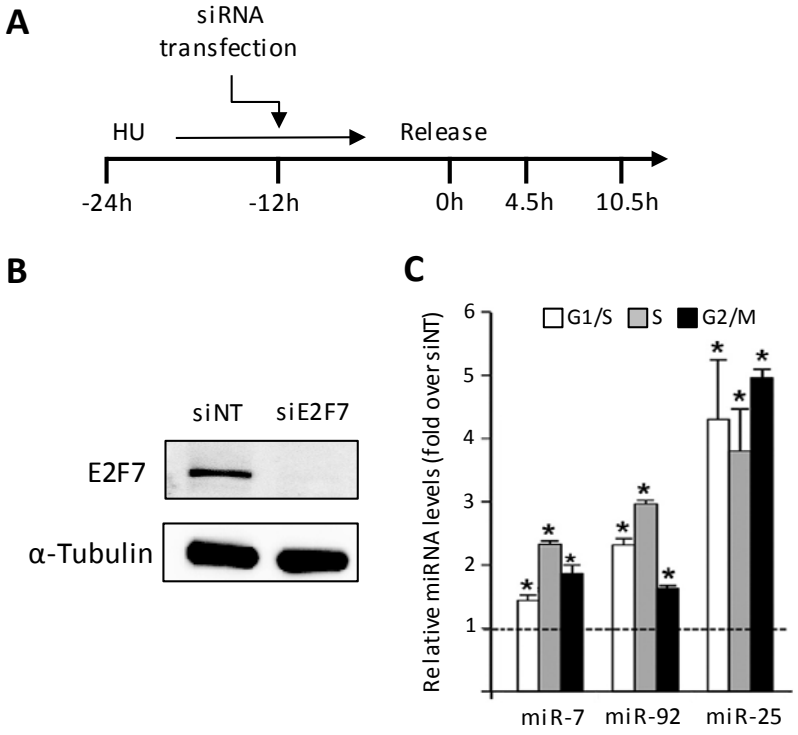

Figure 17: Expression analyses of E2F7 modulated microRNAs. (A) U2OS cells were transfected with E2F7 siRNA or Non-Target (NT) siRNA molecules. (B) E2F7 silencing was checked by Western Blot using specific antibody against E2F7 (C)Transfected cells were treated with HU for 24h microRNA qPCR assays were carried out with RNA samples harvested at 0h (G1/S), 4.5h (S phase) and 10.5h (G2/M) after HU release. Mature miR-25, miR-92 and miR-7 expression levels were normalized to RNU6B and RNU19 small RNA expression, used as standard controls. Data are represented as fold change relative to siNT (*, P<0.05). Dotted line represent siNT microRNA levels.

The expression of the mature microRNAs was compared between siNT and siE2F7-transfected cells which had depleted efficiently E2F7 levels (Figure 17B). Quantification results revealed that miR-7, miR-92 and miR-25 were significantly overexpressed upon E2F7 knockdown all over the cell cycle. The overexpression values ranged between 1.5 and 3-fold for miR-7 and miR-92, and were higher (4-to-5 fold) for miR-25 (Figure 17C), validating the previous screening results (Figure 17).

4.1.2 Regulation of microRNA expression by E2F7

To determine the role of E2F7 in the negative regulation of microRNAs, we first examined the regulatory regions of the microRNAs identified in the gene expression profiling assay previously mentioned. In particular, we searched for putative E2F sites in their regulatory regions, using *Motif locator* tool from TOUCAN program (Aerts *et al.*, 2005).

Many of the E2F7 downregulated microRNAs identified in our study (miR-7, miR-25, miR-26a, miR-27b and miR-153) were located within intronic regions of known protein-coding genes (Table 9). It is known that the expression pattern of this type of microRNAs matches the transcription of their host gene (Baskerville and Bartel, 2005) implying a co-regulation through the generation of a common precursor transcript. Thus, we analyzed the promoter regions of the genes harboring the E2F7-regulated microRNAs to look for E2F binding sites.

Other microRNAs identified in our study were located in regions lacking known protein-coding genes, either individually (miR-30c and miR-331) or clustered with other microRNAs (miR-92, let-7b, miR-195 and let-7f). To search for E2F binding sites in these microRNA coding genes, we analyzed the genomic region upstream of each microRNA transcription start site, thought to harbor their transcriptional regulatory sites (Zhao *et al.*, 2017).

We narrowed down our search to a region comprising -1000/+500 bp from the transcription start site, taking into account previous reports showing that the members of the E2F family of transcription factors are mainly recruited to this proximal region of their target genes (Rabinovich *et al.*, 2008; Lee, Bhinge and Iyer, 2011; Laresgoiti *et al.*, 2013). Using a minimum threshold level of 80% of similarity with the canonical E2F motif recorded in the JASPAR database (http://jaspar.genereg.net), all the E2F7-downregulated microRNAs except for let-7f presented putative E2F-recognition sites in their proximal promoter region, with a similarity of 80% or higher (Table 9), suggesting that their downregulation could be mediated by direct binding of E2F7 to their promoters on these sites.

Table 9: Consensus E2F sites found in the promoter regions of E2F7-regulated microRNAs. The locus, similarity to canonical motif, position and sequence are indicated.

miRNA	Locus	E2F site		
		% similarity[a]	Location from TSS*	Sequence
miR-7	*HNRNPK*	80	+88	GTTCGCGG
		85	+444	TCTCGCGC
		90	-17	GTTCGCGC
		95	-175	TTTGCCGC
miR-92	MIR17HG	80	-233	ATTGGCGG
		80	-3	CTTCGCGG
		85	-82	CTTCGCGC
		85	-72	CTTCGCGC
		85	+281	TTGGCCGC
miR-25	*MCM7*	80	-241	TTTCGAAC
		80	+254	TTTCGCCG
		85	-143	TTTGGCGG
		90	+357	TTTCCCGC
miR-26a	*CTDSPL*	80	-602	TTTACCGC
		80	-484	ATTCGCGG
		85	+311	TTTCTCGC
miR-27b	*C9ORF3*	80	-912	GTTCCCGC
		80	+303	TGTGCCGC
let-7b	MIRLET7BHG	80	+467	TTCCCCGC
		85	-206	TTTGCCGG
miR-195	MIR497HG	80	-679	TTTGGGGC
		85	-580	CTTCGCGC
miR-30c	MIR30C2	90	-326	TTTGGCGA
miR-331	MIR331	85	+301	TTTCTCGC
miR-153	*PTPRN*	80	+159	TTTGCCTC
let-7f	MIRLET7DHG	n.f.	n.f.	n.f.

[a]Threshold level of similarity with the canonical E2F motif recorded in the JASPAR database (TTTSSCGC)
*Transcription Start Site
n.f.: not found

4.1.2.1 In vivo transcription factor binding to the promoter regions of microRNAs regulated by E2F7

To determine whether E2F7 regulates directly the expression of its target microRNAs, we selected the validated microRNAs to carry out Chromatin Immunoprecipitation (ChIP) assays with anti-E2F7 specific antibody. We made use of chromatin extracted from cells collected at 3h following HU release corresponding to early S phase, when E2F7 expression is highest (Mitxelena, 2014). We performed qPCR with the immunoprecipitated chromatin using specific oligonucleotides that hybridize with sequences encompassing the E2F binding sites present in the regulatory regions of the microRNAs. Additionally, parallel ChIP assays were done using an irrelevant antibody (anti-simian virus 40 large T antigen, SV40LT) to assess the nonspecific chromatin immunoprecipitation. The β-actin gene (ACTB), a gene whose promoter lacks E2F sites, was used as negative control (Infante *et al.*, 2008). Quantitative PCR analyses (Figure 18) showed direct E2F7 binding to the regulatory region of miR-7, miR-92 and miR-25, compared with E2F7 binding to the *ACTB* gene. The extent of E2F7 binding activity paralleled the microRNA expression results. A substantially higher E2F7 binding activity to miR-25 regulatory region relative to miR-7 and miR-92 was correlated with a higher expression of miR-25 upon E2F7 depletion.

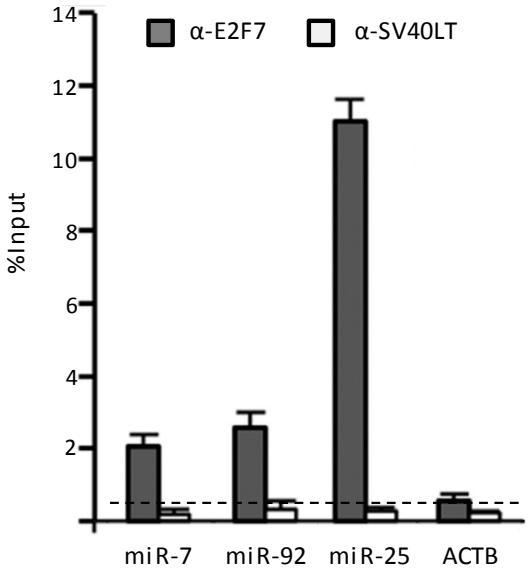

Figure 18: E2F7 is recruited to the promoter regions of selected microRNAs. E2F7 was immunoprecipitated from chromatin lysates harvested from cells in S phase after HU release with specific anti-E2F7 antibodies (α-E2F7). Promoter regions near E2F consensus sites were amplified by qPCR. ACTB amplification values were used as a negative control. An unrelated antibody against the SV40 large T antigen (α-SV40LT) was used as a control for unspecific immunoprecipitation. Data is presented as percentage of input chromatin. These results are representative of three independent experiments.

It has been described that individual E2F sites of the regulatory regions are bound by multiple E2F members *in vivo* (Wells *et al.*, 2000; Infante *et al.*, 2008). To determine whether other E2F family members besides E2F7 are recruited to the regulatory regions of the identified microRNAs we focused on E2F1, E2F2 and E2F3 because they were found to be repressed by E2F7 in our transcriptomic analysis (Mitxelena, 2014), and thus, could potentially be involved in E2F7-dependent microRNA regulation. As shown in Figure 19, in ChIPs carried out with siNT-transfected cells, we found that E2F1 and E2F3 were efficiently recruited to the regulatory regions of miR-7, miR-92 and miR-25, whereas binding of E2F2 was more moderate (about 2-fold over *ACTB* promoter amplification).

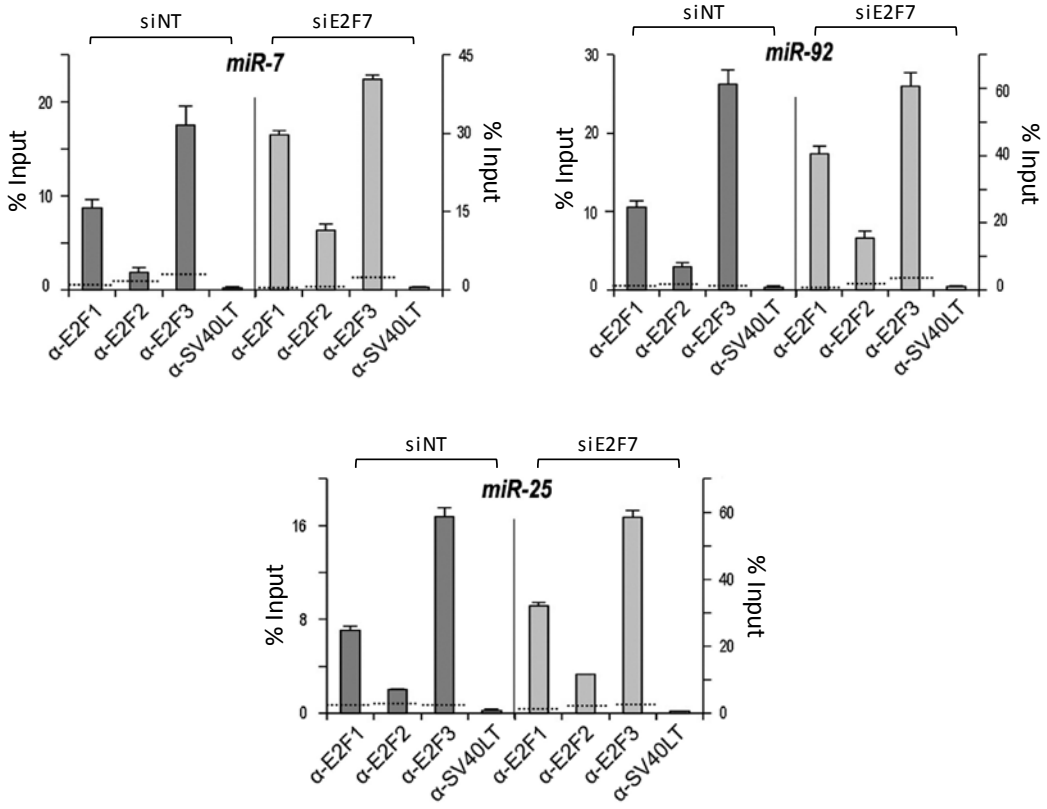

Figure 19: Occupancy of target microRNA regulatory regions by E2F1-3 factors. Cell lysates from siNT and siE2F7-transfected cells were harvested 3 h (early phase S) after HU release and used for ChIP assays with antibodies against E2F1, E2F2 and E2F3. Promoter regions near E2F consensus sites were amplified by qPCR. Promoter binding of E2F1-3 was significantly increased upon E2F7 silencing. Note the Y-axis scale difference in the siE2F7-treated samples. An unrelated antibody against the SV40 large T antigen (SV40LT) was used as a control for unspecific immunoprecipitation. *ACTB* amplification values are represented as dotted horizontal lines. Data is presented as percentage of input chromatin. These results are representative of three independent experiments.

Importantly, E2F7 silencing led to a dramatic increase in recruitment of E2F1, E2F2, and E2F3 to miR-25, miR-92 and miR-7 promoter regions (note right Y-axis scale) consistent with the increased expression of these E2Fs in E2F7-knockdown cells. These results reveal the existence of a complex regulation of miR-7, miR-92 and miR-25 by typical and atypical E2Fs, whereby microRNA expression is bound to be under the influence of both positive and negative signals provided by individual E2Fs.

4.1.2 Functional activity of E2F7-downregulated microRNAs

We next aimed to determine the functional role of the microRNA set identified as E2F7 targets by using the bioinformatics tool miRBase (Griffiths-Jones *et al.*, 2006). We searched for potential pathways regulated by these microRNAs through a bioinformatics analysis of their predicted target genes. To increase the potency of the analysis we carried out a Gene Ontology analysis of the combined predicted targets of all deregulated microRNAs. Interestingly, this study revealed that E2F7-repressed microRNAs preferentially modulate genes involved in cell cycle and mitosis regulation (Figure 20). Other biological processes including hemostasis, signaling by Nerve Growth Factor (NGF) or transmembrane transport also appeared enriched in this analysis, suggesting that E2F7 regulates a diversity of functions through control of microRNA expression.

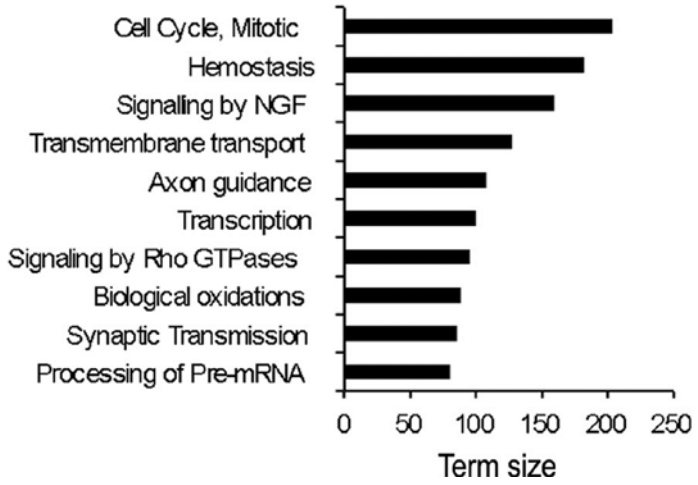

Figure 20: Gene Ontology (GO) analysis of the combined predicted targets of E2F7-repressed microRNAs. Gene ontology (GO) analysis of predicted targets (as identified by miRBase bioinformatic tool) of E2F7-repressed microRNAs using FatiGO tool. Only terms with adjusted *P*-value of > 0.001 were considered.

Given the GO results, we next focused our analysis on determining the contribution of E2F7-regulated microRNAs to cellular proliferation. In addition to miR-7, miR-92 and miR-25 we included for these analyses several other microRNAs with E2F consensus motifs in their regulatory region (miR-26a, miR-27b and let-7b), as well as let-7f, a microRNA with no known E2F sites that we found to be regulated indirectly by E2F7 (Mitxelena, 2014), and we carried out microRNA overexpression as well as inhibition assays to assess their effect in cellular division.

We overexpressed individual microRNAs in U2OS cells and assessed cellular proliferation by the carboxyfluorescein succinimidyl ester (CFSE) method. This method reflects how many cell division cycles have completed the cells over time because the cellular CFSE staining is diluted by 50% with each cell division. U2OS cells transfected with expression vectors coding for a scramble sequence (negative control) or for each individual microRNA, were incubated with the vital dye CFSE. Forty-eight hours later cells were fixed and fluorescence of CFSE-stained cells was quantified by flow cytometry.

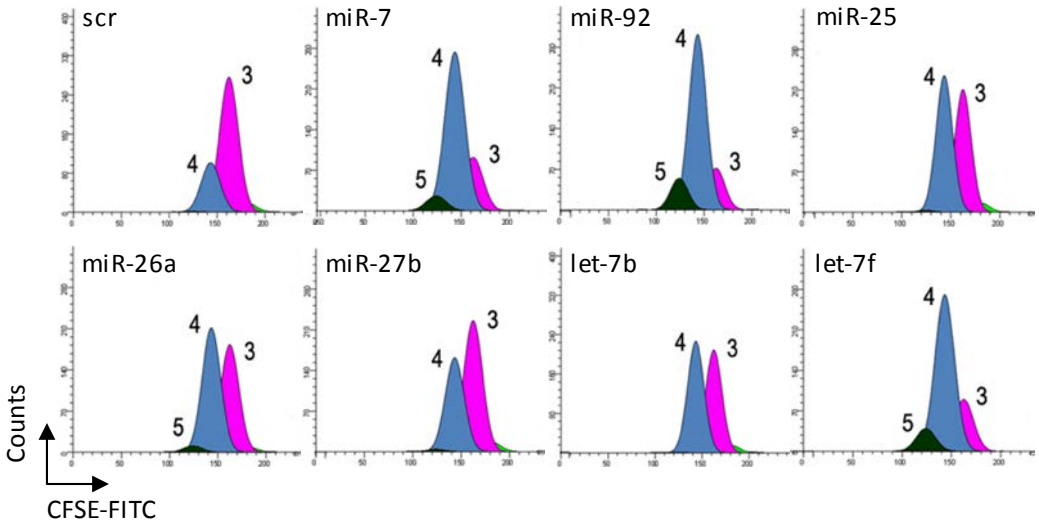

Figure 21: Individual transfection of selected microRNAs accelerates cell cycle progression. U2OS cells were transfected with various microRNA encoding plasmids and incubated with CFSE. A vector coding for a scramble sequence (scr) was used as a negative control. Cells were harvested 48h after transfection and CFSE fluorescence was determined by flow cytometry. The number cellular divisions achieved in each condition is indicated.

As shown in Figure 21, control cells treated with scramble plasmid underwent several cell division cycles, within the 48h time period. Most cells were in generation 3, and a smaller percentage reached up to generation 4.

Remarkably, individual overexpression of microRNAs led to an increase in the cellular proliferation rate, as evidenced by the increased proportion of cells in more advanced cellular generations compared with the scramble-transfected cells (Figure 21). Of those, overexpression of miR-7, miR-92 and let-7f microRNAs led to the strongest effect on proliferation, as shown by the higher proportion of proliferating cells that were able to reach generation 5.

We next analyzed the effect of inhibiting these microRNAs in cell cycle progression. For this purpose, we selected anti-microRNA oligonucleotides specific for miR-7, miR-92 and let-7f since those were the microRNAs whose expression in U2OS cells results in a stronger proliferative effect (Figure 22). These anti-microRNA oligonucleotides (miRVanas) are designed to neutralize the microRNA sequences by preventing selective binding of the microRNAs to the target mRNA molecules (Wang *et al.*, 2012). We pooled all three of them in order to achieve a stronger response and avoid the small effect that individual oligonucleotides could have, and analyzed their impact in cell cycle progression by scoring the fraction of cells able to reach mitosis

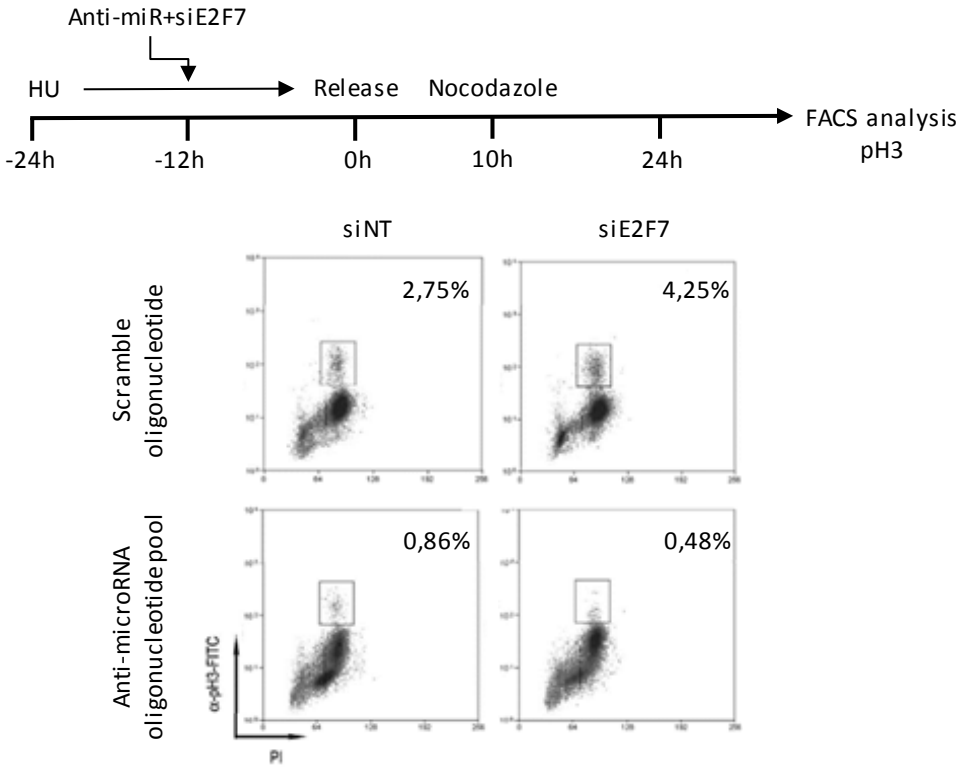

Figure 22: Abrogation of the expression of miR-7, miR92 and let7f interferes with E2F7-dependent cell cycle progression. (A) U2OS cells were synchronized in the presence of 4 mM HU and transfected with siNT or E2F7 siRNA molecules and a pool of anti-microRNA oligonucleotides against miR-7, miR-92 and let-7f. (B) The percentage of mitotic cells was determined by pH3 positivity and FACS analysis 12 hours after cell cycle re-entry. Numbers represent pH3-positive cells (enclosed in boxes).

U2OS cells were synchronized in G1/S with HU and transfected with siNT or siE2F7, along with scramble oligonucleotides and a pool of all three anti-microRNA oligonucleotides. 10h after HU release cells were treated with nocodazole and 24h after HU release, we used FITC-labeled antibodies to phospho-Histone H3 (pH3), a mitotic marker, to study cell cycle progression.

As previously described (Mitxelena, 2014) we observed that depletion of E2F7 caused an acceleration of the cell cycle, as we observed a higher percentage of cells reaching mitosis in cells with reduced E2F7 levels (2.75% in siNT vs 4.25% in siE2F7 in cells transfected with scramble oligonucleotides) (Figure 22). Transfection of anti-microRNA oligonucleotides provoked a reduction in the percentage of cells in mitosis (2.75% in scramble vs 0.86% in anti-microRNA pool). Importantly, inhibition of miR-7/miR-92/let-7f in E2F7 depleted cells abrogated the increased percentage of cells in mitosis seen in the scramble condition (Figure 22). These results suggest that E2F7 negatively regulates cellular proliferation at least in part by repressing the expression of pro-proliferative microRNAs.

To get an insight into the mechanism by which E2F7-regulated microRNAs may contribute to cellular proliferation, we examined the expression of potential mRNA targets of these microRNAs. It has been reported that several genes involved in cell cycle control including $p21^{Cip1}$, $p57^{Kip2}$, PTEN and p130 are potential targets of these microRNAs (Zhang et al. 2015; Knudsen et al. 2015; Feng et al. 2017; Zhu et al. 2018).

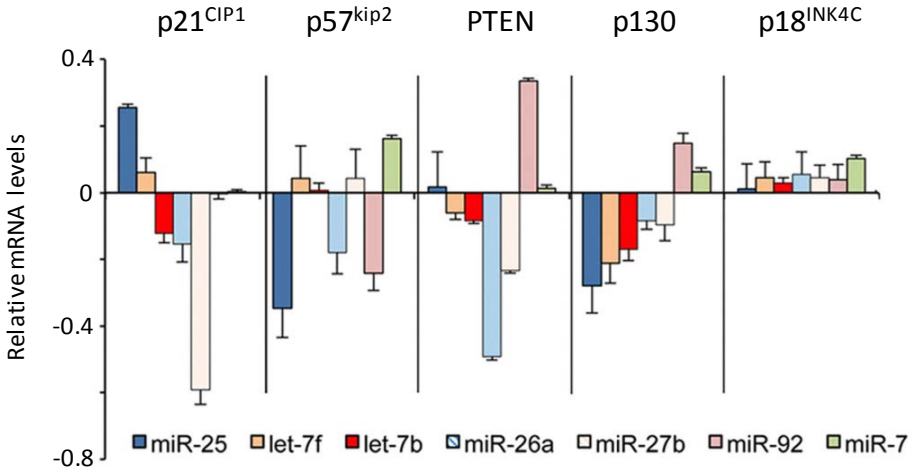

Figure 23: Expression of cell cycle inhibitors upon microRNA overexpression. $p21^{CIP1}$, $p57^{KIP2}$, PTEN, p130 and $p18^{INK4C}$ mRNA levels were assessed by RT-Q-PCR in RNA samples extracted from U2OS cells treated as in Figure 21. Expression values are normalized to the expression of EIF2C2, used as standard control. Data are represented as normalized log2-ratios over control scr transfection.

Individual overexpression of E2F7-regulated microRNAs resulted in the downregulation of some of these genes (Figure 23). In contrast, $p18^{INK4C}$, which has not been described as regulated by these microRNAs, was unaffected by microRNA overexpression compared to controls, ruling out possible general effects due to an overall increase in proliferation rates after microRNA overexpression (Figure 23).

Collectively, our results point to a role for these microRNAs in E2F7-mediated negative regulation of cell proliferation and cell cycle control by modulating the levels of critical cell cycle inhibitors. The findings of this section regarding E2F7-dependent microRNA regulation and function have been included in a recently published manuscript (Mitxelena *et al.*, 2016).

4.2 ROLE OF E2F7 IN DNA DAMAGE RESPONSE AND REPAIR

In this section, we aimed to analyze the role of the E2F7 transcription factor in the DNA damage response and repair. This work has been performed in collaboration with two members of our group, Dr. Mitxelena and Dr. Apraiz.

4.2.1 Characterization of a set of DNA damage response genes as direct E2F7 targets

The role of E2F7 in the maintenance of genomic stability is poorly understood. The transcriptomic results obtained recently in our laboratory showing that a set of genes involved in DNA damage responses are repressed by E2F7 led us to analyze in detail the contribution of E2F7 to the regulation of DNA damage and repair pathways. We first considered whether E2F7 could be regulating the expression of its target genes at the transcriptional level. To this end, we first searched for E2F consensus sites in the promoter regions of the E2F7-responsive genes involved in DNA damage and repair. We focused our analysis on the set of six genes that had been previously validated by RT-Q-PCR as E2F7-repressed genes (Mitxelena, 2014). These genes belong to the Fanconi Anemia, BARD1 and ATR signaling pathways. Using *Motif locator* tool from TOUCAN program (Aerts *et al.*, 2005) we analyzed the promoter region of the selected genes. We narrowed down our search to the region comprising -1000/+500 bp form the transcription start site, as for the microRNA study.

Using a minimum threshold level of 80% of similarity with the canonical E2F motif recorded in the JASPAR database (http://jaspar.genereg.net), all selected genes presented putative E2F-recognition sites in their proximal promoter region (Table 10). With the exception of FANCE, which only encompasses one E2F binding site at 80% similarity with the consensus sequence, the rest of analyzed genes exhibit several E2F binding sites with up to 90% similarity with the consensus site (Table 10).

Table 10: Consensus E2F sites found in the promoter regions of E2F7-regulated protein-coding genes. The similarity of the identified sequence to the canonical motif, the position and sequence are indicated.

Gene	E2F site		
	%similarity[a]	Location from TSS*	Sequence
RAD51	80	+163	TTACGCTC
	85	-528	TTTGGCAC
	85	+434	TTTCGCCC
	90	+10	TTTGGCGG
FANCE	80	+1	GTTCCCGC
FANCI	85	-433	TTTTGCGC
	90	+247	TTTCGCGG
	90	+469	TTTCCCGC
CTIP	80	-22	TTTCGCCG
	80	+120	TTTGCCCC
	80	+460	TTTTGCGA
	85	-379	TTTGGCAC
	85	-356	TTTCGCCC
	90	-289	TTTCGCGA
BARD1	80	-324	TTTCGACC
	80	+49	TTTCGAGT
	80	+81	TTTCCCGA
	80	+356	TCTGCCGC
	85	-582	TTTCCCGG
	85	+202	TTCCGCGC
	85	+394	GTTCCCGC
BRIP1	80	-841	TTTGCCTC
	80	-425	ATTCCCGC
	80	-268	TTTGCTGC
	80	-29	TTGGGCGC
	80	-1	ATTCCCGC
	80	+230	TTTCCCTC
	85	-511	TTTCCCGG
	85	-445	TTTGGCTC

[a]Threshold level of similarity with the canonical E2F motif recorded in the JASPAR database (TTTSSCGC)
*Transcription Start Site

Next, we performed ChIP assays to confirm the direct binding of E2F7 to the selected promoters. To this end, U2OS cells were synchronized with HU and after release they were collected in S phase coinciding with the peak expression of E2F7 (Mitxelena, 2014). In order to detect E2F7 binding, we used an E2F7-specific antibody to immunoprecipitate chromatin followed by qPCR using specific primers hybridizing near the putative E2F7 binding sites in each promoter. The β-actin (*ACTB*) promoter amplification was used as a negative control, since this promoter lacks E2F binding sites but is highly expressed in U2OS cells (Laresgoiti *et al.*, 2013). In addition, as a control for antibody specificity, we used an irrelevant antibody (SV40LT) which has no affinity for chromatin and is unable to immunoprecipitate any of the various E2F target sequences (Infante *et al.*, 2008).

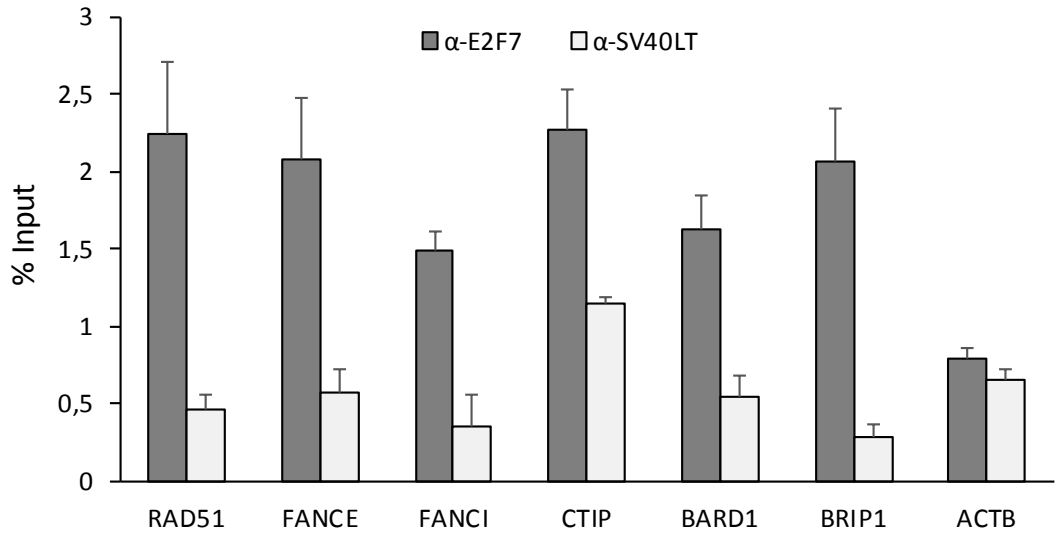

Figure 24: E2F7 is recruited to the promoter regions of validated genes. E2F7 was immunoprecipitated from U2OS chromatin lysates harvested from cells in S phase after HU release. Promoter regions near E2F consensus sites were amplified by qPCR. The promoter of *ACTB* was used as a negative control. An unrelated antibody against the SV40 large T antigen (SV40LT) was used as a control for unspecific immunoprecipitation. Data is presented as percentage of input chromatin. These results are representative of three independent experiments.

As shown in Figure 24, ChIP analyses revealed significant E2F7 binding to the promoters of all the validated genes (*RAD51, FANCE, FANCI, CTIP, BARD1* and *BRIP1*) compared to E2F7 binding to ACTB promoter. These results suggest that DNA damage response genes are repressed by E2F7 through a direct regulation of their transcriptional activity.

4.2.2 Role of E2F7 in the cellular responses to genotoxic DNA damage

Given the overrepresentation of DNA damage response and repair genes directly controlled by E2F7, we hypothesized that E2F7 could be regulating cellular responses following DNA damage.

We focused our attention on the type of damage that is typically repaired by genes that participate in Fanconi Anemia and Homologous Recombination repair, a pathway enriched in the E2F7-regulated transcriptome. We treated the cells with Mitomycin-C (MMC) and Cisplatin (CSP), two compounds known to produce DNA interstrand crosslinks (ICL), which compromise the progression of replication forks typically repaired by the Fanconi Anemia repair pathway (McCabe, Olson and Moses, 2009). Additionally, we included in our analyses double-strand DNA break (DBS)-inducing treatments, which are repaired by mechanisms that do not involve the FA pathway (Ceccaldi, Rondinelli and D 'Andrea, 2016). These treatments include γ-irradiation (γ-IR) or neocarzinostatin (NCS), a radiomimetic drug that mimics DNA damage caused by γ-irradiation by inducing free radical-mediated DSBs (Wang *et al.*, 2002).

4.2.2.1 E2F7 attenuates cell cycle progression upon DNA lesions affecting replication fork progression

We first examined the ability of E2F7-competent of E2F7-deficient cells to recover from cellular checkpoints induced by DNA damage. To this end, non-target and E2F7 siRNA-transfected U2OS cells (see Figure 17B) were synchronized in G1/S with HU and treated with MMC, CSP or γ-IR, following the scheme depicted in Figure 25A. Nocodazole was added to the cell cultures for the last 14h of the experiments to trap cells entering mitosis (Alvarez-Fernández *et al.*, 2010). We determined mitotic index by scoring pH3 positive cells by flow citometry.

All three DNA damaging treatments used in the experiment are known to induce the activation of the DNA-PK/ATM/ATR pathway and the subsequent G2 checkpoint, which results in the accumulation of cells in G2 and a reduction of the cell fraction able to advance to mitosis (Bartek and Lukas, 2003; Toledo, Murga and Fernandez-Capetillo, 2011). This effect can be observed in a representative Figure 25B, in which MMC, CSP and γ-IR treatments reduced significantly the fraction of accumulated mitotic cells relative to untreated cells (15.13% vs 1.83% with MMC, 1.3% with CSP and 8.15% with NCS). Remarkably, we found that transient knockdown of E2F7 in these cells resulted in an increased capacity of the cells to exit from the G2 arrest provoked by MMC (2.8-fold) and CSP (1.5-fold) in comparison with siNT-transfected cells (Figure 25C). By contrast, this recovery was not observed upon γ-IR.

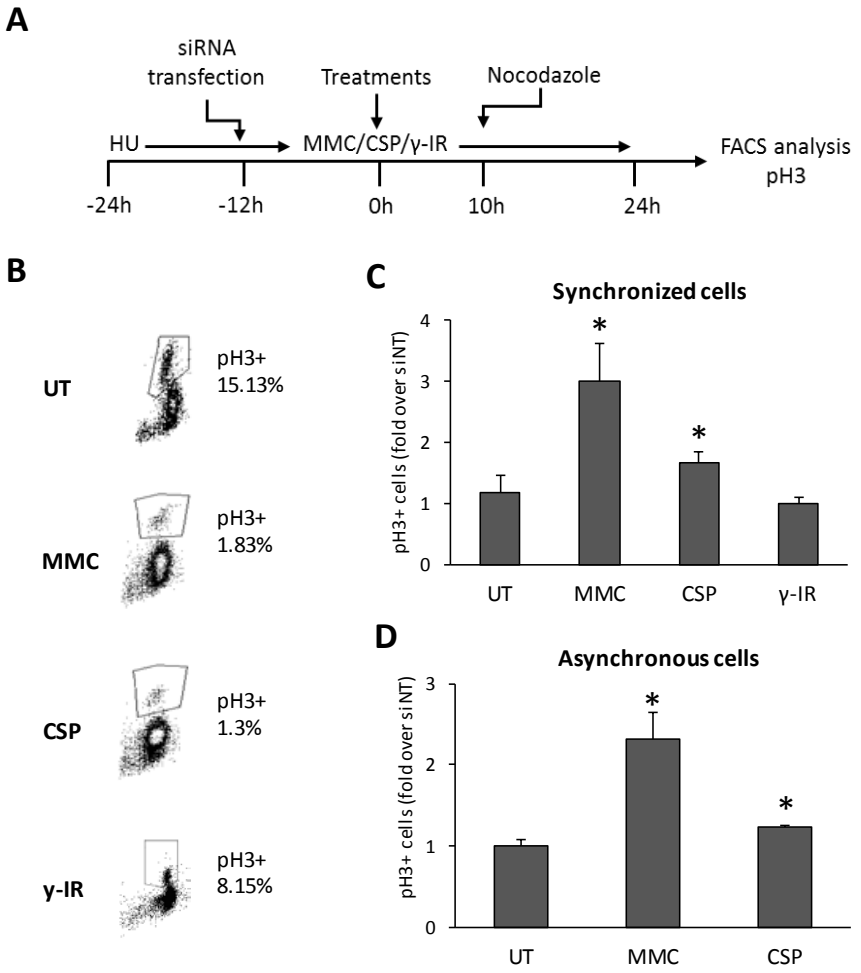

Figure 25: Increased cellular recovery after DNA damage arrest caused by MMC and CSP in E2F7-knockdown cells. (A). Schematic diagram of the cellular recovery experiment. U2OS cells were HU-synchronized and transfected with siNT and siE2F7. After HU treatment for 24 h, cells were released into the cell cycle and treated for 24 hours with 250nM MMC, 30 µM CSP and a dose of 2.5 Gy of γ-IR. Nocodazole was added 10 hours later. (B) All treatments induced an arrest in cell cycle progression in U2OS cells as assessed by the reduction in the proportion of pH3+ mitotic cells present in the cultures. (C) The percentage of mitotic cells determined by pH3 positivity and FACS analysis is shown comparing siE2F7 cells over siNT in synchronized cells. The graph represents fold-change of E2F7-depleted pH3-positive cells over siNT values (mean ± SD) from three independent experiments. (*, $P < 0.05$) (D) The percentage of mitotic cells determined by pH3 positivity and FACS analysis is shown comparing siE2F7 cells over siNT in asynchronous cells without HU treatment. The graph represents fold-change of E2F7-depleted pH3-positive cells over siNT values (mean ± SD) from three independent experiments. (*, $P < 0.05$)

In order to replicate these results in another cellular context, we carried out the protocol described in Figure 25A in asynchronously growing U2OS cells, that is, in the absence of previous HU treatment. We again found that transient knockdown of E2F7 in these cells confers an increased ability to exit from the G2 arrest induced by MMC and CSP in comparison with siNT-transfected cells (Figure 25D).

It has been described that transitory silencing using siRNA technology could impact several off-target effects, which may lead to wrong conclusions regarding the role of the gene under study (Caffrey *et al.*, 2011). We have optimized the siRNA concentration to reduce these effects and have used three different siRNA molecules to target E2F7, with similar results (Mitxelena, 2014). Additionally, in order to repeat our results with more than one system in which expression of E2F7 is depleted, we developed E2F7-knockout U2OS cells using the CRISPR-Cas9 technology, as described in the Materials and Methods section. We confirmed by sequencing the disruption of both E2F7 alleles; one allele was interrupted by the insertion of the puromycin cassette and the other by a premature stop codon provoked by the insertion of a nucleotide. The chronic depletion of E2F7 in U2OS cells (Figure 26B) gave us the opportunity to replicate our results in a different system.

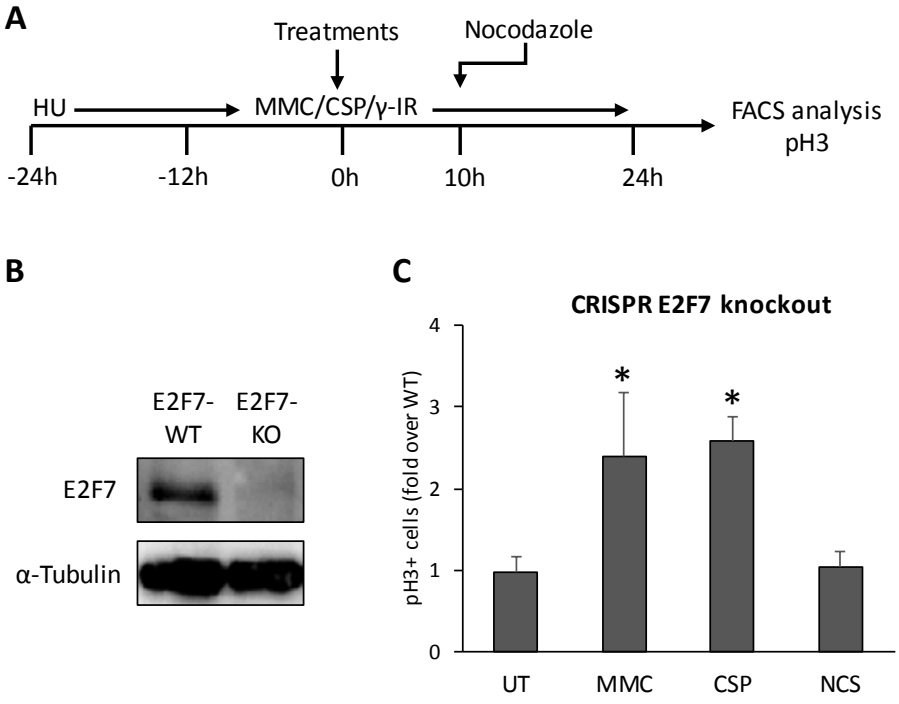

Figure 26: E2F7 controls cellular recovery after DNA damage arrest caused by MMC and CSP. (A) Schematic diagram of the cellular recovery experiment. U2OS cells were transfected with siNT and siE2F7. After HU treatment for 24 h, cells were released into the cell cycle and treated for 24 hours with 250nM MMC, 30 µM CSP and a dose of 20 ng/ml NCS. Nocodazole was added 10 hours later. (B) Western Blot analysis showing the chronic depletion of E2F7 expression in E2F7-KO cells. (C) The percentage of mitotic cells determined by pH3 positivity and FACS analysis is shown comparing E2F7-KO cells over E2F7-WT in synchronized cells. The graph represents fold-change of E2F7-deficient pH3-positive cells over E2F7-proficient cells values (mean ± SD) from three independent experiments. (*, $P < 0.05$)

Wild-type U2OS cells and E2F7-KO U2OS cells were HU-synchronized in G1/S, released from HU-induced block and treated with MMC, CSP or NCS. Next, we added nocodazole to cell cultures for the last 14h of the experiments to trap cells entering mitosis. The percentage of mitotic cells was determined by scoring pH3 positive cells by flow citometry. We observed that knockout of E2F7 in U2OS cells resulted in a significant increase in the fraction of cells capable of exiting from the arrest imposed by MMC and CSP in comparison with U2OS WT cells, consistent with the results gathered with E2F7-kockdown cells (Figure 26). Again, we did not observe any significant recovery after treatment with NCS, raising the possibility that E2F7 depletion affects selectively certain types of DNA damage.

Interstrand DNA crosslinks, such as those generated by MMC and CSP, are known to impact replication fork progression (Jieqiong Zhang *et al.*, 2015). Other genotoxic agents that affect replication fork activity include the compound Olaparib (OLA). This compound has been widely reported to inhibit the DNA repair activity of PARP1, thereby leading to replication fork stalling and cell cycle arrest (Ray Chaudhuri and Nussenzweig, 2017).

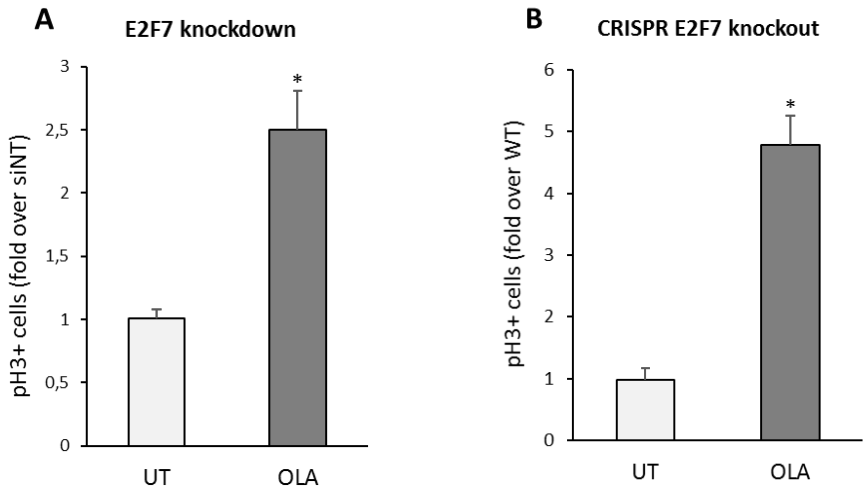

Figure 27: E2F7 controls cellular recovery after the cell cycle arrest caused by inhibition of PARP1. (A) U2OS cells were HU-synchronized and transfected with siNT and siE2F7. After HU treatment for 24 h, cells were released into the cell cycle and treated for 24 hours with 4 µM OLA. Nocodazole was added 10 hours later. The percentage of mitotic cells, as determined by pH3 positivity and FACS analysis is shown comparing siE2F7 cells over siNT. The graph represents fold-change of E2F7-depleted pH3-positive cells over siNT values (mean ± SD) from three independent experiments. (*, $P < 0.05$) (B) U2OS E2F7-WT and U2OS E2F7-KO cells were HU-synchronized. After HU treatment for 24 h, cells were released into the cell cycle and treated for 24 hours with 4 µM OLA. Nocodazole was added 10 hours later. The percentage of mitotic cells determined by pH3 positivity and FACS analysis is shown. The graph represents fold-change values of E2F7-deficient pH3-positive cells over E2F7-proficient pH3-positive cells (mean ± SD) from three independent experiments. (*, $P < 0.05$). (UT= untreated; OLA= Olaparib)

We wondered whether E2F7 could also be involved in the control of cellular recovery following the arrest produced by PARP1 inhibition provoked by OLA. To this end, we followed the protocol described above and compared the behavior of U2OS cells treated with OLA in the absence of E2F7. We found that transient knockdown of E2F7 with specific siRNA-mediated interference in these cells resulted in an up to 2.5-fold increase in the fraction of cells capable of exiting from the cell cycle arrest impaired by OLA, in comparison with siNT-transfected cells (Figure 27A). Similarly, CRISPR/Cas9-mediated knockout of E2F7 in U2OS also resulted in an over 4-fold increase in cells capable of exiting from the arrest imposed by OLA (Figure 27B).

Taken together, these results suggest a role for E2F7 protein in attenuating cell cycle progression after DNA damage induced by ICLs or by PARP1 inhibition, as the absence of E2F7 confers an advantage to overcome the G2 arrest induced by these types of treatments.

Given that interstrand crosslinks and PARP1 inhibition compromise the progression of the replication fork, we next considered whether DNA replication rates were affected after knockdown of E2F7. To analyze the replication rate we carried out a BrDU incorporation assay whereby cells incorporate BrDU as an analog of thymidine as they progress through the S phase of the cell cycle. We measured BrdU incorporation in asynchronously growing cells treated with CSP for 12 h in the presence or absence of E2F7. As expected, DNA synthesis rate was reduced in siNT control cells under CSP treatment, and only 14% of the cells were actively replicating DNA compared to 45% in the untreated condition. By contrast, the reduction in DNA replication was alleviated in E2F7-knockdown cells, and as many as 40% of cells replicated their DNA efficiently. These results suggest that E2F7 inhibits DNA replication when DNA lesions that interfere with fork progression are generated.

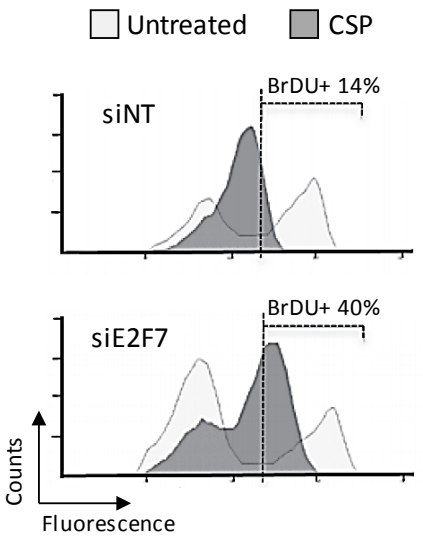

Figure 28: E2F7 inhibits DNA replication with treatments that interfere with replication fork progression. Asynchronously growing U2OS cells were transfected with siNT and siE2F7 and subsequently treated with 16 μM CSP for 12 h. BrdU was present in the cultures for the last 2 h. Cells were stained with anti-BrdU conjugated with FITC and with propidium iodide. A representative FACS analysis is shown.

Having shown that depletion of E2F7 confers an increased ability to damaged cells to replicate their DNA and enter mitosis, we next determined the role of E2F7 in overall cell survival by performing long-term clonogenic assays. To this end, we treated E2F7-knockout cells with several doses of CSP for 24 h and subsequently cultured them at low density for two additional weeks in drug-free medium to allow for colony formation from individual surviving cells.

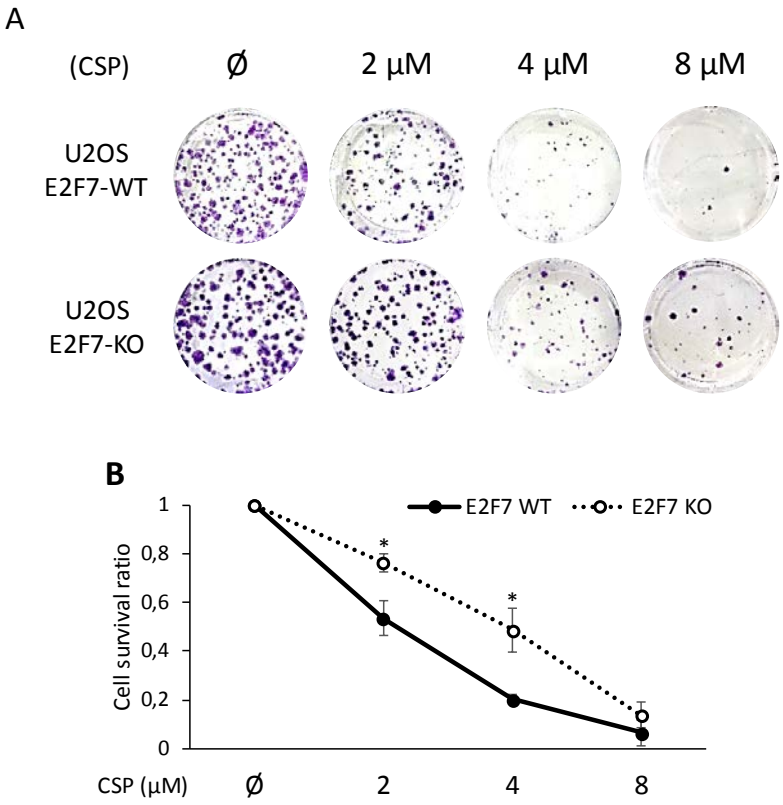

Figure 29: Lack of E2F7 provides long-term resistance against CSP. U2OS cells (E2F7-WT or E2F7-KO) were treated with 2, 4 and 8 µM of CSP for 24 h and cultured at low density for two additional weeks in treatment-free medium. After this period, colonies were stained fixed with paraformaldehyde and stained with crystal violet. Finally, the number of colonies was scored in each condition. (A) Representative images of colony density in each condition. (B) Cell viability ratio was calculated normalizing data against untreated (Ø) samples, which defined as 1. The graph represents colony survival ratio of treated samples against untreated samples (mean ± SD) from three independent experiments. (*, $P < 0.05$)

The number of colonies that were scored in untreated E2F7 knockout cultures was slightly higher than the number of colonies scored in E2F7-competent cultures, which probably reflects the reported role of E2F7 to hinder cellular proliferation (de Bruin et al. 2003; Westendorp et al. 2012; Mitxelena, 2014). As expected, CSP treatment caused a dose-dependent decrease in colony numbers, which reflects the ability of CSP to induce cytotoxicity.

However, as shown in Figure 29, the number of colonies that were scored in E2F7-knockout cultures exposed to all three CSP doses was significantly higher than in E2F7-WT cultures (between 7% and 28% higher depending on the dose), consistent with our pH3 and BrDU results .

Altogether, our results suggest that lack of E2F7 confers an increased recovery competence and survival upon treatment with compounds that affect replication fork progression.

4.2.2.2 E2F7-dependent gene expression regulation of DDR genes upon DNA damage

Our finding that E2F7 negatively affects cellular recovery upon genotoxic damage prompted us to examine the mechanism underlying this phenotype. Several genotoxic drugs such as doxorubicin and etoposide have been reported to induce an accumulation of E2F7 levels (Zalmas *et al.*, 2008; Carvajal *et al.*, 2012). We examined whether E2F7 expression and therefore its transcriptional activity were also regulated upon ICL induction.

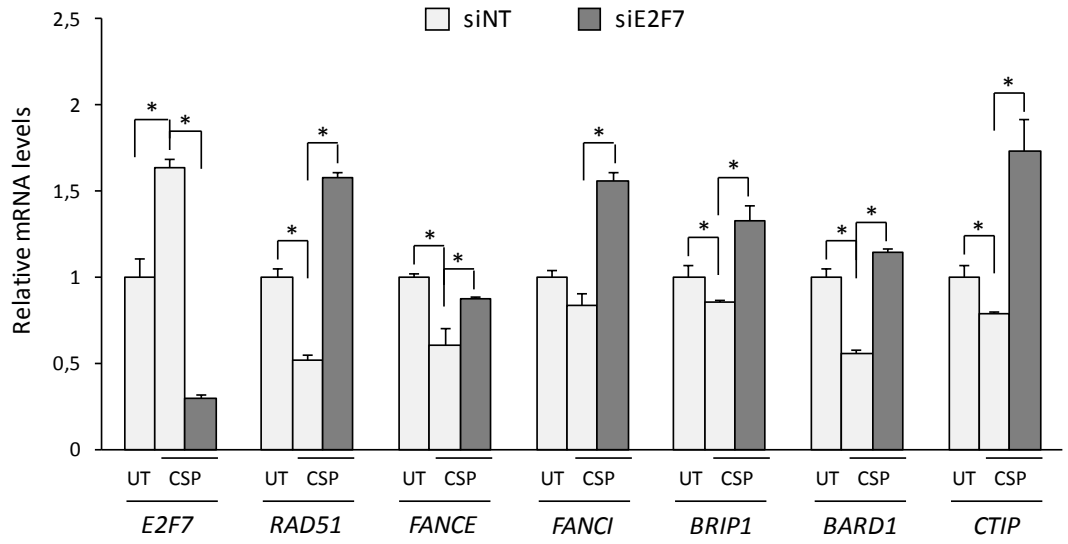

Figure 30: Robust overexpression of DDR genes in CSP-treated cells depleted of E2F7. Asynchronously growing U2OS cells were transfected with siNT and siE2F7 and subsequently treated with 8 µM CSP for 24 h. RT-qPCR analyses of indicated genes are shown. Expression values are normalized to the expression of EIF2C2, used as standard control. Data are represented as relative mRNA levels from three different experiments (*, P<0.05).

To this end, U2OS cells that had been transfected with siNT or siE2F7 molecules were treated with CSP during 24h and target gene expression was analyzed at the mRNA level. A significant increase in E2F7 levels was detected upon CSP exposure, similarly to what has been reported for other treatments, which was blocked in siE2F7-transfected cells (Figure 30). In contrast to E2F7 expression, the mRNA levels of target genes involved in DNA repair identified in our RNA-seq assay were consistently reduced upon CSP treatment. Importantly, silencing of E2F7 led to a robust overexpression of target genes in CSP treated cells (Figure 30). These findings point to a role for E2F7 in the negative regulation of genes involved in DNA damage responses following ICL induction.

At the protein level, E2F7 levels were significantly induced after treatment of U2OS cells with various doses of CSP and MMC (Figure 31A), consistent with mRNA expression results. It has been reported that E2F7 induction upon treatment with topoisomerase II inhibitors doxorubicin and etoposide is p53-dependent (Carvajal *et al.*, 2012). To determine whether the observed accumulation of E2F7 levels upon induction of ICL lesions was mediated by p53, we silenced p53 expression by siRNA interference and examined E2F7 expression upon genotoxic treatment. Surprisingly, loss of p53 did not reduce E2F7 levels (Figure 31B), suggesting that the increase in E2F7 expression upon ICL-producing agents is independent of p53 activity.

Intriguingly, NCS treatment had no effect on E2F7 or p53 accumulation. By contrast, the levels of a p53 target gene, $p21^{Cip1}$, were significantly elevated after NCS treatment, but not after MMC or CSP treatment, reflecting differences in the mechanisms of action of these genotoxic agents at the molecular level.

In functional assays, we found that depletion of p53 did not enhance the recovery of U2OS cells exposed to CSP or MMC as would have been expected if E2F7 levels were controlled by p53 upon ICL-inducing conditions. In fact, the percentage of pH3 positive cells was similar to the siNT condition under p53-depletion conditions (Figure 31C). Conversely, cells with double silencing of E2F7 and p53 exhibited increased recovery competence, which was even higher than the simple silencing of E2F7.

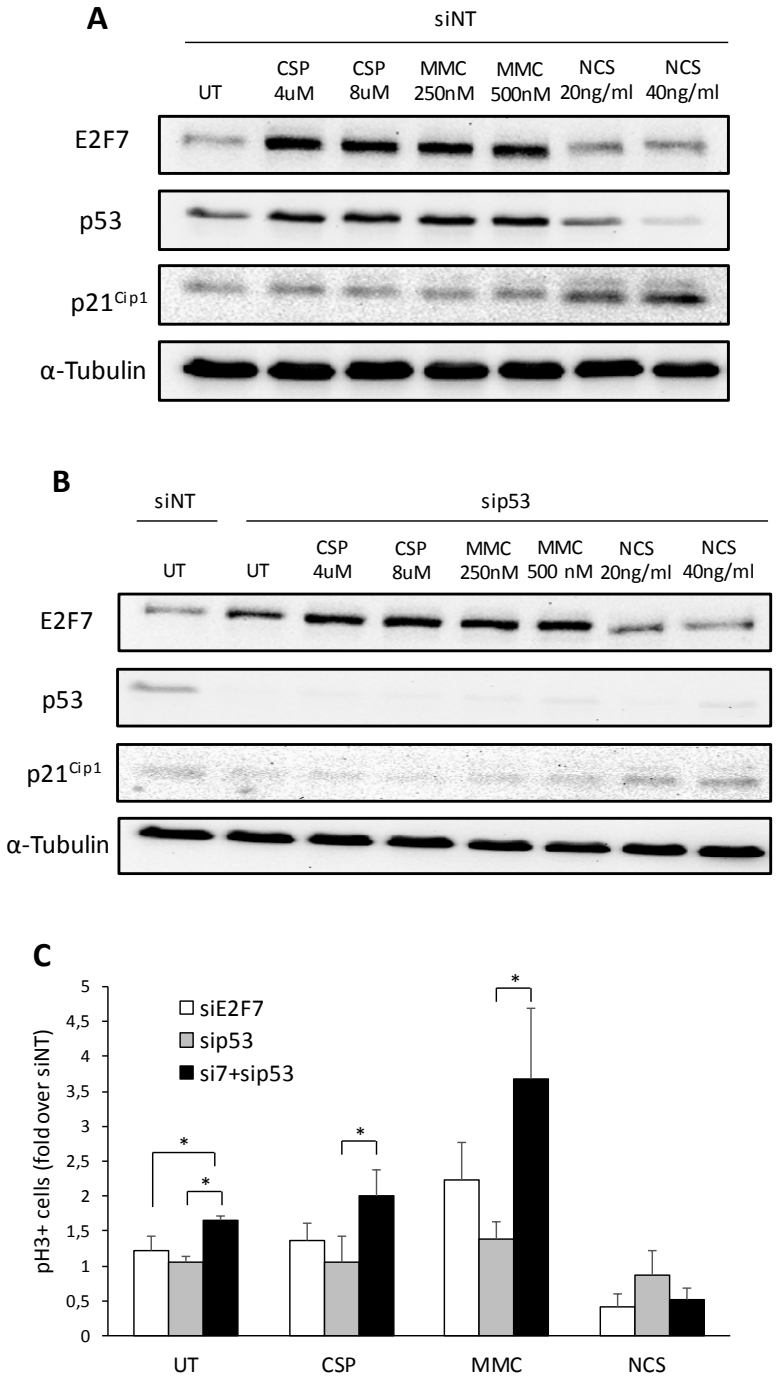

Figure 31: E2F7 induction and functional activity after ICL damage are p53-independent. (A,B) U2OS cells were transfected with siRNA molecules specific for p53 or with siRNA control, and 24 h later treated with MMC (250 and 500 nM), CSP (4 and 8) or NCS (40 ng/ml) for an additional 24 h period. E2F7, p53 and $p21^{Cip1}$ protein levels were analyzed by western blots using specific antibodies. (C) U2OS cells were HU-synchronized and transfected with siNT, siE2F7 and/or sip53. Subsequently, cells were treated as in Figure 26A,B. Finally, cells were treated nocodazole 10 hours later and the percentage of mitotic cells determined by pH3 positivity and FACS analysis. The graphs represent fold-change over siNT values (mean ± SD) of E2F7- and/or p53-depleted pH3-positive cells from three independent experiments. UT, untreated.

To confirm these results we made use of HeLa cells, in which p53 activity is very low due to human papillomavirus derived E6 protein expression in these cells (Haupt *et al.*, 1995). Using the protocol described in Figure 25, we found that transient knockdown of E2F7 in synchronized HeLa cells resulted in a significant increase in cells capable of exiting from the arrest imposed by MMC and CSP in comparison with siNT-transfected cells (Figure 32A). This recovery effect, again, disappeared in E2F7-knockdown cells treated with NCS.

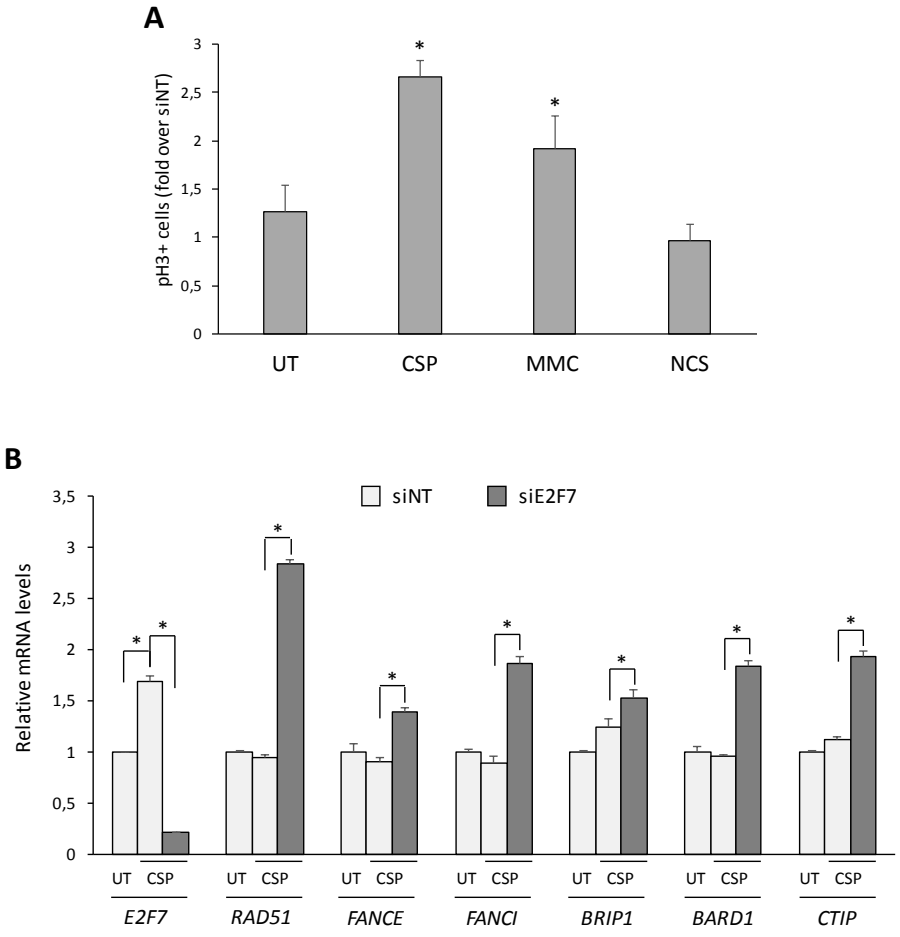

Figure 32: E2F7-mediated cell cycle modulation and transcriptional activity after ICL damage in HeLa cells. (A) Synchronized HeLa cells were transfected and treated as in Figure 31B and the percentage of mitotic pH3-positive cells was analyzed by flow cytometry. The graph represents fold-change of E2F7-depleted pH3-positive cells over siNT values (mean ± SD) from three independent experiments. (*, $P < 0.05$). (B) Asynchronously growing HeLa cells were transfected with siNT and siE2F7 and subsequently treated with 8 M CSP for 24 h. RT-qPCR analyses of indicated genes are shown. Expression values are normalized to the expression of EIF2C2, used as standard control. The graph represents relative mRNA expression average values (mean ± SD) from three independent experiments. (*, $P < 0.05$).

At the gene expression level, exposure to CSP led to a significant induction of E2F7 mRNA levels in HeLa cells (Figure 32B), whereas no effect was observed in the expression of repair genes. However, E2F7 depletion in CSP-treated cells led to a significant increase in the expression of all the analyzed target genes (Figure 32B). Taken together these results point to an essential p53-independent mechanism for E2F7-mediated control of G2 arrest after treatment with compounds producing ICLs.

4.2.3 Role of E2F7 on the repair of ICL-inducing DNA damage

Given the transcriptional repression of E2F7 over genes involved in the repair of ICL-producing DNA damage, we next considered the possibility that E2F7 could specifically contribute to the modulation of this DNA repair pathway. It has been described that treatments with DNA damaging agents that induce interstrand crosslinks give rise to the formation of nuclear foci containing 53BP1 and FANCD2 proteins, two of the main indicators of DNA repair (Rappold *et al.*, 2001; Hussain *et al.*, 2004). Interestingly, we found that depletion of E2F7 caused a significant decrease in the number of 53BP1 and FANCD2 foci upon ICL induction (Mitxelena, 2014).

We next asked whether the lower number of foci detected upon E2F7 depletion was the result of a reduced uploading of repair proteins to damage sites or a more efficient repair activity. In order to answer this question we analyzed foci formation dynamics at early and late treatment time-points. The levels of γ-H2AX, a key protein localized on damage foci were analyzed at 7 and 24h after genotoxic treatments in E2F7-WT and E2F7-KO U2OS cells.

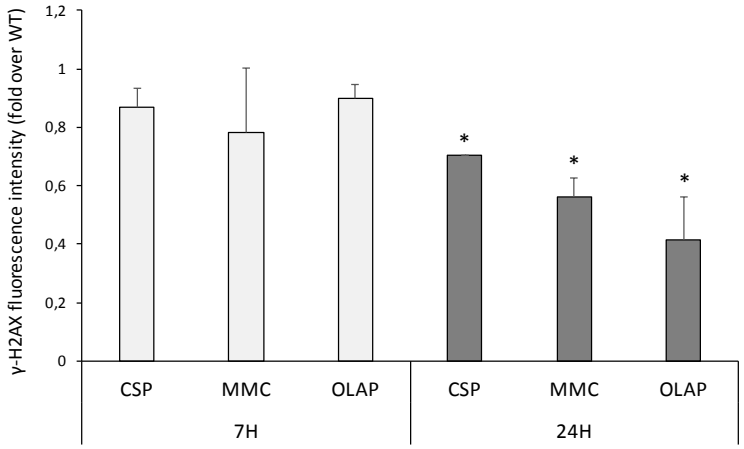

Figure 33: Reduced number of γ-H2AX-positive cells in E2F7-null cells. E2F7- knockout and wild-type U2OS cells were treated with 250nM MMC, 4μM CSP and 2μM OLA, and fixed after 7h or 24h. Cells were stained for γ-H2AX with a FITC-conjugated specific antibody. Fluorescence intensity was analyzed by flow cytometry. Data are represented as the ratio of γ-H2AX-positive cells in E2F7 knockout samples relative to control samples from three independent analyses (*, P<0.05, one sample t-test).

We observed that E2F7-null cells showed lower levels of γ-H2AX compared to E2F7-competent cells after 24 h of genotoxic treatment, whereas the γ-H2AX levels were comparable at earlier time points in both cell lines (Figure 33). These data suggest that E2F7 is dispensable for foci formation. Instead, E2F7 appears to play a key role in the negative control of repair pathways targeting ICL lesions or PARP1 inhibition.

Finally, we assessed one of the main hallmarks of ICL-inducing agents, which is the accumulation of chromosomal aberrations, identified as broken and radial chromosomes in metaphase spreads (Nijman *et al.*, 2005; McCabe, Olson and Moses, 2009). Nearly 40% of the control cells (siNT) displayed radial or broken chromosomes upon MMC exposure whereas silencing of E2F7 provided partial resistance against MMC-induced chromosomal aberrations, with a 2-fold reduction in the number of cells exhibiting radial and broken chromosomes (Figure 34). Thus, E2F7 appears to have a negative role in the repair of chromosomal aberrations resulting from MMC treatment.

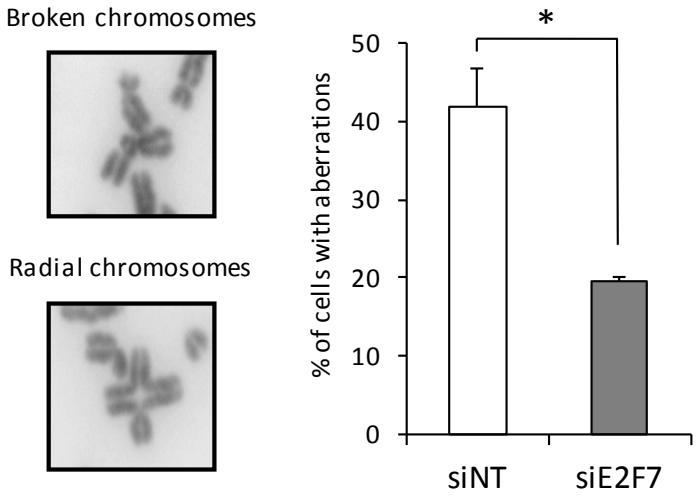

Figure 34: Negative role of E2F7 in the repair of chromosomal aberrations upon ICL damage. siNT and siE2F7 transfected U2OS cells were treated with 250 nM MMC for 48 h and scored for chromosomal aberrations by analyzing metaphase spreads. Representative images of a radial chromosome and a chromatid break are shown. Data are represented as the percentage of cells presenting any chromosomal aberration on each condition (n = 50 cells) in three independent experiments. (*, $P < 0.05$),

4.2.3.1 Role of E2F7 on Homologous Recombination (HR) repair

As has been described in the Introduction section of this report, one of the key steps in the Fanconi Anemia repair pathway is the step mediated by the homologous recombination machinery (Michl, Zimmer and Tarsounas, 2016). In order to assess whether E2F7 has a role in this process we next investigated the efficiency of HR in cells lacking or overexpressing E2F7. For these experiments, we used a U2OS cell line with an integrated direct repeat recombination reporter (DR-GFP). As described in the Materials and Methods section, homology-directed DNA repair can be detected in U2OS-DR-GFP cells when a DSB introduced into the chromosome by the I-SceI endonuclease is repaired by HR to give rise to GFP-positive cells (Richardson, Moynahan and Jasin, 1999).

Knockdown of E2F7 in U2OS-DR-GFP cells resulted in a significant increase in HR efficiency, measured as a percentage of GFP+ cells (Figure 35). Conversely, overexpression of E2F7 in U2OS-DR-GFP cells led to a significant reduction in HR efficiency (Figure 35). Taken together, these results suggest that E2F7 inhibits HR-mediated repair.

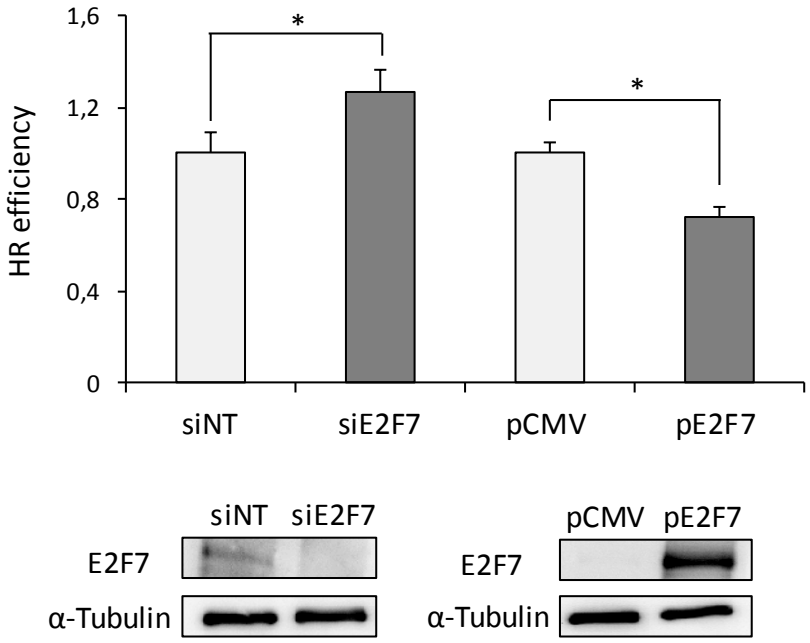

Figure 35: E2F7 affects negatively Homologous Recombination efficiency. U2OS-DR-GFP cells were transfected with siRNAs specific for E2F7 or with a plasmid expressing E2F7, together with an SceI expression vector. GFP-positive cells were analyzed by FACS. Data are shown as a ratio of GFP-positive cells upon E2F7 silencing or overexpressing relative to siNT or empty pCMV transfection. The values shown represent the mean ± SD of three independent experiments (*, $P < 0.05$).

To better define the mechanism underlying E2F7-mediated modulation of DNA repair, we assessed whether the improved homologous recombination, and thus improved genomic stability conferred by loss of E2F7 could be attributed to increased expression of E2F7 target genes that are required for HR repair. We focused on RAD51, a key HR protein and one of the genes identified in this work as direct target of E2F7. Using the DR-GFP reporter system, siRNA-mediated RAD51 depletion led to a reduction in HR repair, whereas E2F7 depletion resulted in increased HR rates, as measured by the differences in the percentages of GFP-positive cells detected by flow cytometry (Figure 36A). In parallel assays, we co-transfected E2F7-specific siRNAs with a concentration of RAD51-specific siRNAs that would attenuate RAD51 expression to the levels found in E2F7 competent cells (Figure 36B).

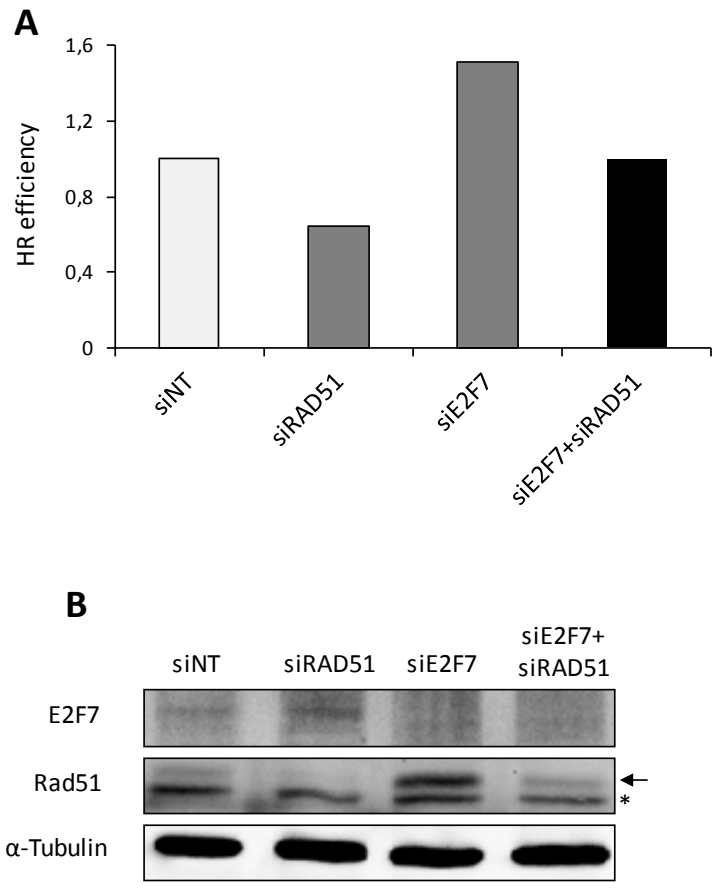

Figure 36: E2F7 suppresses HR through transcriptional repression of DNA repair genes. (A) U2OS-DR-GFP cells were transfected with siRNAs specific for E2F7, RAD51 or with a combination of both and analyzed as in Figure 35. (B) Western blot analysis confirmed knockdown of E2F7 and RAD51 (arrow). Shown is a representative experiment of two independent experiments. A non-specific band in RAD51 blot is indicated with an asterisk.

Interestingly, the increased HR repair efficiency conferred by loss of E2F7 was abrogated under these conditions, and the percentage of GFP positive cells decreased to the levels found in control cells (Figure 36). These results suggest that E2F7 modulates DNA repair through the transcriptional repression of target genes that play a central role in the resolution of DNA lesions requiring homology-directed repair, such as RAD51. These results also suggest that in the absence of E2F7 the HR pathway could become hyperactive and potentially harmful.

4.2.4 Role of E2F7 in genomic stability

Given that E2F7 displays features of an HR inhibitor, we next tested whether downregulation of E2F7 could suppress the genomic instability that characterizes cells with an underlying genetic defect in HR. We hypothesized that the increased recombination capacity conferred by E2F7 depletion might promote DNA repair and protect these cells from genomic instability and cell death.

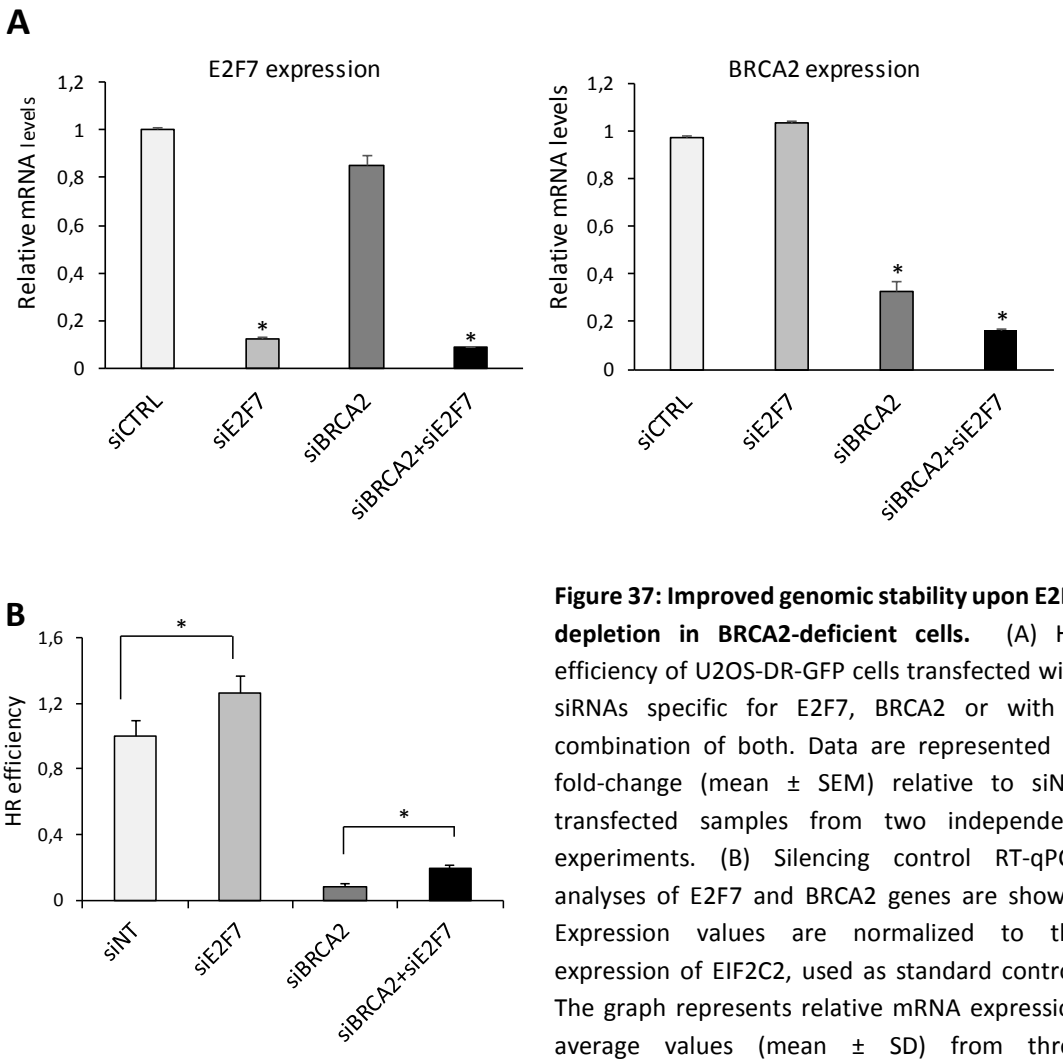

Figure 37: Improved genomic stability upon E2F7 depletion in BRCA2-deficient cells. (A) HR efficiency of U2OS-DR-GFP cells transfected with siRNAs specific for E2F7, BRCA2 or with a combination of both. Data are represented as fold-change (mean ± SEM) relative to siNT-transfected samples from two independent experiments. (B) Silencing control RT-qPCR analyses of E2F7 and BRCA2 genes are shown. Expression values are normalized to the expression of EIF2C2, used as standard control. The graph represents relative mRNA expression average values (mean ± SD) from three independent experiments. (*, $P < 0.05$).

To test this possibility we made use of two systems, both of which involve BRCA2, a key player in HR-mediated repair (Powell and Kachnic, 2003). In the first system, we used RNA interference to attenuate the expression of BRCA2 and E2F7 in the U2OS-DR-GFP cell line (Figure 37A). As expected, knockdown of BRCA2 abolished HR repair in this assay. Interestingly, we observed that co-depletion of E2F7 could improve HR in cells with reduced BRCA2 activity (Figure 37B), suggesting that E2F7 silencing alleviates the genomic instability provoked by the absence of BRCA2.

In the second system, we made use of CAPAN-1 pancreatic adenocarcinoma cells, which are defective in HR due to a loss-of-function mutation of BRCA2 (McCabe *et al.*, 2005). It has been recently demonstrated that, cancer cells deficient in HR repair through loss of BRCA2 are hypersensitive to inhibition of PARP-1, a key protein in the repair of DNA damage involving DSBs (Lord and Ashworth, 2017). Thus, we examined the impact of E2F7 upon PARP1 inhibition in CAPAN-1 cells by performing long-term clonogenic survival assays.

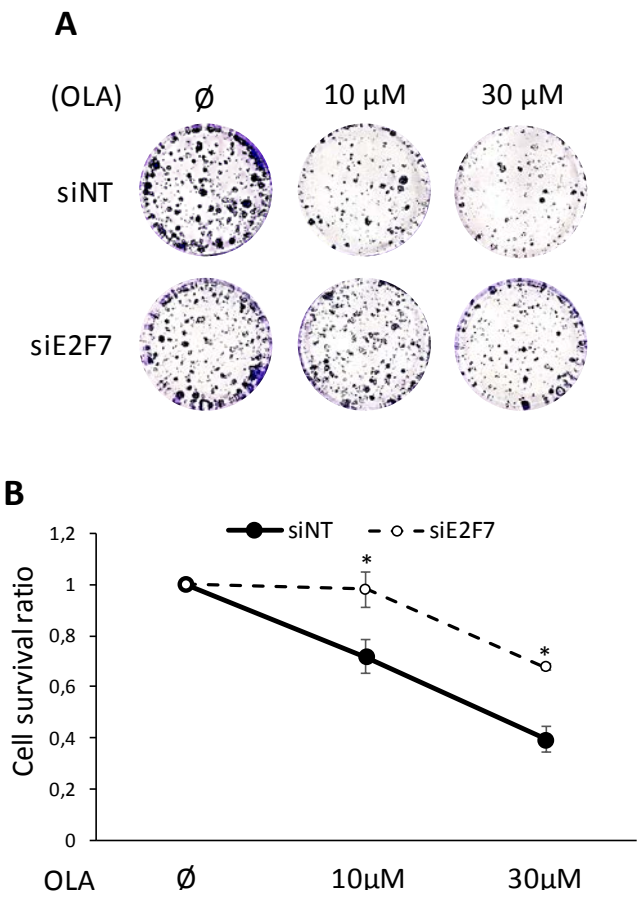

Figure 38: Improved cell survival upon E2F7 depletion in BRCA2-deficient cells. Clonogenic survival assays were carried out with siE2F7 or siNT transfected CAPAN-1. Cells were treated with indicated doses of OLA for 24 h and cultured for two additional weeks at low density in treatment-free medium. After this period, colonies were fixed with paraformaldehyde and stained with crystal violet. Finally, the number of surviving colonies was scored in each condition. (A) Representative images of colony formation in each condition. (B) Colony formation ratio was calculated by normalizing data against untreated (Ø) samples in each transfection condition. The graph represents colony survival ratio of OLA-treated samples against untreated samples (mean ± SD) from three independent experiments. (*, $P < 0.05$)

As expected, treatment of BRCA2-deficient CAPAN-1 cells with PARP1 inhibitor OLA compromised cell viability, by reducing significantly the number of surviving colonies (Figure 38). Remarkably, downregulation of E2F7 expression in CAPAN-1 cells was associated with increased resistance to the PARP1 inhibitor OLA, as the number of colonies scored in E2F7-depleted cells was significantly higher in both OLA concentrations that were tested (Figure 38). These findings suggest that E2F7 knockdown confers an increased resistance to chemotherapy in cells carrying defects in genes involved in HR.

The results compiled in this section regarding the role of E2F7 in the Fanconi Anemia and HR-mediated repair pathways have been recently published (Mitxelena*, Apraiz*, Vallejo-Rodríguez* *et al*, 2018).

4.2.5. Role of E2F7 in the response to DNA alkylation damage

We have shown that lack of E2F7 confers an advantage to cells that have been treated with PARP1 inhibitor Olaparib, as E2F7-depleted cells can progress in the cell cycle more efficiently and show a better clonogenicity than E2F7-competent cells (Figure 27). PARP1 has been described as a key component of several DNA repair pathways. In addition to its role in HR-mediated repair mentioned above, PARP1 has been described as a key member of the machinery responsible for the repair of single-strand DNA breaks (Ray Chaudhuri and Nussenzweig, 2017). Single-strand DNA breaks (SSB) are commonly produced by DNA oxidation or alkylation. They are detected and subsequently processed by the Base Excision Repair (BER) pathway, and finally repaired by a specific SSB-repairing machinery (Kim, Wilson and III, 2012).

Given the impact of E2F7 depletion in the cellular responses to PARP1 inhibition, we wondered whether E2F7 could play a role in the repair pathway that targets single-strand DNA breaks. To address this question we treated E2F7-deficient and E2F7-proficient U2OS cells with methyl methanesulfonate (MMS). This compound produces alkylating damage in the DNA molecule that can be detected by the BER pathway and repaired by the SSB repair machinery (Wyatt and Pittman, 2006).

4.2.4.1. Role of E2F7 in the cellular recovery from alkylating damage on DNA

Following the protocol described in Figure 39A, we analyzed the contribution of E2F7 to cellular responses upon MMS exposure in U2OS cells, measured as the fraction of cells capable of undergoing mitosis. We found that the fraction of cells capable of exiting from the arrest imposed by MMS is significantly increased in the absence of E2F7 (Figure 39B). This result points to a negative role for E2F7 in the cellular recovery from alkylating damage in DNA.

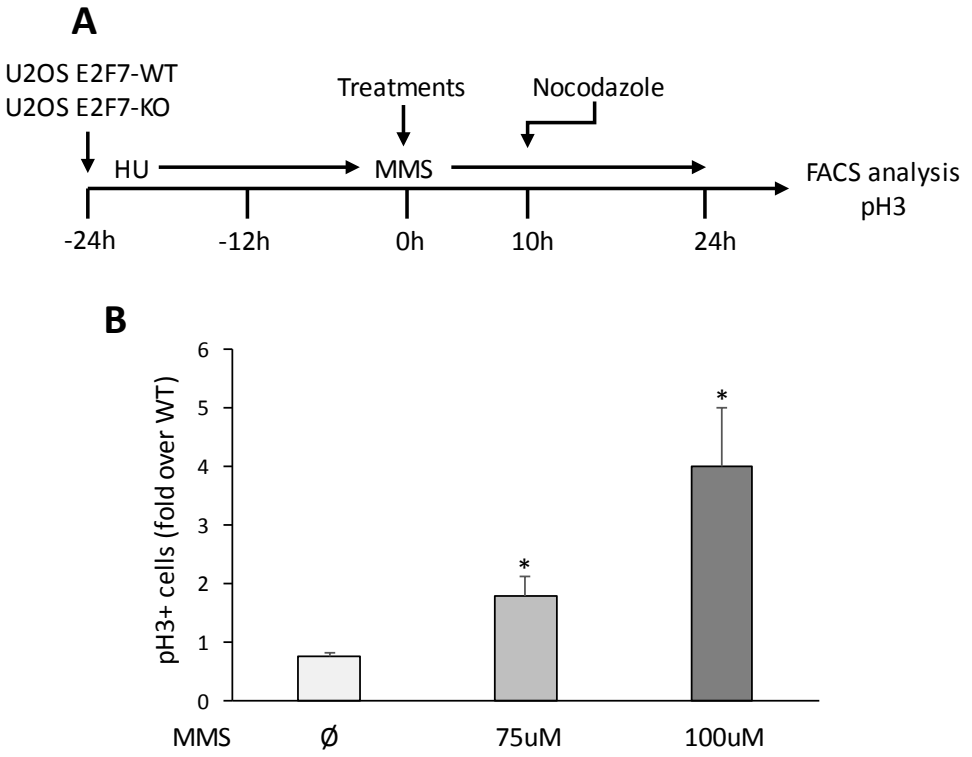

Figure 39: E2F7 controls cellular recovery after DNA alkylation damage caused by MMS. U2OS WT and E2F7 KO cells were HU-synchronized for 24h. After HU treatment, cells were released into the cell cycle and treated for 24 hours with indicated doses of MMS. Nocodazole was added 10 hours later. (A) Schematic diagram of the cellular recovery experiment. (B) The percentage of mitotic cells determined by pH3 positivity after FACS analysis is shown comparing E2F7 KO cells over E2F7 WT cells. The graph represents fold-change of E2F7-deficient pH3-positive cells over E2F7-proficient cells values (mean ± SD) from three independent experiments. (*, $P < 0.05$).

To examine the long-term effect of E2F7 in MMS-treated cells, we carried out clonogenic survival assays with U2OS cells displaying wild-type or null E2F7 levels. Cells were treated with MMS for 24 hours and their viability was assessed by their capacity to form colonies within a period of 14 days. As reported in Lee *et al.*, 2007, increasing amounts of MMS reduced the viability of wild-type control cells. Remarkably, we found that E2F7 knockout cells treated with MMS presented higher clonogenicity rates relative to E2F7-WT cultures (Figure 40).

These results suggest that lack of E2F7 confers a resistance to cell death induced by MMS treatment owing to an improved recovery from the checkpoint imposed by this genotoxic compound.

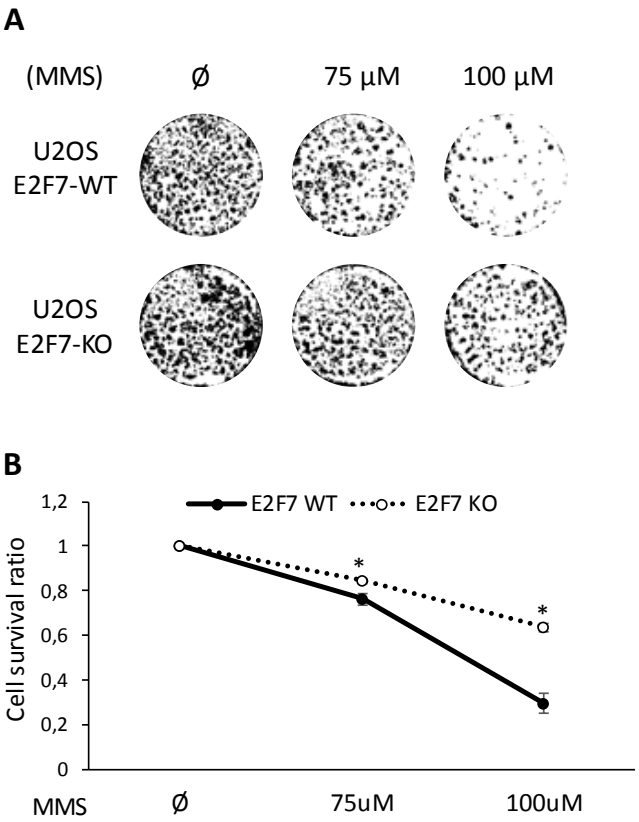

Figure 40: E2F7 silencing provides long-term resistance against MMS. U2OS WT or E2F7 KO cells were treated with 75 and 100 µM of MMS for 24 h and cultured for two additional weeks in treatment-free medium. After this period colonies were stained fixed with paraformaldehyde and stained with crystal violet. Finally, were scored in each condition. (A) Representative images of colony density in each condition. (B) Colony formation ratio was calculated normalizing data against untreated (Ø) samples on each silencing condition. The graph represents colony survival ratio of treated samples against untreated samples (mean ± SD) from three independent experiments. (*, P < 0.05)

4.2.4.2 Role of E2F7 in the expression of alkylation damage repair genes

We have described in the previous section that E2F7 modulates ICL-producing damage repair through the transcriptional regulation of key components of the repair machinery (Figure 30). We next wondered whether E2F7 was similarly involved in modulating responses to DNA alkylation damage through the transcriptional regulation of key proteins involved in BER and SSBR pathways.

XRCC1 and DNA ligase III (LIG3) are key components of BER and SSBR pathways (Kim, Wilson and III, 2012). XCRR1 is a scaffold protein essential for the recruitment of other proteins such as LIG3, which is the ligase responsible of the last step of the repair process. The promoters of both genes harbor consensus E2F binding sites, as it appears from our visual inspection of their regulatory sequences in Ensembl (https://www.ensembl.org/index.html). Moreover, E2F1 protein has been described as a direct transcriptional regulator of XRCC1 protein (Chen *et al.*, 2008). These evidences suggested that E2F7 could be regulating directly the expression of these two proteins that are critical for the repair of DNA alkylation damage.

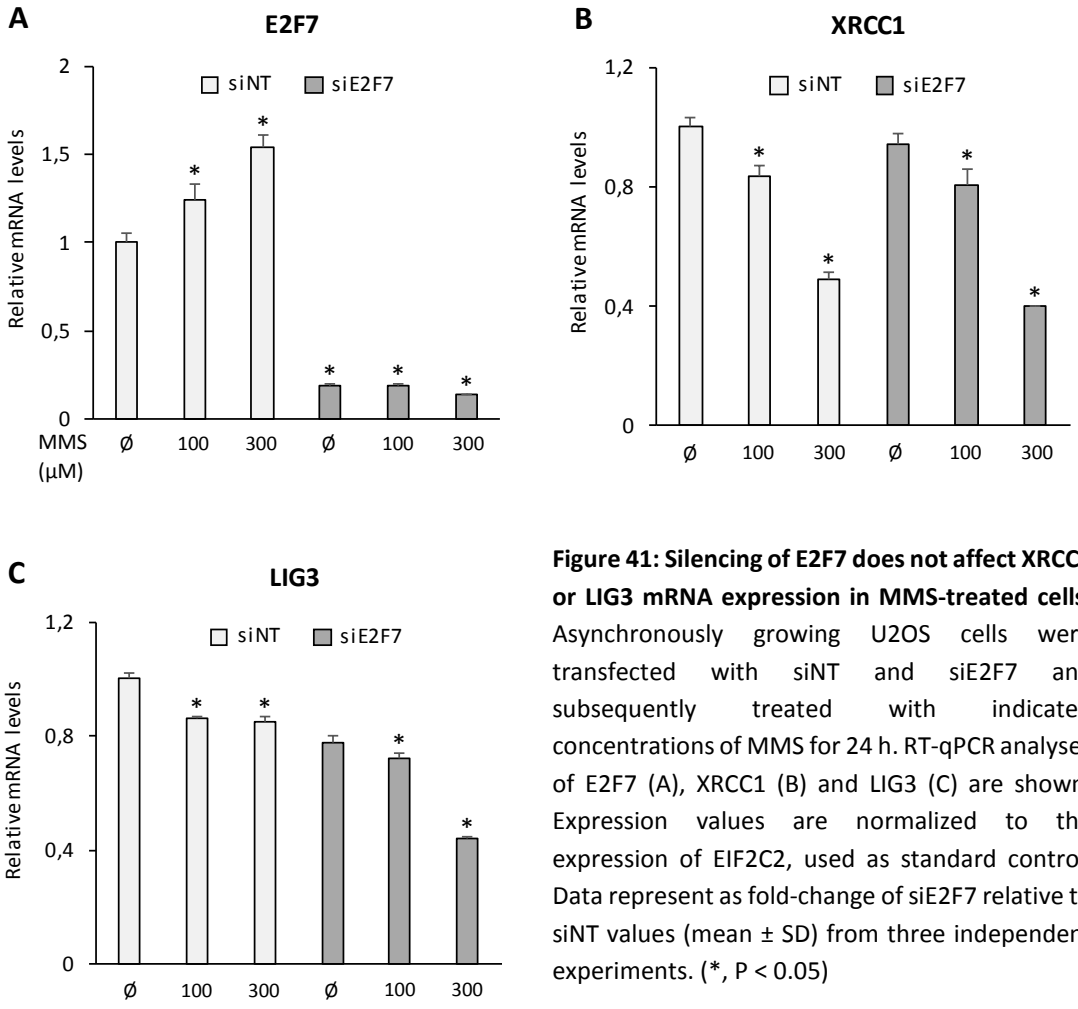

Figure 41: Silencing of E2F7 does not affect XRCC1 or LIG3 mRNA expression in MMS-treated cells. Asynchronously growing U2OS cells were transfected with siNT and siE2F7 and subsequently treated with indicated concentrations of MMS for 24 h. RT-qPCR analyses of E2F7 (A), XRCC1 (B) and LIG3 (C) are shown. Expression values are normalized to the expression of EIF2C2, used as standard control. Data represent as fold-change of siE2F7 relative to siNT values (mean ± SD) from three independent experiments. (*, $P < 0.05$)

To test this hypothesis, we performed gene expression analyses with U2OS cells that had been transfected with siNT or siE2F7 molecules and subsequently treated with MMS. As shown in Figure 41A and Figure 42A,B, MMS treatment induced the expression of E2F7 in a dose-dependent manner at the mRNA and protein level, similarly to what was found for ICL-inducing agents. In contrast to E2F7, the expression of XRCC1 and LIG3 was consistently reduced upon MMS treatment, both at the RNA and protein levels (Figure 41B,C and Figure 42A).

However, contrary to what we found upon treatment with ICL-inducing conditions, silencing of E2F7 did not affect significantly the expression of these genes in MMS treated cells (Figure 41 and Figure 42). These findings suggest that E2F7 does not regulate BER and SSBR pathways at the transcriptional level and points to a fundamental difference in the mechanisms by which E2F7 modulates the cellular responses to specific DNA lesions.

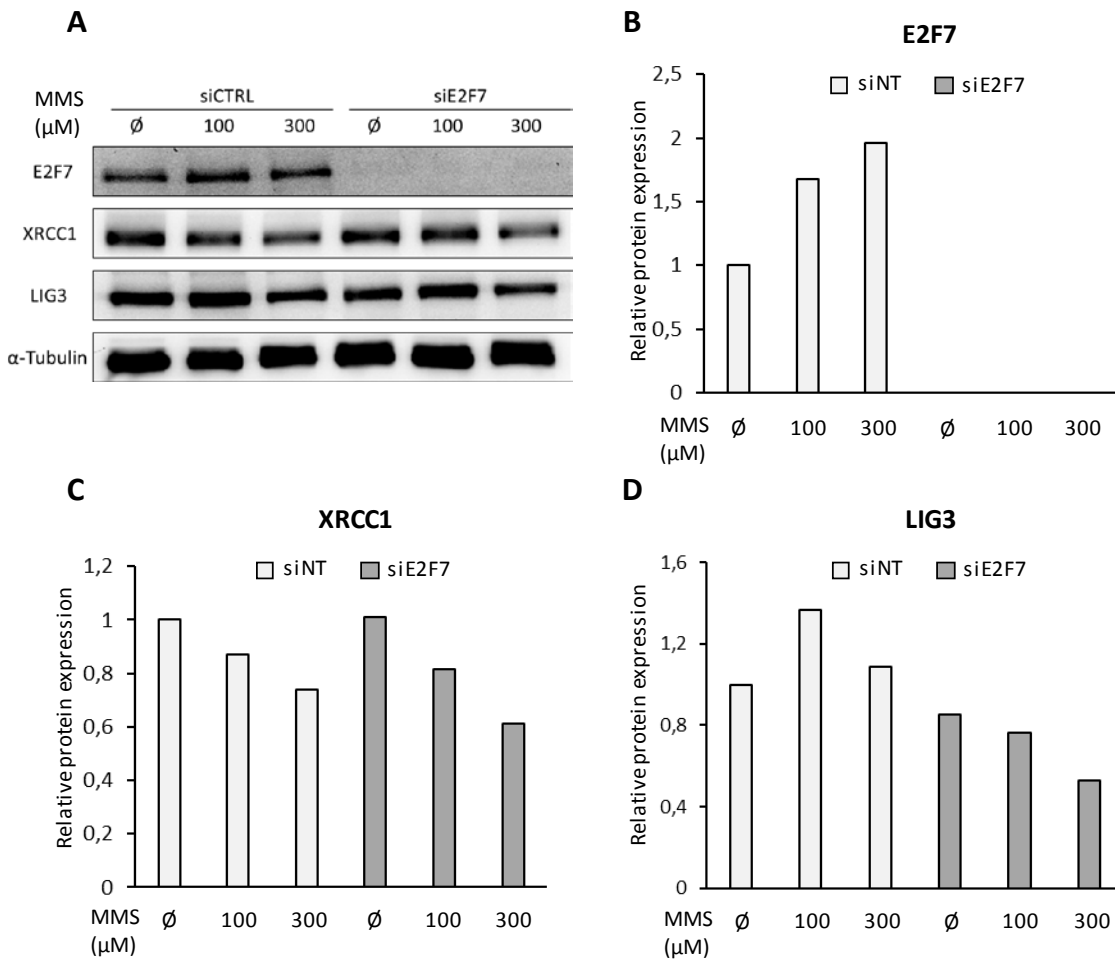

Figure 42: Silencing of E2F7 does not affect XRCC1 or LIG3 protein expression in MMS-treated cells. Asynchronously growing U2OS cells were transfected with siNT and siE2F7 and subsequently treated with indicated concentrations of MMS for 24 h. (A) Protein expression levels were analyzed by western blot using specific antibodies against E2F7, XRCC1, LIG3 and α-Tubulin proteins. Densitometry of E2F7 (B), XRCC1 (C) and LIG3 (D) protein levels relativized to α-Tubulin levels in each sample.

4.2.4.3 Interaction of E2F7 with proteins involved in DNA alkylation repair

We next set out to investigate E2F7-dependent mechanisms for the alkylating damage response that did not involve transcriptional regulation. A central mechanism to regulate protein activity involves direct protein-protein interaction (De Las Rivas and Fontanillo, 2010). We used the bioinformatics tool ELM (http://elm.eu.org/) to search for functional motifs in the amino acid sequence of E2F7 that could be involved in the interaction with other proteins. We identified several functional linear motifs distributed along the sequence of E2F7. Interestingly, this analysis pinpointed a motif in E2F7 that interacts with the BRCT domain, an aminoacid tandem repeat that functions as a phosphoprotein binding domain (Yu *et al.*, 2003).

The BRCT domain was first identified as part of the breast cancer suppressor protein BRCA1 (Bork *et al.*, 1997), but it was subsequently found in many proteins of the DNA damage response such XRCC1 (Zhang *et al.*, 1998). In fact, the BRCT domain in XRCC1 binds and stabilizes DNA Ligase III protein, and disruption of this binding prevents XRCC1-dependent DNA repair (Della-Maria *et al.*, 2012). The presence of this BRCT-binding motif in E2F7 could modulate the activity of repair proteins carrying BRCT motif through a direct protein-protein interaction.

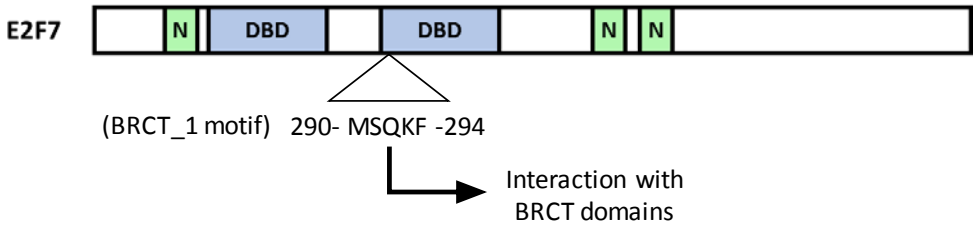

Figure 43: Motif analysis in E2F7 protein sequence. Schematic representation of the protein E2F7 with the localization of BRCT domain interaction motif. BRCT_1 motif was identified between 290 and 294 residues of E2F7 protein, which allows the interaction with BRCT domain present in target proteins. N, nuclear localization motif. DBD, DNA binding domain.

In order to confirm the ELM bioinformatics tool prediction, we next performed protein co-immunoprecipitation experiments. For these experiments, we used U2OS-TetOn cells (described in Materials and Methods section) that were transfected with a plasmid encoding the E2F7 protein tagged with FLAG (U2OS-TRE-E2F7-FLAG) or with an empty plasmid carrying the FLAG tag (U2OS-TRE-FLAG). These plasmids carry the tetracycline response elements in the promoter of the gene, thus allowing the overexpression of transfected recombinant genes in a regulated manner upon the addition of doxycycline, a tetracycline analog (Das, Tenenbaum and Berkhout, 2016).

In order to identify the proteins that could be detected exclusively in E2F7-FLAG overexpressing cells and, therefore, could interact potentially with E2F7, U2OS-TRE-E2F7-FLAG and U2OS-TRE-FLAG cells were seeded and treated with doxycycline 2 µg/ml for 24h hours in order to overexpress E2F7-FLAG or FLAG. Then protein lysates were collected and subsequently immunoprecipitated, as indicated in Materials and Methods section, using antibodies against FLAG tag. As shown in Figure 44, we observed high amounts of E2F7 protein immunoprecipitated in E2F7-FLAG transfected cells (IP1, immunoprecipitation elution 1), which were absent in the IP2 (immunoprecipitation elution 2), or in NB (not bound) fractions. As a control, we showed no E2F7 immunoprecipitated in empty FLAG-transfected cell.

Remarkably, antibodies against FLAG could immunoprecipitate a substantial amount of XRCC1 and LIG3 proteins in E2F7-FLAG transfected cell lysates in comparison with cells transfected with the empty plasmid (compare IP1 elutions in both cases). Although further experiments are needed to confirm these findings, the immunoprecipitation results suggest a direct interaction between E2F7 and the proteins XRCC1 and LIG3 that could account for the E2F7-driven modulation of DNA alkylating damage response found in this work.

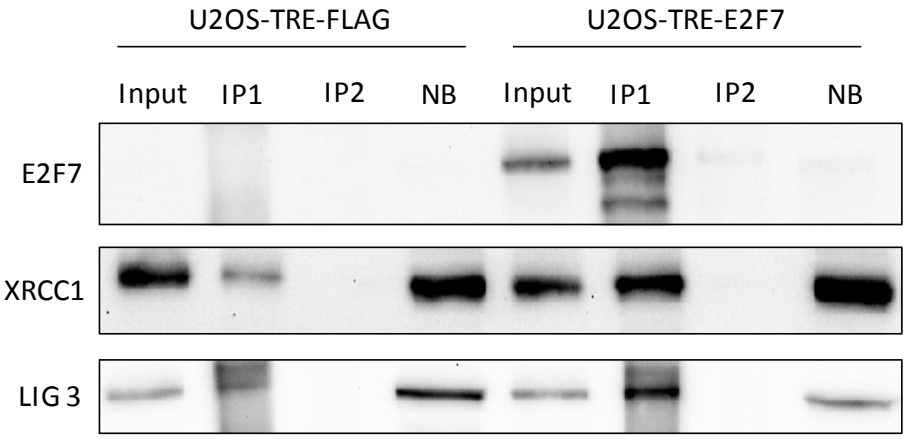

Figure 44: Specific interaction of E2F7 with the repair proteins XRCC1 and LIG3. U2OS TetOn cells were stably transfected with pTre-E2F7-FLAG and pTre-FLAG-empty vectors and after addition of doxycycline these vectors were overexpressed. An immunoprecipitation was carried out against FLAG tag and the elutions were blotted with specific antibodies against E2F7, XRCC1 and LIG3. (Input, immunoprecipitation elution 1 (IP1), immunoprecipitation elution 2 (IP2), Not Bound fraction (NB)). Note: endogenous E2F7 levels are not detected in the input fraction due to the short exposure of the image in order to detect an overexpression.

Collectively, these results point to a novel E2F7-driven regulatory mechanism in DNA alkylation damage response. This novel mechanism could involve protein-protein interaction between E2F7 and key proteins of the repair of this DNA damage, adding a new layer of complexity to the mechanisms underlying E2F7-regulated DNA damage responses.

4.3. THE E2F7-E2F1 AXIS IN CELL PROLIFERATION. A SEARCH FOR MODULATORS OF E2F1-MEDIATED APOPTOSIS

E2F1 is the best known transcriptional target of E2F7 (Li *et al.*, 2008; Moon and Dyson, 2008; Zalmas *et al.*, 2008; Carvajal *et al.*, 2012; Mitxelena, 2014; Thurlings *et al.*, 2016). Increasing cellular levels of E2F7 (and/or E2F8) repress E2F1 expression, whereas reducing the levels of E2F7 (and/or E2F8) results in aberrantly induced E2F1 expression and activation. Furthermore, it has been shown that the high apoptosis rates detected in tissues derived from $E2F7^{-/-}$ or $E2F7^{-/-}$/ $E2F8^{-/-}$ compound mice are triggered by the aberrant levels of E2F1, since ablation of E2F1 in cells derived from $E2F7^{-/-}$/ $E2F8^{-/-}$ mice blocks apoptosis-driven lethality of DKO mice (Li *et al.*, 2008). Moreover, loss of E2F1 accelerates tumorigenesis in E2F7/8-deficient skin tumors (Thurlings *et al.*, 2016). These findings have suggested the existence of an E2F1-E2F7/8 axis that is critical for tissue homeostasis, whose dysregulation can lead to several unfavorable outcomes.

Thus, to gain a better understanding of E2F7 function, it is necessary to learn about the pro-apoptotic activity of E2F1, and how this activity is restrained by counterbalancing signals to facilitate the neoplastic transformation. However, with the exception of PI3K/AKT signaling pathway which can partially block the apoptotic program of E2F1 overexpressing cells (Hallstrom, Mori and Nevins, 2008), little is known about the cellular signals that mediate tumor development under excessive E2F1 activity. The identification and characterization of these modulators could help in the development of therapeutic strategies against tumor progression.

4.3.1. Screening assay to identify modulators of E2F1-driven apoptosis

In order to identify signaling pathways that could be modulating E2F1-driven apoptosis, we carried out a cell-based phenotypic screening assay using a library of 4,216 pharmaceutical compounds (supplied by Chemical Biology Consortium Sweden). We selected this library because all its compounds are approved by the FDA to be used in human clinical trials. Furthermore, they are actively being used for high-throughput screening strategies, so that dose and safety have already been confirmed. This library contains structurally diverse, medicinally active and cell permeable drugs, and a rich documentation on structure and IC50 data is accessible for each compound. All the screening experiments were carried out in Dr. Fernandez-Capetillo´s lab (Karolinska Institutet, Stockholm) as part of our ongoing collaboration, under the supervision of Dr. Jordi Carreras.

To work with an E2F1-driven apoptosis system, we generated U2OS-TRE-E2F1 cells (described in Materials and Methods section). These cells overexpress E2F1 and, therefore, promote E2F1-driven apoptosis upon doxycycline addition in a reproducible manner. Additionally, with this system we avoid cytotoxic effects of transfection reagents used in transitory overexpression systems. U2OS-TRE-E2F1 cultures induce overexpression of E2F1 and apoptosis as early as 24h after doxycycline addition, and the percentage of apoptotic cells increases substantially over time (Figure 45).

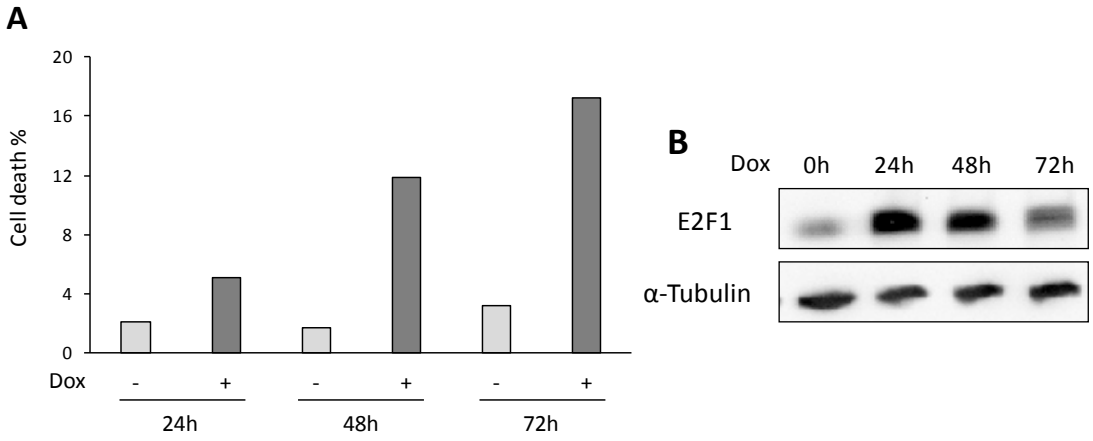

Figure 45: Cell death analysis upon E2F1 overexpression. U2OS-TRE-E2F1 cells were treated with 2 µg/ml doxycycline for the indicated times. (A) Cells were fixed, stained with propidium iodide (PI) and cell cycle profile was analyzed by flow cytometry. Cell death percentages were calculated as the sub-G1 cell fraction over total cell amount. (B) E2F1 overexpression was checked by Western Blot using a specific antibody against E2F1.

To identify new modulators of E2F1-driven apoptosis we selected the 48h doxycycline time point. We reasoned that the percentage of cell death of around 10% triggered by E2F1 at 48h could allow the detection of two types of compounds: those compounds that would increase the apoptotic rate triggered by E2F1 and those compounds that would decrease the apoptotic rate. In the first case we would be looking for compounds that sensitized cells against E2F1-driven apoptosis, that is, compounds that could be inhibiting a pathway that counterbalances E2F1-induced cell death. In the second case, we would be looking for compounds that protected cells against E2F1-driven apoptosis, that is, compounds that could be blocking the apoptosis pathway.

We carried out a high-throughput screening assay as described in Materials and Methods section following a methodology developed by Fernandez-Capetillo´s group. Briefly, U20S-TRE-E2F1 cells were seeded at $1x10^4$/well density in 384-well plates. A total of 45 plates were used to screen the 4216 compounds in triplicates. The following day, doxycycline was added at 2 µg/ml and 24 hours after the activation of E2F1 expression, each triplicate well was treated with an individual compound at a final concentration of 10µM. Subsequently, 24 hours after compound addition, cells were fixed and stained with Propidium Iodide (PI) and Hoechst. We used Propidium Iodide (PI) and Hoechst double staining to detect differences in cell death at high-throughput screening levels. PI positive cells were identified as cells whose membranes had been compromised, which is one of the first hallmarks of cells undergoing apoptosis, and Hoechst staining provided us the total amount of cells in each well. The ratio of PI positive cells/Hoechst positive cells, allowed us to calculate the percentage of cell death in each treatment. Finally, we took individual photos of each well, and image analysis was done using Cell Profiler program (Carpenter *et al.*, 2006) where nuclei were automatically counted. After image acquisition, we calculated the percentage of cell death (PI positive cells/Hoechst positive) for each treatment, which was the average of three replicate wells.

Each plate carried several positive control wells (i.e. treated with doxycycline, and overexpressing E2F1, but without any treatment) and negative control wells (i.e. without E2F1 overexpression and without treatments), which facilitate the comparison of results among plates. As expected, the average of all positive control replicate wells overexpressing E2F1 showed a significantly higher cell death percentage (7.2%±) than the average of all negative control replicate wells (1.24%±) (Figure 46).

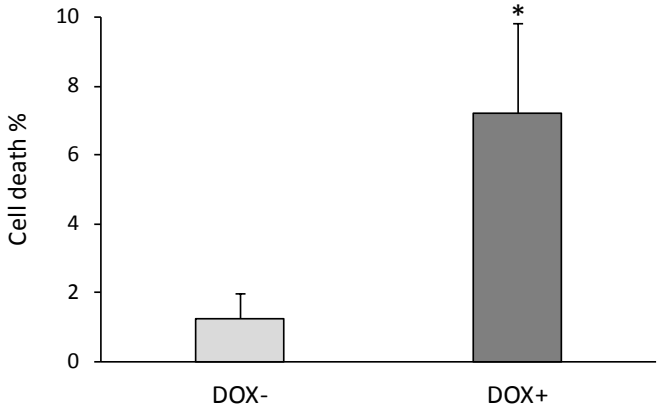

Figure 46: Effect of E2F1 overexpression on cell death percentage in the high-throughput screening. U2OS-TRE-E2F1 cells were cultured for 48 hours in the presence or absence of doxycycline and cell death fraction of each condition (± E2F1 overexpression) was analyzed with PI staining. Data are a compilation of all control wells for each condition in 45 plates. (*, $P < 0.05$)

In order to search for reliable modulators of E2F1-mediated apoptosis, we focused on compounds that changed significantly the percentage of cell death exhibited by the positive controls. On the one hand, we searched for compounds that increased this cell death percentage more than four times the standard deviation of the positive control. We considered these compounds as compounds that increase significantly E2F1-mediated apoptosis. On the other hand, we searched for compounds that decreased this cell death percentage more than two times the standard deviation of the positive control. We considered these compounds as compounds that decrease significantly the E2F1-mediated apoptosis. The different criterion between the two groups is explained because of the small percentage margin between apoptotic rates of negative and positive controls.

Using the described criteria, we identified 315 compounds as significant modulators of E2F1-mediated cell death.

4.3.2. Validation of selected E2F1-driven apoptosis modulators

Our next step consisted of validating the screening results. To this end, we repeated the protocol used in the high-throughput screening with the 315 compounds that gave a significant difference in the first screen. In this occasion, we used six 384-well plates, three of them for cells without doxycycline addition and, therefore, without E2F1 overexpression and three with doxycycline addition and E2F1 overexpression. As in the first screen, the average of all the wells overexpressing E2F1 showed a significantly higher percentage of apoptosis (9.33%±) than in the non-overexpressing control cells (1.42%±) (Figure 47).

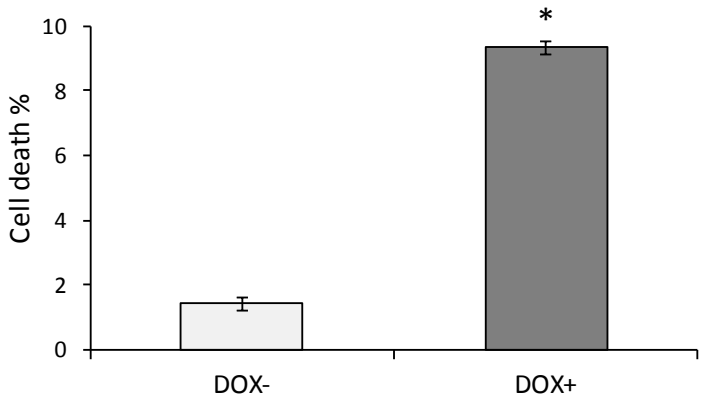

Figure 47: Effect of E2F1 overexpression on cell death in validation screen. U2OS-TRE-E2F1 cells were cultured for 48 hours in the presence and absence of doxycycline and cell death fraction of each condition (± E2F1 overexpression) was analyzed with PI staining. Data are a compilation of all control wells for each condition in 6 plates. (*, $P < 0.05$).

Using the same standard deviation criterion described above, we validated 61 compounds as significant modulators of E2F1-mediated cell death. Among these 61 compounds, we identified HDAC inhibitors (4 different compounds), serotonin receptor antagonists (4 different compounds), calcium channels inhibitors (4 different compounds) and kinase modulators (3 inhibitors and 3 activators) (Figure 48). While most of the compounds acted promoting cell death after E2F1 overexpression, we identified three compounds that activate protein kinases and protect cells with aberrant E2F1 levels.

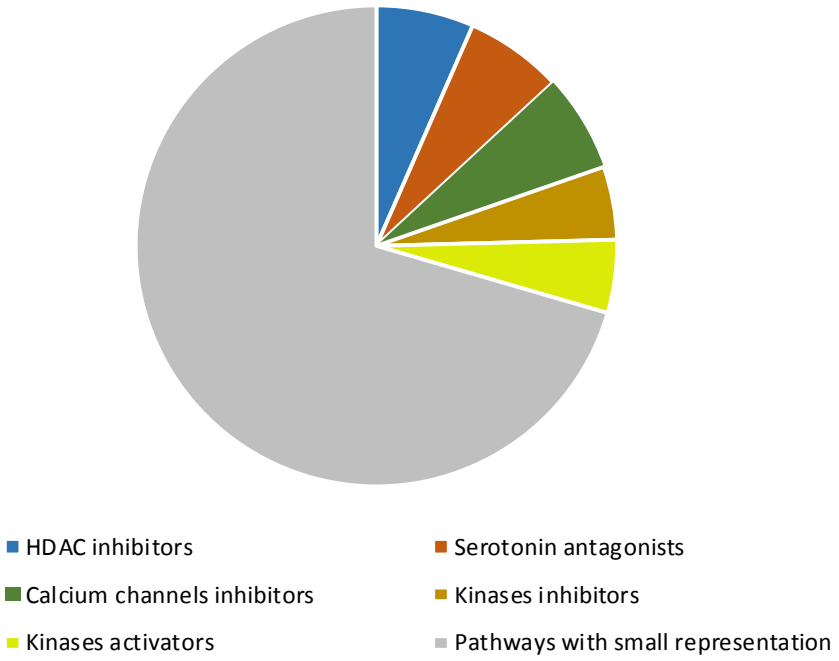

Figure 48: Pathways modulating E2F1-driven cell death. Validated E2F1-driven cell death modulator compounds were classified in pathways. Those pathways with 3 or more compounds identified in the assay as modulators are indicated.

We focused our attention on the group of serotonin receptor antagonists that our screen identified as possible modulators. Serotonin receptors are a large family of proteins (5-HT1 to 5-HT7) required for the membrane transduction of the serotonin signaling cascade. In our validation assay, we identified GR-127935 (5-HT1B/1D antagonist), RS-39604 (5-HT4 antagonist), Indatraline and Vortioxetine (general serotonin receptors antagonists) as compounds that could increase significantly E2F1-induced apoptosis (Table 11). Of these, GR-127935 and RS-39604 stand out as particularly interesting for sensitizing cells that overexpress E2F1: (1) they have minimal effect on cell death in cells without E2F1 overexpression (1.42% vs 2.3% and 4.7%) (2) they have a significant effect upon E2F1 overexpression (9.33% vs 20.6% and 34.4%) and (3) they have shown specificity for serotonin receptors, unlike Indatraline and Vortioxetine (Table 11).

Table 11: List of serotonin receptor antagonists identified as E2F1 driven cell death modulators.

Name	Therapeutic class	% Cell Death	
		DOX -	DOX +
GR 127935 hydrochloride	5-HT1B/1D antagonist	2.30 (±0.44)	20.64 (±2.12)
RS 39604 hydrochloride	5-HT4 antagonist	4.72 (±0.07)	34.45 (±1.41)
Indatraline hydrochloride	5-HT antagonist	5.31 (±0.99)	33.74 (±4,24)
Vortioxetine hydrobromide	5-HT antagonist	52.48 (±3.54)	100 (±3,54)
No compound	-	1.42 (±0.18)	9.33 (±1.79)

4.3.2. Serotonin receptor antagonists as E2F1-mediated cell death modulators

We have started to explore the impact of serotonin receptor antagonists on E2F1-mediated cell death. To this end, we have selected the two compounds that looked more promising in the screening assay, and we have treated the U2OS-TRE-E2F1 cells with several doses of the compounds in the presence or absence of doxycycline for 24 and 48h. Cell viability was determined by measuring the absorbance of crystal violet-stained cells.

As shown in Figure 49, both serotonin receptor antagonists induced a slight reduction in cell viability in cells that did not overexpress E2F1, especially at concentration of 10 µM, which was the one used in the screening assay. Importantly, both serotonin receptor antagonists increased significantly the cell death induced by E2F1. In the case of RS-39604, all the tested concentrations elevated E2F1-driven apoptosis in a dose-dependent manner, with a maximum effect triggered by 10 µM both at 24 and at 48h. In the case of GR-127935, two of the tested concentrations resulted in significant cell death, with a maximum with a maximum effect with the 10 µM, at 24h and with the 5 µM concentration at 48h.

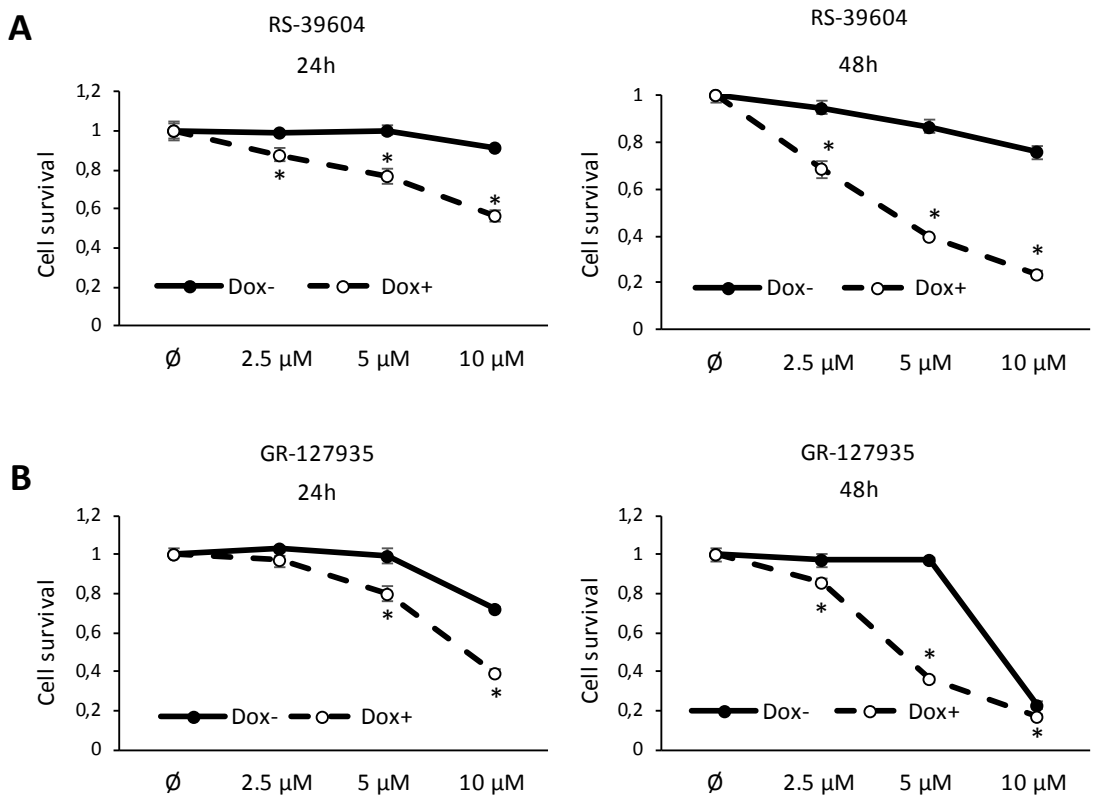

Figure 49: Specific serotonin receptor antagonists sensitize E2F1-overexpressing U2OS cells to cell death. U2OS-TRE-E2F1 cells were treated with doxycycline for 48h and with indicated doses of compounds for 24 and 48h. After that, cell were fixed using paraformaldehyde and stained with crystal violet. Crystal violet was dissolved with acetic acid and the absorbance was measured by spectrophotometry. Cell survival ratio was calculated by normalizing the absorbance of each condition using their untreated (Ø) controls. (A) Graphs obtained with the compound RS-39604 data and (B) Graphs obtained with the compound GR-127935 data. Data represent the mean ±SD from three independent experiments. *, $p<0.05$.

These results suggest a modulation of serotonin antagonists over E2F1-mediated cell death. A detailed study on the impact of the serotonin receptor antagonists on E2F1-driven apoptosis could determine the role of the serotonin pathway as modulator of apoptosis, and could help in the development of therapeutic strategies against tumor progression.

5.- DISCUSSION

E2F transcription factors have been widely described as regulators of gene expression associated with cell cycle regulation and cell growth. Previous studies have detailed the role for E2F factors in the control of the cell cycle through the regulation of genes involved in G1/S transition or in DNA replication (Stanelle et al. 2002; Di Stefano et al. 2003). It has been suggested that the temporal control of gene expression during a cell division cycle not only involves the transcriptional regulation mediated by classical E2Fs (E2F1-5) in quiescence and G1/S transition, but also the repression of these E2F-induced genes as cells advance through the cell cycle, allowing correct progression into the following phases (Infante *et al.*, 2008; Iglesias-Ara *et al.*, 2010; Bertoli, Skotheim and de Bruin, 2013; Laresgoiti *et al.*, 2013). Accumulating evidence points to a role for atypical E2F7 in the repression of E2F-induced transcriptional program as cells move through S- and G2-phases (Di Stefano, Jensen and Helin, 2003; Westendorp *et al.*, 2012), although its full set of target genes are far from being elucidated.

In addition to controlling the expression of genes necessary for cell cycle progression, E2F factors have also been involved in the control of cell surveillance mechanisms. Genomic and proteomic analyses have identified numerous genes regulated by classical E2Fs beyond those involved in S-phase entry and progression, including genes involved in DNA repair pathways (Muller et al., 2001; Polager et al., 2002; Ren et al., 2002; Infante et al., 2008; Westendorp et al., 2012; Laresgoiti et al., 2013). Whether atypical E2F7 is involved in the DNA damage responses has not yet been clarified.

In this work, we have investigated the function of E2F7 by analyzing the contribution of its target genes (microRNAs and protein-coding genes) to the regulation of cellular proliferation and DNA damage responses.

5.1. Regulation of microRNA expression by E2F7

The role of E2F7 in cell cycle progression is now well established. Early overexpression experiments suggested that E2F7 could be a negative regulator of the cell cycle (de Bruin *et al.*, 2003; Di Stefano, Jensen and Helin, 2003), and acute depletion of E2F7 has demonstrated a unique requirement for this E2F member in repressing a timely cell cycle progression, a role that is not shared with E2F8 (Mitxelena *et al.*, 2016). Mechanistically, E2F7 has been found to modulate the expression of protein-coding genes involved in cell cycle regulation (Westendorp *et al.*, 2012; Mitxelena, 2014). We now identify a microRNA set repressed by E2F7 that might play a role in E2F7 function.

Regulation of microRNAs is under tight temporal and spatial control, and changes in their expression are associated with many human diseases, particularly cancer. Recent data suggest that microRNAs are regulated by transcription factors involved in cell cycle regulation such as c-MYC, E2F or p53, and act coordinately with them to finely tune cell cycle progression (Bueno and Malumbres, 2011).

At the onset of this thesis project, no microRNAs regulated by the atypical E2F7 had been reported in the literature. This work was initiated from the results obtained earlier in our group from a microRNA expression profiling analysis using U2OS cells knockdown for E2F7 (Mitxelena, 2014). This expression profiling provided evidence that E2F7 has a major role as a negative regulator of microRNA expression, in line with its role as negative regulator of protein-coding gene expression (de Bruin *et al.*, 2003; Di Stefano, Jensen and Helin, 2003; Carvajal *et al.*, 2012; Westendorp *et al.*, 2012). The Q-RT-PCR results gathered in this work using some of the identified microRNAs confirm the repressor role of E2F7. miR-25 and let-7f exhibited the highest levels of overexpression upon E2F7 loss. Interestingly, these microRNAs have previously been identified as induced by E2F1 and E2F3 in S phase entry (Bueno *et al.*, 2010), indicating that E2F7 might repress during S-phase the expression of microRNAs that have been activated by canonical E2Fs during G1/S (Mitxelena *et al.*, 2016).

A recent study has confirmed the role of E2F7 as transcriptional repressor of microRNA expression, by showing that it downregulates the expression of miR-15a and miR-16 in breast cancer, leading to tamoxifen resistance (Chu *et al.*, 2015). These microRNAs, together with miR-449a/b were previously related to E2F (Lizé, Pilarski and Dobbelstein, 2010; Ofir, Hacohen and Ginsberg, 2011). However, they were not detected in our work, perhaps because of the restrictive criteria that we used in the different steps of RNA-Seq data analysis. On the other hand, our small RNA-Seq experiment has revealed many other differentially expressed microRNAs that have not been previously linked to E2F activity such as miR-7, miR-92 or miR153; thus representing potentially novel E2F-regulated microRNAs (Mitxelena *et al.*, 2016).

microRNA sequences are located within various contexts in the genome. In humans, the majority of canonical microRNAs are encoded by introns of noncoding or protein coding transcripts. Additionally, some microRNAs are encoded by exonic regions of the genome (Rodriguez *et al.*, 2004). In both cases, several microRNA loci are commonly in close proximity to each other, constituting a polycistronic transcription unit (Y. Lee *et al.*, 2002). Although microRNA expression can be regulated throughout their maturation process (Ha and Kim, 2014), regulation of most microRNAs takes place at the transcriptional level, similarly to that of protein-coding genes (Krol, Loedige and Filipowicz, 2010; Gulyaeva and Kushlinskiy, 2016). In fact, factors that regulate protein-coding gene transcription largely overlap with those that control microRNA expression (Davis and Hata, 2009).

Our bioinformatic analysis of regulatory regions has revealed the presence of E2F consensus binding sequences in all the E2F7-responsive microRNAs, except for let-7f, and chromatin immunoprecipitation assays have shown that E2F7 directly binds to the regulatory region of miR-7, miR-92 and miR-25, suggesting that their repression could be carried out through a direct binding of E2F7 to their promoters. Given that individual E2F sites present in gene regulatory regions are commonly bound by multiple E2F members *in vivo* (Wells *et al.*, 2000; Infante *et al.*, 2008), we also tested recruitment of typical E2Fs to the microRNA promoters. E2F1-3 could efficiently bind E2F7-target microRNA promoters (Figure 19). Interestingly, depletion of E2F7 increases dramatically the recruitment of E2F1-3 to the target promoters. An upregulation of E2F1-3 expression in E2F7-knockdown cells may account for this increased binding activity. Thus, E2F7 and E2F1-3 may compete for the same binding sites on miR-7, miR-92 and miR-25 promoters, as has been suggested for the regulation of miR-15a and miR-16 (Chu *et al.*, 2015), implying a complex regulation of miR-7, miR-92 and miR-25 expression by typical and atypical E2Fs. A tightly controlled time-course assay might reveal whether recruitment of these individual E2Fs takes place in a temporal fashion, as expected from their gene expression patterns, and whether expression levels of the microRNAs change accordingly.

A substantially higher E2F7 binding activity was detected at the miR-25 regulatory region relative to miR-7 and miR-92, which correlates with the higher expression of miR-25 upon E2F7 depletion. However, binding activity and microRNA expression did not correlate well with the number of E2F sites or with the degree of similarity of the E2F sites relative to the consensus E2F sequence (TTTXXCGC, where X may be C or G), as identified by the bioinformatic analysis. E2F binding sites in miR-7 are closest to the consensus sequence. However, its E2F7-binding activity was substantially lower than that of miR-25. By contrast, the E2F sites in miR-25 are less similar to the consensus sequence, but it displayed the highest E2F7-binding activity. The reasons for this discrepancy are presently unknown, but could involve a differential affinity of E2F7 for the various E2F motif sequences. ChIP-seq analysis have revealed that E2F7 binds

preferentially to genomic sites containing the TTCCCGCC motif, which is not exactly the same as the consensus motif (Westendorp *et al.*, 2012). However, more recent chromatin immunoprecipitation assays, together with structural and molecular dynamics results found that both typical and atypical E2Fs are recruited to the same sequence motif (Morgunova *et al.*, 2015). Another possibility is that there is a differential accessibility of E2F7 to the regulatory regions of these microRNAs. MCM7, the host gene of miR-25, is a well-recognized E2F-target gene in U2OS cells, whose levels are regulated throughout the cell cycle (Mitxelena *et al.*, 2016). By contrast, it is unknown whether HNRNPK, the host gene of miR-7, and MIR17HG, the host gene of miR-92, are expressed in U2OS cells, and whether they are regulated by E2F7. Analysis of the expression levels of these genes in our cellular system may provide some clues regarding the differential E2F7-mediated binding and expression of their nested microRNAs.

5.1.1. microRNA-dependent cell cycle regulation mediated by E2F7

A Gene Ontology analysis of the combined predicted targets of all deregulated microRNAs revealed that E2F7-repressed microRNAs preferentially modulate genes involved in cell cycle and mitosis regulation suggesting that E2F7 could modulate cell cycle progression through these microRNAs.

Several of the microRNAs that we found to be repressed by E2F7 have previously been described as regulators of proliferation pathways (Bueno *et al.*, 2010; Poliseno *et al.*, 2010), and some of their target mRNAs have been identified. miR-25 has been described to regulate cell cycle progression targeting cell cycle inhibitors such as $p57^{Kip2}$ in gastric cancer cells (Y.-K. Kim *et al.*, 2009) and PTEN in prostate cancer cells (Poliseno *et al.*, 2010), or promoters of proliferation such as CDC42 or CDK2 (Sárközy, Kahán and Csont, 2018). let-7 has been found to target multiple mediators of cell growth, including HMGA2, PRDM1, CDC34, CDK6 or RRM2 (Johnson et al. 2007, Boyerinas 2010). However, their potential roles in cancer have not been clearly established, as these microRNAs appear to have both oncogenic and anti-oncogenic functions in different cellular contexts. Our data evidence that miR-25, let-7f, miR-27b, let-7b, miR-92a, miR-7 and to a lesser extent miR-26a, promote cell proliferation in U2OS cells, at least in part by silencing the expression of anti-proliferative cell cycle regulators ($p21^{Cip1}$, $p57^{Kip2}$, PTEN and p130) (Mitxelena *et al.*, 2016). Thus, by downregulating microRNA expression, E2F7 would indirectly upregulate the levels of cell cycle inhibitors to restrain cell cycle progression. These findings suggest that E2F7 controls cell cycle progression and cellular proliferation through a coordinated performance of both protein-coding and non-coding genes.

Besides their role in cell proliferation control, E2F7-regulated microRNAs are involved in other biological processes including hemostasis, signaling by Nerve Growth Factor (NGF) or transmembrane transport. For example, miR-92 promotes cardiovascular disease via mediating the NRF2-KEAP1-ARE signaling pathway (Liu *et al.*, 2017); let-7 directly targets NGF to mediate the protective effect of melatonin in brain injury (Yang *et al.*, 2018); miR-25 is involved in calcium signaling through targeting the expression of MCU and SERCA2 (Pan, 2015; Sárközy et al. 2018). Thus, E2F7 could regulate a diversity of functions through control of microRNA expression, a field that remains to be explored.

Overall, our study identifies E2F7 as a critical regulator of microRNA biogenesis throughout the cell cycle. Interestingly, we have uncovered a novel interplay between E2F7 and E2F1-3 in the regulation of microRNAs to ensure induction and repression of microRNA genes during the cell division cycle, which in turn could contribute to cell growth control. In this regard, E2F7 might repress microRNA gene expression through binding to its target genes and directly repressing their transcription (miR-25, miR-92a and miR-7). These findings support a model in which the transcriptional activity of E2F-target microRNAs may be dictated by an 'E2F-network' in which E2F1-3 and E2F7 play antagonistic roles. Future studies may help to further identify the components of this novel molecular network as well as its biological relevance.

5.2. E2F7 and the regulation of DNA damage responses

Genome-wide studies performed with gain-of-function and loss-of-function cellular models of E2Fs have led to the recognition of E2F family transcription factors as part of the DNA damage response through the transcriptional regulation of genes involved in this process, such as BRCA1, BARD1 or RAD51 (Wang *et al.*, 2000; Ren *et al.*, 2002; Westendorp *et al.*, 2012). Although E2F7 has been reported to regulate the expression of RRM2 or DHFR, genes involved in DNA metabolism (Carvajal *et al.*, 2012), the role of E2F7 in the maintenance of genome stability is poorly understood. Conflicting results have been reported in the literature regarding the contribution of E2F7 to the cellular response upon genotoxic damage. Zalmas and collaborators described that upon DNA damage E2F7 inhibits apoptosis by repressing E2F1 expression (Zalmas *et al.*, 2008). By contrast, Carvajal and collaborators found that E2F7 is able to block the cell cycle and induce apoptosis through the inhibition of cell cycle-promoting genes after exposure to genotoxic compounds (Carvajal *et al.*, 2012). In this work we have investigated the role of E2F7 in DNA damage responses by analyzing its contribution to the control of gene expression and to cellular responses upon exposure to several genotoxic compounds.

The Gene Set Enrichment Analysis performed with RNA-seq data gathered from cell cycle-synchronized U2OS cells that had been depleted of E2F7, produced a list of pathways that were enriched in E2F7-depleted cells compared to their corresponding controls. Remarkably, we found that in addition to controlling the timely expression of genes necessary for G1/S transition and DNA replication in unperturbed conditions (RB and E2F signaling pathways), E2F7 is involved in the negative regulation of genes controlling DNA repair pathways. These genes are clustered in the categories of Fanconi Anemia (FA), BARD1 signaling and ATR signaling pathway (Mitxelena*, Apraiz*, Vallejo-Rodríguez* *et al*, 2018). These results have led us to propose that E2F7 activity is associated with a suppression of DNA repair reactions.

Interestingly, all upregulated genes included in the DNA damage repair functional group harbor at least one E2F binding site in their promoters, and although many of those have been previously identified as targets of classical E2F proteins (Ren *et al.*, 2002; Bindra and Glazer, 2006; Tategu *et al.*, 2007; Laresgoiti *et al.*, 2013), their regulation by E2F7 has only been demonstrated for some of them (Westendorp *et al.*, 2012). Our RNA-seq followed by ChIP assays have extended the collection of direct E2F7 target genes involved in DNA repair by demonstrating that E2F7 is recruited to the promoter regions of *RAD51*, *FANCE*, *FANCI*, *CTIP*, *BARD1* and *BRIP1*, implying their direct transcriptional repression by E2F7.

5.2.1. Contribution of E2F7 to the cellular responses elicited by ICL-induced DNA damage

Interestingly, the FA pathway, which is known to be involved in ICL repair (Clauson, Schärer and Niedernhofer, 2013), is highly enriched among E2F7- repressed genes. ICLs are extremely toxic for the cell because they produce stalled replication forks that hinder the progression of the cell cycle (Osawa, Davies and Hartley, 2011). ICL-resistant cell lines are known to have elevated gene expression involving the FA/BRCA pathway, including FANCF and RAD51C, which was suggested to be causally related with enhanced removal of ICLs by the resistant cells (Hazlehurst *et al.*, 2003; Chen *et al.*, 2005). We have found evidence that the expression of at least FANCE, FANCI, BRIP1 (also called FANCJ) or RAD51 (also called FANCR) is directly regulated by E2F7, both in unperturbed conditions as well as upon genotoxic exposure, suggesting that E2F7 is tightly involved in the regulation of responses to ICL damage. It will be interesting to analyze whether a correlation can be found between ICL resistance and E2F7 levels in different cancer cell lines in unperturbed conditions, but also upon exposure to ICL-inducing chemotherapy.

The classical E2F family members E2F1-3 have been described to induce the expression of the Fanconi Anemia pathway genes as key determinants for cells to enter into the DNA damage repair pathway and facilitate progression through the cell cycle (Tategu et al. 2007; Hoskins et al. 2008; Laresgoiti et al 2013) although there is no clear demonstration that classical E2Fs are involved in responses elicited by ICLs. We now demonstrated that the atypical member E2F7 impairs cellular recovery during an ongoing DNA damage response induced by ICLs. Firstly, we found that E2F7-depleted U20S cells exhibit increased DNA replication rates after CSP treatment relative to control U2OS cells. Secondly, we show that loss of E2F7 confers an increased recovery competence upon treatment with DNA damage-inducing doses of CSP and MMC, both in the first cell division cycle and in long-term proliferation assays. These results suggest that E2F7 is a factor that negatively controls cellular recovery during an ongoing DNA damage response. This response is not detected upon γ-irradiation or treatment with the radiomimetic drug neocarcinostatin (NCS), suggesting that this role of E2F7 is specific to certain types of DNA damage.

In contrast to our findings, it has been reported that lack of E2F7 sensitizes cells to topoisomerase inhibitors by inducing apoptosis through a mechanism involving E2F1 upregulation (Zalmas *et al.*, 2008; Thurlings *et al.*, 2016). Several reasons could explain the disparity between our results and those from previous studies. On the one hand, we have used a set of genotoxic agents that are known to differ in their mechanism of DNA damage and in the elicited response from the previously analyzed ones. On the other hand, the drug doses used in our study were non-lethal, although sufficient to induce checkpoint arrest in G2, whereas previous studies employed doses sufficiently high to induce apoptosis. Thus, there could be a DNA damage threshold below which cells lacking E2F7 could be involved in repairing the damage, but above which these cells would activate cell death pathways. Systematic analyses using a wide range of doses of a variety of compounds may help resolve these differences.

Regarding the methodology used to carry out our experiments, several points have elicited further discussion. On the one hand, the study of some DNA damage responses has been carried out after having synchronized the cells in the cell cycle with hydroxyurea, a widely used method to analyze cell cycle-dependent processes. Treating cells with HU depletes the cellular pool of dNTPs, and leads to a cell cycle arrest in G1/S (Singh and Xu, 2016). HU treatment also results in stalled replication forks, causing the activation of the DDR and the induction of pathways involved in the protection of stalled forks and fork restart after removal of the drug (Petermann *et al.*, 2010). It is possible that E2F7-depleted cells overcome more easily the HU-induced checkpoint, and this may facilitate their recovery from subsequent ICL induction. Nevertheless, we have repeated the DNA damage recovery experiments in asynchronous cells, and the results

are similar to those in synchronized cells, suggesting that the increased recovery competence upon DNA damage conferred by E2F7 deficiency is specific to CSP and MMC treatments.

Another important point relates to the approaches to deplete E2F7 levels in our studies. Many of the experiments in this study have been carried out using transient E2F7 silencing by siRNA interference, a widely-used method to analyze gene function (Semizarov, Kroeger and Fesik, 2004) which was established previously in the laboratory (Mitxelena, 2014). It has been described that transitory silencing using siRNA technology could impact several off-target genes, which may lead to wrong conclusions regarding the role of the gene under study (Caffrey *et al.*, 2011). In order to avoid these negative effects, we repeated the DNA damage recovery experiments using E2F7-knockout U2OS cells. We find that cells with chronic depletion of E2F7 also present increased recovery competence against under CSP and MMC treatments, confirming the idea that this effect is not due to the off-target effects of transitory silencing.

We decided to extend our studies on the role of E2F7 upon genotoxic damage by inducing replication fork stalling independently of ICL. It has been described that the compound Olaparib (OLA) leads to replication fork stalling and cell cycle arrest by inhibiting the DNA repair activity of PARP1 (Ray Chaudhuri and Nussenzweig, 2017). Repeating our experiments with OLA, we found that E2F7 not only increased recovery competence upon treatment with CSP and MMC, but also with the PARP1 inhibitor. These results suggest a role for E2F7 protein in attenuating cell cycle progression after DNA damage and replication fork block induced by ICLs or by PARP1 inhibition, as the absence of E2F7 confers an advantage to overcome the G2 arrest induced by these types of treatments.

E2F7 levels are increased upon ICL-producing damage both at mRNA and protein levels but not after NCS treatment. Previous studies have linked E2F7 expression and cell-cycle target gene repression to p53 after DNA damage by topoisomerase inhibitors (Carvajal *et al.*, 2012). Unexpectedly, using p53-knockodown U2OS cells and p53-deficient HeLa cells, we found that E2F7 expression and E2F7-modulated cellular recovery after ICL damage is largely p53-independent. Our results point to a fundamental difference in the DNA damage-mediated regulation of E2F7 expression and function between DNA topoisomerase inhibitors and ICL inducers. It will be interesting to determine whether other p53 family members are involved in E2F7 regulation upon ICL induction or whether an entirely distinct pathway mediates E2F7 regulation in this context.

Intriguingly, NCS treatment had no effect on E2F7 or p53 accumulation. By contrast, the levels of $p21^{Cip1}$, a gene that is typically induced by p53 but it can also be regulated in a p53-independent manner (Russo *et al.*, 1995), were significantly elevated after NCS treatment, but not after MMC or CSP treatment. This result could reflect differences in the mechanisms of

action of the tested genotoxic agents at the molecular level. Another possibility could be that the gene expression kinetics are different between NCS and DNA crosslinkers, and that we did not detect them because we only used the 24h time-point. In fact, it has been described that NCS induces an early and transient accumulation of p53 within a few hours after exposure to the compound (Brazina *et al.*, 2015; Stewart-Ornstein, Cheng and Lahav, 2017). Analysis of an earlier time-point may resolve whether E2F7 and p53 are NCS-responsive. However, given that E2F7-depleted cells did not recover after NCS treatment, in contrast to MMC or CSP, suggests that NCS plays a small role, if any, in E2F7 induction.

Regarding the functional assay in the presence or absence of p53, the combined ablation of p53 and E2F7 significantly increased the ability of cells to overcome ICL-producing damage relative to the silencing of each gene individually (Figure 31). This result suggests some kind of complementary interaction between E2F7 and p53, whereby the full phenotypic response is only observed when both genes are silenced. Further experiments are required in order to elucidate these mechanisms.

Upon treatment with DNA damaging agents that induce interstrand crosslinks, cells give rise to the formation of nuclear foci containing 53BP1 and FANCD2 proteins, two of the main indicators of DNA repair (Rappold *et al.*, 2001; Hussain *et al.*, 2004). Previous results from our group have described how depletion of E2F7 caused a significant decrease in the number of 53BP1 and FANCD2 foci upon ICL induction (Mitxelena, 2014). Our finding that γ-H2AX foci number is not altered after 7h of treatment with CSP, MMC or OLA after E2F7 ablation but is reduced after 24h treatment in E2F7 depleted cells significantly contributes to our understanding of E2F function by suggesting that E2F7 is dispensable for foci formation but appears to play a key role in the negative control of repair pathways targeting ICL lesions or PARP1 inhibition. Our observation that E2F7 knockdown has a protective effect against chromosomal aberrations induced by MMC treatment supports this hypothesis.

5.2.3. Role of E2F7 homologous recombination and genomic stability

ICL repair is known to involve homology-directed repair machinery and increased HR is associated with resistance to ICL-inducing agents in human tumor cells (Slupianek *et al.*, 2001; Xu *et al.*, 2005). Our results are consistent with a negative role for E2F7 in HR repair activity. Using a DR-GFP assay to measure the effect of E2F7 in HR, we found that E2F7 negatively affects HR activity. A transcription-independent contribution to DNA repair process for E2F7 and E2F1 has been previously reported, which involves the binding of these E2Fs and recruitment of several factors to damaged DNA sites (Guo *et al.*, 2010, 2011; Chen *et al.*, 2011; Zalmas *et al.*,

2013). We cannot discard the possibility that there is a transcription-independent contribution to E2F7-mediated regulation of ICL lesion repair in our system, which should be important to analyze. However, our data strongly suggest that a major DNA damage response function of E2F7 is through transcription-dependent regulation of DNA repair genes. Several genes involved in HR were found upregulated upon E2F7 depletion, including RAD51, CTIP and BARD1, among others. Most importantly, the results obtained in our E2F7/RAD51 co-depletion experiments suggest that increased HR activity in E2F7 silenced cells is associated with increased levels of RAD51 recombinase, implying a transcriptional role for E2F7 in repair of ICL lesions, through upregulation of target genes involved in homology directed DNA repair. Thus, the transcriptional landscape regulated by E2F7 could provide an additional level of recombination control in addition to that described for several recombinases (Barber *et al.*, 2008; Moldovan *et al.*, 2012), whereby cells can interfere with HR at different steps in the process.

Increasing recombination in HR-deficient cells might result in protective effects. Our results have revealed an intriguing link between genomic integrity of DNA repair deficient cells and E2F7. HR-deficient (BRCA2 mutated) cells exhibit increased genomic instability and accumulation of mutations that ultimately disrupt cell-cycle control pathways, leading to cancer. In this scenario, increased HR activity conferred by inactivation of E2F7 might prevent genomic instability in the cells of these patients and protect against cancer onset, as has been proposed for the depletion of the PCNA-binding protein PARI (Moldovan *et al.*, 2012). However, dysregulated hyper-recombination has also been associated with increased genomic instability and resistance to genotoxic therapy in some cellular contexts, such as after RAD51 upregulation (Martin *et al.*, 2007). In fact, the increased survival of BRCA2- deficient tumor Capan-1 cells treated with OLA that we observe after knockdown of E2F7 implies that loss of E2F7 in the context of HR deficiency confers resistance to chemotherapy, a potentially harmful outcome for cancer treatment.

Although further research is needed to elucidate the molecular mechanisms underlying E2F7-dependent control of genomic stability, our data are consistent with an antioncogenic function for E2F7 whereby E2F7 functions to inhibit or to switch off repair pathways for specific DNA lesions. It has been reported that efficient ICL repair requires negative regulation of the FA pathway. Once repair is completed, the repair factors have to be inactivated to avert inappropriate action and corruption of genetic information (Kim et al. 2009). Thus, the inability to turn off or reset the FA pathway after the repair of specific DNA damage sites may have deleterious effects on genome integrity. In a similar manner, E2F7 might counter-balance the transcriptional program activated in response to ICL repair to fine-tune the cellular response to DNA lesions and ensure response termination.

5.2.4. Role of E2F7 in the response to DNA alkylation damage

In this work, we have shown that E2F7 modulates the cellular responses to multiple types of DNA lesions: DNA crosslink lesions induced by MMC or CSP, as well as DNA alkylation damage induced by methyl methanesulfonate (MMS). DNA alkylation commonly produces single-strand DNA breaks, which are detected and subsequently processed by the Base Excision Repair (BER) pathway, and finally repaired by a specific SSB-repairing machinery (Kim, Wilson and III, 2012). Thus, E2F7 may impair cellular recovery of DNA lesions involving single-strand breaks. The improved cellular responses that we detected in E2F7-depleted cells treated with Olaparib may also have involved the BER pathway, since PARP1 participates in the machinery responsible for the repair of SSBs (Campalans *et al.*, 2013).

Some of key components of single-strand break repair pathway are XRCC1 and DNA ligase III (Kim, Wilson and III, 2012). XCRR1 is a scaffold protein essential for the recruitment of other proteins such as LIG3, which is the ligase responsible of the last step of the repair process. Interestingly, their regulatory regions harbor consensus E2F binding sites, and E2F1 has been described as a direct regulator of XRCC1 gene expression (Chen *et al.*, 2008; Jin *et al.*, 2011), supporting the idea that XRCC1 and LIG3 are E2F-responsive genes. However, we did not observe any change in XRCC1 and LIG3 expression after E2F7 depletion, not at mRNA or at protein level, discarding an E2F7-mediated transcriptional regulation of their expression. Although further experiments, such as ChIPs or luciferase reporter assays are needed to unequivocally elucidate whether these genes or others in the pathway are E2F7-target genes, our results suggest that the mechanisms by which E2F7 modulates BER repair responses are substantially different from ICL repair responses. The first one would involve non-transcriptional mechanisms whereas the second one would rely on transcriptional mechanisms for modulating DNA damage responses.

The mechanism by which E2F7 impairs BER repair responses remains to be elucidated. One possibility is that E2F7 might be recruited to SSB sites. It has been described that, after treatment with topoisomerase inhibitors, E2F7, together with CTBP and HDAC, can be recruited to double-strand breaks (Zalmas *et al.*, 2013). The complex could then alter the local chromatin environment of the DNA lesion and modulate the repair activity. Our finding that XRCC1 interacts with E2F7 through the BRCT1-binding motif suggests a mechanism by which binding of E2F7 to XRCC1 could negatively impact XRCC1 repair activity since this is the motif used by XRCC1 to interact with LIG3 and initiate DNA repair. However, further experiments are needed in order to better describe this interaction and its functional role.

5.3 Modulators of E2F1-driven apoptosis

Some of the best recognized mechanisms for E2F7 function involve E2F1 and the negative feedback loop established between the two E2F members. E2F1 induces E2F7 expression, which in turn targets E2F1 for transcriptional repression (Li *et al.*, 2008; Moon and Dyson, 2008; Zalmas *et al.*, 2008; Carvajal *et al.*, 2012; Mitxelena, 2014; Thurlings *et al.*, 2016).

Non-tumor cells maintain in balance the pro-survival and pro-apoptotic activities of E2F1. However, cancer cells, whereby E2F1 amplification or aberrant E2F1 activity is commonly observed, the pro-apoptotic activity of E2F1 must be restrained by counterbalancing signals in order to facilitate the neoplastic transformation. With the exception of PI3K/AKT signaling pathway, which can partially block the apoptotic program of E2F1 overexpressing cells (Hallstrom, Mori and Nevins, 2008), little is known about the cellular signals that mediate tumor development under excessive E2F1 activity. The high-throughput screening system using a collection of FDA-approved inhibitors that we have employed could be useful to identify modulators of E2F1-induced apoptosis. Our preliminary results suggest that the serotonin regulatory pathway could be a modulator of the cell death triggered by E2F1.

Serotonin receptor antagonists have been previously used in order to dissect the serotonin signaling pathway. It has been established that this pathway is a key regulator of cell viability and apoptosis in tumoral processes (Siddiqui *et al.*, 2006). Ketanserin, a selective 5-HT2A serotonin receptor antagonist, has been described as a cell viability inhibitor through the inactivation of ERK1/2 and JAK2/STAT3 signaling pathways in human choriocarcinoma cell lines (Oufkir *et al.*, 2010). Additionally, SB216641, a selective 5-HT1B serotonin receptor antagonist has been described as an apoptosis inducer in human uterine leiomyoma cells (Gurbuz *et al.*, 2016). The results gathered in our apoptosis screening assay are consistent with a role for the serotonin signaling in mediating cell survival. Serotonin receptor antagonists emerge as promising inhibitors of E2F1-mediated apoptosis. A more throrough characterization of the effect of the serotonin signaling pathway in E2F1-driven apoptosis in cancer, should provide a better understanding of apoptosis inhibitory processes in tumor progression and help in the development of therapeutic strategies against it.

6.- CONCLUSIONS

1. E2F7 represses the expression of a set of microRNAs. E2F7-responsive microRNAs harbor E2F binding sites in their regulatory regions, and E2F7 directly binds to the promoters of miR-7, miR-92 and miR-25.

2. E2F7-target microRNAs regulate expression of cell cycle inhibitors and promote cellular proliferation, implying a negative regulatory role for E2F7 in cell cycle progression through suppression of microRNA expression.

3. E2F7 directly binds to the promoters of FANCE, FANCI, CTIP, RAD51, BARD1 and BRIP1 genes and represses their expression- These genes are key to several DNA repair pathways such as Fanconi Anemia or Homologous Recombination that modulate the DNA damage response.

4. E2F7 transcriptionally regulates the cellular response to DNA lesions induced by interstrand-crosslinks and PARP1 inhibition. Loss of E2F7 confers an increase on the short-term and long-term cellular recovery to these lesions, which compromise replication fork progression.

5. E2F7 restricts short-term and long-term cellular recovery to DNA damage induced by alkylating treatments. Present evidence suggests that this response is not regulated transcriptionally by E2F7.

6. E2F7 suppresses homologous recombination-directed DNA repair activity and prevents genomic instability in HR-deficient cells.

7. Serotonin receptor antagonists amplify E2F1-driven apoptosis in a tumor model.

7.- REFERENCES

Adams, M. R., Sears, R., Nuckolls, F., Leone, G. and Nevins, J. R. (2000) 'Complex transcriptional regulatory mechanisms control expression of the E2F3 locus.', *Molecular and cellular biology*, 20(10), pp. 3633–9.

Aerts, S., Van Loo, P., Thijs, G., Mayer, H., de Martin, R., Moreau, Y. and De Moor, B. (2005) 'TOUCAN 2: the all-inclusive open source workbench for regulatory sequence analysis.', *Nucleic acids research*. Oxford University Press, 33(Web Server issue), pp. W393-6. doi: 10.1093/nar/gki354.

Alvarez-Fernández, M., Halim, V. A., Krenning, L., Aprelia, M., Mohammed, S., Heck, A. J. and Medema, R. H. (2010) 'Recovery from a DNA-damage-induced G2 arrest requires Cdk-dependent activation of FoxM1', *EMBO reports*, 11(6), pp. 452–458. doi: 10.1038/embor.2010.46.

Arbi, M., Pefani, D., Kyrousi, C., Lalioti, M., Kalogeropoulou, A., Papanastasiou, A. D., Taraviras, S. and Lygerou, Z. (2016) 'GemC1 controls multiciliogenesis in the airway epithelium', *EMBO reports*, 17(3), pp. 400–413. doi: 10.15252/embr.201540882.

Attwooll, C., Lazzerini Denchi, E. and Helin, K. (2004) 'The E2F family: specific functions and overlapping interests.', *The EMBO journal*. European Molecular Biology Organization, 23(24), pp. 4709–16. doi: 10.1038/sj.emboj.7600481.

Attwooll, C., Oddi, S., Cartwright, P., Prosperini, E., Agger, K., Steensgaard, P., Wagener, C., Sardet, C., Moroni, M. C. and Helin, K. (2005) 'A Novel Repressive E2F6 Complex Containing the Polycomb Group Protein, EPC1, That Interacts with EZH2 in a Proliferation-specific Manner', *Journal of Biological Chemistry*, 280(2), pp. 1199–1208. doi: 10.1074/jbc.M412509200.

Balciunaite, E., Spektor, A., Lents, N. H., Cam, H., te Riele, H., Scime, A., Rudnicki, M. A., Young, R. and Dynlacht, B. D. (2005) 'Pocket Protein Complexes Are Recruited to Distinct Targets in Quiescent and Proliferating Cells', *Molecular and Cellular Biology*, 25(18), pp. 8166–8178. doi: 10.1128/MCB.25.18.8166-8178.2005.

Barber, L. J., Youds, J. L., Ward, J. D., McIlwraith, M. J., O'Neil, N. J., Petalcorin, M. I. R., Martin, J. S., Collis, S. J., Cantor, S. B., Auclair, M., Tissenbaum, H., West, S. C., Rose, A. M. and Boulton, S. J. (2008) 'RTEL1 Maintains Genomic Stability by Suppressing Homologous Recombination', *Cell*, 135(2), pp. 261–271. doi: 10.1016/j.cell.2008.08.016.

Bartek, J. and Lukas, J. (2003) 'Chk1 and Chk2 kinases in checkpoint control and cancer', *Cancer Cell*. Cell Press, 3(5), pp. 421–429. doi: 10.1016/S1535-6108(03)00110-7.

Baskerville, S. and Bartel, D. P. (2005) 'Microarray profiling of microRNAs reveals frequent coexpression with neighboring miRNAs and host genes', *RNA*, 11(3), pp. 241–247. doi: 10.1261/rna.7240905.

Bertoli, C., Skotheim, J. M. and de Bruin, R. A. M. (2013) 'Control of cell cycle transcription during G1 and S phases.', *Nature reviews. Molecular cell biology*. NIH Public Access, 14(8), pp. 518–28. doi: 10.1038/nrm3629.

Bieda, M., Xu, X., Singer, M. A., Green, R. and Farnham, P. J. (2006) 'Unbiased location analysis of E2F1-binding sites suggests a widespread role for E2F1 in the human genome', *Genome Research*, 16(5), pp. 595–605. doi: 10.1101/gr.4887606.

Bieging, K. T., Mello, S. S. and Attardi, L. D. (2014) 'Unravelling mechanisms of p53-mediated tumour suppression', *Nature Reviews Cancer*, 14(5), pp. 359–370. doi: 10.1038/nrc3711.

Bindra, R. S. and Glazer, P. M. (2006) 'Cancer Biology & Therapy Basal repression of BRCA1 by multiple E2Fs and pocket proteins at adjacent E2F sites'. doi: 10.4161/cbt.5.10.3454org/10.4161/cbt.5.10.3454.

Biswas, A. K., Mitchell, D. L. and Johnson, D. G. (2014) 'E2F1 Responds to Ultraviolet Radiation by Directly Stimulating DNA Repair and Suppressing Carcinogenesis', *Cancer Research*, 74(12), pp. 3369–3377. doi: 10.1158/0008-5472.CAN-13-3216.

Blackford, A. N. and Jackson, S. P. (2017) 'ATM, ATR, and DNA-PK: The Trinity at the Heart of the DNA Damage Response', *Molecular Cell*, 66(6), pp. 801–817. doi: 10.1016/j.molcel.2017.05.015.

De Bont, R. and van Larebeke, N. (2004) 'Endogenous DNA damage in humans: a review of quantitative data.', *Mutagenesis*, 19(3), pp. 169–85.

Bork, P., Hofmann, K., Bucher, P., Neuwald, A. F., Altschul, S. F. and Koonin, E. V (1997) 'A superfamily of conserved domains in DNA damage-responsive cell cycle checkpoint proteins.', *FASEB journal : official publication of the Federation of American Societies for Experimental Biology*, 11(1), pp. 68–76. doi: 10.1096/FASEBJ.11.1.9034168.

Bracken, A. P., Ciro, M., Cocito, A. and Helin, K. (2004) 'E2F target genes: unraveling the biology', *Trends in Biochemical Sciences*, 29(8), pp. 409–417. doi: 10.1016/j.tibs.2004.06.006.

Brazina, J., Svadlenka, J., Macurek, L., Andera, L., Hodny, Z., Bartek, J. and Hanzlikova, H. (2015) 'DNA damage-induced regulatory interplay between DAXX, p53, ATM kinase and Wip1 phosphatase', *Cell Cycle*, 14(3), pp. 375–387. doi: 10.4161/15384101.2014.988019.

Bretones, G., Delgado, M. D. and León, J. (2015) 'Myc and cell cycle control', *Biochimica et Biophysica Acta (BBA) - Gene Regulatory Mechanisms*, 1849(5), pp. 506–516. doi: 10.1016/j.bbagrm.2014.03.013.

de Bruin, A., Maiti, B., Jakoi, L., Timmers, C., Buerki, R. and Leone, G. (2003) 'Identification and Characterization of *E2F7* , a Novel Mammalian E2F Family Member Capable of Blocking Cellular Proliferation', *Journal of Biological Chemistry*, 278(43), pp. 42041–42049. doi: 10.1074/jbc.M308105200.

Budhavarapu, V. N., White, E. D., Mahanic, C. S., Chen, L., Lin, F.-T. and Lin, W.-C. (2012) 'Regulation of E2F1 by APC/C Cdh1 via K11 linkage-specific ubiquitin chain formation.', *Cell cycle (Georgetown, Tex.)*. Taylor & Francis, 11(10), pp. 2030–8. doi: 10.4161/cc.20643.

Bueno, M. J., Gómez de Cedrón, M., Laresgoiti, U., Fernández-Piqueras, J., Zubiaga, A. M. and Malumbres, M. (2010) 'Multiple E2F-induced microRNAs prevent replicative stress in response to mitogenic signaling.', *Molecular and cellular biology*. American Society for Microbiology, 30(12), pp. 2983–95. doi: 10.1128/MCB.01372-09.

Bueno, M. J. and Malumbres, M. (2011) 'MicroRNAs and the cell cycle', *Biochimica et Biophysica Acta (BBA) - Molecular Basis of Disease*, 1812(5), pp. 592–601. doi: 10.1016/j.bbadis.2011.02.002.

Caffrey, D. R., Zhao, J., Song, Z., Schaffer, M. E., Haney, S. A., Subramanian, R. R., Seymour, A. B. and Hughes, J. D. (2011) 'siRNA Off-Target Effects Can Be Reduced at Concentrations That Match Their Individual Potency', *PLoS ONE*. Edited by T. Preiss. Public Library of Science, 6(7), p. e21503. doi: 10.1371/journal.pone.0021503.

Caldecott, K. W. (2008) 'Single-strand break repair and genetic disease', *Nature Reviews Genetics*. Nature Publishing Group, 9(8), pp. 619–631. doi: 10.1038/nrg2380.

Campalans, A., Kortulewski, T., Amouroux, R., Menoni, H., Vermeulen, W. and Radicella, J. P. (2013) 'Distinct spatiotemporal patterns and PARP dependence of XRCC1 recruitment to single-strand break and base excision repair', *Nucleic Acids Research*, 41(5), pp. 3115–3129. doi: 10.1093/nar/gkt025.

Canman, C. E., Lim, D. S., Cimprich, K. A., Taya, Y., Tamai, K., Sakaguchi, K., Appella, E., Kastan, M. B. and Siliciano, J. D. (1998) 'Activation of the ATM kinase by ionizing radiation and phosphorylation of p53.', *Science (New York, N.Y.)*, 281(5383), pp. 1677–9.

Carcagno, A. L., Giono, L. E., Marazita, M. C., Castillo, D. S., Pregi, N. and Cánepa, E. T. (2012) 'E2F1 induces p19INK4d, a protein involved in the DNA damage response, following UV irradiation', *Molecular and Cellular Biochemistry*, 366(1–2), pp. 123–129. doi: 10.1007/s11010-012-1289-8.

Carpenter, A. E., Jones, T. R., Lamprecht, M. R., Clarke, C., Kang, I., Friman, O., Guertin, D. A., Chang, J., Lindquist, R. A., Moffat, J., Golland, P. and Sabatini, D. M. (2006) 'CellProfiler: image analysis software for identifying and quantifying cell phenotypes', *Genome Biology*. BioMed Central, 7(10), p. R100. doi: 10.1186/gb-2006-7-10-r100.

Carvajal, L. A., Hamard, P.-J., Tonnessen, C. and Manfredi, J. J. (2012) 'E2F7, a novel target, is up-regulated by p53 and mediates DNA damage-dependent transcriptional repression', *Genes & Development*, 26(14), pp. 1533–1545. doi: 10.1101/gad.184911.111.

Castillo, D. S., Campalans, A., Belluscio, L. M., Carcagno, A. L., Radicella, J. P., Cánepa, E. T. and Pregi, N. (2015) 'E2F1 and E2F2 induction in response to DNA damage preserves genomic stability in neuronal cells', *Cell Cycle*, 14(8), pp. 1300–1314. doi: 10.4161/15384101.2014.985031.

Ceccaldi, R., Rondinelli, B. and D 'andrea, A. D. (2016) 'Repair Pathway Choices and Consequences at the Double-Strand Break'. doi: 10.1016/j.tcb.2015.07.009.

Chafin, C. B., Regna, N. L., Caudell, D. L. and Reilly, C. M. (2014) 'MicroRNA-let-7a promotes E2F-mediated cell proliferation and NFκB activation in vitro', *Cellular & Molecular Immunology*, 11(1), pp. 79–83. doi: 10.1038/cmi.2013.51.

Chen, D., Yu, Z., Zhu, Z. and Lopez, C. D. (2008) 'E2F1 regulates the base excision repair gene XRCC1 and promotes DNA repair.', *The Journal of biological chemistry*. American Society for Biochemistry and Molecular Biology, 283(22), pp. 15381–9. doi: 10.1074/jbc.M710296200.

Chen, D., Chen, Y., Forrest, D. and Bremner, R. (2013) 'E2f2 induces cone photoreceptor apoptosis independent of E2f1 and E2f3', *Cell Death & Differentiation*, 20(7), pp. 931–940. doi: 10.1038/cdd.2013.24.

Chen, H.-Z., Tsai, S.-Y. and Leone, G. (2009) 'Emerging roles of E2Fs in cancer: an exit from cell cycle control', *Nature Reviews Cancer*, 9(11), pp. 785–797. doi: 10.1038/nrc2696.

Chen, J., Zhu, F., Weaks, R. L., Biswas, A. K., Guo, R., Li, Y. and Johnson, D. G. (2011) 'E2F1 promotes the recruitment of DNA repair factors to sites of DNA double-strand breaks', *Cell Cycle*, 10(8), pp. 1287–1294. doi: 10.4161/cc.10.8.15341.

Chen, Q., Van der Sluis, P. C., Boulware, D., Hazlehurst, L. A. and Dalton, W. S. (2005) 'The FA/BRCA pathway is involved in melphalan-induced DNA interstrand cross-link repair and accounts for melphalan resistance in multiple myeloma cells', *Blood*, 106(2), pp. 698–705. doi: 10.1182/blood-2004-11-4286.

Chong, J.-L., Wenzel, P. L., Sáenz-Robles, M. T., Nair, V., Ferrey, A., Hagan, J. P., Gomez, Y. M., Sharma, N., Chen, H.-Z., Ouseph, M., Wang, S.-H., Trikha, P., Culp, B., Mezache, L., Winton, D. J., Sansom, O. J., Chen, D., Bremner, R., Cantalupo, P. G., Robinson, M. L., Pipas, J. M. and Leone, G. (2009) 'E2f1–3 switch from activators in progenitor cells to repressors in differentiating cells', *Nature*, 462(7275), pp. 930–934. doi: 10.1038/nature08677.

Christensen, J., Cloos, P., Toftegaard, U., Klinkenberg, D., Bracken, A. P., Trinh, E., Heeran, M., Di Stefano, L. and Helin, K. (2005) 'Characterization of E2F8, a novel E2F-like cell-cycle regulated repressor of E2F-activated transcription.', *Nucleic acids research*. Oxford University Press, 33(17), pp. 5458–70. doi: 10.1093/nar/gki855.

Chu, J., Zhu, Y., Liu, Y., Sun, L., Lv, X., Wu, Y., Hu, P., Su, F., Gong, C., Song, E., Liu, B. and Liu, Q. (2015) 'E2F7 overexpression leads to tamoxifen resistance in breast cancer cells by competing with E2F1 at miR-15a/16 promoter', *Oncotarget*, 6(31), pp. 31944–57. doi: 10.18632/oncotarget.5128.

Chuang, T.-D. and Khorram, O. (2018) 'Regulation of Cell Cycle Regulatory Proteins by MicroRNAs in Uterine Leiomyoma', *Reproductive Sciences*, p. 193371911876869. doi: 10.1177/1933719118768692.

Ciccia, A. and Elledge, S. J. (2010) 'The DNA Damage Response: Making It Safe to Play with Knives'. doi: 10.1016/j.molcel.2010.09.019.

Clauson, C., Schärer, O. D. and Niedernhofer, L. (2013) 'Advances in understanding the complex mechanisms of DNA interstrand cross-link repair.', *Cold Spring Harbor perspectives in biology*. Cold Spring Harbor Laboratory Press, 5(10), p. a012732. doi: 10.1101/cshperspect.a012732.

Coleman, M. L., Marshall, C. J. and Olson, M. F. (2004) 'RAS and RHO GTPases in G1-phase cell-cycle regulation', *Nature Reviews Molecular Cell Biology*, 5(5), pp. 355–366. doi: 10.1038/nrm1365.

Collin, G., Huna, A., Warnier, M., Flaman, J.-M. and Bernard, D. (2018) 'Transcriptional repression of DNA repair genes is a hallmark and a cause of cellular senescence', *Cell Death and Disease*, 9. doi: 10.1038/s41419-018-0300-z.

Crosio, C., Fimia, G. M., Loury, R., Kimura, M., Okano, Y., Zhou, H., Sen, S., Allis, C. D. and Sassone-Corsi, P. (2002) 'Mitotic phosphorylation of histone H3: spatio-temporal regulation by mammalian Aurora kinases.', *Molecular and cellular biology*, 22(3), pp. 874–85.

Dagnino, L., Kaur, R. and Judah, D. (2011) 'Post-Transcriptional Regulation of E2F Transcription Factors: Fine-Tuning DNA Repair, Cell Cycle Progression and Survival in Development & Disease', in *DNA Repair*. InTech. doi: 10.5772/22159.

Das, A. T., Tenenbaum, L. and Berkhout, B. (2016) 'Tet-On Systems For Doxycycline-inducible Gene Expression.', *Current gene therapy*, 16(3), pp. 156–67.

Davis, B. N. and Hata, A. (2009) 'Regulation of MicroRNA Biogenesis: A miRiad of mechanisms', *Cell Communication and Signaling*, 7(1), p. 18. doi: 10.1186/1478-811X-7-18.

DeGregori, J. (2002) 'The genetics of the E2F family of transcription factors: shared functions and unique roles.', *Biochimica et biophysica acta*, 1602(2), pp. 131–50.

DeGregori, J. and Johnson, D. G. (2006) 'Distinct and Overlapping Roles for E2F Family Members in Transcription, Proliferation and Apoptosis.', *Current molecular medicine*, 6(7), pp. 739–48.

Della-Maria, J., Hegde, M. L., Mcneill, D. R., Matsumoto, Y., Tsai, M.-S., Ellenberger, T., Wilson Iii, D. M., Mitra, S. and Tomkinson, A. E. (2012) 'The Interaction between Polynucleotide Kinase Phosphatase and the DNA Repair Protein XRCC1 Is Critical for Repair of DNA Alkylation Damage and Stable Association at DNA Damage Sites *', *Published JBC Papers in Press*. doi: 10.1074/jbc.M112.369975.

Dimova, D. K. and Dyson, N. J. (2005) 'The E2F transcriptional network: old acquaintances with new faces', *Oncogene*, 24(17), pp. 2810–2826. doi: 10.1038/sj.onc.1208612.

Dynlacht, B. D. (2008) 'Live or Let Die: E2F1 and PI3K Pathways Intersect to Make Life or Death Decisions', *Cancer Cell*. Cell Press, 13(1), pp. 1–2. doi: 10.1016/J.CCR.2007.12.017.

Dyson, N. (1998) 'The regulation of E2F by pRB-family proteins.', *Genes & development*, 12(15), pp. 2245–62.

Elford, H. L. (1968) 'Effect of hydroxyurea on ribonucleotide reductase.', *Biochemical and biophysical research communications*, 33(1), pp. 129–35.

Emmrich, S. and Pützer, B. M. (2010) 'Checks and balances: E2F—microRNA crosstalk in cancer control', *Cell Cycle*, 9(13), pp. 2555–2567. doi: 10.4161/cc.9.13.12061.

Endo-Munoz, L., Dahler, A., Teakle, N., Rickwood, D., Hazar-Rethinam, M., Abdul-Jabbar, I., Sommerville, S., Dickinson, I., Kaur, P., Paquet-Fifield, S. and Saunders, N. (2009) 'E2F7 Can Regulate Proliferation, Differentiation, and Apoptotic Responses in Human Keratinocytes: Implications for Cutaneous Squamous Cell Carcinoma Formation', *Cancer Research*, 69(5), pp. 1800–1808. doi: 10.1158/0008-5472.CAN-08-2725.

Engelmann, D., Knoll, S., Ewerth, D., Steder, M., Stoll, A. and Pü, B. M. (2009) 'Functional interplay between E2F1 and chemotherapeutic drugs defines immediate E2F1 target genes crucial for cancer cell death'. doi: 10.1007/s00018-009-0222-0.

Falck, J., Mailand, N., Syljuåsen, R. G., Bartek, J. and Lukas, J. (2001) 'The ATM–Chk2–Cdc25A checkpoint pathway guards against radioresistant DNA synthesis', *Nature*, 410(6830), pp. 842–847. doi: 10.1038/35071124.

Feng, S., Wang, Y., Zhang, R., Yang, G., Liang, Z., Wang, Z. and Zhang, G. (2017) 'Curcumin exerts its antitumor activity through regulation of miR-7/Skp2/p21 in nasopharyngeal carcinoma cells', *OncoTargets and Therapy*, Volume 10, pp. 2377–2388. doi: 10.2147/OTT.S130055.

Fernandez-Capetillo, O., Chen, H.-T., Celeste, A., Ward, I., Romanienko, P. J., Morales, J. C., Naka, K., Xia, Z., Camerini-Otero, R. D., Motoyama, N., Carpenter, P. B., Bonner, W. M., Chen, J. and Nussenzweig, A. (2002) 'DNA damage-induced G2–M checkpoint activation by histone H2AX and 53BP1', *Nature Cell Biology*, 4(12), pp. 993–997. doi: 10.1038/ncb884.

Field, S. J., Tsai, F. Y., Kuo, F., Zubiaga, A. M., Kaelin, W. G., Livingston, D. M., Orkin, S. H. and Greenberg, M. E. (1996) 'E2F-1 functions in mice to promote apoptosis and suppress proliferation.', *Cell*, 85(4), pp. 549–61.

Fischer, M. and Müller, G. A. (2017) 'Cell cycle transcription control: DREAM/MuvB and RB-E2F complexes', *Critical Reviews in Biochemistry and Molecular Biology*. Taylor & Francis, 52(6), pp. 638–662. doi: 10.1080/10409238.2017.1360836.

Friend, S. H., Bernards, R., Rogelj, S., Weinberg, R. A., Rapaport, J. M., Albert, D. M. and Dryja, T. P. (1986) 'A human DNA segment with properties of the gene that predisposes to retinoblastoma and osteosarcoma', *Nature*, 323(6089), pp. 643–646. doi: 10.1038/323643a0.

Garaycoechea, J. I., Crossan, G. P., Langevin, F., Daly, M., Arends, M. J. and Patel, K. J. (2012) 'Genotoxic consequences of endogenous aldehydes on mouse haematopoietic stem cell function', *Nature*, 489(7417), pp. 571–575. doi: 10.1038/nature11368.

García, I., Murga, M., Vicario, A., Field, S. J. and Zubiaga, A. M. (2000) 'A role for E2F1 in the induction of apoptosis during thymic negative selection.', *Cell growth & differentiation : the molecular biology journal of the American Association for Cancer Research*. AACR, 11(2), pp. 91–8.

Gaubatz, S., Lindeman, G. J., Ishida, S., Jakoi, L., Nevins, J. R., Livingston, D. M. and Rempel, R. E. (2000) 'E2F4 and E2F5 play an essential role in pocket protein-mediated G1 control.', *Molecular cell*, 6(3), pp. 729–35.

Gaubatz, S., Lees, J. A., Lindeman, G. J. and Livingston, D. M. (2001) 'E2F4 Is Exported from the Nucleus in a CRM1-Dependent Manner', *Molecular and Cellular Biology*, 21(4), pp. 1384–1392. doi: 10.1128/MCB.21.4.1384-1392.2001.

Glorian, V., Allègre, J., Berthelet, J., Dumetier, B., Boutanquoi, P.-M., Droin, N., Kayaci, C., Cartier, J., Gemble, S., Marcion, G., Gonzalez, D., Boidot, R., Garrido, C., Michaud, O., Solary, E. and Dubrez, L. (2017) 'DNA damage and S phase-dependent E2F1 stabilization requires the cIAP1 E3-ubiquitin ligase and is associated with K63-poly-ubiquitination on lysine 161/164 residues', *Cell Death and Disease*, 8(5), p. e2816. doi: 10.1038/cddis.2017.222.

Gong, C., Liu, H., Song, R., Zhong, T., Lou, M., Wang, T., Qi, H., Shen, J., Zhu, L. and Shao, J. (2016) 'ATR–CHK1–E2F3 signaling transactivates human ribonucleotide reductase small subunit M2 for DNA repair induced by the chemical carcinogen MNNG', *Biochimica et Biophysica Acta (BBA) - Gene Regulatory Mechanisms*, 1859(4), pp. 612–626. doi: 10.1016/j.bbagrm.2016.02.012.

Griffiths-Jones, S., Grocock, R. J., van Dongen, S., Bateman, A. and Enright, A. J. (2006) 'miRBase: microRNA sequences, targets and gene nomenclature', *Nucleic Acids Research*. Oxford University Press, 34(90001), pp. D140–D144. doi: 10.1093/nar/gkj112.

Guiley, K. Z., Liban, T. J., Felthousen, J. G., Ramanan, P., Litovchick, L. and Rubin, S. M. (2015) 'Structural mechanisms of DREAM complex assembly and regulation.', *Genes & development*. Cold Spring Harbor Laboratory Press, 29(9), pp. 961–74. doi: 10.1101/gad.257568.114.

Gulyaeva, L. F. and Kushlinskiy, N. E. (2016) 'Regulatory mechanisms of microRNA expression', *J Transl Med*, 14, p. 143. doi: 10.1186/s12967-016-0893-x.

Guo, R., Chen, J., Zhu, F., Biswas, A. K., Berton, T. R., Mitchell, D. L. and Johnson, D. G. (2010) 'E2F1 Localizes to Sites of UV-induced DNA Damage to Enhance Nucleotide Excision Repair', *Journal of Biological Chemistry*, 285(25), pp. 19308–19315. doi: 10.1074/jbc.M110.121939.

Guo, R., Chen, J., Mitchell, D. L. and Johnson, D. G. (2011) 'GCN5 and E2F1 stimulate nucleotide excision repair by promoting H3K9 acetylation at sites of damage', *Nucleic Acids Research*, 39(4), pp. 1390–1397. doi: 10.1093/nar/gkq983.

Gurbuz, N., Asoglu, M. R., Ashour, A. A., Salama, S., Kilic, G. S. and Ozpolat, B. (2016) 'A selective serotonin 5-HT1B receptor inhibition suppresses cells proliferation and induces apoptosis in human uterine leiomyoma cells.', *European journal of obstetrics, gynecology, and reproductive biology*. Elsevier, 206, pp. 114–119. doi: 10.1016/j.ejogrb.2016.08.006.

Ha, M. and Kim, V. N. (2014) 'Regulation of microRNA biogenesis', *Nature Reviews Molecular Cell Biology*, 15(8), pp. 509–524. doi: 10.1038/nrm3838.

Hallstrom, T. C., Mori, S. and Nevins, J. R. (2008) 'An E2F1-Dependent Gene Expression Program That Determines the Balance Between Proliferation and Cell Death', *Cancer Cell*, 13, pp. 11–22.

Harvey, S. L., Charlet, A., Haas, W., Gygi, S. P. and Kellogg, D. R. (2005) 'Cdk1-dependent regulation of the mitotic inhibitor Wee1.', *Cell*. Elsevier, 122(3), pp. 407–20. doi: 10.1016/j.cell.2005.05.029.

Hauck, L. and von Harsdorf, R. (2005) 'E2F transcription factors and pRb pocket proteins in cell cycle progression.', *Methods in molecular biology (Clifton, N.J.)*, 296, pp. 239–45.

Haupt, Y., Rowan, S., Shaulian, E., Vousden, K. H. and Oren, M. (1995) 'Induction of apoptosis in HeLa cells by trans-activation-deficient p53.', *Genes & development*, 9(17), pp. 2170–83.

Hazlehurst, L. A., Enkemann, S. A., Beam, C. A., Argilagos, R. F., Painter, J., Shain, K. H., Saporta, S., Boulware, D., Moscinski, L., Alsina, M. and Dalton, W. S. (2003) 'Genotypic and phenotypic comparisons of de novo and acquired melphalan resistance in an isogenic multiple myeloma cell line model.', *Cancer research*, 63(22), pp. 7900–6.

He, J., Zhao, Y., Zhao, E., Wang, X., Dong, Z., Chen, Y., Yang, L. and Cui, H. (2018) 'Cancer-testis specific gene OIP5: a downstream gene of E2F1 that promotes tumorigenesis and metastasis in glioblastoma by stabilizing E2F1 signaling', *Neuro-Oncology*. doi: 10.1093/neuonc/noy037.

Helin, K. (1998) 'Regulation of cell proliferation by the E2F transcription factors.', *Current opinion in genetics & development*, 8(1), pp. 28–35.

Holliday, R. and Ho, T. (1998) 'Gene silencing and endogenous DNA methylation in mammalian cells.', *Mutation research*, 400(1–2), pp. 361–8.

Hong, S., Paulson, Q. X. and Johnson, D. G. (2008) 'Cell Cycle E2F1 and E2F3 activate ATM through distinct mechanisms to promote E1A-induced apoptosis', *Cell Cycle*, 7, pp. 1–10. doi: 10.4161/cc.7.3.5286.

Hoskins, E. E., Gunawardena, R. W., Habash, K. B., Wise-Draper, T. M., Jansen, M., Knudsen, E. S. and Wells, S. I. (2008) 'Coordinate regulation of Fanconi anemia gene expression occurs through the Rb/E2F pathway', *Oncogene*, 27(35), pp. 4798–4808. doi: 10.1038/onc.2008.121.

Huang, Y. and Li, L. (2013) 'DNA crosslinking damage and cancer - a tale of friend and foe.', *Translational cancer research*, 2(3), pp. 144–154. doi: 10.3978/j.issn.2218-676X.2013.03.01.

Hühn, D., Bolck, H. A. and Sartori, A. A. (2013) 'Targeting DNA double-strand break signalling and repair: recent advances in cancer therapy.', *Swiss medical weekly*, p. w13837. doi: 10.4414/smw.2013.13837.

Hussain, S., Wilson, J. B., Medhurst, A. L., Hejna, J., Witt, E., Ananth, S., Davies, A., Masson, J.-Y., Moses, R., West, S. C., de Winter, J. P., Ashworth, A., Jones, N. J. and Mathew, C. G. (2004) 'Direct interaction of FANCD2 with BRCA2 in DNA damage response pathways', *Human Molecular Genetics*. Oxford University Press, 13(12), pp. 1241–1248. doi: 10.1093/hmg/ddh135.

Ianari, A., Gallo, R., Palma, M., Alesse, E. and Gulino, A. (2004) 'Specific Role for p300/CREB-binding Protein-associated Factor Activity in E2F1 Stabilization in Response to DNA Damage', *Journal of Biological Chemistry*, 279(29), pp. 30830–30835. doi: 10.1074/jbc.M402403200.

Iglesias, A., Murga, M., Laresgoiti, U., Skoudy, A., Bernales, I., Fullaondo, A., Moreno, B., Lloreta, J., Field, S. J., Real, F. X. and Zubiaga, A. M. (2004) 'Diabetes and exocrine pancreatic insufficiency in E2F1/E2F2 double-mutant mice', *Journal of Clinical Investigation*, 113(10), pp. 1398–1407.

doi: 10.1172/JCI18879.

Iglesias-Ara, A., Zenarruzabeitia, O., Fernandez-Rueda, J., Sánchez-Tilló, E., Field, S. J., Celada, A. and Zubiaga, A. M. (2010) 'Accelerated DNA replication in E2F1- and E2F2-deficient macrophages leads to induction of the DNA damage response and p21CIP1-dependent senescence', *Oncogene*, 29(41), pp. 5579–5590. doi: 10.1038/onc.2010.296.

Iglesias-Ara, A., Zenarruzabeitia, O., Buelta, L., Merino, J. and Zubiaga, A. M. (2015) 'E2F1 and E2F2 prevent replicative stress and subsequent p53-dependent organ involution', *Cell Death & Differentiation*, 22(10), pp. 1577–1589. doi: 10.1038/cdd.2015.4.

Infante, A., Laresgoiti, U., Fernández-Rueda, J., Fullaondo, A., Galán, J., Díaz-Uriarte, R., Malumbres, M., Field, S. J. and M. Zubiaga, A. (2008) 'E2F2 represses cell cycle regulators to maintain quiescence', *Cell Cycle*, 7(24), pp. 3915–3927. doi: 10.4161/cc.7.24.7379.

Irwin, M., Marin, M. C., Phillips, A. C., Seelan, R. S., Smith, D. I., Liu, W., Flores, E. R., Tsai, K. Y., Jacks, T., Vousden, K. H. and Kaelin Jr, W. G. (2000) 'Role for the p53 homologue p73 in E2F-1-induced apoptosis', *Nature*. Nature Publishing Group, 407(6804), pp. 645–648. doi: 10.1038/35036614.

Iyer, D. R. and Rhind, N. (2017) 'The Intra-S Checkpoint Responses to DNA Damage.', *Genes*. Multidisciplinary Digital Publishing Institute (MDPI), 8(2). doi: 10.3390/genes8020074.

Jiang, X., Nevins, J. R., Shats, I. and Chi, J.-T. (2015) 'E2F1-Mediated Induction of NFYB Attenuates Apoptosis via Joint Regulation of a Pro-Survival Transcriptional Program', *PLOS ONE*. Edited by M. M. Alonso, 10(6), p. e0127951. doi: 10.1371/journal.pone.0127951.

Jiang, Y., Rabbi, M., Kim, M., Ke, C., Lee, W., Clark, R. L., Mieczkowski, P. A. and Marszalek, P. E. (2009) 'UVA Generates Pyrimidine Dimers in DNA Directly', *Biophysical Journal*, 96(3), pp. 1151–1158. doi: 10.1016/j.bpj.2008.10.030.

Jin, R., Sun, Y., Qi, X., Zhang, H., Zhang, Y., Li, N., Ding, W. and Chen, D. (2011) 'E2F1 is involved in DNA single-strand break repair through cell-cycle-dependent upregulation of XRCC1 expression', *DNA Repair*, 10(9), pp. 926–933. doi: 10.1016/j.dnarep.2011.05.006.

Johnson, C. D., Esquela-Kerscher, A., Stefani, G., Byrom, M., Kelnar, K., Ovcharenko, D., Wilson, M., Wang, X., Shelton, J., Shingara, J., Chin, L., Brown, D. and Slack, F. J. (2007) 'The let-7 MicroRNA Represses Cell Proliferation Pathways in Human Cells', *Cancer Research*, 67(16), pp. 7713–7722. doi: 10.1158/0008-5472.CAN-07-1083.

Johnson, D. G., Ohtani, K. and Nevins, J. R. (1994) 'Autoregulatory control of E2F1 expression in response to positive and negative regulators of cell cycle progression.', *Genes & development*, 8(13), pp. 1514–25.

Kikuchi, J., Shimizu, R., Wada, T., Ando, H., Nakamura, M., Ozawa, K. and Furukawa, Y. (2007) 'E2F-6 Suppresses Growth-Associated Apoptosis of Human Hematopoietic Progenitor Cells by Counteracting Proapoptotic Activity of E2F-1', *Stem Cells*, 25(10), pp. 2439–2447. doi: 10.1634/stemcells.2007-0207.

Kim, J. M., Parmar, K., Huang, M., Weinstock, D. M., Ruit, C. A., Kutok, J. L. and D'Andrea, A. D. (2009) 'Inactivation of Murine Usp1 Results in Genomic Instability and a Fanconi Anemia Phenotype', *Developmental Cell*, 16(2), pp. 314–320. doi: 10.1016/j.devcel.2009.01.001.

Kim, Y.-J., Wilson, D. M. and III (2012) 'Overview of base excision repair biochemistry.', *Current molecular pharmacology*. NIH Public Access, 5(1), pp. 3–13.

Kim, Y.-K., Yu, J., Han, T. S., Park, S.-Y., Namkoong, B., Kim, D. H., Hur, K., Yoo, M.-W., Lee, H.-J., Yang, H.-K. and Kim, V. N. (2009) 'Functional links between clustered microRNAs: suppression of cell-cycle inhibitors by microRNA clusters in gastric cancer', *Nucleic Acids Research*, 37(5), pp. 1672–1681. doi: 10.1093/nar/gkp002.

Knudsen, K. N., Nielsen, B. S., Lindebjerg, J., Hansen, T. F., Holst, R. and Sørensen, F. B. (2015) 'microRNA-17 Is the Most Up-Regulated Member of the miR-17-92 Cluster during Early Colon Cancer Evolution', *PLOS ONE*. Edited by J. Q. Cheng, 10(10), p. e0140503. doi: 10.1371/journal.pone.0140503.

Kovesdi, I., Reichel, R. and Nevins, J. R. (1986) 'Identification of a cellular transcription factor involved in E1A trans-activation.', *Cell*, 45(2), pp. 219–28.

Kowalik, T. F., DeGregori, J., Leone, G., Jakoi, L. and Nevins, J. R. (1998) 'E2F1-specific induction of apoptosis and p53 accumulation, which is blocked by Mdm2.', *Cell growth & differentiation : the molecular biology journal of the American Association for Cancer Research*. AACR, 9(2), pp. 113–8.

Krol, J., Loedige, I. and Filipowicz, W. (2010) 'The widespread regulation of microRNA biogenesis, function and decay', *Nature Reviews Genetics*, 11(9), pp. 597–610. doi: 10.1038/nrg2843.

Kuo, L. J. and Yang, L.-X. (2008) 'Gamma-H2AX - a novel biomarker for DNA double-strand breaks.', *In vivo (Athens, Greece)*. International Institute of Anticancer Research, 22(3), pp. 305–9.

Lang, S. E., McMahon, S. B., Cole, M. D. and Hearing, P. (2001) 'E2F transcriptional activation requires TRRAP and GCN5 cofactors.', *The Journal of biological chemistry*. American Society for Biochemistry and Molecular Biology, 276(35), pp. 32627–34. doi: 10.1074/jbc.M102067200.

Langevin, F., Crossan, G. P., Rosado, I. V., Arends, M. J. and Patel, K. J. (2011) 'Fancd2 counteracts the toxic effects of naturally produced aldehydes in mice', *Nature*. Nature Publishing Group, 475(7354), pp. 53–58. doi: 10.1038/nature10192.

Laresgoiti, U., Apraiz, A., Olea, M., Mitxelena, J., Osinalde, N., Rodriguez, J. A., Fullaondo, A. and Zubiaga, A. M. (2013) 'E2F2 and CREB cooperatively regulate transcriptional activity of cell cycle genes', *Nucleic Acids Research*, 41(22), pp. 10185–10198. doi: 10.1093/nar/gkt821.

De Las Rivas, J. and Fontanillo, C. (2010) 'Protein-protein interactions essentials: key concepts to building and analyzing interactome networks.', *PLoS computational biology*. Public Library of Science, 6(6), p. e1000807. doi: 10.1371/journal.pcbi.1000807.

Latorre, I., Chesney, M. A., Garrigues, J. M., Stempor, P., Appert, A., Francesconi, M., Strome, S. and Ahringer, J. (2015) 'The DREAM complex promotes gene body H2A.Z for target repression'. doi: 10.1101/gad.255810.114.

Lazzerini Denchi, E. and Helin, K. (2005) 'E2F1 is crucial for E2F-dependent apoptosis.', *EMBO reports*. EMBO Press, 6(7), pp. 661–8. doi: 10.1038/sj.embor.7400452.

Lee, B.-K., Bhinge, A. A. and Iyer, V. R. (2011) 'Wide-ranging functions of E2F4 in transcriptional activation and repression revealed by genome-wide analysis', *Nucleic Acids Research*, 39(9), pp. 3558–3573. doi: 10.1093/nar/gkq1313.

Lee, C., Chang, J. H., Lee, H. S. and Cho, Y. (2002) 'Structural basis for the recognition of the E2F transactivation domain by the retinoblastoma tumor suppressor', *Genes & Development*, 16(24), pp. 3199–3212. doi: 10.1101/gad.1046102.

Lee, M.-Y., Kim, M.-A., Kim, H.-J., Bae, Y.-S., Park, J.-I., Kwak, J.-Y., Chung, J. H. and Yun, J. (2007) 'Alkylating agent methyl methanesulfonate (MMS) induces a wave of global protein hyperacetylation: Implications in cancer cell death'. doi: 10.1016/j.bbrc.2007.06.084.

Lee, Y., Jeon, K., Lee, J.-T., Kim, S. and Kim, V. N. (2002) 'MicroRNA maturation: stepwise processing and subcellular localization.', *The EMBO journal*, 21(17), pp. 4663–70.

Leung, J. Y. and Nevins, J. R. (2012) 'E2F6 Associates with BRG1 in Transcriptional Regulation', *PLoS ONE*. Edited by F. Kashanchi, 7(10), p. e47967. doi: 10.1371/journal.pone.0047967.

Li, J. M., Hu, P. P., Shen, X., Yu, Y. and Wang, X. F. (1997) 'E2F4-RB and E2F4-p107 complexes suppress gene expression by transforming growth factor beta through E2F binding sites.', *Proceedings of the National Academy of Sciences of the United States of America*. National Academy of Sciences, 94(10), pp. 4948–53.

Li, J., Ran, C., Li, E., Gordon, F., Comstock, G., Siddiqui, H., Cleghorn, W., Chen, H.-Z., Kornacker, K., Liu, C.-G., Pandit, S. K., Khanizadeh, M., Weinstein, M., Leone, G. and de Bruin, A. (2008) 'Synergistic Function of E2F7 and E2F8 Is Essential for Cell Survival and Embryonic Development', *Developmental Cell*, 14(1), pp. 62–75. doi: 10.1016/j.devcel.2007.10.017.

Liang, C.-C., Zhan, B., Yoshikawa, Y., Haas, W., Gygi, S. P. and Cohn, M. A. (2015) 'UHRF1 Is a Sensor for DNA Interstrand Crosslinks and Recruits FANCD2 to Initiate the Fanconi Anemia Pathway', *Cell Reports*. Cell Press, 10(12), pp. 1947–1956. doi: 10.1016/J.CELREP.2015.02.053.

Liban, T. J., Thwaites, M. J., Dick, F. A. and Rubin, S. M. (2016) 'Structural Conservation and E2F Binding Specificity within the Retinoblastoma Pocket Protein Family', *Journal of Molecular Biology*, 428(20), pp. 3960–3971. doi: 10.1016/j.jmb.2016.08.017.

Lin, W. C., Lin, F. T. and Nevins, J. R. (2001) 'Selective induction of E2F1 in response to DNA damage, mediated by ATM-dependent phosphorylation.', *Genes & development*, 15(14), pp. 1833–44.

Liu, B., Shats, I., Angus, S. P., Gatza, M. L. and Nevins, J. R. (2013) 'Interaction of E2F7 Transcription Factor with E2F1 and C-terminal-binding Protein (CtBP) Provides a Mechanism for E2F7-dependent Transcription Repression', *Journal of Biological Chemistry*, 288(34), pp. 24581–24589. doi: 10.1074/jbc.M113.467506.

Liu, H., Wu, H.-Y., Wang, W.-Y., Zhao, Z.-L., Liu, X.-Y. and Wang, L.-Y. (2017) 'Regulation of miR-92a on vascular endothelial aging via mediating Nrf2-KEAP1-ARE signal pathway.', *European review for medical and pharmacological sciences*, 21(11), pp. 2734–2742.

Liu, K., Lin, F.-T., Ruppert, J. M. and Lin, W.-C. (2003) 'Regulation of E2F1 by BRCT domain-containing protein TopBP1.', *Molecular and cellular biology*, 23(9), pp. 3287–304.

Lizé, M., Pilarski, S. and Dobbelstein, M. (2010) 'E2F1-inducible microRNA 449a/b suppresses cell proliferation and promotes apoptosis', *Cell Death & Differentiation*, 17(3), pp. 452–458. doi: 10.1038/cdd.2009.188.

Logan, N., Delavaine, L., Graham, A., Reilly, C., Wilson, J., Brummelkamp, T. R., Hijmans, E. M., Bernards, R. and La Thangue, N. B. (2004) 'E2F-7: a distinctive E2F family member with an unusual organization of DNA-binding domains', *Oncogene*, 23(30), pp. 5138–5150. doi: 10.1038/sj.onc.1207649.

Lord, C. J. and Ashworth, A. (2017) 'PARP inhibitors: Synthetic lethality in the clinic', *Science*, 355(6330), pp. 1152–1158. doi: 10.1126/science.aam7344.

Lu, Z., Bauzon, F., Fu, H., Cui, J., Zhao, H., Nakayama, K., Nakayama, K. I. and Zhu, L. (2014) 'Skp2 suppresses apoptosis in Rb1-deficient tumours by limiting E2F1 activity.', *Nature communications*. NIH Public Access, 5, p. 3463. doi: 10.1038/ncomms4463.

Luo, W., Li, G., Yi, Z., Nie, Q. and Zhang, X. (2016) 'E2F1-miR-20a-5p/20b-5p auto-regulatory feedback loop involved in myoblast proliferation and differentiation', *Scientific Reports*, 6(1), p. 27904. doi: 10.1038/srep27904.

Lv, Y., Xiao, J., Liu, J. and Xing, F. (2017) 'E2F8 is a Potential Therapeutic Target for Hepatocellular Carcinoma', *Journal of Cancer*, 8(7), pp. 1205–1213. doi: 10.7150/jca.18255.

Mahaney, B. L., Meek, K. and Lees-Miller, S. P. (2009) 'Repair of ionizing radiation-induced DNA double-strand breaks by non-homologous end-joining', *Biochemical Journal*, 417(3), pp. 639–650. doi: 10.1042/BJ20080413.

Maiti, B., Li, J., de Bruin, A., Gordon, F., Timmers, C., Opavsky, R., Patil, K., Tuttle, J., Cleghorn, W. and Leone, G. (2005) 'Cloning and Characterization of Mouse *E2F8* , a Novel Mammalian *E2F* Family Member Capable of Blocking Cellular Proliferation', *Journal of Biological Chemistry*, 280(18), pp. 18211–18220. doi: 10.1074/jbc.M501410200.

Marques, M., Laflamme, L., Gervais, A. L. and Gaudreau, L. (2010) 'Reconciling the positive and negative roles of histone H2A.Z in gene transcription'. doi: 10.4161/epi.5.4.11520.

Marti, A., Wirbelauer, C., Scheffner, M. and Krek, W. (1999) 'Interaction between ubiquitin–protein ligase SCFSKP2and E2F-1 underlies the regulation of E2F-1 degradation', *Nature Cell Biology*, 1(1), pp. 14–19. doi: 10.1038/8984.

Martin, R. W., Orelli, B. J., Yamazoe, M., Minn, A. J., Takeda, S. and Bishop, D. K. (2007) 'RAD51 Up-regulation Bypasses BRCA1 Function and Is a Common Feature of BRCA1-Deficient Breast Tumors', *Cancer Research*, 67(20), pp. 9658–9665. doi: 10.1158/0008-5472.CAN-07-0290.

Martinez, L. A., Goluszko, E., Chen, H.-Z., Leone, G., Post, S., Lozano, G., Chen, Z. and Chauchereau, A. (2010) 'E2F3 is a mediator of DNA damage-induced apoptosis.', *Molecular and cellular biology*. American Society for Microbiology (ASM), 30(2), pp. 524–36. doi: 10.1128/MCB.00938-09.

Martínez-Balbás, M. A., Bauer, U. M., Nielsen, S. J., Brehm, A. and Kouzarides, T. (2000) 'Regulation of E2F1 activity by acetylation.', *The EMBO journal*. EMBO Press, 19(4), pp. 662–71. doi: 10.1093/emboj/19.4.662.

Matas-Rico, E., van Veen, M., Leyton-Puig, D., van den Berg, J., Koster, J., Kedziora, K. M., Molenaar, B., Weerts, M. J. A., de Rink, I., Medema, R. H., Giepmans, B. N. G., Perrakis, A., Jalink, K., Versteeg, R. and Moolenaar, W. H. (2016) 'Glycerophosphodiesterase GDE2 Promotes Neuroblastoma Differentiation through Glypican Release and Is a Marker of Clinical Outcome', *Cancer Cell*, 30(4), pp. 548–562. doi: 10.1016/j.ccell.2016.08.016.

McCabe, K. M., Olson, S. B. and Moses, R. E. (2009) 'DNA interstrand crosslink repair in mammalian cells', *Journal of Cellular Physiology*, 220(3), pp. 569–573. doi: 10.1002/jcp.21811.

McCabe, N., Lord, C. J., Tutt, A. N. J., Martin, N. M. B., Smith, G. C. M. and Ashworth, A. (2005) 'BRCA2-deficient CAPAN-1 cells are extremely sensitive to the inhibition of Poly (ADP-Ribose) polymerase: an issue of potency.', *Cancer biology & therapy*, 4(9), pp. 934–6.

Meek, K., Dang, V. and Lees-Miller, S. P. (2008) 'Chapter 2 DNA-PK: The Means to Justify the Ends?', *Advances in Immunology*. Academic Press, 99, pp. 33–58. doi: 10.1016/S0065-

2776(08)00602-0.

Michl, J., Zimmer, J. and Tarsounas, M. (2016) 'Interplay between Fanconi anemia and homologous recombination pathways in genome integrity.', *The EMBO journal*. European Molecular Biology Organization, 35(9), pp. 909–23. doi: 10.15252/embj.201693860.

Mikhailov, A., Cole, R. W. and Rieder, C. L. (2002) 'DNA damage during mitosis in human cells delays the metaphase/anaphase transition via the spindle-assembly checkpoint.', *Current biology : CB*, 12(21), pp. 1797–806.

Mitxelena, J. (2014) *Transcriptional mechanisms regulating cell cycle progression and DNA damage response by E2F7 transcription factor*. Doctoral thesis dissertation.

Mitxelena, J., Apraiz, A., Vallejo-Rodríguez, J., Malumbres, M. and Zubiaga, A. M. (2016) 'E2F7 regulates transcription and maturation of multiple microRNAs to restrain cell proliferation', *Nucleic Acids Research*, 44(12), pp. 5557–5570. doi: 10.1093/nar/gkw146.

Mitxelena, J.*, Apraiz, A.*, Vallejo-Rodríguez, J.*, García-Santisteban, I., Fullaondo, A., Alvarez-Fernández, M., Malumbres, M. and Zubiaga, A. M. (2018) 'An E2F7-dependent transcriptional program modulates DNA damage repair and genomic stability', *Nucleic Acids Research*, 46(9), pp. 4546–4559. doi: 10.1093/nar/gky218.* Equal contribution.

Moldovan, G.-L., Dejsuphong, D., Petalcorin, M. I. R., Hofmann, K., Takeda, S., Boulton, S. J. and D'Andrea, A. D. (2012) 'Inhibition of Homologous Recombination by the PCNA-Interacting Protein PARI', *Molecular Cell*, 45(1), pp. 75–86. doi: 10.1016/j.molcel.2011.11.010.

Moon, N.-S. and Dyson, N. (2008) 'E2F7 and E2F8 Keep the E2F Family in Balance', *Developmental Cell*. Cell Press, 14(1), pp. 1–3. doi: 10.1016/J.DEVCEL.2007.12.017.

Morey, L. and Helin, K. (2010) 'Polycomb group protein-mediated repression of transcription', *Trends in Biochemical Sciences*, 35(6), pp. 323–332. doi: 10.1016/j.tibs.2010.02.009.

Morgunova, E., Yin, Y., Jolma, A., Dave, K., Schmierer, B., Popov, A., Eremina, N., Nilsson, L. and Taipale, J. (2015) 'Structural insights into the DNA-binding specificity of E2F family transcription factors', *Nature Communications*. Nature Publishing Group, 6(1), p. 10050. doi: 10.1038/ncomms10050.

Murga, M., Fernández-Capetillo, O., Field, S. J., Moreno, B., Borlado, L. R., Fujiwara, Y., Balomenos, D., Vicario, A., Carrera, A. C., Orkin, S. H., Greenberg, M. E. and Zubiaga, A. M. (2001) 'Mutation of E2F2 in mice causes enhanced T lymphocyte proliferation, leading to the development of autoimmunity.', *Immunity*, 15(6), pp. 959–70.

Narasimha, A. M., Kaulich, M., Shapiro, G. S., Choi, Y. J., Sicinski, P. and Dowdy, S. F. (2014) 'Cyclin D activates the Rb tumor suppressor by mono-phosphorylation', *eLife*, 3. doi: 10.7554/eLife.02872.

Nevins, J. R. (1992) 'E2F: a link between the Rb tumor suppressor protein and viral oncoproteins.', *Science (New York, N.Y.)*, 258(5081), pp. 424–9.

Nevins, J. R. (1998) 'Toward an understanding of the functional complexity of the E2F and retinoblastoma families.', *Cell growth & differentiation : the molecular biology journal of the American Association for Cancer Research*, 9(8), pp. 585–93.

Nevins, J. R. (2001) 'The Rb/E2F pathway and cancer.', *Human molecular genetics*, 10(7), pp. 699–703.

Nijman, S. M. B., Huang, T. T., Dirac, A. M. G., Brummelkamp, T. R., Kerkhoven, R. M., D'Andrea, A. D. and Bernards, R. (2005) 'The deubiquitinating enzyme USP1 regulates the Fanconi anemia pathway.', *Molecular cell*. Elsevier, 17(3), pp. 331–9. doi: 10.1016/j.molcel.2005.01.008.

O'Donnell, K. A., Wentzel, E. A., Zeller, K. I., Dang, C. V. and Mendell, J. T. (2005) 'c-Myc-regulated microRNAs modulate E2F1 expression', *Nature*. Nature Publishing Group, 435(7043), pp. 839–843. doi: 10.1038/nature03677.

Ofir, M., Hacohen, D. and Ginsberg, D. (2011) 'miR-15 and miR-16 Are Direct Transcriptional Targets of E2F1 that Limit E2F-Induced Proliferation by Targeting Cyclin E', *Molecular Cancer Research*, 9(4), pp. 440–447. doi: 10.1158/1541-7786.MCR-10-0344.

Orlando, V. (2000) 'Mapping chromosomal proteins in vivo by formaldehyde-crosslinked-chromatin immunoprecipitation.', *Trends in biochemical sciences*, 25(3), pp. 99–104.

Osawa, T., Davies, D. and Hartley, J. A. (2011) 'Mechanism of cell death resulting from DNA interstrand cross-linking in mammalian cells', *Cell Death & Disease*. Nature Publishing Group, 2(8), pp. e187–e187. doi: 10.1038/cddis.2011.70.

Oufkir, T., Arseneault, M., Sanderson, J. T. and Vaillancourt, C. (2010) 'The 5-HT 2A serotonin receptor enhances cell viability, affects cell cycle progression and activates MEKeERK1/2 and JAK2eSTAT3 signalling pathways in human choriocarcinoma cell lines'. doi: 10.1016/j.placenta.2010.02.019.

Pagliarini, V., Giglio, P., Bernardoni, P., De Zio, D., Fimia, G. M., Piacentini, M. and Corazzari, M. (2015) 'Downregulation of E2F1 during ER stress is required to induce apoptosis', *Journal of Cell Science*, 128(6), pp. 1166–1179. doi: 10.1242/jcs.164103.

Peart, M. J., Poyurovsky, M. V., Kass, E. M., Urist, M., Verschuren, E., Summers, M. K., Jackson, P. K. and Prives, C. (2010) 'APC/C ^{Cdc20} targets E2F1 for degradation in prometaphase', *Cell Cycle*, 9(19), pp. 3956–3964. doi: 10.4161/cc.9.19.13162.

Petermann, E., Orta, M. L., Issaeva, N., Schultz, N. and Helleday, T. (2010) 'Hydroxyurea-Stalled Replication Forks Become Progressively Inactivated and Require Two Different RAD51-Mediated Pathways for Restart and Repair', *Molecular Cell*, 37(4), pp. 492–502. doi: 10.1016/j.molcel.2010.01.021.

Pierce, A. J., Johnson, R. D., Thompson, L. H. and Jasin, M. (1999) 'XRCC3 promotes homology-directed repair of DNA damage in mammalian cells'.

Polager, S., Kalma, Y., Berkovich, E. and Ginsberg, D. (2002) 'E2Fs up-regulate expression of genes involved in DNA replication, DNA repair and mitosis', *Oncogene*, 21(3), pp. 437–446. doi: 10.1038/sj.onc.1205102.

Polager, S. and Ginsberg, D. (2008) 'E2F – at the crossroads of life and death', *Trends in Cell Biology*, 18(11), pp. 528–535. doi: 10.1016/j.tcb.2008.08.003.

Poliseno, L., Salmena, L., Riccardi, L., Fornari, A., Song, M. S., Hobbs, R. M., Sportoletti, P., Varmeh, S., Egia, A., Fedele, G., Rameh, L., Loda, M. and Pandolfi, P. P. (2010) 'Identification of the miR-106b~25 microRNA cluster as a proto-oncogenic PTEN-targeting intron that cooperates with its host gene MCM7 in transformation.', *Science Signaling*, 3(117), p. ra29-ra29. doi: 10.1126/scisignal.2000594.

Pomerantz, J., Schreiber-Agus, N., Liégeois, N. J., Silverman, A., Alland, L., Chin, L., Potes, J., Chen, K., Orlow, I., Lee, H. W., Cordon-Cardo, C. and DePinho, R. A. (1998) 'The Ink4a tumor suppressor

gene product, p19Arf, interacts with MDM2 and neutralizes MDM2's inhibition of p53.', *Cell*. Elsevier, 92(6), pp. 713–23. doi: 10.1016/S0092-8674(00)81400-2.

Powell, S. N. and Kachnic, L. A. (2003) 'Roles of BRCA1 and BRCA2 in homologous recombination, DNA replication fidelity and the cellular response to ionizing radiation', *Oncogene*, 22, pp. 5784–5791. doi: 10.1038/sj.onc.1206678.

Pusapati, R. V., Weaks, R. L., Rounbehler, R. J., McArthur, M. J. and Johnson, D. G. (2009) 'E2F2 suppresses Myc-induced proliferation and tumorigenesis', *Molecular Carcinogenesis*, 49(2), p. n/a-n/a. doi: 10.1002/mc.20584.

Pützer, B. M. (2007) 'E2F1 death pathways as targets for cancer therapy', *Journal of Cellular and Molecular Medicine*, 11(2), pp. 239–251. doi: 10.1111/j.1582-4934.2007.00030.x.

Qin, X. Q., Livingston, D. M., Kaelin, W. G. and Adams, P. D. (1994) 'Deregulated transcription factor E2F-1 expression leads to S-phase entry and p53-mediated apoptosis.', *Proceedings of the National Academy of Sciences of the United States of America*, 91(23), pp. 10918–22.

Rabinovich, A., Jin, V. X., Rabinovich, R., Xu, X. and Farnham, P. J. (2008) 'E2F in vivo binding specificity: Comparison of consensus versus nonconsensus binding sites', *Genome Research*, 18(11), pp. 1763–1777. doi: 10.1101/gr.080622.108.

Rappold, I., Iwabuchi, K., Date, T. and Chen, J. (2001) 'Tumor suppressor p53 binding protein 1 (53BP1) is involved in DNA damage-signaling pathways.', *The Journal of cell biology*. The Rockefeller University Press, 153(3), pp. 613–20.

Ray Chaudhuri, A. and Nussenzweig, A. (2017) 'The multifaceted roles of PARP1 in DNA repair and chromatin remodelling', *Nature Reviews Molecular Cell Biology*. Nature Publishing Group, 18(10), pp. 610–621. doi: 10.1038/nrm.2017.53.

Remeseiro, S., Cuadrado, A., Carretero, M., Martínez, P., Drosopoulos, W. C., Cañamero, M., Schildkraut, C. L., Blasco, M. A. and Losada, A. (2012) 'Cohesin-SA1 deficiency drives aneuploidy and tumourigenesis in mice due to impaired replication of telomeres', *The EMBO Journal*, 31(9), pp. 2076–2089. doi: 10.1038/emboj.2012.11.

Ren, B., Cam, H., Takahashi, Y., Volkert, T., Terragni, J., Young, R. A. and Dynlacht, B. D. (2002) 'E2F integrates cell cycle progression with DNA repair, replication, and G(2)/M checkpoints.', *Genes & development*. Cold Spring Harbor Laboratory Press, 16(2), pp. 245–56. doi: 10.1101/gad.949802.

Richardson, C., Moynahan, M. E. and Jasin, M. (1999) 'Homologous recombination between heterologs during repair of a double-strand break. Suppression of translocations in normal cells.', *Annals of the New York Academy of Sciences*, 886, pp. 183–6.

Rodriguez, A., Griffiths-Jones, S., Ashurst, J. L. and Bradley, A. (2004) 'Identification of mammalian microRNA host genes and transcription units.', *Genome research*. Cold Spring Harbor Laboratory Press, 14(10A), pp. 1902–10. doi: 10.1101/gr.2722704.

Rogakou, E. P., Pilch, D. R., Orr, A. H., Ivanova, V. S. and Bonner, W. M. (1998) 'DNA double-stranded breaks induce histone H2AX phosphorylation on serine 139.', *The Journal of biological chemistry*, 273(10), pp. 5858–68.

Romagosa, C., Simonetti, S., López-Vicente, L., Mazo, A., Lleonart, M. E., Castellvi, J. and Ramon y Cajal, S. (2011) 'p16Ink4a overexpression in cancer: a tumor suppressor gene associated with senescence and high-grade tumors', *Oncogene*. Nature Publishing Group, 30(18), pp. 2087–

2097. doi: 10.1038/onc.2010.614.

Roots, R., Kraft, G. and Gosschalk, E. (1985) 'The formation of radiation-induced DNA breaks: the ratio of double-strand breaks to single-strand breaks.', *International journal of radiation oncology, biology, physics*, 11(2), pp. 259–65.

Rounbehler, R. J., Rogers, P. M., Conti, C. J. and Johnson, D. G. (2002) 'Inactivation of E2f1 enhances tumorigenesis in a Myc transgenic model.', *Cancer research*. American Association for Cancer Research, 62(11), pp. 3276–81.

Russo, T., Zambrano, N., Esposito, F., Ammendola, R., Cimino, F., Fiscella, M., Jackman, J., O'Connor, P. M., Anderson, C. W. and Appella, E. (1995) 'A p53-independent pathway for activation of WAF1/CIP1 expression following oxidative stress.', *The Journal of biological chemistry*. American Society for Biochemistry and Molecular Biology, 270(49), pp. 29386–91. doi: 10.1074/JBC.270.49.29386.

Saenz-Ponce, N., Pillay, R., de Long, L. M., Kashyap, T., Argueta, C., Landesman, Y., Hazar-Rethinam, M., Boros, S., Panizza, B., Jacquemyn, M., Daelemans, D., Gannon, O. M. and Saunders, N. A. (2018) 'Targeting the XPO1-dependent nuclear export of E2F7 reverses anthracycline resistance in head and neck squamous cell carcinomas', *Science Translational Medicine*, 10(447), p. eaar7223. doi: 10.1126/scitranslmed.aar7223.

Salvatori, B., Iosue, I., Mangiavacchi, A., Loddo, G., Padula, F., Chiaretti, S., Peragine, N., Bozzoni, I., Fazi, F. and Fatica, A. (2012) 'The microRNA-26a target E2F7 sustains cell proliferation and inhibits monocytic differentiation of acute myeloid leukemia cells', *Cell Death & Disease*, 3(10), pp. e413–e413. doi: 10.1038/cddis.2012.151.

Santamaria, D. and Ortega, S. (2006) 'Cyclins and CDKS in development and cancer: lessons from genetically modified mice.', *Frontiers in bioscience : a journal and virtual library*, 11, pp. 1164–88.

Sárközy, M., Kahán, Z. and Csont, T. (2018) 'A myriad of roles of miR-25 in health and disease', *Oncotarget*, 9(30), pp. 21580–21612. doi: 10.18632/oncotarget.24662.

Sears, R., Ohtani, K. and Nevins, J. R. (1997) 'Identification of positively and negatively acting elements regulating expression of the E2F2 gene in response to cell growth signals.', *Molecular and cellular biology*, 17(9), pp. 5227–35.

Semizarov, D., Kroeger, P. and Fesik, S. (2004) 'siRNA-mediated gene silencing: a global genome view.', *Nucleic acids research*. Oxford University Press, 32(13), pp. 3836–45. doi: 10.1093/nar/gkh714.

Ben Shachar, B., Feldstein, O., Hacohen, D. and Ginsberg, D. (2010) 'The Tumor Suppressor Maspin Mediates E2F1-Induced Sensitivity of Cancer Cells to Chemotherapy', *Molecular Cancer Research*, 8(3), pp. 363–372. doi: 10.1158/1541-7786.MCR-09-0137.

Shaltiel, I. A., Krennin, L., Bruinsma, W. and Medema, R. H. (2015) 'The same, only different – DNA damage checkpoints and their reversal throughout the cell cycle', *Journal of Cell Science*, 128, pp. 607–620. doi: 10.1242/jcs.163766.

Shats, I., Deng, M., Davidovich, A., Zhang, C., Kwon, J. S., Manandhar, D., Gordân, R., Yao, G. and You, L. (2017) 'Expression level is a key determinant of E2F1-mediated cell fate', 24. doi: 10.1038/cdd.2017.12.

Siddiqui, E. J., Shabbir, M., Mikhailidis, D. P., Thompson, C. S. and Mumtaz, F. H. (2006) 'The Role

of Serotonin (5-Hydroxytryptamine1A and 1B) Receptors in Prostate Cancer Cell Proliferation', *The Journal of Urology*, 176(4), pp. 1648–1653. doi: 10.1016/j.juro.2006.06.087.

Singh, A. and Xu, Y.-J. (2016) 'The Cell Killing Mechanisms of Hydroxyurea.', *Genes*. Multidisciplinary Digital Publishing Institute (MDPI), 7(11). doi: 10.3390/genes7110099.

Skotheim, J. M., Di Talia, S., Siggia, E. D. and Cross, F. R. (2008) 'Positive feedback of G1 cyclins ensures coherent cell cycle entry', *Nature*, 454(7202), pp. 291–296. doi: 10.1038/nature07118.

Slupianek, A., Schmutte, C., Tombline, G., Nieborowska-Skorska, M., Hoser, G., Nowicki, M. O., Pierce, A. J., Fishel, R. and Skorski, T. (2001) 'BCR/ABL regulates mammalian RecA homologs, resulting in drug resistance.', *Molecular cell*, 8(4), pp. 795–806.

Stanelle, J., Stiewe, T., Theseling, C. C., Peter, M. and Pützer, B. M. (2002) 'Gene expression changes in response to E2F1 activation.', *Nucleic acids research*, 30(8), pp. 1859–67.

Di Stefano, L., Jensen, M. R. and Helin, K. (2003) 'E2F7, a novel E2F featuring DP-independent repression of a subset of E2F-regulated genes.', *The EMBO journal*. European Molecular Biology Organization, 22(23), pp. 6289–98. doi: 10.1093/emboj/cdg613.

Stern, L. L., Mason, J. B., Selhub, J. and Choi, S. W. (2000) 'Genomic DNA hypomethylation, a characteristic of most cancers, is present in peripheral leukocytes of individuals who are homozygous for the C677T polymorphism in the methylenetetrahydrofolate reductase gene.', *Cancer epidemiology, biomarkers & prevention : a publication of the American Association for Cancer Research, cosponsored by the American Society of Preventive Oncology*, 9(8), pp. 849–53.

Stevens, C. and La Thangue, N. B. (2004) 'The emerging role of E2F-1 in the DNA damage response and checkpoint control', *DNA Repair*, 3(8–9), pp. 1071–1079. doi: 10.1016/j.dnarep.2004.03.034.

Stewart-Ornstein, J., Cheng, H. W. (Jacky) and Lahav, G. (2017) 'Conservation and Divergence of p53 Oscillation Dynamics across Species', *Cell Systems*, 5(4), p. 410–417.e4. doi: 10.1016/j.cels.2017.09.012.

Stiewe, T. and Pützer, B. M. (2000) 'Role of the p53-homologue p73 in E2F1-induced apoptosis', *Nature Genetics*, 26(4), pp. 464–469. doi: 10.1038/82617.

Takahashi, Y., Rayman, J. B. and Dynlacht, B. D. (2000) 'Analysis of promoter binding by the E2F and pRB families in vivo: distinct E2F proteins mediate activation and repression.', *Genes & development*. Cold Spring Harbor Laboratory Press, 14(7), pp. 804–16.

Talluri, S. and Dick, F. A. (2012) 'Regulation of transcription and chromatin structure by pRB: Here, there and everywhere', *Cell Cycle*, 11(17), pp. 3189–3198. doi: 10.4161/cc.21263.

Tategu, M., Arauchi, T., Tanaka, R., Nakagawa, H. and Yoshida, K. (2007) 'Systems biology-based identification of crosstalk between E2F transcription factors and the Fanconi anemia pathway.', *Gene regulation and systems biology*, 1, pp. 1–8.

Taubert, S., Gorrini, C., Frank, S. R., Parisi, T., Fuchs, M., Chan, H.-M., Livingston, D. M. and Amati, B. (2004) 'E2F-dependent histone acetylation and recruitment of the Tip60 acetyltransferase complex to chromatin in late G1.', *Molecular and cellular biology*, 24(10), pp. 4546–56.

Teplyuk, N. M., Uhlmann, E. J., Wong, A. H.-K., Karmali, P., Basu, M., Gabriely, G., Jain, A., Wang, Y., Chiocca, E. A., Stephens, R., Marcusson, E., Yi, M. and Krichevsky, A. M. (2015) 'MicroRNA-

10b inhibition reduces E2F1-mediated transcription and miR-15/16 activity in glioblastoma', *Oncotarget*, 6(6), pp. 3770–83. doi: 10.18632/oncotarget.3009.

TGCA Network (2014) 'Comprehensive genomic characterization of head and neck squamous cell carcinomas', *Nature*, 517. doi: 10.1038/nature14129.

Thurlings, I., Martínez-López, L., Westendorp, B., Zijp, M., Kuiper, R., Tooten, P., Kent, L., Leone, G., Vos, H., Burgering, B. and De Bruin, A. (2016) 'Synergistic functions of E2F7 and E2F8 are critical to suppress stress-induced skin cancer', *Oncogene*, 36. doi: 10.1038/onc.2016.251.

Toledo, L. I., Murga, M. and Fernandez-Capetillo, O. (2011) 'Targeting ATR and Chk1 kinases for cancer treatment: A new model for new (and old) drugs', *Molecular Oncology*. No longer published by Elsevier, 5(4), pp. 368–373. doi: 10.1016/J.MOLONC.2011.07.002.

Toledo, L., Neelsen, K. J. and Lukas, J. (2017) 'Replication Catastrophe: When a Checkpoint Fails because of Exhaustion.', *Molecular cell*. Elsevier, 66(6), pp. 735–749. doi: 10.1016/j.molcel.2017.05.001.

Trimarchi, J. M., Fairchild, B., Wen, J. and Lees, J. A. (2001) 'The E2F6 transcription factor is a component of the mammalian Bmi1-containing polycomb complex', *Proceedings of the National Academy of Sciences*, 98(4), pp. 1519–1524. doi: 10.1073/pnas.041597698.

Trimarchi, J. M. and Lees, J. A. (2002) 'Sibling rivalry in the E2F family', *Nature Reviews Molecular Cell Biology*. Nature Publishing Group, 3(1), pp. 11–20. doi: 10.1038/nrm714.

Uchida, C. (2016) 'Roles of pRB in the Regulation of Nucleosome and Chromatin Structures', *BioMed Research International*. Hindawi, 2016, pp. 1–11. doi: 10.1155/2016/5959721.

Voorhoeve, P. M., le Sage, C., Schrier, M., Gillis, A. J. M., Stoop, H., Nagel, R., Liu, Y.-P., van Duijse, J., Drost, J., Griekspoor, A., Zlotorynski, E., Yabuta, N., De Vita, G., Nojima, H., Looijenga, L. H. J. and Agami, R. (2006) 'A Genetic Screen Implicates miRNA-372 and miRNA-373 As Oncogenes in Testicular Germ Cell Tumors', *Cell*, 124(6), pp. 1169–1181. doi: 10.1016/j.cell.2006.02.037.

Walden, H. and Deans, A. J. (2014) 'The Fanconi Anemia DNA Repair Pathway: Structural and Functional Insights into a Complex Disorder', *Annual Review of Biophysics*. Annual Reviews , 43(1), pp. 257–278. doi: 10.1146/annurev-biophys-051013-022737.

Wang, A., Schneider-Broussard, R., Kumar, A. P., MacLeod, M. C. and Johnson, D. G. (2000) 'Regulation of BRCA1 expression by the Rb-E2F pathway.', *The Journal of biological chemistry*. American Society for Biochemistry and Molecular Biology, 275(6), pp. 4532–6. doi: 10.1074/JBC.275.6.4532.

Wang, P., Lee, J. W., Yu, Y., Turner, K., Zou, Y., Jackson-Cook, C. K. and Povirk, L. F. (2002) 'Gene rearrangements induced by the DNA double-strand cleaving agent neocarzinostatin: conservative non-homologous reciprocal exchanges in an otherwise stable genome.', *Nucleic acids research*. Oxford University Press, 30(12), pp. 2639–46.

Wang, W., Corrigan-Cummins, M., Hudson, J., Maric, I., Simakova, O., Neelapu, S. S., Kwak, L. W., Janik, J. E., Gause, B., Jaffe, E. S. and Calvo, K. R. (2012) 'MicroRNA profiling of follicular lymphoma identifies microRNAs related to cell proliferation and tumor response', *Haematologica*, 97(4), pp. 586–594. doi: 10.3324/haematol.2011.048132.

Weijts, B. G. M. W., Bakker, W. J., Cornelissen, P. W. A., Liang, K.-H., Schaftenaar, F. H., Westendorp, B., de Wolf, C. A. C. M. T., Paciejewska, M., Scheele, C. L. G. J., Kent, L., Leone, G., Schulte-Merker, S. and de Bruin, A. (2012) 'E2F7 and E2F8 promote angiogenesis through

transcriptional activation of VEGFA in cooperation with HIF1', *The EMBO Journal*, 31(19), pp. 3871–3884. doi: 10.1038/emboj.2012.231.

Weinberg, R. A. (1995) 'The retinoblastoma protein and cell cycle control.', *Cell*, 81(3), pp. 323–30.

Weinmann, A. S., Yan, P. S., Oberley, M. J., Huang, T. H.-M. and Farnham, P. J. (2002) 'Isolating human transcription factor targets by coupling chromatin immunoprecipitation and CpG island microarray analysis', *Genes & Development*, 16(2), pp. 235–244. doi: 10.1101/gad.943102.

Wells, J., Boyd, K. E., Fry, C. J., Bartley, S. M. and Farnham, P. J. (2000) 'Target gene specificity of E2F and pocket protein family members in living cells.', *Molecular and cellular biology*. American Society for Microbiology, 20(16), pp. 5797–807. doi: 10.1128/MCB.20.16.5797-5807.2000.

Westendorp, B., Mokry, M., Groot Koerkamp, M. J. A., Holstege, F. C. P., Cuppen, E. and de Bruin, A. (2012) 'E2F7 represses a network of oscillating cell cycle genes to control S-phase progression', *Nucleic Acids Research*, 40(8), pp. 3511–3523. doi: 10.1093/nar/gkr1203.

Witzel, I.-I., Koh, L. F. and Perkins, N. D. (2010) 'Regulation of cyclin D1 gene expression.', *Biochemical Society transactions*. Portland Press Limited, 38(Pt 1), pp. 217–22. doi: 10.1042/BST0380217.

Woods, K., Thomson, J. M. and Hammond, S. M. (2007) 'Direct Regulation of an Oncogenic Micro-RNA Cluster by E2F Transcription Factors', *Journal of Biological Chemistry*, 282(4), pp. 2130–2134. doi: 10.1074/jbc.C600252200.

Wyatt, M. D. and Pittman, D. L. (2006) 'Methylating Agents and DNA Repair Responses: Methylated Bases and Sources of Strand Breaks', *Chemical Research in Toxicology*, 19(12), pp. 1580–1594. doi: 10.1021/tx060164e.

Xie, Y., Si, J., Wang, Y.-P., Li, H.-Y., Di, C.-X., Yan, J.-F., Ye, Y.-C., Zhang, Y.-S. and Zhang, H. (2018) 'E2F is involved in radioresistance of carbon ion induced apoptosis via Bax/caspase 3 signal pathway in human hepatoma cell', *Journal of Cellular Physiology*, 233(2), pp. 1312–1320. doi: 10.1002/jcp.26005.

Xu, X., Bieda, M., Jin, V. X., Rabinovich, A., Oberley, M. J., Green, R. and Farnham, P. J. (2007) 'A comprehensive ChIP chip analysis of E2F1, E2F4, and E2F6 in normal and tumor cells reveals interchangeable roles of E2F family members', *Genome Research*, 17(11), pp. 1550–1561. doi: 10.1101/gr.6783507.

Xu, X., Cai, N., Zhi, T., Bao, Z., Wang, D., Liu, Y., Jiang, K., Fan, L., Ji, J. and Liu, N. (2017) 'MicroRNA-1179 inhibits glioblastoma cell proliferation and cell cycle progression via directly targeting E2F transcription factor 5.', *American journal of cancer research*, 7(8), pp. 1680–1692.

Xu, Z.-Y., Loignon, M., Han, F.-Y., Panasci, L. and Aloyz, R. (2005) 'Xrcc3 Induces Cisplatin Resistance by Stimulation of Rad51-Related Recombinational Repair, S-Phase Checkpoint Activation, and Reduced Apoptosis', *Journal of Pharmacology and Experimental Therapeutics*, 314(2), pp. 495–505. doi: 10.1124/jpet.105.084053.

Yang, S., Tang, W., He, Y., Wen, L., Sun, B. and Li, S. (2018) 'Long non-coding RNA and microRNA-675/let-7a mediates the protective effect of melatonin against early brain injury after subarachnoid hemorrhage via targeting TP53 and neural growth factor', *Cell Death & Disease*. Nature Publishing Group, 9(2), p. 99. doi: 10.1038/s41419-017-0155-8.

Yang, W.-W., Shu, B., Zhu, Y. and Yang, H.-T. (2008) 'E2F6 Inhibits Cobalt Chloride-Mimetic

Hypoxia-induced Apoptosis through E2F1', *Molecular Biology of the Cell*. Edited by K. Luo, 19(9), pp. 3691–3700. doi: 10.1091/mbc.e08-02-0171.

Yao, G., Lee, T. J., Mori, S., Nevins, J. R. and You, L. (2008) 'A bistable Rb–E2F switch underlies the restriction point', *Nature Cell Biology*. Nature Publishing Group, 10(4), pp. 476–482. doi: 10.1038/ncb1711.

Yu, X., Chini, C. C. S., He, M., Mer, G. and Chen, J. (2003) 'The BRCT domain is a phospho-protein binding domain.', *Science (New York, N.Y.)*. American Association for the Advancement of Science, 302(5645), pp. 639–42. doi: 10.1126/science.1088753.

Yuan, R., Vos, H. R., Van Es, R. M., Chen, J., Burgering, B. M., Westendorp, B. and De Bruin, A. (2018) 'Chk1 and 14-3-3 proteins inhibit atypical E2Fs to prevent a permanent cell cycle arrest', *The EMBO Journal*, 37. doi: 10.15252/embj.

Zalmas, L. P., Zhao, X., Graham, A. L., Fisher, R., Reilly, C., Coutts, A. S. and La Thangue, N. B. (2008) 'DNA-damage response control of E2F7 and E2F8', *EMBO reports*, 9(3), pp. 252–259. doi: 10.1038/sj.embor.7401158.

Zalmas, L.-P., Coutts, A., Helleday, T. and La Thangue, N. B. (2013) 'E2F-7 couples DNA damage-dependent transcription with the DNA repair process', *Cell Cycle*, 12(18), pp. 3037–3051. doi: 10.4161/cc.26078.

Zhan, L., Zhang, Y., Wang, W., Song, E., Fan, Y. and Wei, B. (2016) 'E2F1: a promising regulator in ovarian carcinoma', *Tumor Biology*. doi: 10.1007/s13277-015-4770-7.

Zhang, J., Dewar, J. M., Budzowska, M., Motnenko, A., Cohn, M. A. and Walter, J. C. (2015) 'DNA interstrand cross-link repair requires replication-fork convergence.', *Nature structural & molecular biology*. NIH Public Access, 22(3), pp. 242–7. doi: 10.1038/nsmb.2956.

Zhang, J., Gong, X., Tian, K., Chen, D., Sun, J., Wang, G. and Guo, M. (2015) 'miR-25 promotes glioma cell proliferation by targeting CDKN1C', *Biomedicine & Pharmacotherapy*, 71, pp. 7–14. doi: 10.1016/j.biopha.2015.02.005.

Zhang, P., Pei, C., Wang, X., Xiang, J., Sun, B.-F., Cheng, Y., Qi, X., Marchetti, M., Xu, J.-W., Sun, Y.-P., Edgar, B. A. and Yuan, Z. (2017) 'A Balance of Yki/Sd Activator and E2F1/Sd Repressor Complexes Controls Cell Survival and Affects Organ Size', *Developmental Cell*, 43(5), p. 603–617.e5. doi: 10.1016/j.devcel.2017.10.033.

Zhang, X., Moréra, S., Bates, P. A., Whitehead, P. C., Coffer, A. I., Hainbucher, K., Nash, R. A., Sternberg, M. J., Lindahl, T. and Freemont, P. S. (1998) 'Structure of an XRCC1 BRCT domain: a new protein-protein interaction module.', *The EMBO journal*, 17(21), pp. 6404–11. doi: 10.1093/emboj/17.21.6404.

Zhao, J., Ramos, R. and Demma, M. (2013) 'CDK8 regulates E2F1 transcriptional activity through S375 phosphorylation', *Oncogene*, 32(30), pp. 3520–3530. doi: 10.1038/onc.2012.364.

Zhao, L.-J., Subramanian, T., Vijayalingam, S. and Chinnadurai, G. (2014) 'CtBP2 proteome: Role of CtBP in E2F7-mediated repression and cell proliferation', *Genes & Cancer*, 5(1–2), p. 31. doi: 10.18632/genesandcancer.2.

Zhao, Y., Wang, F., Chen, S., Wan, J. and Wang, G. (2017) 'Methods of MicroRNA Promoter Prediction and Transcription Factor Mediated Regulatory Network', *BioMed Research International*. Hindawi, 2017, pp. 1–8. doi: 10.1155/2017/7049406.

Zhu, Y., Gu, J., Li, Y., Peng, C., Shi, M., Wang, X., Wei, G., Ge, O., Wang, D., Zhang, B., Wu, J., Zhong, Y., Shen, B. and Chen, H. (2018) 'MiR-17-5p enhances pancreatic cancer proliferation by altering cell cycle profiles via disruption of RBL2/E2F4-repressing complexes', *Cancer Letters*, 412, pp. 59–68. doi: 10.1016/j.canlet.2017.09.044.

8.- SUPPLEMENTARY INFORMATION

Solutions

Protein lysis buffer

10 mM NaH_2PO_4 (pH7.2)

1 mM EDTA

1 mM EGTA

150 mM NaCl

1% NP-40 (v/v)

10 mM β-glycerophosphate

10 mM PMSF

10 mM Na_3VO_4

10 µg/ml Leupeptin

10 µg/ml Aprotinin

10 µg/ml Pepstatin

1X PBS (pH 7.6)

137 mM NaCl

2.7 mM KCl

1.8 mM KH_2PO_4

8.1 mM Na_2HPO_4

6X Protein Loading Buffer

350 mM Tris-HCl pH 6.8

34.4% Glycerol (v/v)

10% SDS (w/v)

10% β-mercaptoethanol (v/v)

0.06% Bromophenol blue (w/v)

SDS-PAGE Running buffer

0.25 mM Tris base

1.92 mM Glycine

1% SDS

Transfer buffer

120 mM Tris base

40 mM Glycine

20% Methanol

Tris Buffered Saline (TBS) (pH 7.6)

20 mM Tris base

137 mM NaCl

Stacking gel for SDS-PAGE

63 mM Tris HCl pH6.8

0.1% SDS (v/v)

5% Acrylamide

0.1% TEMED

0.1% APS

Resolving gel for SDS-PAGE

376 mM Tris HCl pH8.8

0.1% SDS (v/v)

Acrylamide (variable %)

0.04% TEMED

0.1% APS

Formaldehyde dilution buffer (ChIP)

50mM Hepes/KOH pH8

100mM NaCl

1mM EDTA pH8

0.5mM EGTA pH8

Cell lysis buffer (ChIP)

5mM PIPES pH8

85mM KCl

0.5% NP-40

1mM PMSF

1X Protease inhibitor cocktail

Nuclei lysis buffer (ChIP)

50mM Tris-Cl pH8

10mM EDTA pH8

1% SDS

1mM PMSF

1X Protease inhibitor cocktail

ChIP dilution buffer (ChIP)

0.01% SDS

1.1% Triton X-100

1.2mM EDTA

16.7mM Tris-Cl pH8

167mM NaCl

Low Salt Wash Buffer (ChIP)

20mM Tris HCl pH8

0.1% SDS

1% Triton X-100

2mM EDTA pH8

150mM NaCl

High Salt Wash Buffer (ChIP)

20mM Tris HCl pH8

0.1% SDS

1% Triton X-100

2mM EDTA pH8

500mM NaCl

LiCl Wash Buffer (ChIP)

10mM Tris HCl pH8

0.25M LiCl

1% NP-40

1% Na-deoxycholate

1mM EDTA pH8

TE

10mM Tris HCl pH8

1mM EDTA pH8

Published online 9 March 2016

Nucleic Acids Research, 2016, Vol. 44, No. 12 ***5557–5570***
doi: 10.1093/nar/gkw146

E2F7 regulates transcription and maturation of multiple microRNAs to restrain cell proliferation

Jone Mitxelena[1], Aintzane Apraiz[2], Jon Vallejo-Rodríguez[1], Marcos Malumbres[3] and Ana M. Zubiaga[1,*]

[1]Department of Genetics, Physical Anthropology and Animal Physiology, University of the Basque Country UPV/EHU, 48080 Bilbao, Spain, [2]Department of Cell Biology and Histology, University of the Basque Country UPV/EHU, 48080 Bilbao, Spain and [3]Cell Division and Cancer Group, Spanish National Cancer Research Centre (CNIO), 28029 Madrid, Spain

Received October 4, 2015; Revised February 29, 2016; Accepted March 1, 2016

ABSTRACT

E2F transcription factors (E2F1-8) are known to coordinately regulate the expression of a plethora of target genes, including those coding for microRNAs (miRNAs), to control cell cycle progression. Recent work has described the atypical E2F factor E2F7 as a transcriptional repressor of cell cycle-related protein-coding genes. However, the contribution of E2F7 to miRNA gene expression during the cell cycle has not been defined. We have performed a genome-wide RNA sequencing analysis to identify E2F7-regulated miRNAs and show that E2F7 plays as a major role in the negative regulation of a set of miRNAs that promote cellular proliferation. We provide mechanistic evidence for an interplay between E2F7 and the canonical E2F factors E2F1-3 in the regulation of multiple miRNAs. We show that miR-25, -26a, -27b, -92a and -7 expression is controlled at the transcriptional level by the antagonistic activity of E2F7 and E2F1-3. By contrast, let-7 miRNA expression is controlled indirectly through a novel E2F/c-MYC/LIN28B axis, whereby E2F7 and E2F1-3 modulate c-MYC and LIN28B levels to impact let-7 miRNA processing and maturation. Taken together, our data uncover a new regulatory network involving transcriptional and post-transcriptional mechanisms controlled by E2F7 to restrain cell cycle progression through repression of proliferation-promoting miRNAs.

INTRODUCTION

Since the initial identification of E2F as the cellular factor required for activation of the E2 adenoviral promoter, the E2F family of transcription factors has expanded through the addition of new members in mammals and through the discovery of homologs in other eukaryotes. Eight mammalian E2F family members (E2F1-8) have been identified, which orchestrate a complex gene regulatory network to ensure proper cell cycle progression, cellular differentiation and development (1,2). However, it is still unclear what the precise roles of each individual E2F member are, and how the activity of the whole E2F family is coordinated to achieve an integrated regulation of gene expression.

Canonical E2F proteins (E2F1-6) bear one DNA-binding domain (DBD) immediately followed by a dimerization domain, which mediates interaction with the dimerization partner protein (DP). This dimerization enables E2Fs to bind DNA with high affinity, and to function as transcriptional regulators (3). According to the prevailing model, transcriptional regulation by canonical E2Fs is controlled through association with the retinoblastoma (RB) family of tumor suppressor proteins (pRB, p107 and p130) in the case of E2F1-5, or with polycomb group (PcG) proteins, in the case of E2F6 (4). These associations facilitate recruitment of histone deacetylases and methyltransferases to target promoters and subsequent transcriptional repression. Disruption of repressor complexes unleashes E2F activity, thereby triggering target gene transcription (3).

By contrast to canonical E2Fs, the atypical members E2F7 and E2F8, display two tandem DBDs and lack sequences that mediate RB and DP binding (5). The mechanisms by which atypical E2Fs regulate gene expression as well as their biological roles are still unclear. Gain-of-function experiments have revealed that E2F7 and E2F8 are recruited to promoters of several E2F target genes involved in DNA replication and DNA repair, and repress E2F site-dependent transcription in a RB-independent manner (6–11). Furthermore, overexpression of either E2F7 or E2F8 disrupts cell cycle progression, suggesting that they might promote negative cell cycle control through transcriptional repression of cell cycle genes (6–11). However, knockout

*To whom correspondence should be addressed. Tel: +34 94 601 2603; Fax: +34 94 601 3143; Email: ana.zubiaga@ehu.es
Present address: Jone Mitxelena, Department of Molecular Mechanisms of Disease, University of Zurich, Switzerland.

(KO) of E2F7 or E2F8 in mice has no significant effect on cell cycle progression, and a concomitant inactivation of E2F7 and E2F8 is needed to impact on cell cycle progression *in vivo* (12). This is probably due to compensatory mechanisms between both E2Fs, a common outcome in constitutive KO mouse models. Thus, the specific contribution of E2F7 and E2F8 to cell cycle control remains to be elucidated.

Significant progress in the understanding of E2F-mediated regulation of gene expression has been achieved by the finding that many microRNA-coding genes are *bona fide* E2F target genes (13–20). In line with the complex nature of the E2F pathway, many reports have uncovered an essential role for E2F-regulated microRNAs in modulating distinct cellular processes, most notably pathways involved in neoplastic transformation (21,22). Some of these E2F-regulated miRNAs, including miR-17-92, miR-106b-25, mir-15b-16-2 and miR-15a-16-1, appear to function as tumor suppressors that modulate and restrict progression through the cell cycle by limiting the expression of E2Fs themselves as well as other pathway components, thereby creating negative feedback loops (14,16,18). By contrast, there is also evidence for an oncogenic potential for some E2F-dependent miRNAs. For instance, miR-17-92 and miR-106b-25 clusters have been found to suppress the expression of anti-proliferative and pro-apoptotic genes, such as $p21^{CIP1}$, pRB, p130, $p57^{KIP2}$, PTEN and BIM (13,17,23–25). Given that each miRNA can regulate the expression of numerous genes, the list of genes regulated by miRNAs under E2F control is likely to include other, yet to be identified, targets.

The contribution of atypical E2F factors to miRNA expression regulation, and the effect that target miRNAs have on the biological roles mediated by E2F7 and E2F8, are still unknown. In this work, we have investigated the role of E2F7 in the regulation of miRNA-coding gene expression. We show that E2F7 is required for the timely repression of a set of miRNAs that function to promote cell proliferation. Importantly, our data uncover both transcriptional and post-transcriptional mechanisms for E2F7-mediated regulation of these miRNAs, and provide new insights to the understanding of E2F-regulated gene network.

MATERIALS AND METHODS

Cell culture conditions and flow cytometry

Human U2OS osteosarcoma cell line and human embryonic kidney (HEK) 293T cells were maintained in Dulbecco's modified Eagle's medium supplemented with 10% fetal bovine serum (FBS). For cell synchronization in G1/S, exponentially growing cells were incubated with 4 mM hydroxyurea (HU) for 24 h and subsequently washed and cultured in complete medium. For cell synchronization at mitosis, cell cultures were incubated with thymidine (2 mM) for 18 h. Subsequently, cells were washed and cultured for an additional 20 h in fresh medium. Nocodazole (50 ng/ml) was added to the cultures for the last 16 h. Mitotic cells were collected by shaking off the plates and seeded in complete medium for subsequent analyses. To assess the cell cycle distribution, cells were fixed with chilled 70% ethanol, stained with 50 μg/ml propidium iodide (PI) and analyzed by flow cytometry (FACSCalibur, BD). To analyze the percentage of cells in mitosis, ethanol-fixed cells were stained with an antibody recognizing Histone H3 phosphorylated on Serine 10 (p-H3) conjugated with FITC (06-570, Millipore), subsequently incubated with PI and analyzed by flow cytometry. Cell cycle distribution and mitotix index analysis was performed with Summit 4.3 software. For cell proliferation assays, cells were stained with 0.5 μM carboxyfluorescein diacetate succinimidyl ester (CFSE) (MolecularProbes) in phosphate buffered saline for 15 min at 37°C, washed with complete medium for 20 min and then treated and cultured as indicated. Cells were fixed for 10 min in a solution of buffered formaldehyde (3.7%) and fluorescence was detected and analyzed by flow cytometry. Proliferation Wizard software was used to identify cells in different cellular generations and determine proliferation index, which was calculated as the sum of the cells in all generations including the parental divided by the computed number of original parent cells present at the start of the experiment.

Transfections

Plasmid transfection was performed using XtremeGENE HD (Roche) transfection reagent following manufacturer´s recommendations. Mammalian expression plasmids pRc-CMV-HA-E2F1, pRc-CMV-HA-E2F2, pRc-CMV-HA-E2F3, pCEFL-MYC and pFRT/FLAG/HA-DEST-LIN28B have been previously described (26–28). For exogenous expression of miRNAs, miRNA genes were expressed in the pMirVec vector (29). To silence endogenous expression of E2F1, E2F2, E2F3, E2F7, c-MYC and LIN28B, and to inhibit endogenous microRNA activity, cells were transfected with commercial siRNAs and with miRVana microRNA Inhibitors, respectively (Life Technologies), at a final concentration of 10 nM using Lipofectamine RNAiMAX (Life Technologies) following manufacturer's recommendations.

RNA expression analyses

Total RNA extraction was performed with TRIzol Reagent (Life Technologies) and purified using the miRNeasy kit (Qiagen) following the manufacturer's recommendations. For small RNA-Sequencing (RNA-Seq), 2 μg of total RNA containing the small RNA fraction including miRNAs was processed using the TruSeq Small RNA Sample Preparation kit from Illumina. The resulting libraries were sequenced on the Genome Analyzer IIx with SBS TruSeq v5 reagents following manufacturer's protocols. To test for differential miRNA expression between different samples the Bioconductor DESeq package was used (30). The list of differentially expressed miRNAs produced by DESeq was further filtered to remove miRNAs with fewer than 10 reads in the different samples under comparison (31). Clustering analysis of differentially expressed miRNAs was performed with Perseus software (http://www.perseus-framework.org/).

Predicted targets of microRNAs were identified using the DIANA-microT-CDS miRNA target prediction server (32) and then analyzed for pathway enrichment using terms from the Reactome database (33). We used low *P*-values (*P*

< 0.001) to avoid inconsistent results due to the use of different databases or algorithms, as suggested previously (34). Gene ontology analysis was performed using the FatiScan algorithm (35).

Mature microRNA and Primary microRNA (Pri-miRNA) RT-Q-PCR analyses were performed using specific TaqMan microRNA and Pri-miRNA assays, respectively (Life Technologies) (Supplementary Table S1). For mRNA expression analysis, RNA was reverse-transcribed into cDNA with the High-Capacity cDNA RT Kit (Life Technologies) and Q-PCR was performed as described previously (36). Sequences of Q-PCR primers are listed in Supplementary Table S2.

Protein expression analyses

For western blot analyses, cells were lysed in buffer containing 10 mM NaH_2PO_4 pH 7.2; 1 mM EDTA; 1 mM EGTA; 150 mM NaCl; 1% NP-40 and a cocktail of protease and phosphatase inhibitors (Roche). Protein concentrations in supernatants were determined using a commercially available kit (DC Protein Assay from Bio-Rad). A total of 20 μg of protein were loaded per lane, fractionated in 8–10% sodium dodecyl sulphate-polyacrylamide gels and transferred onto nitrocellulose membranes (Bio-Rad). Antibodies against the following proteins were used: E2F7 (sc-32574, Santa Cruz), Cyclin E1 (4129, Cell Signaling), c-MYC (sc-42, Santa Cruz), LIN28B (4192, Cell Signaling), HA (MMS-101R, Covance), p-H3 (06-570, Millipore), α-Tubulin (T-9026, Sigma), β-Actin (A5441, Sigma). Immunocomplexes were visualized with horseradish peroxidase-conjugated anti-mouse, anti-goat or anti-rabbit IgG antibodies (Santa Cruz), followed by chemiluminiscence detection (ECL, Amersham) with a ChemiDoc camera (Bio-Rad).

Chromatin immunoprecipitation

Chromatin immunoprecipitations (ChIPs) and the quantification of immunoprecipitated DNA sequences by Q-PCR were performed as described previously (36). The localization of E2F motifs in E2F7-regulated miRNAs was carried out with the MotifLocator tool of the TOUCAN program (37). The search was restricted to the proximal promoter region (−1000 and +500 bp relative to the transcription start site) (38). Sequences of Q-PCR primers are listed in Supplementary Table S3. Antibodies used for ChIP analysis were: E2F1 (sc-193, Santa Cruz), E2F2 (sc-633, Santa Cruz), E2F3 (sc-878, Santa Cruz), E2F4 (sc-1082, Santa Cruz), E2F7 (sc-66870, Santa Cruz), RB (sc-50 Santa Cruz), p107 (sc-318 Santa Cruz), p130 (sc-317 Santa Cruz), MYC (sc-764 Santa Cruz), RNA polymerase II (sc-899, Santa Cruz) and SV40LT (sc-147, Santa Cruz).

Statistical analysis

Data are presented as mean ± SD. The significance of the difference between two groups was assessed using the Student two-tailed *t*-test. A $P < 0.05$ was considered statistically significant.

RESULTS

Acute loss of E2F7 accelerates cell cycle progression

E2F7 gene expression is regulated in a cell cycle-dependent manner in U2OS cells, with reduced levels at M and G1 phases and a peak expression in G1/S transition and S phase (Supplementary Figure S1 A and B), consistent with previous reports (11). We assessed whether E2F7 is required for timely cell cycle progression by acutely depleting E2F7 and examining cell cycle distribution over time. Endogenous E2F7 was depleted very efficiently in U2OS cells individually transfected with three independent RNAi molecules specific for E2F7 (siE2F7), but not in cells transfected with an oligonucleotide whose sequence has no specificity to any human protein (siNT) used as a control (Figure 1A and Supplementary Figure S2). Importantly, E2F7 depletion resulted in substantially increased mRNA levels of known E2F7-downregulated genes (*E2F1*, *E2F2*, *E2F3* and *Cyclin E1*), confirming loss of E2F7-mediated repression in siE2F7-transfected cells (Figure 1A and Supplementary Figure S2).

To monitor cell cycle progression upon acute silencing of E2F7, U2OS cells were HU-synchronized at G1/S boundary and subsequently transfected with E2F7-specific siRNAs. Upon removal of the drug, cells were harvested every 3 h for FACS analyses (Figure 1B). DNA content analyses revealed a comparable block in G1/S in non-target control and E2F7 siRNA transfected cells. Remarkably, upon HU release, entry into S-phase in E2F7-depleted cells was significantly accelerated compared to control cells. This effect was visible as early as 3 h after HU release (48% in siE2F7 versus 40% siNT). Likewise, E2F7 depleted cells showed an earlier entry into G2 phase 6 h after exiting from HU-induced block (41 versus 27%) and it was also evident at the 9 h time point (67 versus 52%). Similarly, E2F7 depleted cells synchronized in M-phase with nocodazole showed accelerated entry and progression into S phase as well as into G2 (50% in siE2F7 versus 39% siNT at the 15 h-time-point following exit from mitotic arrest) in comparison with control siRNA transfected cells (Supplementary Figure S3). Consistent with these results, E2F7 siRNA transfected cells exhibited earlier and increased levels of the mitotic marker p-H3 after cell cycle re-entry from a HU-induced block (Figure 1C). By contrast, E2F8 depletion in U2OS cells did not result in a significant impact on cell cycle progression, even though E2F7 and E2F8 showed similar expression levels in U2OS cells (Supplementary Figure S4).

In parallel, we examined the rate of cell proliferation by labeling the cells with the vital fluorescent dye CFSE, which is diluted ∼2-fold with each cell division. Consistent with cell cycle analyses, E2F7-depleted cells displayed a higher proliferation rate compared to siNT cells (Figure 1D). Thus, by inducing acute loss of E2F7, our data reveal that E2F7 is indispensable for correct progression through the cell cycle and for cellular proliferation, and that this role is not satisfied by E2F8 or by other E2F family members upon E2F7 knockdown.

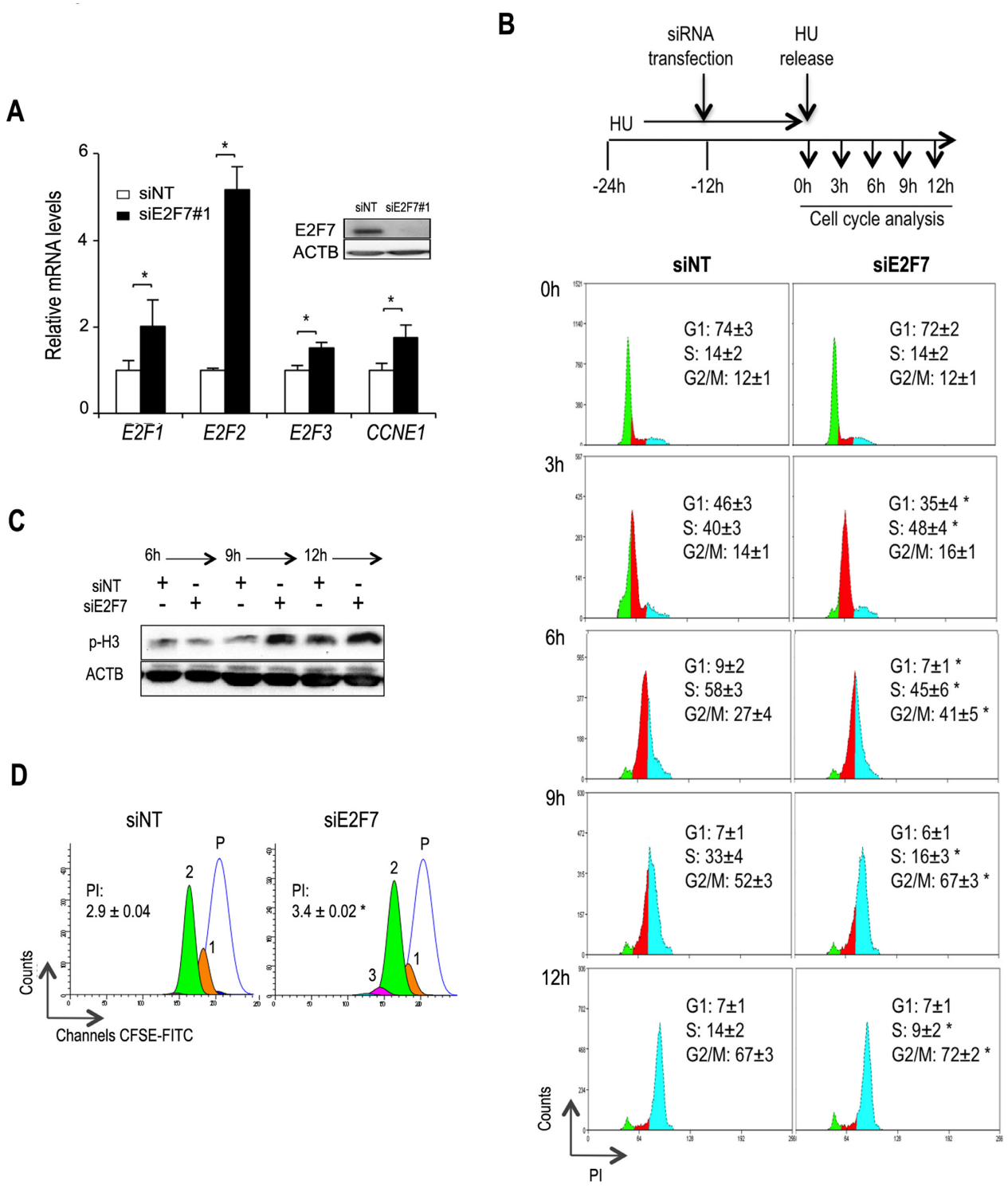

Figure 1. Accelerated cell cycle progression and increased proliferation in cells lacking E2F7. (**A**) RT-Q-PCR analyses of *E2F1, E2F2*, *E2F3* and Cyclin E1 (*CCNE1)* in cells treated with siE2F7 #1 or a non-target siRNA (siNT) for 12 h. Western blot analysis shows efficient depletion of E2F7 by transfection of specific siRNA molecules. mRNA expression values are normalized to the expression of *EIF2C2*, used as a standard control. Results are expressed as fold over siNT values (mean ± SD) from three independent experiments. (**B**) U2OS cells were treated with 4 mM HU and 12 h later were transfected with NT siRNA and E2F7 siRNA (#1). Cells were washed after 24 h of HU treatment, harvested every 3 h and processed for FACS analysis. Shown is the experimental design followed. The percentage of cells in G1 (green), S (red) and G2/M (blue) ± SEM (standard error of the mean) is indicated and correspond to the average of three independent replicates. (**C**) Lysates from cells treated as in panel B, harvested at indicated times after HU release were used for western blot analyses of p-H3 (Ser 10). (**D**) Proliferation of representative siNT and siE2F7 transfected cultures. U2OS cells were incubated with CFSE, transfected with indicated siRNAs and cultured for 24 h. Proliferation Index (PI) corresponds to the average of three experiments. Shown are representative images of the parental population (P) and the proliferative cellular generations in each condition (indicated with numbers). Asterisks (*) indicate significant differences ($P < 0.05$), and were derived from a two-tailed *t*-test between siE2F7- and siNT-transfected cells.

Identification of E2F7-regulated miRNAs

We set out to identify microRNAs that could contribute to E2F7-mediated cell cycle and proliferation control. To this end, unbiased RNA-Seq experiments were conducted using RNA derived from E2F7-competent and E2F7-depleted cells at G1/S transition (0 h), S phase (3 h) and G2/M boundary (12 h) of cell cycle following exit from HU-induced block. The expression level of endogenous E2F7 was appreciable in all three time-points (Supplementary Figure S1B). Three independent RNA-Seq experiments were performed for each condition (siE2F7 versus siNT) and time-point. Close to 1100 miRNAs were identified in the three time-points analyzed. A list of differentially expressed miRNAs between control and E2F7-depleted cells was produced by *Bioconductor DESeq* package (30) and only those miRNAs with fold-changes higher than 1.5 (siE2F7 versus siNT) in at least two of the three experiments were considered. Using these criteria a total of 18 miRNAs were found to be consistently deregulated upon E2F7 knockdown (Figure 2A and Supplementary Table S4), 15 of which were upregulated in at least two time-points of the cell cycle. These data suggest a major role for E2F7 as a negative regulator of miRNA expression throughout the cell cycle.

Within the set of E2F7-regulated miRNAs, miR-25, let-7f and miR-92a have been previously identified as E2F1 and E2F3 targets (14,17–19,39). Of note, whereas E2F1 and E2F3 are known to induce the expression of these miRNAs, our data indicate that E2F7 represses their expression. In addition, our deep-sequencing analyses produced many other miRNAs that represent potentially novel E2F-regulated miRNAs (Figure 2A and Supplementary Table S4). E2F7 has been reported to repress E2F site-dependent transcription (7,8,11). To identify potential E2F motifs within E2F7-repressed microRNAs, we made use of the MotifLocator tool provided by TOUCAN program (37). Using a threshold level of 0.8 for similarity with the canonical E2F motif recorded in the TRANSFAC database, we found that 67% of E2F7-repressed genes harbored at least one canonical E2F motif within the −1000/+500 bp regulatory region (Supplementary Table S5).

From the collection of miRNAs that were differentially expressed in E2F7-depleted cells, we selected those that have been previously related with E2F (miR-25, let-7f and miR-92a) as well as a set of miRNAs bearing E2F motifs in their promoter regions (let-7b, miR-26a, miR-27b and miR-7) (Supplementary Table S5) for further analyses. Conventional RT-Q-PCR assays of the selected miRNAs showed significantly increased expression levels upon E2F7 knockdown in the three cell cycle phases analyzed (Figure 2B), thus validating the small RNA-Seq experiment results. We subsequently examined potential pathways regulated by these miRNAs by performing a bioinformatics analysis of their predicted targets. Interestingly, Gene Ontology analysis of the combined predicted targets revealed that E2F7-repressed miRNAs preferentially modulate genes involved in cell cycle and mitotic regulation (Figure 2C). Other biological processes including hemostasis, signaling by Nerve Growth Factor (NGF) or transmembrane transport also appeared enriched in this analysis, suggesting that E2F7 regulates a diversity of functions through control of microRNA expression.

E2F7-repressed miRNAs modulate cell proliferation

We tested whether miRNAs repressed by E2F7 (miR-25, let-7f, let-7b, miR-26a, miR-27b, miR-92a and miR-7) could contribute to E2F7-dependent control of the cell cycle. U2OS cells were transfected with expression vectors coding for these miRNAs, and cell cycle distribution profiles were analyzed. Ectopic expression of individual miRNAs gave rise to a slight acceleration of the first cell division cycle relative to *scramble* control-transfected cells (Supplementary Figures S5, S6 and data not shown). Importantly, this effect was amplified after several cell division cycles, and we observed significantly increased proliferation rates when fluorescence of CFSE-stained cells was quantified after overexpression of individual miRNAs (Figure 3A and Supplementary Table S6). Furthermore, blocking endogenous miRNA activity with a pool of anti-miRNA oligonucleotides reversed the accelerated cell cycle progression induced by E2F7 knockdown (Supplementary Figure S7).

We next assessed whether E2F7-regulated miRNAs could promote cell proliferation by limiting the expression of miRNA target genes involved in cell growth inhibition. Several critical cell cycle inhibitors reported to be regulated by these miRNAs, such as $p21^{Cip1}$, $p57^{Kip2}$, PTEN and p130, were indeed downregulated in U2OS cells overexpressing individual E2F7-repressed miRNAs (Figure 3B). $p18^{INK4C}$, which has not been reported to be regulated by microRNAs, showed no differences in this assay, ruling out possible general effects due to an overall proliferation increase. Collectively, these results point to a role for these microRNAs in E2F7-mediated negative regulation of cell proliferation and cell cycle control by modulating the levels of critical cell cycle inhibitors.

E2F factors are bound to the promoter region of miR-25, miR-26a, miR-27b, miR-92a and miR-7

To begin to dissect the mechanism by which E2F7 represses the expression of miRNAs during the cell cycle, we examined binding of E2F7 to the regulatory regions of the validated miRNAs. Binding of E2F7 was examined by ChIP analyses followed by Q-PCR with specific oligonucleotides for each miRNA regulatory region bearing E2F consensus sites (Figure 4A). The regulatory region of let-7f lacks putative E2F binding sites, and was therefore discarded for binding studies. The β-actin gene (ACTB), whose promoter lacks active E2F sites (36), was used as a negative promoter control. We made use of chromatin derived from cells collected at 3 h following HU release (corresponding to S-phase cells). Additionally, as a control for non-specific ChIP, parallel ChIP assays were carried out with an irrelevant antibody (SV40LT). As shown in Figure 4B, ChIP analyses revealed robust E2F7 binding to the regulatory region of miR-25, miR-92a and miR-7 (compare binding to ACTB), suggesting that E2F7 represses miR-25, miR-92a and miR-7 expression by directly binding to their regulatory region. By contrast, we did not to detect binding of E2F7 to the regulatory regions of miR-26a, miR-27b and let-7b, which harbor consensus E2F sites (Figure 4A and B).

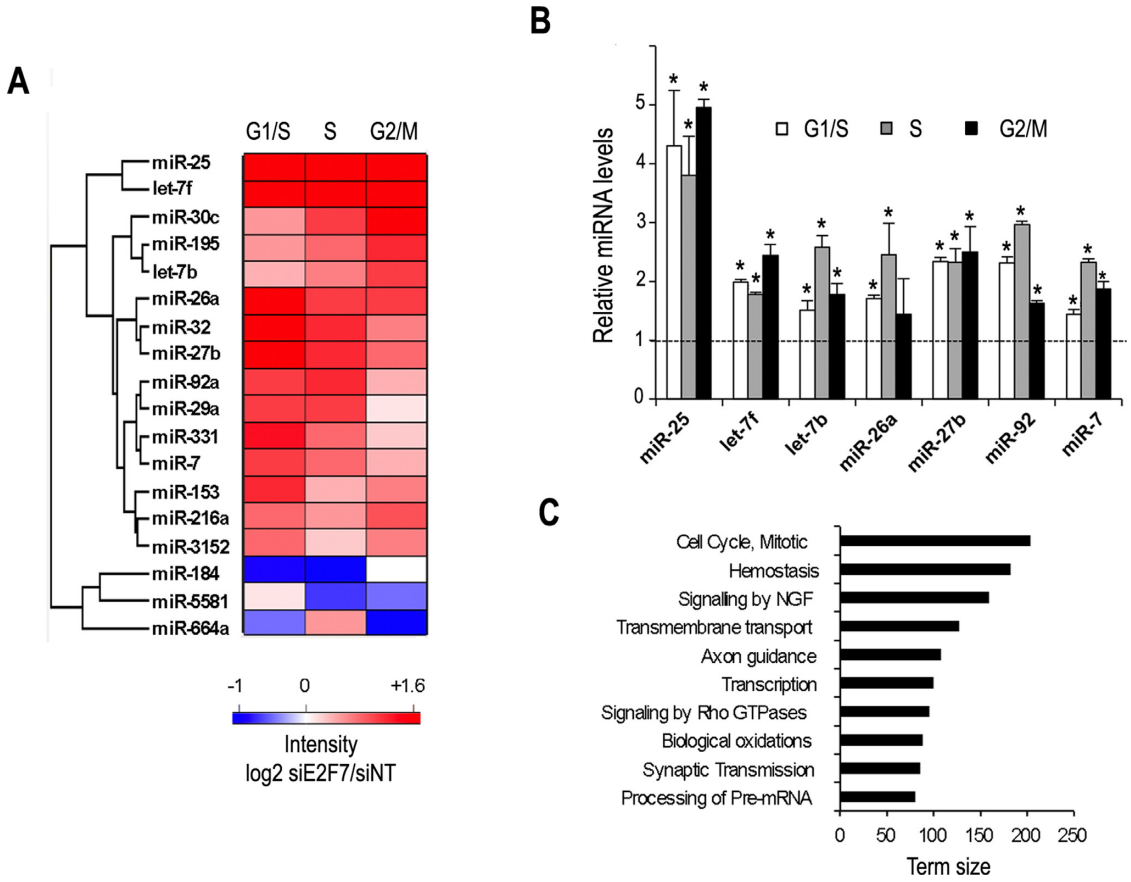

Figure 2. Identification of E2F7-regulated miRNAs by small RNA-Seq analysis. (**A**) MicroRNA expression profiles in siE2F7#1 transfected cells at various time-points after HU release. Data are normalized to the levels of siNT-treated cells. Red indicates upregulation and blue indicates downregulation. (**B**) Confirmatory RT-Q-PCR expression analyses in E2F7-depleted cells at various time-points after HU release. Mature miR-25, let-7f, let-7b, miR-26a, miR-27b, miR-92a and miR-7 expression levels were analyzed and normalized to RNU6B and RNU19 levels. Data are represented as fold-change relative to siNT-transfected samples (*$P < 0.05$). (**C**) Gene ontology (GO) analysis of predicted targets of E2F7-repressed miRNAs using FatiGO tool. Only terms with adjusted P-value of > 0.001 were considered.

It has been shown that individual E2F target promoters are bound by multiple E2Fs *in vivo* (36,40). Therefore, we tested whether other E2F family members could occupy the regulatory regions of these miRNAs. We focused on E2F1, E2F2 and E2F3 because they are regulated by E2F7 (Figure 1A), and thus, could potentially be involved in E2F7-dependent miRNA regulation. As shown in Figure 4C, we found that E2F1, E2F2 and E2F3 were efficiently recruited to the promoter region of miR-25 and miR-92a (>2-fold over β-actin promoter amplification), supporting previous data (14,18,19). Interestingly, miR-26a regulatory region was bound by E2F3, and both, E2F1 and E2F3, occupied miR-27b and miR-7 promoters. None of them was significantly recruited to let-7b. Remarkably, E2F7 depletion led to a dramatic increase in recruitment of E2F1, E2F2 and E2F3 to miR-25, miR-26a, miR-27b, miR-92a and miR-7 promoters (Figure 4C, note scale difference), consistent with the increased expression of these E2Fs in E2F7-knockdown cells (Figure 1A). Moreover, ectopic expression of E2F1-3 factors led to an induction of E2F7-regulated miRNAs (Supplementary Figure S8). These results point to a direct role for E2F1, E2F2 and E2F3 in the transcriptional activation of E2F7-repressed miRNAs.

E2F7 regulates let-7 microRNA maturation

The absence of consensus E2F motifs in let-7f regulatory region and the lack of binding of E2F factors to let-7b, points to an indirect mechanism for E2F7 in the regulation of these miRNAs. We examined the abundance of let-7f and let-7b immature primary transcripts in U2OS cells transfected with non-target or E2F7-specific siRNAs. We included miR-25 in our assay as a control of a miRNA whose promoter is bound by E2F7 (Figure 4B). Unprocessed pri-miR-25 levels were increased in E2F7-depleted cells (Figure 5A), demonstrating that E2F7 regulates miR-25 expression at the transcriptional level. By contrast, pri-let-7f and pri-let-7b levels remained unaffected upon E2F7 knockdown. These findings rule out a transcriptional regulation of let-7f and let-7b by E2F7 and point to a role of this E2F factor in the maturation pathway of let-7 miRNAs.

The RNA binding proteins LIN28A and LIN28B have been reported to directly bind to let-7 precursor miRNA molecules and inhibit their processing into mature and functional miRNAs (41–45). We tested whether E2F7 depletion had an effect on LIN28 expression. Interestingly, RT-Q-PCR and western blot analyses showed a substantial reduction of LIN28B mRNA and protein levels (both al-

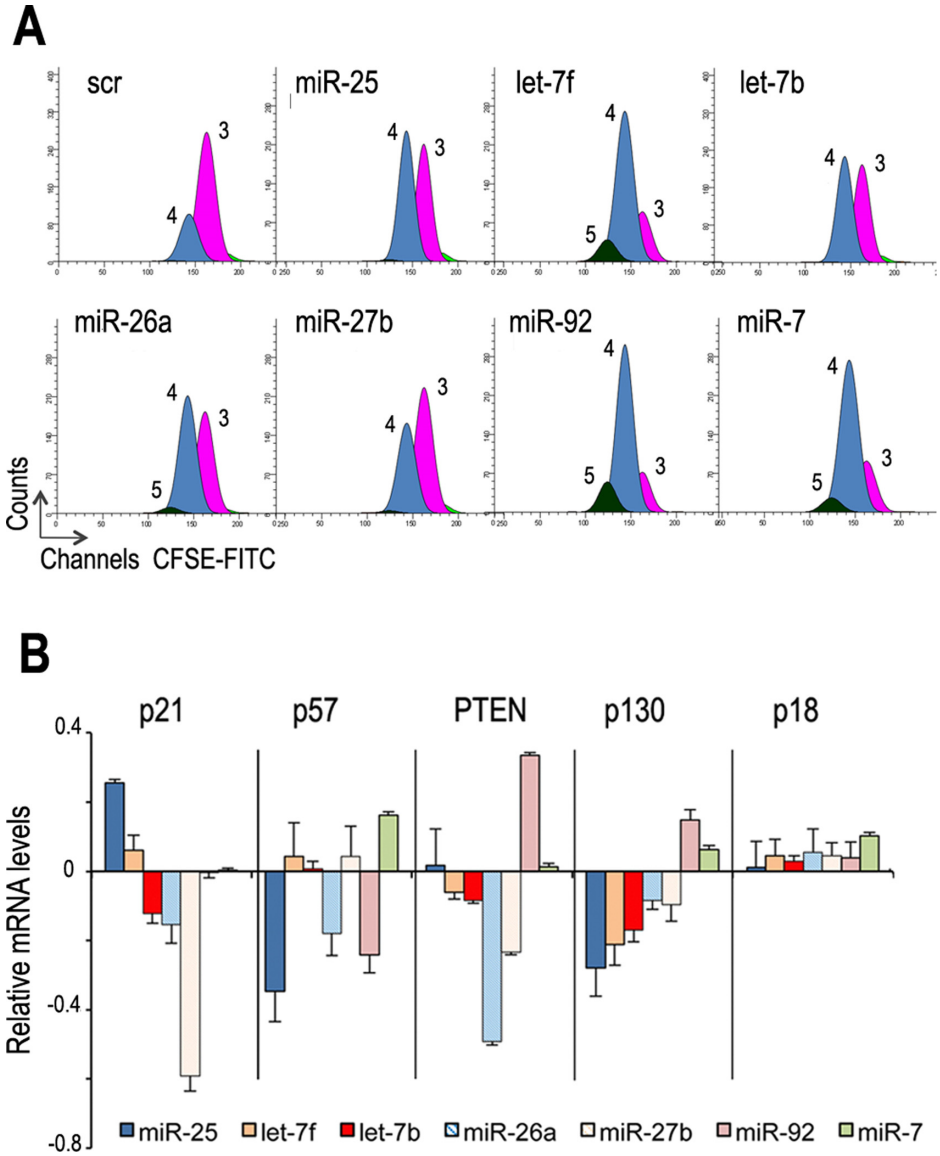

Figure 3. E2F7-regulated miRNAs target critical cell cycle regulators and enhance cell proliferation. (**A**) U2OS cells were transfected with various miRNA-coding plasmids and incubated with CFSE. A vector coding a scramble sequence (scr) was used as a negative control. Cells were harvested 24, 48 and 72 h after transfection and CFSE fluorescence was determined by flow cytometry. Shown are representative images of the distribution of cellular generations 48 h after transfection (indicated with numbers). (**B**) $p21^{CIP1}$, $p57^{KIP2}$, PTEN, p130 and $p18^{INK4C}$ mRNA levels were assessed by RT-Q-PCR in RNA samples extracted from cells treated as in panel A. Data are represented as normalized log_2-ratios over control scr transfection.

ternatively spliced forms) upon E2F7 knockdown (Figure 5B). LIN28A levels were not detected in U2OS cells (data not shown).

We next assessed whether LIN28B was required for downregulation of let-7b and let-7f in cell cycle synchronized U2OS cells. Knockdown of LIN28B by RNAi led to an increased expression of endogenous let-7b and let-7f (Figure 5C). Conversely, ectopic LIN28B expression abolished the increased expression levels exhibited by let-7f and let-7b in cells lacking E2F7, but not the levels of miR-25 (Figure 5D). Collectively, these results imply a post-transcriptional pathway regulated by E2F7 and LIN28B in dictating the levels of let-7 miRNAs.

E2F7 regulation of let-7 involves the LIN28/c-MYC axis

LIN28B expression has not been previously linked to E2F. Instead, LIN28B expression is known to be induced by c-MYC (46). In addition to the c-MYC binding site previously reported (46), inspection of LIN28B promoter region revealed three putative E2F-recognition sites near the transcription start site (Figure 6A). However, ChIP analyses did not detect endogenous E2F7 bound to LIN28B promoter. Likewise, E2F1, E2F2 and E2F3 were absent from LIN28B promoter both in control- and E2F7-depleted cells (Supplementary Figure S9 and data not shown). In contrast, c-MYC was efficiently recruited to the promoter region of LIN28B (Figure 6A), and subsequent functional analyses showed that knockdown of c-MYC led to decreased

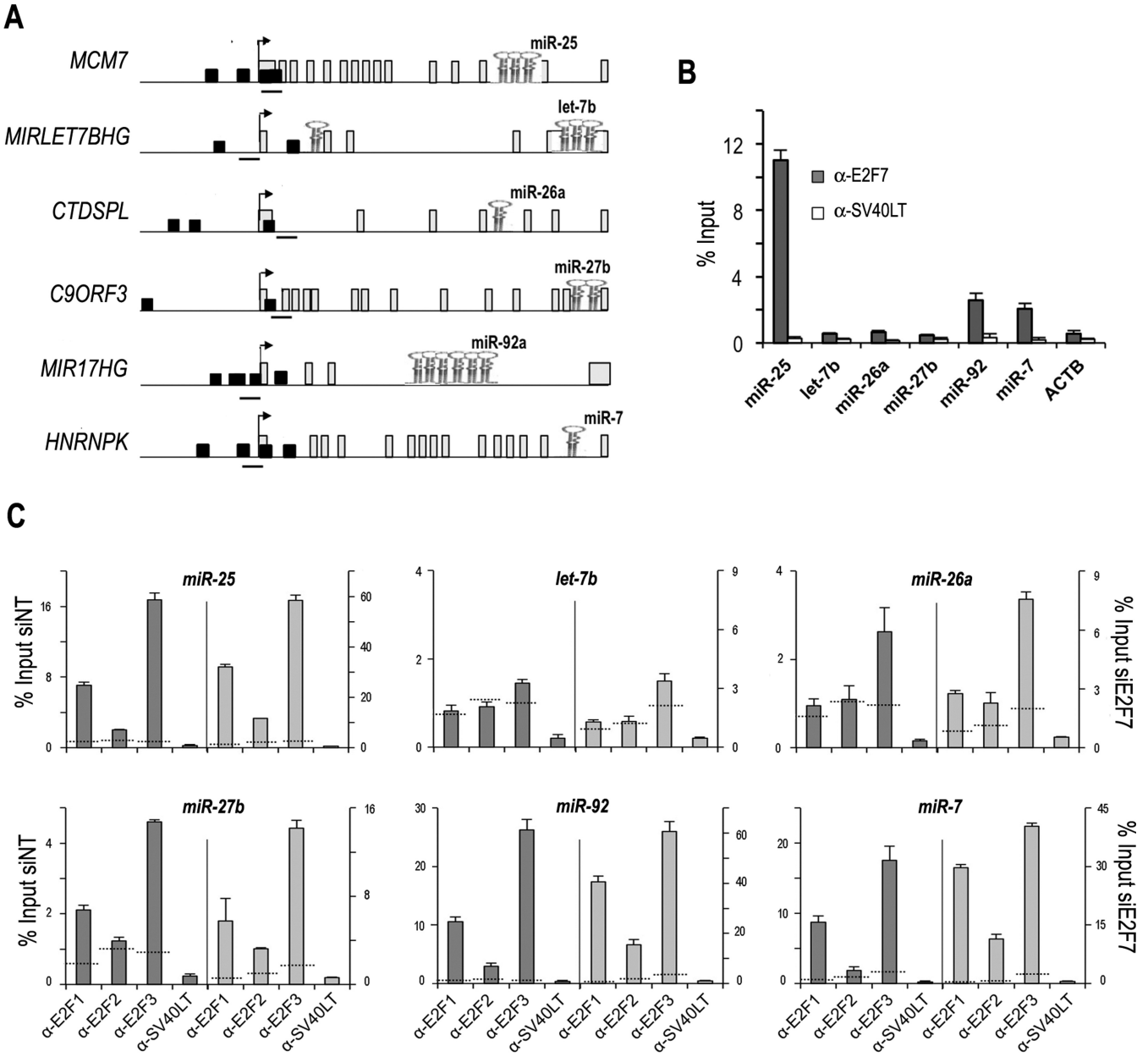

Figure 4. E2F factors are recruited to the promoter region of multiple microRNAs. (**A**) Schematic representation of human miR-25, let-7b, miR-26a, miR-27b, miR-92a and miR-7 loci within the human *MCM7, MIRLET7BHG, CTDSPL, C9ORF3, MIR17HG and HRNPK* transcription units, respectively. The predicted E2F recognition sites are indicated by small filled boxes. Horizontal lines depict the chromatin sequences amplified by Q-PCR. (**B**) ChIP-Q-PCR analyses of E2F7-regulated miRNAs. Cell lysates were harvested 3 h after HU release and used for ChIP assays with an antibody against E2F7. Promoter regions near E2F consensus sites were amplified by Q-PCR. The promoter of β-Actin (*ACTB)* was used as a negative control. An unrelated antibody against the SV40 large T antigen (SV40LT) was used as a control for background immunoprecipitation. Data are presented as percentage of input chromatin (representative experiment of three independent experiments where the values are the mean ± SD of triplicate determinations). (**C**) Cell lysates from siNT and siE2F7-transfected cells were harvested 3 h after HU release and used for ChIP assays with antibodies against E2F1, E2F2 and E2F3. Note the Y-axis scale difference in the siE2F7-treated samples. *ACTB* amplification values are represented as dotted horizontal lines.

LIN28B mRNA and protein levels (Figure 6B), suggesting that c-MYC directly transactivates LIN28B expression in U2OS cells.

Importantly, ectopic expression of c-MYC impaired the reduction of LIN28B expression in E2F7-depleted cells, and led to a recovery of LIN28B levels close to those in siNT-treated cells (Figure 6C), suggesting that E2F7 could control LIN28B expression indirectly through the modulation of c-MYC levels. Furthermore, let-7b upregulation in siE2F7 treated cells was partially reversed upon c-MYC expression, whereas miR-25 expression was not negatively affected by c-MYC (Figure 6D).

The above results raised the possibility that E2F7 may control let-7 and LIN28B expression through c-MYC. Indeed, we found that c-MYC expression was significantly decreased upon knockdown of endogenous E2F7 by two inde-

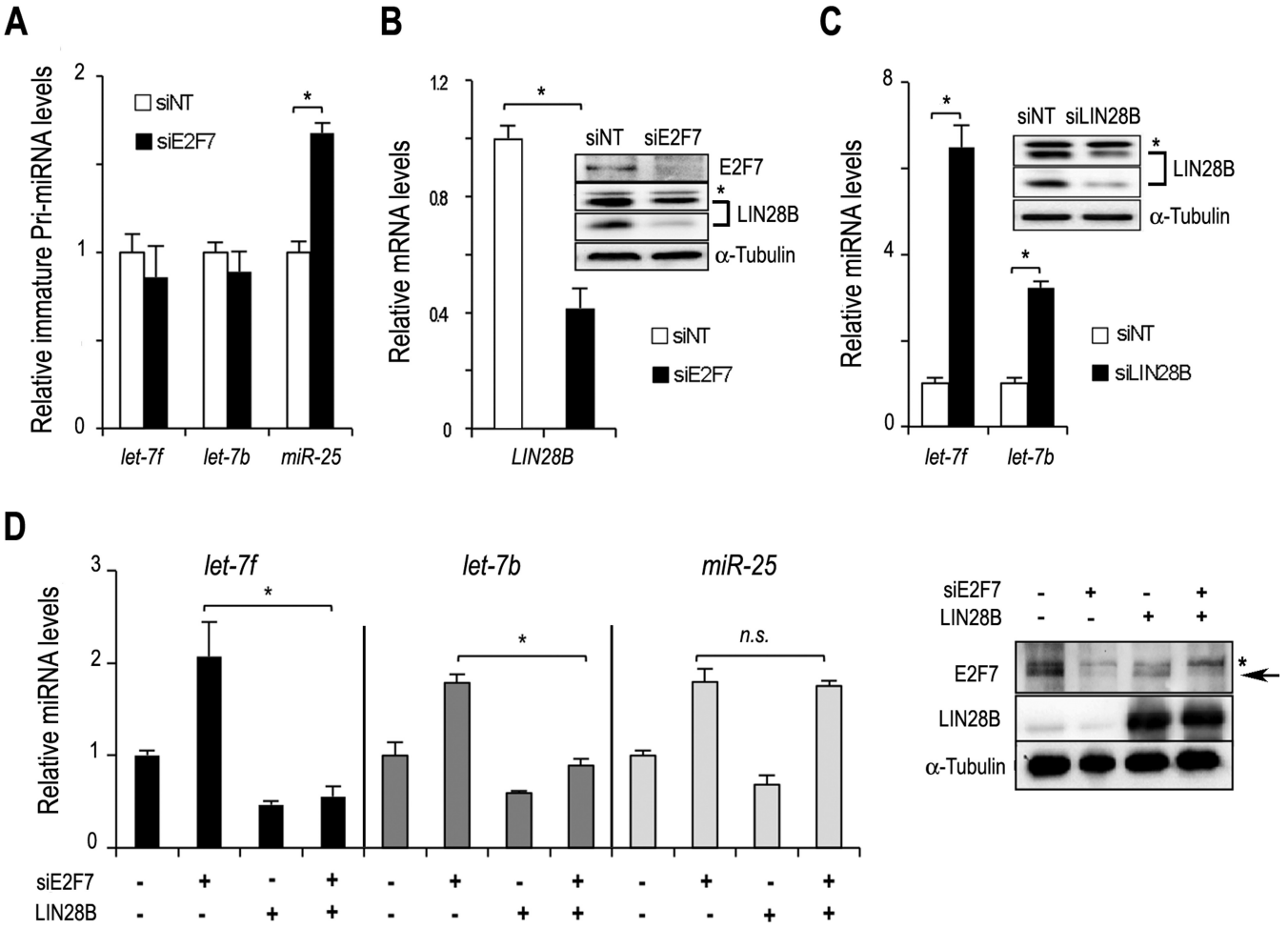

Figure 5. E2F7 controls let-7f and let-7b maturation through LIN28B (**A**) E2F7 does not regulate let-7f and let-7b transcription. HU-synchronized cells were transfected with siNT and siE2F7 and RNA was purified 3 h after cell cycle re-entry. Expression analyses of the indicated pri-miRNAs were performed using specific Taqman assays. (**B**) LIN28B expression was analyzed by RT-Q-PCR in cells transfected with siNT or siE2F7 RNAs. mRNA expression values are normalized to the expression of *EIF2C2*, used as a standard control. Western blot analysis shows significant downregulation of LIN28B expression after E2F7 depletion. Specific bands corresponding to two isoforms of LIN28B are indicated with arrows. A non-specific band is indicated with an asterisk. (**C**) LIN28B controls let-7f and let-7b expression in U2OS cells. U2OS cells were synchronized in mitosis by nocodazole treatment and transfected with LIN28B siRNA molecules. RT-Q-PCR analyses of let-7f and let-7b were carried out with RNA samples after 6 h of mitotic block release. Let-7f and let-7b expression was normalized to *RNU6B* and *RNU19* small RNAs expression, used as standard controls. Data are represented as fold change relative to siNT. Western blot shows efficient siRNA-mediated knockdown of LIN28B. (**D**) E2F7 and LIN28B cooperate to regulate let-7f and let-7b expression. let-7f, let-7b and miR-25 levels were determined in U2OS cells synchronized in mitosis and transfected with E2F7 siRNA together with an expression plasmid encoding LIN28B (pFRT-LIN28B). Cells were harvested 6 h after block release. miRNA expression levels are shown over the empty transfection. (*$P <$ 0.05 in all graphs). Western blot shows expression of E2F7 and LIN28B in the samples used for miRNA expression analysis. A non-specific band in E2F7 blot is indicated with an asterisk.

pendent siRNA molecules (Figure 6E and Supplementary Figure S10). This surprising result prompted us to examine c-MYC regulation in more detail. c-MYC promoter region has been reported to contain several E2F elements (47), and our bioinformatic analysis confirmed this point (Figure 7A). However, whether E2Fs are involved in c-MYC regulation has not been clarified. We assessed c-MYC promoter occupancy by E2F7 as well as by its targets E2F1, E2F2 and E2F3. ChIP analyses revealed robust binding by all four E2Fs to c-MYC promoter. In addition, E2F7-depleted cells exhibited dramatically increased promoter binding by E2F1, E2F2 and E2F3 factors (Figure 7A, note scale difference), suggesting that E2F7-dependent c-MYC regulation might be mediated, at least in part, by E2F1-3. Accordingly, c-MYC mRNA and protein levels were increased upon E2F1, E2F2 and E2F3 depletion (Figure 7B and Supplementary Figure S11A). By contrast, another E2F target (Cyclin E1) showed decreased expression upon the combined knockdown of E2F1-3 (Figure 7B), as previously reported (48). Moreover, c-MYC expression was negatively affected by the ectopic expression of E2F1-3, both at the mRNA and protein levels (Figure 7C and Supplementary Figure S11B).

Modulation of c-MYC levels by E2F1-3 was not the result of altered cell-cycle profiles in these cells (Supplementary Figure S11C) and it did not involve increased promoter binding by classical E2F repressors, such as E2F4, or by pocket proteins (Supplementary Figure S12 and data

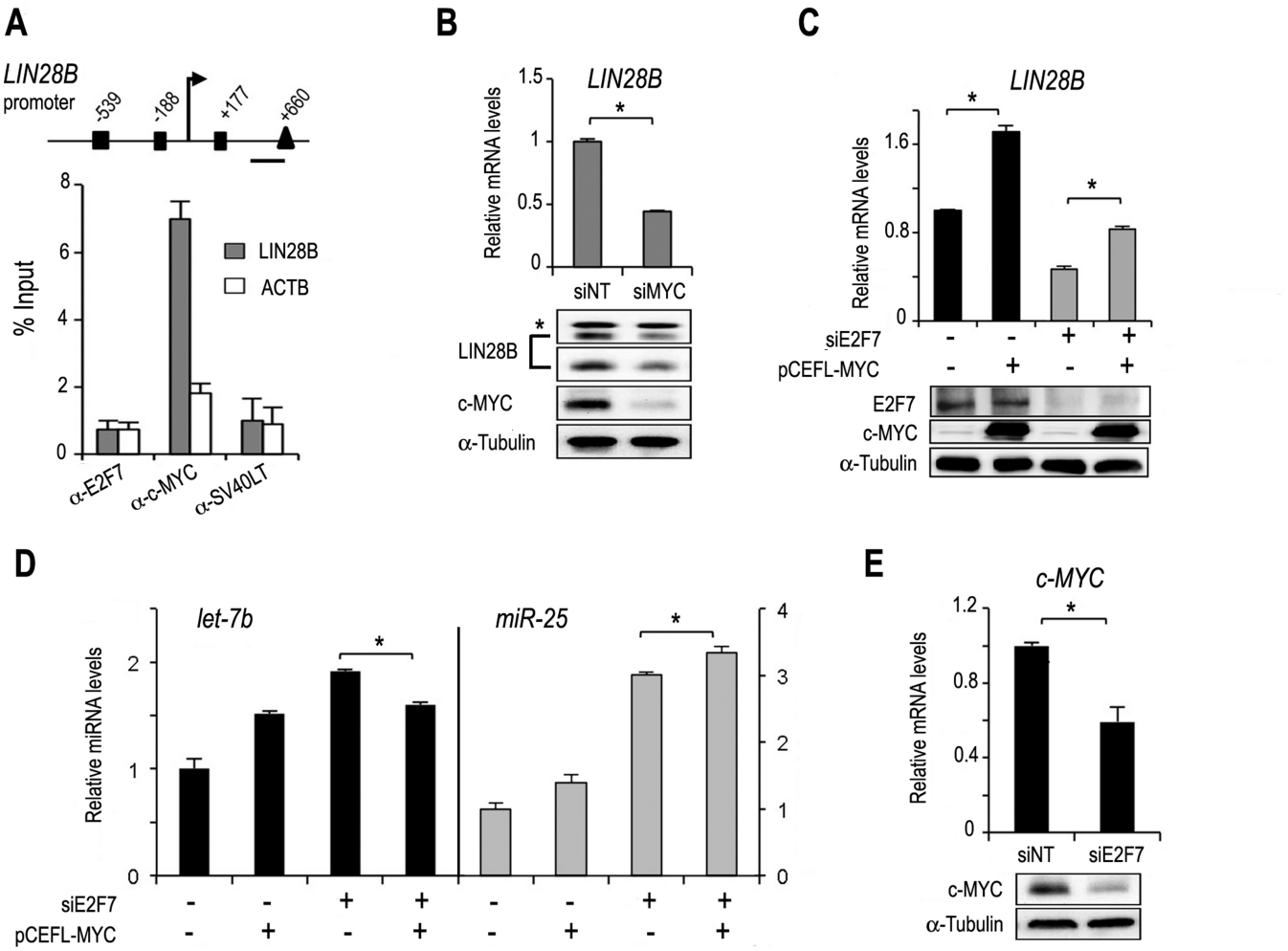

Figure 6. E2F7 controls LIN28B expression through c-MYC. (**A**) Schematic representation of LIN28B promoter region, indicating the localization of consensus E2F (boxes; −539: TTTCGGGC; −188: GCACGAAA; +177: TTTGGAGC) and c-MYC (triangle; TCCTCGTGCCC) binding motifs. ChIP analyses were performed with the indicated antibodies and Q-PCR was performed using primers spanning genomic regions around or close to E2F and c-MYC sites. The horizontal line depicts the chromatin sequence amplified by Q-PCR. Data correspond to a representative experiment of three independent replicates. (**B**) RT-Q-PCR and western blot analyses of LIN28B levels in c-MYC depleted cells. Cells blocked in mitosis were transfected with siNT or siMYC molecules and RNA and protein extracts were harvested 9 h after block release. Western blot shows efficient knockdown of c-MYC in U2OS cells. mRNA data are shown as fold-change over siNT. (**C**) RT-Q-PCR analysis of LIN28B mRNA levels in U2OS cells synchronized in mitosis and transfected with E2F7 siRNA along with an expression plasmid encoding c-MYC (pCEFL-MYC). Cells were harvested 9 h after block release. Data are shown as fold over the empty vector transfection. Western blot shows c-MYC and E2F7 expression levels in samples used for LIN28B expression analysis. (**D**) miRNA levels were assessed in cells treated as in panel C. (**E**) c-MYC mRNA and protein levels were analyzed in cells synchronized in the cell cycle by HU treatment and transfected with siNT or siE2F7. mRNA expression values are normalized to the expression of *EIF2C2*, used as a standard control. (*$P < 0.05$).

not shown), suggesting that repression of c-MYC by E2F1-3 could involve RB-independent mechanisms. Consistent with this, a similar level of c-MYC repression by E2F1-3 was detected in HEK293T cells (Supplementary Figure S13), which harbor inactive RB (49).

Importantly, modulation of E2F1-3 levels affected RNA Pol II occupancy downstream of c-MYC transcription start site (Figure 7D), which is a measure of c-MYC transcription rate (50). ChIP data revealed increased association of RNA Pol II with c-MYC gene in E2F1-3 depleted cells, whereas RNA Pol II occupancy in Cyclin E1 gene was decreased in the same experiment. Conversely, ectopic E2F2 expression negatively impacted on RNA Pol II association to c-MYC promoter, while Cyclin E1 gene showed an increased occupancy by RNA Pol II in these samples. These results further demonstrate that E2F1-3 repress c-MYC at the transcriptional level. Thus, we conclude that E2F7 regulates let-7 miRNA expression through a miRNA maturation pathway involving several intermediate steps controlled by the transcriptional activity of E2F and c-MYC factors.

DISCUSSION

In this work, we have analyzed the contribution of E2F7 transcription factor to the regulation of a subset of novel target miRNAs during the cell division cycle. We have discovered transcriptional and post-transcriptional mechanisms by which E2F7 modulates target miRNA expression. Our data support a model whereby E2F7 ensures repression

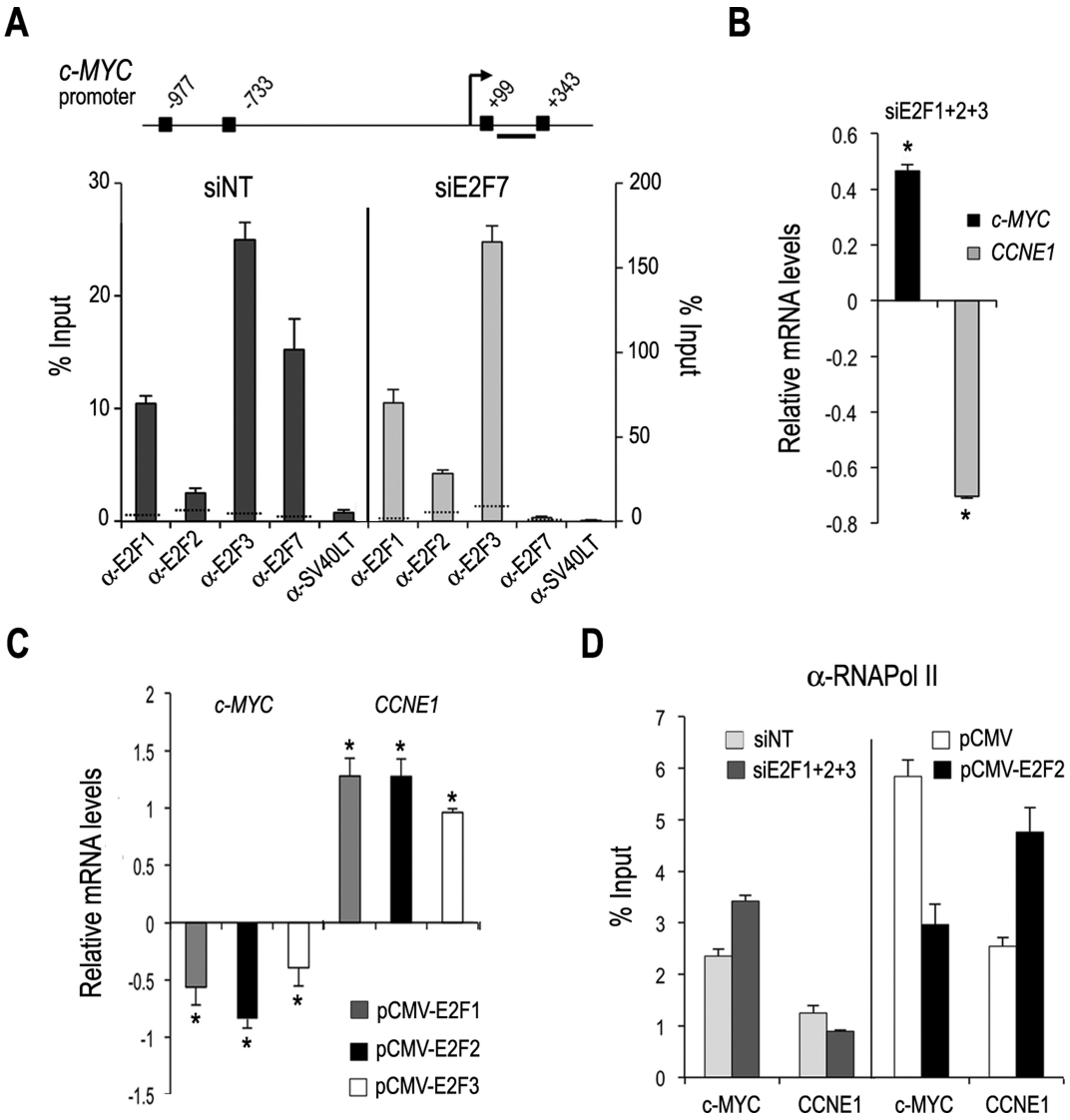

Figure 7. E2F1, E2F2, E2F3 and E2F7 bind to c-MYC promoter and regulate its expression. (**A**) Schematic representation of c-MYC promoter region, indicating the localization of consensus E2F motifs (filled boxes; −977: GCGCCACA; −733: GCAGCAAA; +99: GCGGGAAA; +343: CTTGCCGC). The horizontal line depicts the ChIP-Q-PCR amplicon. Binding of E2F1, E2F2, E2F3 and E2F7 was assessed by ChIP-Q-PCR in HU-synchronized cells transfected with E2F7 siRNA or control NT siRNAs. Cell lysates of siNT and siE2F7 treated cells were harvested 3 h after HU release. Note scale difference between siNT and siE2F7. Dotted horizontal lines represent *ACTB* amplification values. Data correspond to a representative experiment of three independent replicates. (**B**) c-MYC and CCNE1 expression was analyzed by RT-Q-PCR in cells transfected with siNT or a pool of E2F1, E2F2 and E2F3 specific siRNAs. mRNA data are presented as normalized log2-ratios over siNT transfection. (**C**) U2OS cells were synchronized in mitosis and transfected with plasmids expressing HA-tagged E2F1, E2F2 and E2F3. *c-MYC* and *CCNE1* levels were analyzed by RT-Q-PCR in samples harvested 6 h after block release. mRNA data are shown as log2-ratios over the empty pCMV transfection. (**D**) ChIP analyses of RNA-Pol II binding at downstream regions (>1 kb) of *c-MYC* and *CCNE1* genes. U2OS cells transfected with E2F1, E2F2 and E2F3 specific siRNAs or pCMV-E2F2-HA were used for ChIP assays with an antibody against RNA-Pol II. Immunoprecipitated DNA was analyzed by Q-PCR using primers in *c-MYC* and *CCNE1* +1 kb region. Data correspond to a representative experiment of three independent replicates.

of a set of miRNA genes throughout the cell cycle, which in turn may finely tune pathways controlling cell proliferation.

The role of E2F7 in cell cycle progression has not been clearly established. Early overexpression experiments suggested that E2F7 could be a negative regulator of the cell cycle (7,8). However, chronic ablation of E2F7 did not impact cellular proliferation (12). By inducing acute depletion of E2F7, and thus largely avoiding compensatory mechanisms that are common after chronic ablation, our data clearly establish a unique requirement for E2F7 in dictating proper cell cycle kinetics, a role that is not shared with E2F8 in U2OS cells. Our observation that E2F7 restrains cell cycle progression raises the possibility that E2F7 could function as a tumor suppressor gene, and is consistent with recent data showing that E2F7 loss together with RB inactivation promotes oncogenic transformation of murine cells (51).

E2F7 has been shown to repress a set of protein-coding genes involved in DNA replication and metabolism (11). The miRNA expression profiling analysis performed in the present work significantly expands our understanding of

E2F7 function, by providing evidence that this factor has a major role as a negative regulator of miRNA expression. miR-25 and let-7f exhibited the highest levels of overexpression upon E2F7 loss. Interestingly, these miRNAs have previously been identified as induced by E2F1 and E2F3 in S phase entry (14), indicating that E2F7 might repress the expression of miRNAs activated by canonical E2Fs. Other miRNAs previously related to E2F, such as miR-449a/b and miR-15 (15,16,20), were not detected in our work, perhaps because of the restrictive criteria that we used in the different steps of RNA-Seq data analysis. On the other hand, our small RNA-Seq experiment has revealed many other differentially expressed miRNAs that have not been previously linked to E2F activity, and thus represent potentially novel E2F-regulated miRNAs.

Several of the miRNAs that we found to be repressed by E2F7 have previously been described as regulators of proliferation pathways (13,14,17,23,24,52–59). However, their potential roles in cancer have not been clearly established, as these miRNAs appear to have both oncogenic and anti-oncogenic functions in different cellular contexts. Our data evidence that miR-25, let-7f, miR-27b, let-7b, miR-92a, miR-7 and to a lesser extent miR-26a, promote cell proliferation in U2OS cells, at least in part by silencing the expression of anti-proliferative cell cycle regulators. Thus, by downregulating miRNA expression, E2F7 would indirectly upregulate the levels of cell cycle inhibitors to restrain cell cycle progression. These findings suggest that E2F7 controls cell cycle progression and cellular proliferation through a coordinated performance of both protein-coding and non-coding genes.

According to our promoter occupancy analyses, the chromatin binding properties of E2F7 and canonical E2F factors in the regulation of target genes appear to be different. The finding that E2F7 is only bound to E2F sites present in miR-25, miR-92a, miR-7 and c-MYC, suggests that the affinity of E2F7 for its binding site could be more restricted than that of canonical E2F1-3 factors. The basis for this selectivity remains unknown, and could involve unique interactions between E2F7 and other transcription factors at a particular promoter, as it has been proposed for other members of the E2F family (60).

miRNA biogenesis is thought to be regulated at multiple levels through mechanisms that are still not well understood. Our work reveals that regulation of let-7f and let-7b maturation by E2F7 involves both transcriptional and post-transcriptional mechanisms mediated by c-MYC and LIN28B, adding a new level of complexity to E2F-mediated miRNA regulation. The mechanism by which E2F7 modulates c-MYC expression is presently unknown, although our findings suggest that it involves negative regulation of E2F1-3 and RNA Pol II activities. Interestingly, an interplay between E2F7 and c-MYC activity has recently been suggested (61). Interfering with E2F7 expression resulted in inhibition of c-MYC functional activity in acute myeloid leukemia (AML) cells by an unknown mechanism. However, the authors did not report changes in c-MYC or LIN28B expression. It would be interesting to examine if E2F7 regulates c-MYC gene expression in AML cells, similarly to what we have observed in U2OS cells, and inquire into the biological relevance of this novel E2F7-c-MYC-LIN28B axis in AML cells.

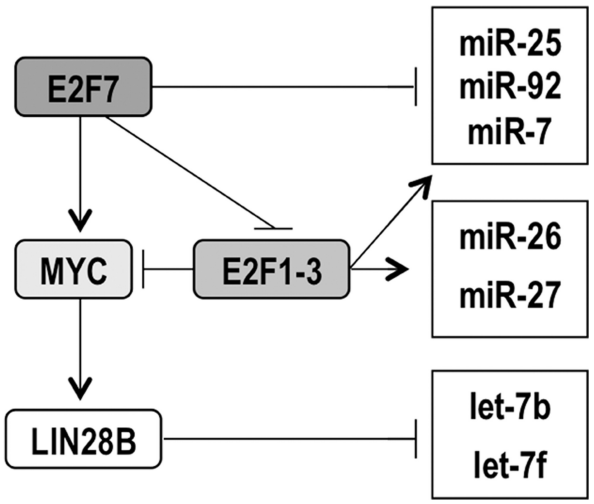

Figure 8. Model summarizing the mechanism of action of E2F factors, c-MYC and LIN28B in miRNA expression regulation described in this study.

Overall, our study identifies E2F7 as a critical regulator of miRNA biogenesis throughout the cell cycle (Figure 8). Interestingly, we have uncovered a novel interplay between E2F7 and E2F1-3 in the regulation of miRNAs to ensure induction and repression of miRNA genes during the cell division cycle, which in turn could contribute to cell growth control. In this regard, E2F7 might repress miRNA gene expression through multiple mechanisms: by binding to its target genes and directly repressing their transcription (miR-25, miR-92a and miR-7); by repressing the expression of E2F1-3, and indirectly suppressing miRNA expression at the level of transcription (miR-25, miR-26a, miR-27b) or maturation (let-7b, let-7f); or probably by a combination of both mechanisms. These findings support a model in which the transcriptional activity of E2F-target miRNAs may be dictated by an 'E2F-network' in which E2F1-3 and E2F7 play antagonistic roles. A similar mechanism may also be operating in E2F7-mediated regulation of protein-coding genes. Future studies may help to further identify the components of this novel molecular network as well as its biological relevance.

SUPPLEMENTARY DATA

Supplementary Data are available at NAR Online.

ACKNOWLEDGEMENT

We thank members of the Zubiaga and Malumbres laboratory for helpful discussions, Naiara Zorrilla for technical support, Ainhoa Iglesias and Asier Fullaondo for assistance with figures, Jose Antonio Rodriguez and Nerea Osinalde for critical reading of the manuscript and J.R. Nevins, T. Tuschl and J. León for kindly providing vectors.

FUNDING

This work was supported by the Spanish Ministry [SAF2012-33551, co-funded by the European Regional Development fund to A.M.Z., SAF2012-38215 to M.M., SAF2014-57791-REDC to A.M.Z. and to M.M.]; Basque Government [IT634-13 to A.M.Z.]; University of the Basque Country UPV/EHU [UFI11/20 to A.M.Z.]; Excellence Network CellSYS [BFU2014-52125-REDT to M.M.]; Comunidad de Madrid [S2010/BMD-2470 to M.M.]; Basque Government Fellowship for graduate studies (to J.M.). Funding for open access charge: Basque Government [IT634-13].

Conflict of interest statement. None declared.

REFERENCES

1. Bertoli,C., Skotheim,J.M. and de Bruin,R.A. (2013) Control of cell cycle transcription during G1 and S phases. *Nat. Rev. Mol. Cell Biol.*, **14**, 518–528.
2. Chen,H.Z., Tsai,S.Y. and Leone,G. (2009) Emerging roles of E2Fs in cancer: an exit from cell cycle control. *Nat. Rev. Cancer*, **9**, 785–797.
3. Dimova,D.K. and Dyson,N.J. (2005) The E2F transcriptional network: old acquaintances with new faces. *Oncogene*, **24**, 2810–2826.
4. van den Heuvel,S and Dyson,N.J. (2008) Conserved functions of the pRB and E2F families. *Nat. Rev. Mol. Cell Biol.*, **9**, 713–724.
5. Lammens,T., Li,J., Leone,G. and De Veylder,L. (2009) Atypical E2Fs: new players in the E2F transcription factor family. *Trends Cell Biol.*, **19**, 111–118.
6. Christensen,J., Cloos,P., Toftegaard,U., Klinkenberg,D., Bracken,A.P., Trinh,E., Heeran,M., Di Stefano,L. and Helin,K. (2005) Characterization of E2F8, a novel E2F-like cell-cycle regulated repressor of E2F-activated transcription. *Nucleic Acids Res.*, **33**, 5458–5470.
7. de Bruin,A., Maiti,B., Jakoi,L., Timmers,C., Buerki,R. and Leone,G. (2003) Identification and characterization of E2F7, a novel mammalian E2F family member capable of blocking cellular proliferation. *J. Biol. Chem.*, **278**, 42041–42049.
8. Di Stefano,L., Jensen,M.R. and Helin,K. (2003) E2F7, a novel E2F featuring DP-independent repression of a subset of E2F-regulated genes. *EMBO J.*, **22**, 6289–6298.
9. Logan,N., Graham,A., Zhao,X., Fisher,R., Maiti,B., Leone,G. and La Thangue,N.B. (2005) E2F-8: an E2F family member with a similar organization of DNA-binding domains to E2F-7. *Oncogene*, **24**, 5000–5004.
10. Maiti,B., Li,J., de Bruin,A., Gordon,F., Timmers,C., Opavsky,R., Patil,K., Tuttle,J., Cleghorn,W. and Leone,G. (2005) Cloning and characterization of mouse E2F8, a novel mammalian E2F family member capable of blocking cellular proliferation. *J. Biol. Chem.*, **280**, 18211–18220.
11. Westendorp,B., Mokry,M., Groot Koerkamp,M.J., Holstege,F.C., Cuppen,E. and de Bruin,A. (2012) E2F7 represses a network of oscillating cell cycle genes to control S-phase progression. *Nucleic Acids Res.*, **40**, 3511–3523.
12. Li,J., Ran,C., Li,E., Gordon,F., Comstock,G., Siddiqui,H., Cleghorn,W., Chen,H.Z., Kornacker,K., Liu,C.G. *et al.* (2008) Synergistic function of E2F7 and E2F8 is essential for cell survival and embryonic development. *Dev. Cell*, **14**, 62–75.
13. Brosh,R., Shalgi,R., Liran,A., Landan,G., Korotayev,K., Nguyen,G.H., Enerly,E., Johnsen,H., Buganim,Y., Solomon,H. *et al.* (2008) p53-Repressed miRNAs are involved with E2F in a feed-forward loop promoting proliferation. *Mol. Syst. Biol.*, **4**, 229.
14. Bueno,M.J., Gomez de,C.M., Laresgoiti,U., Fernandez-Piqueras,J., Zubiaga,A.M. and Malumbres,M. (2010) Multiple E2F-induced microRNAs prevent replicative stress in response to mitogenic signaling. *Mol. Cell. Biol.*, **30**, 2983–2995.
15. Lize,M., Pilarski,S. and Dobbelstein,M. (2010) E2F1-inducible microRNA 449a/b suppresses cell proliferation and promotes apoptosis. *Cell Death. Differ.*, **17**, 452–458.
16. Ofir,M., Hacohen,D. and Ginsberg,D. (2011) MiR-15 and miR-16 are direct transcriptional targets of E2F1 that limit E2F-induced proliferation by targeting cyclin E. *Mol. Cancer Res.*, **9**, 440–447.
17. Petrocca,F., Visone,R., Onelli,M.R., Shah,M.H., Nicoloso,M.S., De Martino,I., Iliopoulos,D., Pilozzi,E., Liu,C.G., Negrini,M. *et al.* (2008) E2F1-regulated microRNAs impair TGFbeta-dependent cell-cycle arrest and apoptosis in gastric cancer. *Cancer Cell*, **13**, 272–286.
18. Sylvestre,Y., De Guire,V., Querido,E., Mukhopadhyay,U.K., Bourdeau,V., Major,F., Ferbeyre,G. and Chartrand,P. (2007) An E2F/miR-20a autoregulatory feedback loop. *J. Biol. Chem.*, **282**, 2135–2143.
19. Woods,K., Thomson,J.M. and Hammond,S.M. (2007) Direct regulation of an oncogenic micro-RNA cluster by E2F transcription factors. *J. Biol. Chem.*, **282**, 2130–2134.
20. Yang,X., Feng,M., Jiang,X., Wu,Z., Li,Z., Aau,M. and Yu,Q. (2009) miR-449a and miR-449b are direct transcriptional targets of E2F1 and negatively regulate pRb-E2F1 activity through a feedback loop by targeting CDK6 and CDC25A. *Genes Dev.*, **23**, 2388–2393.
21. Bueno,M.J., Perez de Castro,I. and Malumbres,M. (2008) Control of cell proliferation pathways by microRNAs. *Cell Cycle*, **7**, 3143–3148.
22. Bueno,M.J. and Malumbres,M. (2011) MicroRNAs and the cell cycle. *Biochim. Biophys. Acta*, **1812**, 592–601.
23. Kim,Y.K., Yu,J., Han,T.S., Park,S.Y., Namkoong,B., Kim,D.H., Hur,K., Yoo,M.W., Lee,H.J., Yang,H.K. *et al.* (2009) Functional links between clustered microRNAs: suppression of cell-cycle inhibitors by microRNA clusters in gastric cancer. *Nucleic Acids Res.*, **37**, 1672–1681.
24. Poliseno,L., Salmena,L., Riccardi,L., Fornari,A., Song,M.S., Hobbs,R.M., Sportoletti,P., Varmeh,S., Egia,A., Fedele,G. *et al.* (2010) Identification of the miR-106b~25 microRNA cluster as a proto-oncogenic PTEN-targeting intron that cooperates with its host gene MCM7 in transformation. *Sci. Signal.*, **3**, ra29.
25. Ventura,A., Young,A.G., Winslow,M.M., Lintault,L., Meissner,A., Erkeland,S.J., Newman,J., Bronson,R.T., Crowley,D., Stone,J.R. *et al.* (2008) Targeted deletion reveals essential and overlapping functions of the miR-17-92 family of miRNA clusters. *Cell*, **132**, 875–86.
26. Hafner,M., Max,K.E., Bandaru,P., Morozov,P., Gerstberger,S., Brown,M., Molina,H. and Tuschl,T. (2013) Identification of mRNAs bound and regulated by human LIN28 proteins and molecular requirements for RNA recognition. *RNA*, **19**, 613–626.
27. Krek,W., Livingston,D.M. and Shirodkar,S. (1993) Binding to DNA and the retinoblastoma gene product promoted by complex formation of different E2F family members. *Science*, **262**, 1557–1560.
28. Mauleon,I., Lombard,M.N., Muñoz-Alonso,M.J., Cañelles,M. and Leon,J. (2004) Kinetics of myc-max-mad gene expression during hepatocyte proliferation in vivo: Differential regulation of mad family and stress-mediated induction of c-myc. *Mol. Carcinog.*, **39**, 85–90.
29. Voorhoeve,P.M., le Sage,C., Schrier,M., Gillis,A.J., Stoop,H., Nagel,R., Liu,Y.P., van Duijse,J., Drost,J., Griekspoor,A. *et al.* (2007) A genetic screen implicates miRNA-372 and miRNA-373 as oncogenes in testicular germ cell tumors. *Adv. Exp. Med. Biol.*, **604**, 17–46.
30. Anders,S. and Huber,W. (2010) Differential expression analysis for sequence count data. *Genome Biol.*, **11**, R106.
31. Dhahbi,J.M., Atamna,H., Boffelli,D., Magis,W., Spindler,S.R. and Martin,D.I. (2011) Deep sequencing reveals novel microRNAs and regulation of microRNA expression during cell senescence. *PLoS One*, **6**, e20509.
32. Paraskevopoulou,M.D., Georgakilas,G., Kostoulas,N., Vlachos,I.S., Vergoulis,T., Reczko,M., Filippidis,C., Dalamagas,T. and Hatzigeorgiou,A.G. (2013) DIANA-microT web server v5.0: service integration into miRNA functional analysis workflows. *Nucleic Acids Res.*, **41**, 169–173.
33. Joshi-Tope,G., Gillespie,M., Vastrik,I., D'Eustachio,P., Schmidt,E., de Bono,B., Jassal,B., Gopinath,G.R., Wu,G.R., Matthews,L. *et al.* (2005) Reactome: a knowledgebase of biological pathways. *Nucleic Acids Res.*, **1**, 428–432.
34. Ritchie,W., Flamant,S. and Rasko,J.E. (2009) Predicting microRNA targets and functions: traps for the unwary. *Nat. Methods*, **6**, 397–398.
35. Al-Shahrour,F., Minguez,P., Vaquerizas,J.M., Conde,L. and Dopazo,J.2005. BABELOMICS: a suite of web tools for functional annotation and analysis of groups of genes in high-throughput experiments. *Nucleic Acids Res.*, **33**, W460–W464.

36. Infante,A., Laresgoiti,U., Fernandez-Rueda,J., Fullaondo,A., Galan,J., Diaz-Uriarte,R., Malumbres,M., Field,S.J. and Zubiaga,A.M. (2008) E2F2 represses cell cycle regulators to maintain quiescence. *Cell Cycle*, **7**, 3915–3927.
37. Aerts,S., Van Loo,P., Thijs,G., Mayer,H., de Martin,R., Moreau,Y. and De Moor,B. (2005) TOUCAN 2: the all-inclusive open source workbench for regulatory sequence analysis. *Nucleic Acids Res.*, **33**, W393–W396.
38. Laresgoiti,U., Apraiz,A., Olea,M., Mitxelena,J., Osinalde,N., Rodriguez,J.A., Fullaondo,A. and Zubiaga,A.M. (2013) E2F2 and CREB cooperatively regulate transcriptional activity of cell cycle genes. *Nucleic Acids Res.*, **41**, 10185–10198.
39. Thangavel,C., Boopathi,E., Ertel,A., Lim,M., Addya,S., Fortina,P., Witkiewicz,A.K. and Knudsen,E.S. (2013) Regulation of miR106b cluster through the RB pathway: mechanism and functional targets. *Cell Cycle*, **12**, 98–111.
40. Wells,J., Boyd,K.E., Fry,C.J., Bartley,S.M. and Farnham,P.J. (2000) Target gene specificity of E2F and pocket protein family members in living cells. *Mol. Cell. Biol.*, **20**, 5797–5807.
41. Heo,I., Joo,C., Cho,J., Ha,M., Han,J. and Kim,V.N. (2008) Lin28 mediates the terminal uridylation of let-7 precursor MicroRNA. *Mol. Cell*, **32**, 276–284.
42. Newman,M.A., Thomson,J.M. and Hammond,S.M. (2008) Lin-28 interaction with the Let-7 precursor loop mediates regulated microRNA processing. *RNA*, **14**, 1539–1549.
43. Piskounova,E., Viswanathan,S.R., Janas,M., LaPierre,R.J., Daley,G.Q., Sliz,P. and Gregory,R.I. (2008) Determinants of microRNA processing inhibition by the developmentally regulated RNA-binding protein Lin28. *J. Biol. Chem.*, **283**, 21310–21314.
44. Rybak,A., Fuchs,H., Smirnova,L., Brandt,C., Pohl,E.E., Nitsch,R. and Wulczyn,F.G. (2008) A feedback loop comprising lin-28 and let-7 controls pre-let-7 maturation during neural stem-cell commitment. *Nat. Cell Biol.*, **10**, 987–993.
45. Viswanathan,S.R., Daley,G.Q. and Gregory,R.I. (2008) Selective blockade of microRNA processing by Lin28. *Science*, **320**, 97–100.
46. Chang,T.C., Zeitels,L.R., Hwang,H.W., Chivukula,R.R., Wentzel,E.A., Dews,M., Jung,J., Gao,P., Dang,C.V., Beer,M.A. *et al.* (2009) Lin-28B transactivation is necessary for Myc-mediated let-7 repression and proliferation. *Proc. Natl. Acad. Sci. U.S.A.*, **106**, 3384–3389.
47. Bretones,G., Delgado,M.D. and Leon,J. (2015) Myc and cell cycle control. *Biochim. Biophys. Acta*, **1849**, 506–516.
48. DeGregori,J. and Johnson,D.G. (2006) Distinct and overlapping roles for E2F family members in transcription, proliferation and apoptosis. *Curr. Mol. Med.*, **6**, 739–748.
49. Martelli,F. and Livingston,D.M. (1999) Regulation of endogenous E2F1 stability by the retinoblastoma family proteins. *Proc. Natl. Acad. Sci. U.S.A.*, **96**, 2858–2863.
50. Sandoval,J., Rodríguez,J.L., Tur,G., Serviddio,G., Pereda,J., Boukaba,A., Sastre,J., Torres,L., Franco,L. and López-Rodas,G. (2004) RNAPol-ChIP: a novel application of chromatin immunoprecipitation to the analysis of real-time gene transcription. *Nucleic Acids Res.*, **32**, e88.
51. Aksoy,O., Chicas,A., Zeng,T., Zhao,Z., McCurrach,M., Wang,X. and Lowe,S.W. (2012) The atypical E2F family member E2F7 couples the p53 and RB pathways during cellular senescence. *Genes Dev.*, **26**, 1546–1557.
52. Johnson,C.D., Esquela-Kerscher,A., Stefani,G., Byrom,M., Kelnar,K., Ovcharenko,D., Wilson,M., Wang,X., Shelton,J., Shingara,J. *et al.* (2007) The let-7 microRNA represses cell proliferation pathways in human cells. *Cancer Res.*, **67**, 7713–7722.
53. Kim,H., Huang,W., Jiang,X., Pennicooke,B., Park,P.J. and Johnson,M.D. (2010) Integrative genome analysis reveals an oncomir/oncogene cluster regulating glioblastoma survivorship. *Proc. Natl. Acad. Sci. U.S.A.*, **107**, 2183–2188.
54. Kota,J., Chivukula,R.R., O'Donnell,K.A., Wentzel,E.A., Montgomery,C.L., Hwang,H.W., Chang,T.C., Vivekanandan,P., Torbenson,M., Clark,K.R. *et al.* (2009) Therapeutic microRNA delivery suppresses tumorigenesis in a murine liver cancer model. *Cell*, **137**, 1005–1017.
55. Lee,J.J., Drakaki,A., Iliopoulos,D. and Struhl,K. (2012) MiR-27b targets PPARgamma to inhibit growth, tumor progression and the inflammatory response in neuroblastoma cells. *Oncogene*, **31**, 3818–3825.
56. Schultz,J., Lorenz,P., Gross,G., Ibrahim,S. and Kunz,M. (2008) MicroRNA let-7b targets important cell cycle molecules in malignant melanoma cells and interferes with anchorage-independent growth. *Cell Res.*, **18**, 549–557.
57. Suh,S.S., Yoo,J.Y., Nuovo,G.J., Jeon,Y.J., Kim,S., Lee,T.J., Kim,T., Bakacs,A., Alder,H., Kaur,B. *et al.* (2012) MicroRNAs/TP53 feedback circuitry in glioblastoma multiforme. *Proc. Natl. Acad. Sci. U.S.A.*, **109**, 5316–5321.
58. Wang,Y., Rathinam,R., Walch,A. and Alahari,S.K. (2009) ST14 (suppression of tumorigenicity 14) gene is a target for miR-27b, and the inhibitory effect of ST14 on cell growth is independent of miR-27b regulation. *J. Biol. Chem.*, **284**, 23094–23106.
59. He,L., Thomson,J.M., Hemann,M.T., Hernando-Monge,E., Mu,D., Goodson,S., Powers,S., Cordon-Cardo,C., Lowe,S.W., Hannon,G.J. *et al.* (2005) A microRNA polycistron as a potential human oncogene. *Nature*, **435**, 828–833.
60. Mitxelena,J., Osinalde,N., Arizmendi,J.M., Fullaondo,A. and Zubiaga,A.M. (2012) Proteomic approaches to unraveling the RB/E2F regulatory pathway. In: Man,TK and Flores,RJ (eds). *Proteomics—Human Diseases and Protein Functions*, INTECH Open Access Publisher, Rijeka, 135–160.
61. Salvatori,B., Iosue,I., Mangiavacchi,A., Loddo,G., Padula,F., Chiaretti,S., Peragine,N., Bozzoni,I., Fazi,F. and Fatica,A. (2012) The microRNA-26a target E2F7 sustains cell proliferation and inhibits monocytic differentiation of acute myeloid leukemia cells. *Cell Death Dis.*, **3**, e413.

4546–4559 *Nucleic Acids Research, 2018, Vol. 46, No. 9* *Published online 24 March 2018*
doi: 10.1093/nar/gky218

An E2F7-dependent transcriptional program modulates DNA damage repair and genomic stability

Jone Mitxelena[1,†], Aintzane Apraiz[2,†], Jon Vallejo-Rodríguez[1,†], Iraia García-Santisteban[1], Asier Fullaondo[1], Mónica Alvarez-Fernández[3], Marcos Malumbres[3] and Ana M. Zubiaga[1,*]

[1]Department of Genetics, Physical Anthropology and Animal Physiology, University of the Basque Country UPV/EHU, 48080 Bilbao, Spain, [2]Department of Cell Biology and Histology, University of the Basque Country UPV/EHU, 48080 Bilbao, Spain and [3]Cell Division and Cancer Group, Spanish National Cancer Research Centre (CNIO), 28029 Madrid, Spain

Received July 20, 2017; Revised February 09, 2018; Editorial Decision March 12, 2018; Accepted March 15, 2018

ABSTRACT

The cellular response to DNA damage is essential for maintaining the integrity of the genome. Recent evidence has identified E2F7 as a key player in DNA damage-dependent transcriptional regulation of cell-cycle genes. However, the contribution of E2F7 to cellular responses upon genotoxic damage is still poorly defined. Here we show that E2F7 represses the expression of genes involved in the maintenance of genomic stability, both throughout the cell cycle and upon induction of DNA lesions that interfere with replication fork progression. Knockdown of E2F7 leads to a reduction in 53BP1 and FANCD2 foci and to fewer chromosomal aberrations following treatment with agents that cause interstrand crosslink (ICL) lesions but not upon ionizing radiation. Accordingly, E2F7-depleted cells exhibit enhanced cell-cycle re-entry and clonogenic survival after exposure to ICL-inducing agents. We further report that expression and functional activity of E2F7 are p53-independent in this context. Using a cell-based assay, we show that E2F7 restricts homologous recombination through the transcriptional repression of RAD51. Finally, we present evidence that downregulation of E2F7 confers an increased resistance to chemotherapy in recombination-deficient cells. Taken together, our results reveal an E2F7-dependent transcriptional program that contributes to the regulation of DNA repair and genomic integrity.

INTRODUCTION

Mammalian E2F transcription factors (E2F1-E2F8) are key components of the Retinoblastoma (RB) pathway that control cell-cycle progression through the activation or repression of target genes. Deregulation of E2F activity has a high impact on health and disease (1). An insight into the specific functions of E2F family members has been provided by the identification of a large set of genes regulated by each individual factor (2). These studies have revealed a key role for RB-dependent classical E2Fs (E2F1-5) in cell-cycle control and DNA damage response (DDR). By contrast, the contribution of RB-independent atypical E2F factors, E2F7-8, to these processes has not been clearly defined.

E2F7, a predominantly transcriptional repressor, is known to be induced in late G1 by E2F1, together with a large array of E2F target genes (3,4). E2F7 binds to promoters of microRNA and protein-coding genes bearing E2F consensus motifs, such as *E2F1*, *CDC6*, *MCM2* or *miR-25* during S-phase, thereby repressing their expression (4,5). These findings have raised the possibility that E2F7 protein may be a key component of a negative feedback loop required to turn off transcription of E2F-driven G1/S target genes, thus allowing progression through the cell cycle. Accordingly, overexpression of E2F7 blocks S-phase entry (4,6,7), whereas acute loss of E2F7 accelerates cell-cycle progression (5).

Involvement of E2F7 in stress responses is supported by various lines of evidence, although the mechanisms by which E2F7 participates in these processes remain unresolved. E2F7 and E2F8 double knockout mouse embryos exhibit widespread apoptosis, suggesting a role for these E2Fs in cell survival (8). Furthermore, depletion of atypical E2Fs has been shown to reduce survival of tumor cells, primary mouse keratinocytes and embryonic fibroblasts after treatment with several DNA damaging compounds, indicating that sensitivity to cytotoxic/genotoxic stimuli is enhanced by loss of E2F7 or by the combined loss of E2F7/8 (8–10). Co-depletion of E2F1 under these circumstances could rescue stress-induced apoptosis (8,11) and acceler-

*To whom correspondence should be addressed. Tel: +34 94 601 2603; Fax: +34 94 601 3143; Email: ana.zubiaga@ehu.es
†The authors wish it to be known that, in their opinion, the first three authors should be regarded as joint First Authors.
Present Address: Jone Mitxelena, Department of Molecular Mechanisms of Disease, University of Zurich, Switzerland.

ate tumorigenesis in a two-stage skin carcinogenesis model (10), implying a key role for E2F1 in E2F7/8-dependent stress responses. Additional mediators of E2F7-dependent resistance to DNA damaging drugs include the sphingosine kinase SPHK1 and its downstream target AKT (12), although the precise role of E2F7 in this pathway remains to be elucidated.

Both transcription-independent and transcription-dependent roles of E2F7 in the response to DNA damage have been suggested. On the one hand, a recruitment of E2F7 to the sites of DNA breaks has been reported, and it has been suggested that E2F7 represses DNA repair process directly on the lesion (13). On the other hand, a p53-dependent E2F7 transactivation has been described after treatment with DNA topoisomerase inhibitors, which leads to repression of a subset of cell-cycle genes, including *DHFR*, *RRM2* and *E2F1* (14), suggesting a key transcriptional role for E2F7 in cell-cycle arrest upon DNA damage.

Genes involved in DNA repair have been reported as targets of E2F factors, including E2F7 (4,15), but whether E2F7 modulates responses to DNA damage through regulation of DNA repair gene expression remains to be established. In this work we have investigated the role of E2F7 in the transcriptional regulation of genes involved in DNA repair, and the functional consequences of E2F7-mediated transcriptional program upon genotoxic damage. Our results suggest that E2F7 plays a p53-independent role in the attenuation of DNA repair function through transcriptional repression of target genes that are required for the timely regulation of replication fork-associated DNA damage repair.

MATERIALS AND METHODS

Cell culture and flow cytometry

Human cell lines were maintained in Dulbecco's modified Eagle's medium supplemented with fetal bovine serum (10% for U2OS and HeLa cells; 20% for CAPAN-1 cells). For cell synchronization in G1/S, exponentially growing U2OS cells were incubated with 4 mM hydroxyurea (HU) for 24 h and subsequently washed and cultured in complete medium. For cell synchronization at mitosis, cell cultures were incubated with nocodazole (50–100 ng/ml) for the last 14 h of culture. To assess cell-cycle distribution, cells were fixed with chilled 70% ethanol, stained with 50 μg/ml propidium iodide (PI) and analyzed by flow cytometry (FACSCalibur, BD). To analyze the percentage of mitotic or γ-H2AX-positive cells, ethanol-fixed cells were stained with an antibody recognizing Histone H3 phosphorylated on Serine 10 (pH3) conjugated with FITC (06-570, Millipore), or an antibody recognizing γ-H2AX protein conjugated with FITC (05-636, Millipore), subsequently incubated with PI and analyzed by flow cytometry. Cell-cycle distribution, mitotic index and γ-H2AX accumulation analyses were performed with Summit 4.3 software. To analyze the percentage of cells replicating DNA, cells were pulse-labeled with 10 μM BrdU for the last 2 h of cell culture, washed in ice-cold phosphate-buffered saline and fixed in ice-cold 70% ethanol. Cells were stained with an antibody recognizing BrdU (M0744, Dako) and analyzed by flow cytometry as described (16).

Generation of U2OS E2F7 knockout cells

E2F7 knockout cells were generated using the CRISPR/Cas9 system. A CRISPR guide RNA (gRNA) targeting the first coding exon of E2F7 was designed using Benchling, and cloned into the BbsI site of pX330 (42230, Addgene). U2OS cells were co-transfected with this plasmid, together with a plasmid containing a gRNA to the zebrafish TIA gene (5′-GGTATGTCGGGAACCTCTCC-3′) and a P2A-puromycin resistance cassette flanked by two TIA target sites. Co-transfection results in excision of the cassette and subsequent sporadic incorporation at the site of the targeted genomic locus as previously described (17). Successful integration of the cassette into the targeted gene disrupts the allele and renders cells resistant to puromycin. After puromycin selection, resistant clones were expanded, screened for cassette integration and indels into the target gene.

Clonogenic survival assays

Cells were treated with cisplatin (CSP) at the indicated concentrations for 24 h. Cells were then washed free of the drug and incubated in fresh medium for 14 days or left untreated. The number of colonies of more than 50 cells in each dish was counted after staining with crystal violet.

Analysis of chromosomal aberrations

Chromosomal aberrations were visualized in chromosome spreads following published protocols, with minor modifications (18). Cells were arrested in metaphase after treating cell cultures with Karyomax Colcemid (Life Technologies) for 12 h at a final concentration of 100 ng/ml. Metaphase-arrested cells were subsequently harvested and fixed in Carnoy solution. An aliquot of the cellular suspension was dropped onto microscopy slides to obtain chromosome spreads, which were stained and mounted with ProLong Gold Antifade with DAPI reagent (Life Technologies). Image acquisition was performed on a Leica DMI 6000B fluorescence microscope.

Transfections and homologous recombination assay

To silence endogenous expression of E2F7, p53, BRCA2 and RAD51, cells were transfected with commercial siRNAs (Life Technologies), at a final concentration of 10 nM (sequences provided in Supplementary Table S1) using Lipofectamine RNAiMAX (Life Technologies) following manufacturer's recommendation. Plasmid transfection was performed with various amounts of DNA in 6-well culture dishes using XtremeGENE HP transfection reagent (Roche Pharma), following manufacturer's recommendations. The mixture was incubated for 15 min at room temperature and added dropwise to cell cultures.

Homologous recombination (HR)-dependent DNA double stranded break (DSB) repair was assessed using the DR-GFP/SceI assay described by M. Jasin's group (19). For these experiments we used a U2OS cell line that carries a recombination substrate, DR–GFP, inserted in the genome (U2OS DR-GFP cell line). To induce a double-strand break in the HR reporter, U2OS-DR-GFP cells were

transfected with I-SceI restriction enzyme expression construct (pCBAI-SceI) (20). HR repair was analyzed using flow cytometry by scoring GFP-positive cells.

RNA expression analyses

Total RNA extraction was performed with TRIzol Reagent (Life Technologies) and purified using the RNeasy Mini kit (Qiagen) following the manufacturer's recommendations. mRNA was used to build a cDNA library using the reagents provided in the Illumina TruSeq RNA Sample Preparation Kit following the manufacturer's instructions. The resulting purified cDNA library was sequenced on the Genome Analyzer IIx with SBS TruSeq v5 reagents following manufacturer's protocols.

Sequencing reads obtained in each condition were mapped to the human reference genome (GRCh37/hg19) with TopHat software tool (21). After running TopHat, the resulting alignment files were supplied to Cufflinks tool to generate a transcriptome assembly for each sample. The reads were subsequently fed to Cuffdiff, which calculates the expression levels of each identified transcript and tests the statistical significance of the expression changes between conditions. This tool assumes that the number of sequencing reads generated from a transcript is directly proportional to the relative abundance of that transcript in the sample. Expression levels were represented by FPKM values (fragments per kilobase per million sequenced reads), which incorporate two normalization steps to ensure that expression levels of different transcripts can be compared across different runs (longer transcripts produce more sequencing fragments than shorter transcripts and different sequencing runs may produce different volumes of sequencing reads). Changes in gene expression between samples were considered significant at a false discovery rate (FDR)-adjusted P-value (q-value) < 0.05.

For individual mRNA expression analysis, RNA was reverse-transcribed into cDNA with the High-Capacity cDNA RT Kit (Life Technologies) and qPCR was performed as described previously (22), following Minimal Information for Publication of Quantitative Real-Time PCR Experiments (MIQE) guidelines. Sequences of RT-qPCR primers are listed in Supplementary Table S2.

Bioinformatic tools

For gene set enrichment analysis (GSEA) analyses we tested whether 137 pathways obtained from the Pathway Interaction Database (NCI-Nature) are enriched among E2F7-regulated genes. We considered as statistically enriched those pathways with normalized enrichment scores (NES) higher than 1.5 and FDRs $< 10\%$.

Search for E2F motifs in E2F7-regulated genes was carried out with the MotifLocator tool from TOUCAN program (https://gbiomed.kuleuven.be/english/research/50000622/lcb /tools/toucan) (23). The search was restricted to the proximal promoter region (−1000 and +500 bp relative to the transcription start site). Cutoffs of 0.8, 0.85 and 0.9 were applied, and the 'Human 1 Kb Proximal 1000 ENSMUSG' was used as background.

Identification of over-represented transcription factor binding motifs in the regulatory regions of E2F7-regulated genes was performed using the DiRE server (http://DiRE.dcode.org/) (24). For these analyses, the list of up-regulated genes and the list of downregulated genes obtained in the RNA-seq experiments were submitted independently. A list of 5000 human genes randomly selected by DiRE were used as background.

Protein expression and chromatin immunoprecipitation analyses

For western blot analyses, cells were lysed in buffer containing 10 mM NaH_2PO_4 pH 7.2; 1 mM ethylenediaminetetraacetic acid; 1 mM Ethylene glycol tetraacetic acid (EGTA); 150 mM NaCl; 1% NP-40, and a cocktail of protease and phosphatase inhibitors (Roche). Protein concentrations in supernatants were determined using a commercially available kit (DC Protein Assay from Bio-Rad). A total of 20 μg of protein were loaded per lane, fractionated in 8–10% sodium dodecyl sulphate-polyacrylamide gels and transferred onto nitrocellulose membranes (Bio-Rad). Antibodies against the following proteins were used: E2F7 (sc-32574, Santa Cruz), Cyclin E1 (4129, Cell Signaling), p53 (sc-1312, Santa Cruz), RAD51 (sc-8349, Santa Cruz), pH3 (06-570, Millipore), α-Tubulin (T-9026, Sigma), β-Actin (A5441, Sigma). Immunocomplexes were visualized with horseradish peroxidase-conjugated anti-mouse, anti-goat or anti-rabbit IgG antibodies (Santa Cruz), followed by chemiluminiscence detection (ECL, Amersham) with a ChemiDoc camera (Bio-Rad).

Chromatin immunoprecipitations (ChIPs) and the quantification of immunoprecipitated DNA sequences by qPCR were performed as described previously (25). Sequences of qPCR primers are listed in Supplementary Table S3. Antibodies used for ChIP analysis were: E2F7 (sc-66870, Santa Cruz), and SV40LT (sc-147, Santa Cruz).

Immunoflorescence/high-throughput microscopy (HTM)

For standard immunofluorescence, cells were grown on coverslips in 12-well plates. For FANCD2 staining, cells were fixed for 10 min with 3.7% paraformaldehyde in phosphate-buffered saline (PBS) and permeabilized in PBS containing 0.5% Triton X-100. Primary antibodies against FANCD2 (sc-20022, Santa Cruz) and RAD51 (sc-8349, Santa Cruz) were applied to the coverslips for 2 h at room temperature. After washing twice with PBS-T, samples were incubated with the corresponding diluted fluorescent secondary antibody for 1 h. Finally, samples were stained with DAPI and mounted on a microscopy slide using Prolong Gold antifade (Life Technologies) mounting medium. Image acquisition was performed on a Leica DMI 6000B fluorescence microscope. FANCD2 foci quantification was performed with the Definiens Tissue Phenomics analysis software.

High-throughput microscopy (HTM) was performed with the protocol described above, except that in this case cells were grown in 96-well plates with flattened glass bottom (mCLEAR, Greiner Bio-One) at a density of 7500 cells per well. An antibody against 53BP1 (NB100-304, Novus) was used. As a final step nuclei were stained with a DAPI containing solution and the preparations were kept in PBS. Images were automatically acquired with the Opera High

Content Screening platform (Perkin Elmer). Data analysis was performed with the Acapella Imaging and analysis software (Perkin Elmer) as described previously (26). Data were represented with the Prism software (GraphPad Software).

Statistical analysis

Data are presented as mean ± SD. The significance of the difference between two groups was assessed using the Student two-tailed *t*-test. A $P < 0.05$ was considered statistically significant.

RESULTS

E2F7-regulated gene expression profiling in the cell cycle

To better define E2F7 function we analyzed global gene expression profiles during the cell cycle after acute depletion of E2F7. To this end, U2OS cells were synchronized in G1/S transition with HU, and subsequently transfected with siRNAs specific for E2F7 (siE2F7) or with non-target control siRNAs (siNT), as previously described (5). RNA was isolated at three time-points following exit from cell-cycle arrest, which represent G1/S transition (0 h), S phase (3 h) and G2/M boundary (12 h) of the cell cycle (Supplementary Figure S1A). Kinetics of CCNE1 protein levels confirmed the cell-cycle phases of the selected time-points, with high levels at 0 h (G1/S) and a stepwise reduction in the following time-points (Supplementary Figure S1B). Furthermore, we showed efficient E2F7 protein depletion upon siE2F7 transfection, with a concomitant increase in CCNE1 levels, in line with an E2F7-dependent regulation of this gene (Supplementary Figure S1B) (7).

RNA samples were harvested from three independent experiments and subsequently pooled. PolyA+ enriched samples from siNT- and siE2F7-transfected cells were used to build cDNA libraries that were sequenced by RNA-seq. Close to 10^7 high quality reads were obtained per sample. Changes in gene expression between siE2F7-transfected relative to siNT-transfected cells were scored as significant at *q*-value < 0.05. In all three time-points under study, RNA-seq analyses showed close to 500 genes with altered expression upon E2F7 knockdown in comparison with control cells. The proportion of overexpressed and underexpressed genes was similar (data not shown).

We analyzed the potential pathways regulated by E2F7 by performing GSEA. We considered as significantly enriched the pathways with an NES above 1.5 and an FDR below 10%. In concordance with the role of E2F7 as transcriptional repressor of RB/E2F-regulated cell-cycle genes (4), GSEA analyses showed highest enrichment values for E2F and RB pathways (Figure 1A) among the set of E2F7-repressed genes. This group included many genes previously described as E2F targets: *CCND3*, *CDC6*, *DHFR* and several *MCM*-s among others.

Interestingly, pathways involved in (DDR) and repair, including BARD1, Fanconi anemia (FA) and Ataxia telangiectasia and Rad3-related protein (ATR) pathways were also over-represented among the genes repressed by E2F7 in all cell-cycle phases (Figure 1A). We confirmed E2F7-mediated repression of genes belonging to these functional groups by RT-qPCR analysis (Figure 1B). RNAi-mediated depletion of E2F7 resulted in a significantly increased expression of genes involved in HR-mediated repair of damaged DNA (RAD51, CTIP, BARD1) or in FA pathway (FANCE, FANCI, BRIP1). These results suggest that, in addition to the previously reported regulation of cell-cycle genes, E2F7 might also mediate repression of genes involved in DNA damage response and repair pathways.

E2F7 is recruited to the promoters of DNA damage repair genes

A search for promoter regulatory elements of the differentially expressed genes showed that about 40% of overexpressed genes in E2F7-depleted cells harbor E2F binding sites. In fact, the canonical E2F-binding motif was the most over-represented transcription factor-binding site among the upregulated set of genes in the three time-points analyzed according to DiRE analysis. By contrast, this motif was not over-represented among the set of genes displaying decreased mRNA levels in cells lacking E2F7. This finding supports a role for E2F7 in transcriptional repression through binding to consensus E2F motifs, in agreement with previous data (4,5).

To identify the E2F motifs within E2F7-repressed RNAs we made use of MotifLocator tool provided by TOUCAN program. We focused our search on the genes belonging to BARD1, FA and ATR pathways that showed aberrant expression upon E2F7 attenuation in at least two of the analyzed time-points. Taking into account previous evidence suggesting that E2F factors are predominantly recruited to the proximal promoter of their target genes (4,15,27,28), we limited our search to a region spanning −1000 to +500 bp relative to transcription initiation. Using a threshold level of 0.8 for similarity with the canonical E2F motif recorded in the JASPAR database, we found that all E2F7-repressed genes included in the selected subset harbored at least one canonical E2F motif (Figure 2A and Supplementary Table S4).

We next assessed E2F7 binding activity to the promoters of E2F7-regulated genes by performing ChIP analyses with an anti-E2F7 specific antibody followed by qPCR using promoter-specific primers. Amplification of the β-actin promoter was used as a negative control, since this promoter lacks E2F binding sites but is highly expressed in U2OS cells (5). In addition, as a control for antibody specificity, we used an irrelevant antibody (anti-SV40LT), which has no affinity for chromatin and is unable to immunoprecipitate any of the various E2F target sequences (25). As shown in Figure 2B, ChIP analyses revealed efficient binding of E2F7 to all analyzed promoters, suggesting an important role for E2F7 in the direct transcriptional repression of DNA repair genes.

E2F7 controls cellular responses after genotoxic damage

Given the enrichment in DDR and DNA repair genes within the list of E2F7-regulated transcripts, and having validated several of them as direct E2F7 target genes, we hypothesized that E2F7 could control cellular responses following DNA damage. To test this possibility, G1/S-synchronized cells were transfected with siNT or siE2F7, and subsequently cultured under several genotoxic conditions (Figure 3A): mitomycin C (MMC) and CSP are

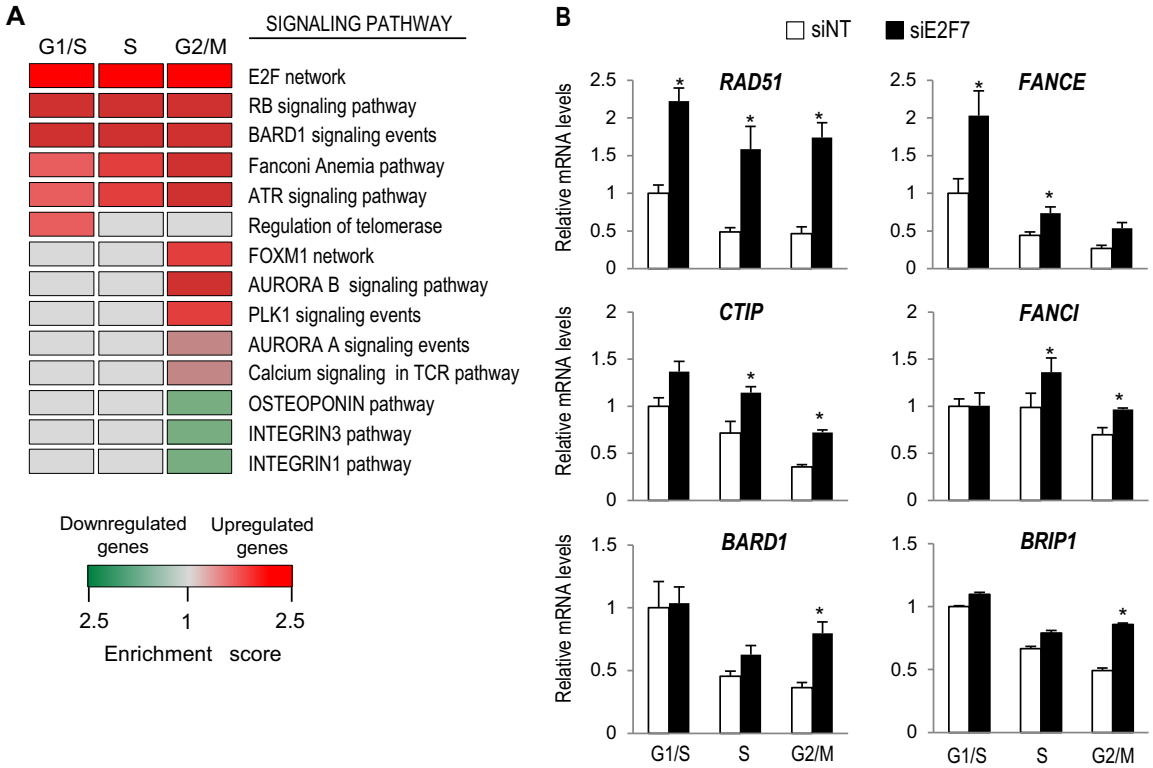

Figure 1. E2F7 represses the expression of genes involved in cell cycle and DNA repair pathways. (**A**) Functional classification of E2F7-regulated genes by GSEA analysis using Pathway Interaction Database. The heat map shows the enriched pathways among the list of genes differentially expressed in cells lacking E2F7. Normalized enrichment ratios obtained in GSEA analyses are represented as colors (red for upregulated genes, green for downregulated genes). Only pathways with FDR < 10% were considered significantly enriched. (**B**) Validation of RNA-seq results. U2OS cells transfected with NT control or E2F7 siRNAs were synchronized in the cell cycle by HU treatment. RT-qPCR analyses of indicated genes were carried out with RNA samples harvested at 0h (G1/S), 3 h (S phase) and 12 h (G2/M) after HU treatment release. Expression values are normalized to the expression of *EIF2C2*, used as standard control. Data are represented as fold-change (mean ± SEM) relative to siNT-transfected samples from three independent experiments (*, $P < 0.05$).

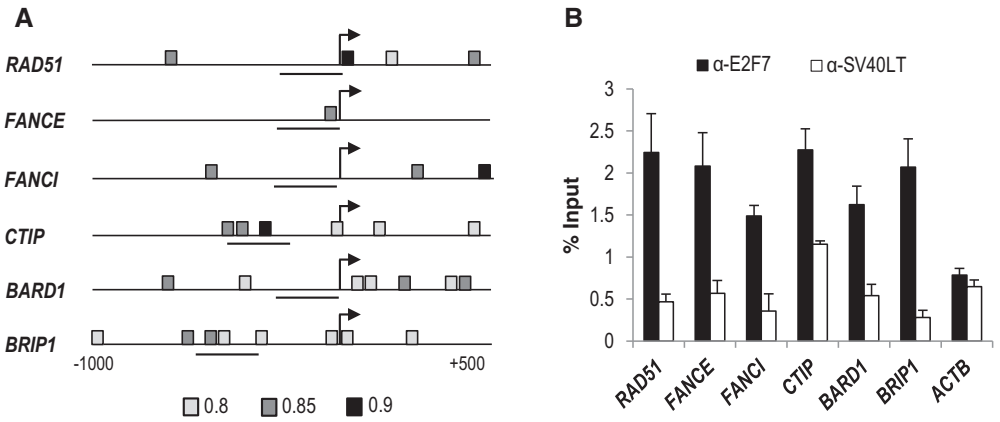

Figure 2. E2F7 occupies the promoter regions of a set of genes involved in the DNA damage response. (**A**) Schematic representation of human RAD51, FANCE, FANCI, CTIP, BARD1, BRIP1 promoter regions (−1000, +500), indicating the localization of consensus E2F motifs detected by Motiflocator tool from TOUCAN at 0.8 (light gray), 0.85 (gray) and 0.9 (dark gray) threshold levels. Horizontal lines depict the chromatin sequences amplified by qPCR. (**B**) ChIP-qPCR analyses of E2F7-regulated genes. Cell lysates were harvested 3 h after HU release and used for ChIP assays with an antibody against E2F7. Promoter regions near E2F consensus sites were amplified by qPCR. The promoter of β-Actin (*ACTB*) was used as a negative control. An unrelated antibody against the SV40 large T antigen (SV40LT) was used as a control for background immunoprecipitation. Data are presented as percentage of input chromatin (representative experiment of three independent experiments where the values are the mean ± SD of triplicate determinations).

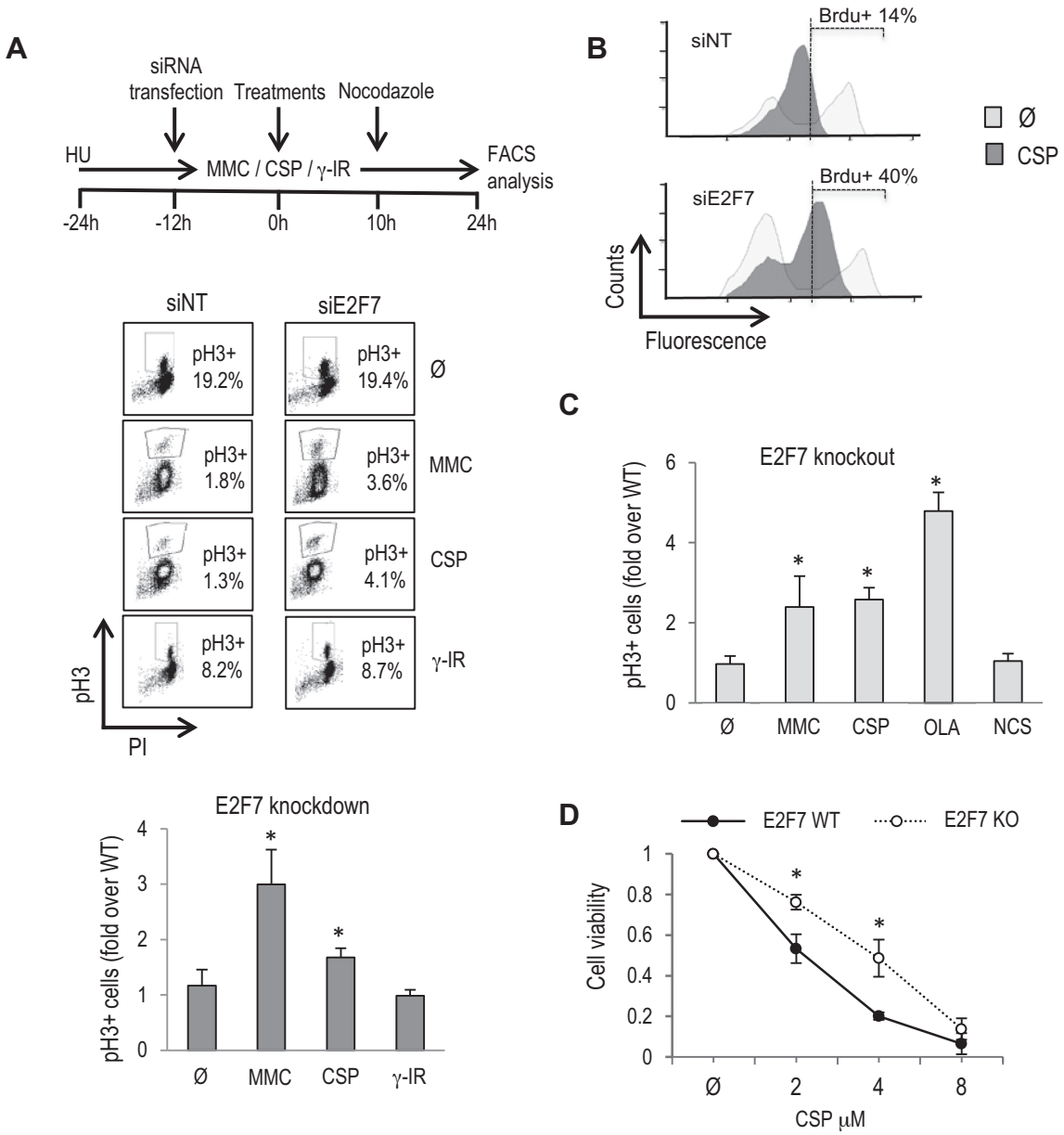

Figure 3. E2F7 controls cellular recovery after DNA lesions that interfere with fork progression. (**A**) As shown in the schematic diagram, U2OS cells were HU-synchronized and transfected with siNT and siE2F7. Subsequently, cells were released into the cell cycle and treated for 24 h with 250 nM MMC, 8 μM CSP and a dose of 2.5 Gy of γ-IR. Nocodazole was present in the culture for the last 14 h of culture. The percentage of mitotic pH3-positive cells is shown in a representative figure obtained by FACS analysis. The graphs represent fold-change over siNT values (mean ± SD) of E2F7-depleted pH3-positive cells from four independent experiments. (**B**) Asynchronously growing U2OS cells were transfected with siNT and siE2F7 and subsequently treated with 8 μM CSP for 12 h. BrdU was present in the cultures for the last 2 h. Cells were stained with anti-BrdU conjugated with FITC and with propidium iodide. A representative FACS analysis is shown. (**C**) E2F7 knockout and wild-type cells were treated and analyzed as in (A). NCS (20 ng/ml) and OLA (4 μM) were also analyzed in these cells. The graphs represent fold-change of E2F7-knockout pH3-positive cells over parental wild-type values (mean ± SD) from three independent experiments. (**D**) Clonogenic survival assays were carried out with E2F7-knockout and parental U2OS cells treated with indicated doses of CSP. For each cell line tested, cell viability of untreated cells was defined as 1. Data represent mean ± SD from two independent experiments. Ø, untreated.

known to generate DNA interstrand crosslinks (ICL), in which FA repair pathway is involved (29), whereas γ-irradiation (IR) or neocarzinostatin (NCS), which mimics DNA damage caused by γ-IR (30) are known to induce DNA double-stranded breaks (31).

Cell-cycle progression was assessed by recording the accumulation of pH3-positive mitotic cells after nocodazole addition. Only a small fraction of siNT-transfected cells exposed to non-lethal doses of DNA-damaging agents was able to enter mitosis, reflecting the efficient arrest in G2 caused by these genotoxic agents (Figure 3A and Supplementary Figure S2A). Strikingly, knockdown of E2F7 led to a significant increase in the fraction of cells capable of exiting from the G2 arrest imposed by MMC and CSP relative to siNT-transfected cells (Figure 3A). This difference in recovery capacity between siNT and siE2F7-transfected

cells was not observed upon ionizing radiation-induced G2 arrest. Results compiled from multiple biological replicates of synchronized as well as asynchronous cells confirmed the significant increase in the percentage of E2F7-silenced mitotic cells after treatment with MMC and CSP (Figure 3A and Supplementary Figure S2B). Similar results were obtained after treatment with Olaparib (OLA), an inhibitor of poly(ADP-ribose) polymerase-1 (PARP1) that induces single-strand break accumulation and reduced fork stability (32) (Supplementary Figure S2B and C).

Given the known effect of these drugs in replication fork progression, we next examined DNA replication rates after knockdown of E2F7 by measuring BrdU incorporation in asynchronously growing cells treated with CSP for 12 h. As expected, DNA synthesis rate was reduced in siNT cells under this treatment. By contrast, the reduction in DNA replication was alleviated in siE2F7 cells (Figure 3B), suggesting that E2F7 inhibits DNA replication when DNA lesions that interfere with fork progression are generated.

To confirm the functional significance of E2F7 in DNA damage responses, a CRISPR/Cas9 mediated E2F7 gene knockout was established in U2OS cells using a gRNA that targets the N-terminal region of E2F7 protein. Efficient E2F7 knockout of a selected cell line was demonstrated by DNA sequencing and Western analysis (Supplementary Figure S3). E2F7 knockout cells were treated with DNA damaging compounds, and pH3-positive mitotic cells were scored. Similarly to our finding with E2F7-knockdown cells, the fraction E2F7 knockout cells that was positive for pH3 was significantly increased relative to parental E2F7 wild-type cells after ICL induction or PARP inhibition (Figure 3C).

We next determined whether the improved cell-cycle progression of E2F7-deficient cells after genotoxic damage impacted their long-term clonogenic survival. To this end, we treated E2F7-knockout cells with CSP for 24 h and cultured them for two additional weeks to allow for colony formation from individual surviving cells. As shown in Figure 3D, the number of colonies that were scored in E2F7-knockout cultures exposed to CSP was significantly higher than in wild-type cultures, in concordance with cell-cycle analyses (Supplementary Figure S4). Altogether, our results suggest that lack of E2F7 confers an increased checkpoint recovery competence upon treatment with compounds that affect replication fork progression (CSP, MMC, OLA).

E2F7 expression and activity in cells exposed to DNA crosslinkers is p53-independent

It has been reported that E2F7 expression is induced when DNA lesions are generated upon treatment with selected drugs (11,14). We tested whether E2F7 expression and transcriptional activity are also regulated upon ICL induction. Asynchronously growing U2OS cells transfected with siE2F7 or siNT were treated with CSP or left untreated for 24 h, and gene expression was analyzed at the mRNA level. A significant increase in E2F7 levels was detected upon CSP exposure, which was blocked in siE2F7-transfected cells (Figure 4A). In contrast to E2F7 expression, the mRNA levels of target genes involved in DNA replication and repair identified in our RNA-seq were consistently reduced upon CSP treatment. Importantly, silencing of E2F7 led to a robust overexpression of target genes in CSP treated cells (Figure 4A and Supplementary Figure S5). Similar results were obtained after MMC treatment (data not shown). These findings point to a role for E2F7 in the negative regulation of genes involved in DNA damage responses during cell-cycle progression, but also following ICL induction.

ICL damage and PARP inhibition also led to a substantial induction of E2F7 at the protein level, concomitant with p53 accumulation (Figure 4B). To determine whether the observed accumulation of E2F7 levels was mediated by p53, as had been reported previously for cells treated with DNA topoisomerase II inhibitors (14), we silenced p53 expression by specific siRNA transfection and examined E2F7 expression upon genotoxic treatment. Remarkably, loss of p53 did not reduce E2F7 levels (Figure 4B). In functional assays, we found that depletion of p53 had no effect on the recovery of U2OS cells exposed to CSP, MMC or OLA, whereas concomitant depletion of p53 and E2F7 led to a significant increase in the number of mitotic cells (Figure 4C), suggesting that E2F7's role in cell-cycle recovery from ICL damage or PARP inhibition is p53-independent.

To confirm these results we made use of HeLa cells, in which p53 activity is very low due to human papillomavirus-derived E6 protein expression in these cells (33). HeLa cells that were transfected with siRNA molecules specific for E2F7 and subsequently treated with genotoxic compounds accumulated a significantly higher percentage of pH3-positive mitotic cells compared to control cells transfected with non-target siRNAs (Figure 4D). Furthermore, exposure to CSP led to an induction of E2F7 mRNA levels and to an upregulation of target gene expression in E2F7-depleted HeLa cells (Figure 4E). These results suggest a p53-independent role in the regulation of cellular responses by E2F7 after DNA damage by ICLs and PARP inhibition.

Reduced number of DNA repair foci and chromosome breaks after E2F7 silencing

We next considered the possibility that E2F7 could contribute to the modulation of DNA repair pathways involved in ICL resolution. To test this hypothesis, we examined the accumulation of 53BP1 foci in the nuclei of damaged cells. 53BP1 has been involved in DNA damage signaling and repair, and is well characterized for its ability to localize to DNA lesions in cells exposed to genotoxic agents, including ICL-inducing agents (34). U2OS cells were transfected with E2F7-specific siRNAs and subsequently treated with MMC, CSP or the radiomimetic drug NCS. Twenty-four hours after treatments, cells were fixed and 53BP1 foci were analyzed and quantified by immunofluorescence and high-throughput microscopy (Figure 5A). As expected, treatments with DNA damaging agents resulted in an increased number of foci relative to untreated cells. Interestingly, depletion of E2F7 caused a significant decrease in MMC or CSP-induced 53BP1 foci, but did not alter NCS-derived foci number. Furthermore, E2F7-null cells showed lower levels of γ-H2AX compared to E2F7-competent cells after 24 h of genotoxic treatment, whereas the γ-H2AX levels were comparable at earlier time points in both cell lines (Supplementary Figure S6). These data imply that E2F7 does not affect

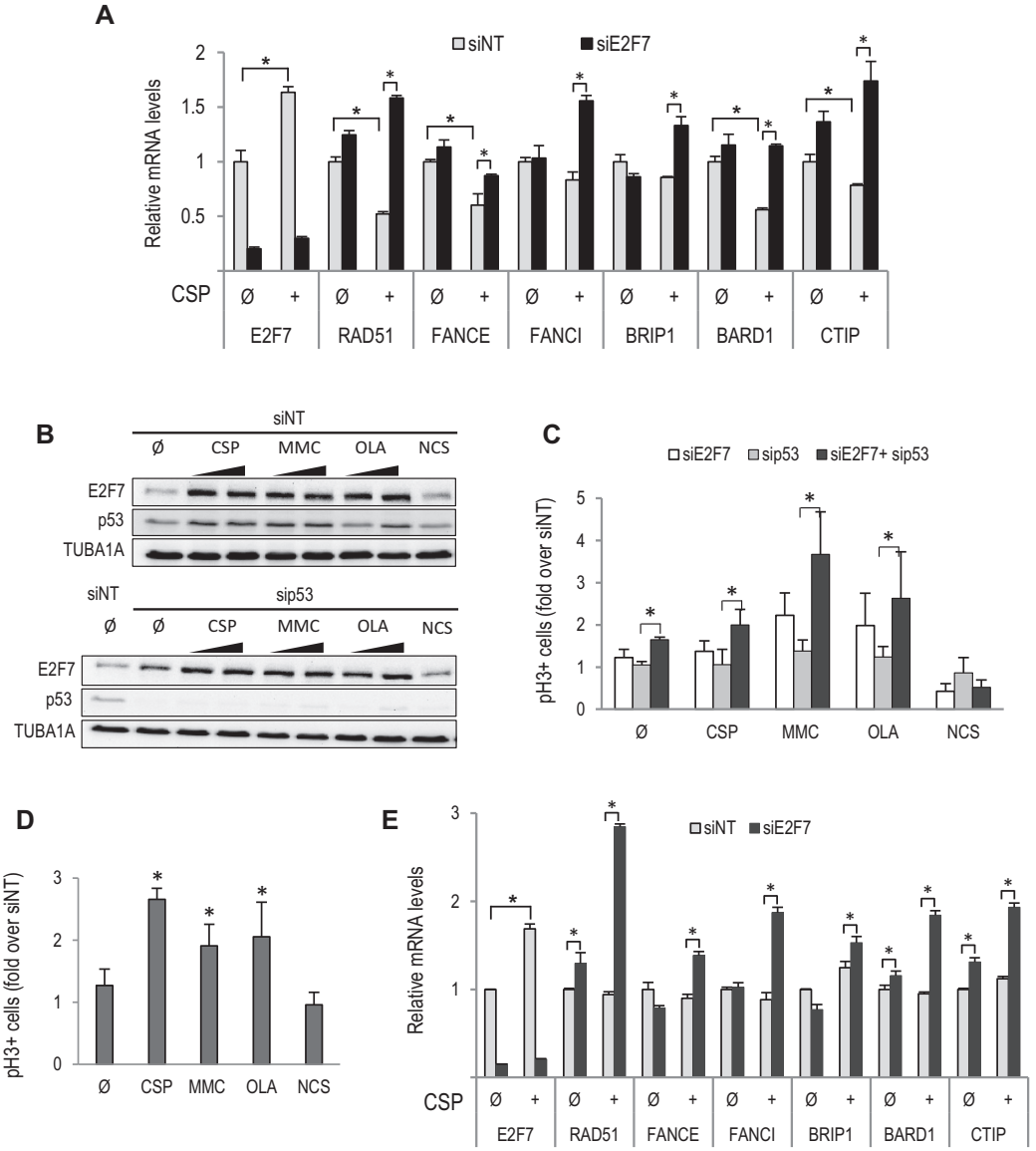

Figure 4. E2F7 expression and activity are regulated in a p53-independent manner after ICL induction and PARP inhibition. (**A**) Asynchronously growing U2OS cells were transfected with siNT and siE2F7 and subsequently treated with 8 μM CSP for 24 h. RT-qPCR analyses of indicated genes are shown. Expression values are normalized to the expression of *EIF2C2*, used as standard control. Data are represented as fold-change (mean ± SEM) relative to siNT-transfected samples from three independent experiments. (**B**) U2OS cells were transfected with siRNA molecules specific for p53 or with siRNA control, and 24 h later treated with MMC (250 and 500 nM), CSP (4 and 8 μM), OLA (2 and 4 μM) or NCS (40 ng/ml) for an additional 24 h period. E2F7 and p53 protein levels were analyzed by western blots using specific antibodies. (**C**) U2OS cells were HU-synchronized and transfected with siNT, siE2F7 and/or sip53. Subsequently, cells were treated as in Figure 3B. The graphs represent fold-change over siNT values (mean ± SD) of E2F7- and/or p53-depleted pH3-positive cells from three independent experiments. (**D**) Asynchronously growing HeLa cells were transfected and treated as in (A). Shown are RT-qPCR analyses of indicated genes. (**E**) HeLa cells were treated as in Figure 3B, and the percentage of mitotic pH3-positive cells was analyzed by flow cytometry. The graph represents fold-change of E2F7-depleted pH3-positive cells over siNT values (mean ± SD) from three independent experiments. Ø, untreated. (*, $P < 0.05$)

foci formation, but instead E2F7 plays a role in the negative control of pathways involved specifically in ICL repair.

It has been shown that FANCD2 recruitment to sites of DNA crosslinks is an essential step for ICL repair (35,36). Thus, we analyzed FANCD2 foci by immunofluorescence, and quantified the number of foci per nucleus in E2F7-depleted cells exposed to MMC or CSP. As expected, MMC and CSP treatments increased the number of FANCD2 foci/nucleus. Importantly, depletion of E2F7 caused a significant decrease in MMC or CSP-induced FANCD2 foci (Figure 5B).

We next assessed the accumulation of chromosomal aberrations, a hallmark of ICL-inducing agents (29,37), visualized in metaphase spreads. Numerous control cells (siNT) displayed radial and broken chromosomes (nearly 0.5 aberrations per metaphase) upon MMC exposure. Silencing of E2F7 provided partial resistance against MMC-induced chromosomal aberrations, with a reduced presence of radial

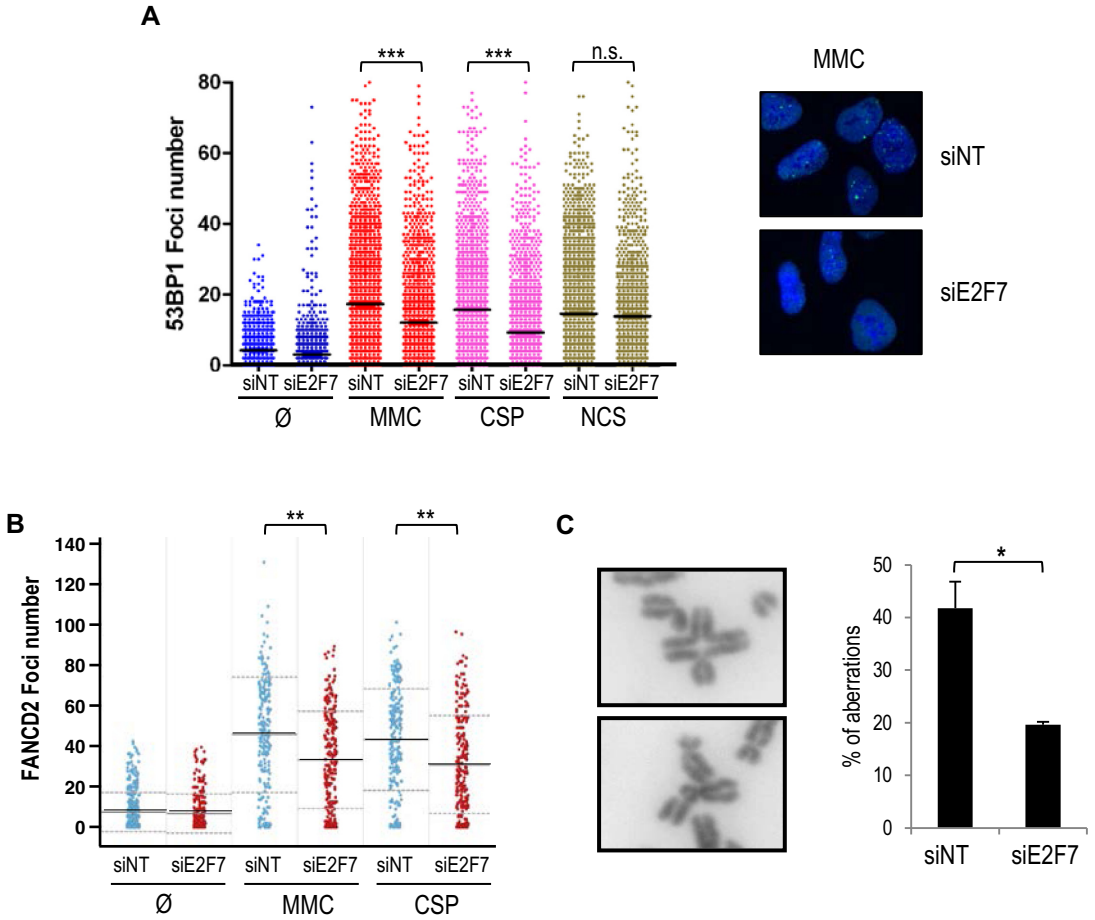

Figure 5. E2F7 knockdown results in reduced foci and chromosome break number after ICL induction. (**A**) siNT and siE2F7 transfected U2OS cells were treated with MMC, CSP and NCS and fixed 24 h later. Cells were stained for 53BP1 with a FITC-conjugated specific antibody. Nuclear DNA was stained with DAPI. The number of 53BP1 foci was scored by HTM. Data are representative of three independent analyses. Horizontal lines indicate mean vales. (**B**) siNT and siE2F7 transfected U2OS cells were treated with 250nM MMC or with 4 μM CSP. Twenty fours hours later, samples were fixed and stained for FANCD2. The number of FANCD2 foci was scored on fluorescence microscope images. Continuous horizontal lines indicate mean values. Data are representative of three independent analyses. (**C**) siNT and siE2F7 transfected U2OS cells were treated with 250 nM MMC for 48 h and scored for chromosomal aberrations by analyzing metaphase spreads. Representative images of a radial chromosome and a chromatid break are shown. Chromosomal aberrations are expressed as the average breaks and radial chromosomes found per metaphase ($n = 50$ cells) in three independent experiments. (*, $P < 0.05$; ***, $P < 0.001$), Ø, untreated, n.s. not significant.

and broken chromosomes (Figure 5C). Thus, E2F7 appears to have a negative role in the repair of chromosomal aberrations resulting from MMC treatment. The reduction in 53BP1 and FANCD2 foci upon MMC treatment shown by cells lacking E2F7 supports this hypothesis.

E2F7 modulates homology-directed DNA repair

We next investigated the efficiency of HR in cells depleted of E2F7. We used a U2OS cell line with an integrated direct repeat recombination reporter (DR-GFP). With this reporter, homology-directed DNA repair is detected when a DSB introduced into the chromosome by the I-SceI endonuclease is repaired by HR to give rise to GFP-positive cells (20). Knockdown of E2F7 resulted in a significant increase in HR efficiency (Figure 6A). Conversely, overexpression of E2F7 in U2OS-DR-GFP cells to levels that are comparable to those observed after ICL induction led to a significant reduction in HR efficiency, suggesting that E2F7 inhibits HR-mediated repair.

To better define the mechanism underlying E2F7-mediated modulation of DNA repair, we analyzed whether the improved genomic stability conferred by loss of E2F7 could be attributed to increased expression of E2F7 target genes necessary for HR repair. We examined RAD51 recombinase activity, a surrogate marker of HR efficiency and transcriptional target of E2F7 (Figures 1B and 2). In E2F7-depleted U2OS cells, RAD51 foci were significantly increased under both basal and ICL-inducing conditions (Supplementary Figure S7), suggesting that HR may be hyperactive upon loss of E2F7. Using the DR-GFP reporter system, siRNA-mediated RAD51 depletion led to a reduction in HR repair, whereas E2F7 depletion resulted in increased HR rates, as measured by the differences in the percentages of GFP-positive cells detected by flow cytometry (Figure 6B). Western blot analysis of protein extracts derived from E2F7-silenced cells showed overexpression of

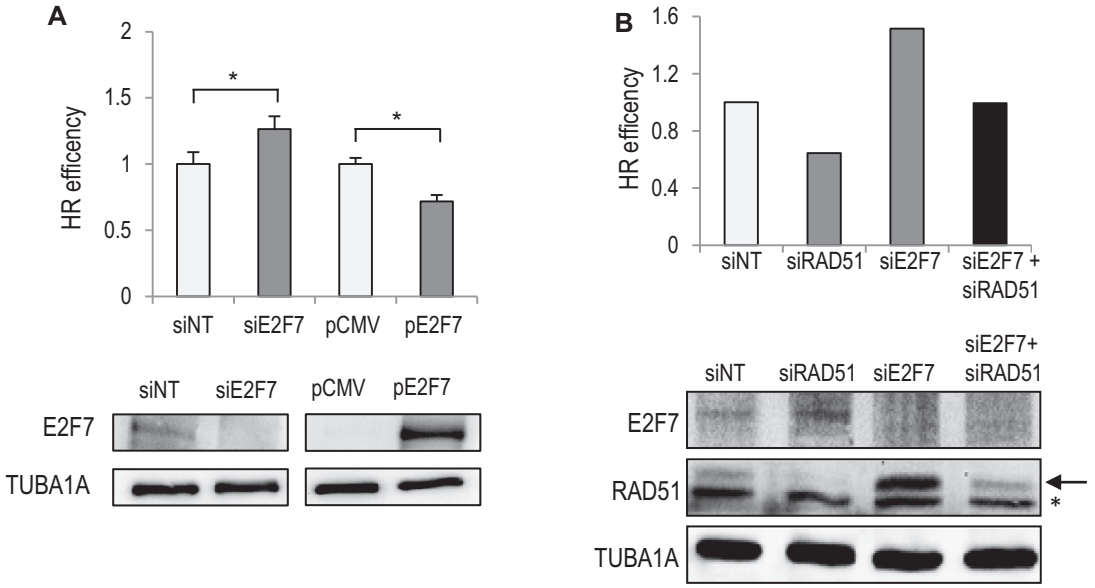

Figure 6. E2F7 suppresses HR through transcriptional repression of DNA repair genes. (**A**) U2OS-DR-GFP cells were transfected with siRNAs specific for E2F7 or with a plasmid expressing E2F7 together with an SceI expression vector. GFP-positive cells were analyzed by FACS. Data are shown as a percentage over siNT or over empty pCMV transfection. The values shown represent the mean ± SD of three independent experiments (*, $P < 0.05$). (**B**) U2OS-DR-GFP cells were transfected with siRNAs specific for E2F7, RAD51 or with a combination of both and analyzed as in (A). Western blot analysis confirms knockdown of E2F7 and RAD51 (arrow). Shown is a representative experiment of two independent experiments. A non-specific band in RAD51 blot is indicated with an asterisk.

RAD51 protein levels, in line with the mRNA results described in Figure 1B. We next co-transfected E2F7-specific siRNAs with a concentration of RAD51-specific siRNAs that would attenuate RAD51 expression to the levels found in E2F7 competent cells. Interestingly, the increased HR repair efficiency conferred by loss of E2F7 was abrogated under these conditions, and the percentage of GFP positive cells decreased to the levels found in control cells (Figure 6B and Supplementary Figure S8). These results suggest that E2F7 modulates DNA repair through the transcriptional repression of target genes that play a central role in the resolution of DNA lesions requiring homology-directed repair, such as RAD51. In the absence of E2F7 the HR pathway could become hyperactive and potentially harmful.

Improved genomic stability in HR-deficient cells after E2F7 depletion

Given that E2F7 displays features of an HR inhibitor, we next tested whether downregulation of E2F7 could suppress genomic instability in cells with an underlying genetic defect in HR. We hypothesized that the increased recombination conferred by E2F7 depletion might promote DNA repair and protect cells from genomic instability and cell death. To test this possibility we used RNA interference to attenuate the expression of BRCA2 in the U2OS DR-GFP cell line. As expected, knockdown of BRCA2 abolished HR repair in this assay. Interestingly, we observed that E2F7 co-depletion could improve HR in cells with reduced BRCA2 activity, therefore ensuring genomic stability (Figure 7A and Supplementary Figure S9). We next made use of CAPAN-1 pancreatic adenocarcinoma cells, which are defective in HR due to a loss-of-function mutation of BRCA2 (38). Treatment of these cells with PARP1 inhibitor OLA compromised cell viability as seen in short-term and long-term clonogenic survival assays (Figure 7B and Supplementary Figure S10), consistent with the finding that cancer cells deficient in HR repair through loss of BRCA2 are hypersensitive to PARP inhibitors (39). Importantly, downregulation of E2F7 expression in CAPAN-1 cells was associated with increased resistance to the PARP1 inhibitor OLA (Figure 7B and Supplementary Figure S10). Thus, E2F7 knockdown confers an increased resistance to chemotherapy in cells carrying defects in genes involved in HR.

DISCUSSION

In this work we have investigated the role of the atypical E2F member E2F7 in DNA damage repair by analyzing its contribution to the control of gene expression and to cellular responses upon exposure to genotoxic damage. We find that in addition to controlling the timely expression of genes necessary for G1/S transition and DNA replication in unperturbed conditions, E2F7 is involved in the negative regulation of genes controlling DNA repair pathways. Consequently, E2F7 activity is associated with a suppression of DNA repair reactions.

The expression of genes that are involved in various aspects of the DDR and DNA repair pathways is cell-cycle regulated, showing highest expression in G1/S transition and decreasing thereafter. Here, we show that the downregulation of these genes throughout the cell cycle is E2F7-dependent. Interestingly, all upregulated genes included in the DNA damage repair functional group harbor at least one E2F binding site in their promoters, and although many of those have been previously identified as targets of classical E2F proteins (15,40–44), their regulation by E2F7 has only been demonstrated for some of them (4). Our

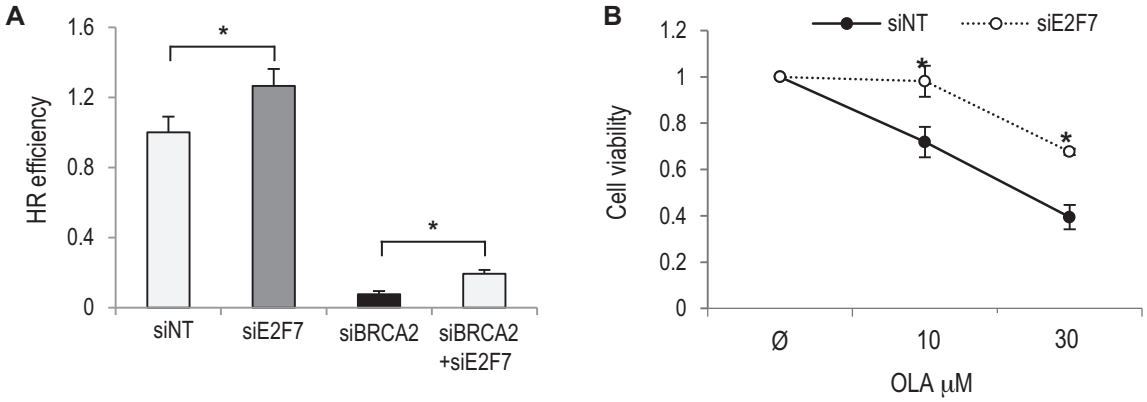

Figure 7. Improved genomic stability and survival upon E2F7 depletion in BRCA2-deficient cells. (**A**) Direct repeat recombination was measured in U2OS-DR-GFP cells transfected with siRNAs specific for E2F7, BRCA2 or with a combination of both. E2F7 knockdown partly rescued the severe defect caused by BRCA2 depletion. Data are represented as fold-change (mean ± SEM) relative to siNT-transfected samples from two independent experiments. (**B**) Clonogenic survival assays were carried out with siE2F7 or siNT transfected CAPAN-1 cells treated with indicated doses of OLA. For each siRNA, cell viability of untreated cells was defined as 1. Data represent mean ± SD from two independent experiments. Ø, untreated. (*, $P < 0.05$).

RNA-seq and ChIP experiments have extended the collection of direct E2F7 target genes involved in DNA repair by demonstrating that E2F7 is recruited to the promoter regions of *RAD51*, *FANCE*, *FANCI*, *CTIP*, *BARD1* and *BRIP1*, implying their direct transcriptional repression by E2F7. An E2F7-dependent downregulation of replication fork-associated DNA damage repair genes in the cell cycle could help restrict DNA repair activities to the S phase, which might otherwise give rise to unscheduled DNA repair activity and genome instability.Exposure of siE2F7-transfected cells to ICL-inducing DNA damaging agents results in higher levels of DNA replication and mitotic cells compared to siNT-transfected cells, consistent with a role for E2F7 in cell-cycle arrest. Supporting this possibility, we demonstrate that loss of E2F7 confers an increased recovery competence upon treatment with DNA damage-inducing doses of CSP, MMC or OLA, suggesting that E2F7 is a factor that controls cellular recovery during an ongoing DNA damage response. In contrast to our findings, it has been reported that lack of E2F7 sensitizes cells to topoisomerase inhibitors by inducing apoptosis through a mechanism involving E2F1 upregulation (10,11). Several reasons could explain the disparity between our results and those from previous studies. On the one hand, we have used a set of genotoxic agents that are known to differ in their mechanism of DNA damage and in the elicited response from the previously analyzed ones. On the other hand, the drug doses used in our study were non-lethal although sufficient to induce checkpoint arrest in G2, whereas previous studies employed doses sufficiently high to induce apoptosis. Thus, there could be a DNA damage threshold below which cells lacking E2F7 could be involved in repairing the damage, but above which these cells would activate cell death pathways. Systematic analyses using a wide range of doses of a variety of compounds may help resolve these differences.

E2F7 expression and cell-cycle target gene repression have been previously linked to p53 after DNA damage by topoisomerase inhibitors (14). Unexpectedly, we found that E2F7 expression and E2F7-modulated cellular recovery upon ICL damage is largely p53-independent. Our results point to a fundamental difference in the DNA damage-mediated regulation of E2F7 expression and function between DNA topoisomerase inhibitors and interstrand crosslink inducers. Further studies should determine whether other p53 family members are involved in E2F7 regulation upon ICL induction or whether a distinct pathway mediates E2F7 regulation in this context. In contrast to DNA crosslinkers, ionizing radiation did not induce E2F7 expression in U2OS cells, which may explain why depletion of E2F7 did not confer increased cellular recovery after radiation.

Remarkably, our data show that E2F7 has additional roles beyond inhibition of DNA replication in the presence of DNA damage. In fact, DNA damage foci are significantly reduced upon MMC and CSP treatments in E2F7-depleted cells. These results point to a uniquely increased DNA repair competence upon treatment with ICL-inducing agents in cells lacking E2F7, leading to an earlier release from the chromatin of γ-H2AX, 53BP1 and FANCD2. Our observation that E2F7 knockdown has a protective effect against chromosomal aberrations induced by MMC treatment supports this hypothesis.

Interestingly, the FA pathway, which is known to be involved in ICL repair (45), is highly enriched among E2F7-repressed genes. ICL-resistant cell lines are known to have elevated gene expression involving the FA/BRCA pathway, including FANCF and RAD51C, which was suggested to be causally related with enhanced removal of ICLs by the resistant cells (46,47). We have found evidence that the expression of at least FANCE, FANCI, BRIP1 (also called FANCJ) or RAD51 (also called FANCR) is directly regulated by E2F7, and that E2F7 depletion results in enhanced expression of these FA genes, particularly during S/G2 phases or after DNA damage, two cellular contexts exhibiting high E2F7 levels (5) (Figure 4B). By contrast, this enhanced expression of E2F7 target genes was not observed in asynchronously growing cells, probably because most of these cells are in G1, a time-point where E2F7 levels are very low (5) and therefore unable to repress target gene expression. It will be interesting to analyze whether a correlation

can be found between ICL resistance and E2F7 levels in different cancer cell lines in unperturbed conditions, but also upon exposure to ICL-inducing chemotherapy.

ICL repair is known to involve homology-directed repair machinery and increased HR is associated with resistance to ICL-inducing agents in human tumor cells (48,49). Our results are consistent with a negative role for E2F7 in HR repair activity. Indeed, using a DR-GFP assay to measure the effect of E2F7 in HR, we found that E2F7 negatively affects HR activity. A transcription-independent contribution to DNA repair process for E2F7 and E2F1 has been previously reported, which involves the binding of these E2Fs and recruitment of several factors to damaged DNA sites (13,50–52). We cannot discard the possibility that there is a transcription-independent contribution to E2F7-mediated regulation of ICL lesion repair in our system, which should be important to analyze. However, our data strongly suggest that a major DNA damage response function of E2F7 is through transcription-dependent regulation of DNA repair genes. Several genes involved in HR were found upregulated upon E2F7 depletion, including RAD51, CTIP and BARD1, among others. Most importantly, the results obtained in our E2F7/RAD51 co-depletion experiments suggest that increased HR activity in E2F7 silenced cells is associated with increased levels of RAD51 recombinase, implying a transcriptional role for E2F7 in repair of ICL lesions, through upregulation of target genes involved in homology-directed DNA repair. Thus, the transcriptional landscape regulated by E2F7 could provide an additional level of recombination control in addition to that described for several recombinases (53,54), whereby cells can interfere with HR at different steps in the process.

Increasing recombination in HR-deficient cells might result in protective effects. Our results have revealed an intriguing link between genomic integrity of DNA repair-deficient cells and E2F7. HR-deficient (BRCA2 mutated) cells exhibit increased genomic instability and accumulation of mutations that ultimately disrupt cell-cycle control pathways, leading to cancer. In this scenario, increased HR activity conferred by inactivation of E2F7 might prevent genomic instability in the cells of these patients and protect against cancer onset, as has been proposed for the depletion of the PCNA-binding protein PARI (54). However, dysregulated hyper-recombination has also been associated with increased genomic instability and resistance to genotoxic therapy in some cellular contexts, such as after RAD51 upregulation (55). In fact, the increased survival of BRCA2-deficient tumor cells treated with a PARP inhibitor that we observe after knockdown of E2F7 implies that loss of E2F7 in the context of HR deficiency confers resistance to chemotherapy, a potentially harmful outcome for cancer treatment.

Although further research will be needed to elucidate the molecular mechanisms underlying E2F7-dependent control of genomic stability, our data are consistent with an antioncogenic function for E2F7 whereby E2F7 functions to inhibit or to switch off repair pathways for specific DNA lesions. It has been reported that efficient ICL repair requires negative regulation of the FA pathway. Once repair is completed, the repair factors have to be inactivated to avert inappropriate action and corruption of genetic information (56). Thus, the inability to turn off or reset the FA pathway after the repair of specific DNA damage sites may have deleterious effects on genome integrity. In a similar manner, E2F7 might counter-balance the transcriptional program activated in response to ICL repair to fine-tune the cellular response to DNA lesions and ensure response termination.

DATA AVAILABILITY

RNA-seq datasets generated in this study were deposited in the NCBI Gene Expression Omnibus (GEO; https://www.ncbi.nlm.nih.gov/geo/) under accession number GSE107216.

SUPPLEMENTARY DATA

Supplementary Data are available at NAR Online.

ACKNOWLEDGEMENTS

We thank members of the Zubiaga and Malumbres laboratory for helpful discussions, Naiara Zorrilla for technical support, José Antonio Rodríguez for critical reading of the manuscript, D. Olmos and J. Surrallés for kindly providing cell lines and R. Medema for providing CRISPR/Cas9 plasmids.

FUNDING

This work was supported by grants from the Spanish Ministry [SAF2012-33551 and SAF2015-67562-R, co-financed by FEDER funds, and SAF2014-57791-REDC], the Basque Government [IT634-13 and KK-2015/89], and the University of the Basque Country UPV/EHU [UFI11/20] to AMZ; and grants from the Spanish Ministry [SAF2015-69920-R], and Worldwide Cancer Research [15-0278] to MM. JM was recipient of a Basque Government fellowship for graduate studies and JVR is recipient of a UPV/EHU fellowship for graduate studies. M.A.F. was supported by a young investigator grant from MINECO [SAF2014-60442-JIN; co-financed by FEDER funds]. Funding for open access charge: Spanish Ministry [SAF2015-67562-R, co-financed by FEDER funds]; Basque Government [IT634-13].
Conflict of interest statement. None declared.

REFERENCES

1. Chen,H.Z., Tsai,S.Y. and Leone,G. (2009) Emerging roles of E2Fs in cancer: an exit from cell cycle control. *Nat. Rev. Cancer*, **9**, 785–797.
2. Dimova,D.K. and Dyson,N.J. (2005) The E2F transcriptional network: old acquaintances with new faces. *Oncogene*, **24**, 2810–2826.
3. Bertoli,C., Skotheim,J.M. and de Bruin,R.A. (2013) Control of cell cycle transcription during G1 and S phases. *Nat. Rev. Mol. Cell Biol.*, **14**, 518–528.
4. Westendorp,B., Mokry,M., Groot Koerkamp,M.J., Holstege,F.C., Cuppen,E. and de Bruin,A. (2012) E2F7 represses a network of oscillating cell cycle genes to control S-phase progression. *Nucleic Acids Res.*, **40**, 3511–3523.
5. Mitxelena,J., Apraiz,A., Vallejo-Rodriguez,J., Malumbres,M. and Zubiaga,A.M. (2016) E2F7 regulates transcription and maturation of multiple microRNAs to restrain cell proliferation. *Nucleic Acids Res.*, **44**, 5557–5570.

6. de Bruin,A., Maiti,B., Jakoi,L., Timmers,C., Buerki,R. and Leone,G. (2003) Identification and characterization of E2F7, a novel mammalian E2F family member capable of blocking cellular proliferation. *J. Biol. Chem.*, **278**, 42041–42049.
7. Di Stefano,L., Jensen,M.R. and Helin,K. (2003) E2F7, a novel E2F featuring DP-independent repression of a subset of E2F-regulated genes. *EMBO J.*, **22**, 6289–6298.
8. Li,J., Ran,C., Li,E., Gordon,F., Comstock,G., Siddiqui,H., Cleghorn,W., Chen,H.Z., Kornacker,K., Liu,C.G *et al.* (2008) Synergistic function of E2F7 and E2F8 is essential for cell survival and embryonic development. *Dev. Cell*, **14**, 62–75.
9. Endo-Munoz,L., Dahler,A., Teakle,N., Rickwood,D., Hazar-Rethinam,M., Abdul-Jabbar,I., Sommerville,S., Dickinson,I., Kaur,P., Paquet-Fifield,S *et al.* (2009) E2F7 can regulate proliferation, differentiation, and apoptotic responses in human keratinocytes: implications for cutaneous squamous cell carcinoma formation. *Cancer Res.*, **69**, 1800–1808.
10. Thurlings,I., Martinez-Lopez,L.M., Westendorp,B., Zijp,M., Kuiper,R., Tooten,P., Kent,L.N., Leone,G., Vos,H.J., Burgering,B *et al.* (2017) Synergistic functions of E2F7 and E2F8 are critical to suppress stress-induced skin cancer. *Oncogene*, **36**, 829–839.
11. Zalmas,L.P., Zhao,X., Graham,A.L., Fisher,R., Reilly,C., Coutts,A.S. and La Thangue,N.B. (2008) DNA-damage response control of E2F7 and E2F8. *EMBO Rep.*, **9**, 252–259.
12. Hazar-Rethinam,M., Cameron,S.R., Dahler,A.L., Endo-Munoz,L.B., Smith,L., Rickwood,D. and Saunders,N.A. (2011) Loss of E2F7 expression is an early event in squamous differentiation and causes derepression of the key differentiation activator Sp1. *J. Invest. Dermatol.*, **131**, 1077–1084.
13. Zalmas,L.P., Coutts,A.S., Helleday,T. and La Thangue,N.B. (2013) E2F-7 couples DNA damage-dependent transcription with the DNA repair process. *Cell Cycle*, **12**, 3037–3051.
14. Carvajal,L.A., Hamard,P.J., Tonnessen,C. and Manfredi,J.J. (2012) E2F7, a novel target, is up-regulated by p53 and mediates DNA damage-dependent transcriptional repression. *Genes Dev.*, **26**, 1533–1545.
15. Laresgoiti,U., Apraiz,A., Olea,M., Mitxelena,J., Osinalde,N., Rodriguez,J.A., Fullaondo,A. and Zubiaga,A.M. (2013) E2F2 and CREB cooperatively regulate transcriptional activity of cell cycle genes. *Nucleic Acids Res.*, **41**, 10185–10198.
16. Iglesias-Ara,A., Zenarruzabeitia,O., Fernandez-Rueda,J., Sanchez-Tillo,E., Field,S.J., Celada,A. and Zubiaga,A.M. (2010) Accelerated DNA replication in E2F1- and E2F2-deficient macrophages leads to induction of the DNA damage response and p21(CIP1)-dependent senescence. *Oncogene*, **29**, 5579–5590.
17. Blomen,V.A., Majek,P., Jae,L.T., Bigenzahn,J.W., Nieuwenhuis,J., Staring,J., Sacco,R., van Diemen,F.R., Olk,N., Stukalov,A *et al.* (2015) Gene essentiality and synthetic lethality in haploid human cells. *Science*, **350**, 1092–1096.
18. Remeseiro,S., Cuadrado,A., Carretero,M., Martinez,P., Drosopoulos,W.C., Canamero,M., Schildkraut,C.L., Blasco,M.A. and Losada,A. (2012) Cohesin-SA1 deficiency drives aneuploidy and tumourigenesis in mice due to impaired replication of telomeres. *EMBO J.*, **31**, 2076–2089.
19. Pierce,A.J., Johnson,R.D., Thompson,L.H. and Jasin,M. (1999) XRCC3 promotes homology-directed repair of DNA damage in mammalian cells. *Genes Dev.*, **13**, 2633–2638.
20. Richardson,C., Moynahan,M.E. and Jasin,M. (1999) Homologous recombination between heterologs during repair of a double-strand break. Suppression of translocations in normal cells. *Ann. N. Y. Acad. Sci.*, **886**, 183–186.
21. Trapnell,C., Roberts,A., Goff,L., Pertea,G., Kim,D., Kelley,D.R., Pimentel,H., Salzberg,S.L., Rinn,J.L. and Pachter,L. (2012) Differential gene and transcript expression analysis of RNA-seq experiments with TopHat and Cufflinks. *Nat. Protoc.*, **7**, 562–578.
22. Osinalde,N., Olea,M., Mitxelena,J., Aloria,K., Rodriguez,J.A., Fullaondo,A., Arizmendi,J.M. and Zubiaga,A.M. (2013) The Nuclear Protein ALY binds to and modulates the activity of transcription factor E2F2. *Mol. Cell Proteomics*, **12**, 1087–1098.
23. Aerts,S., Van Loo,P., Thijs,G., Mayer,H., de Martin,R., Moreau,Y. and De Moor,B. (2005) TOUCAN 2: the all-inclusive open source workbench for regulatory sequence analysis. *Nucleic Acids Res.*, **33**, W393–W396.
24. Gotea,V. and Ovcharenko,I. (2008) DiRE: identifying distant regulatory elements of co-expressed genes. *Nucleic Acids Res.*, **36**, W133–W139.
25. Infante,A., Laresgoiti,U., Fernandez-Rueda,J., Fullaondo,A., Galan,J., Diaz-Uriarte,R., Malumbres,M., Field,S.J. and Zubiaga,A.M. (2008) E2F2 represses cell cycle regulators to maintain quiescence. *Cell Cycle*, **7**, 3915–3927.
26. Lopez-Contreras,A.J., Specks,J., Barlow,J.H., Ambrogio,C., Desler,C., Vikingsson,S., Rodrigo-Perez,S., Green,H., Rasmussen,L.J., Murga,M *et al.* (2015) Increased Rrm2 gene dosage reduces fragile site breakage and prolongs survival of ATR mutant mice. *Genes Dev.*, **29**, 690–695.
27. Rabinovich,A., Jin,V.X., Rabinovich,R., Xu,X. and Farnham,P.J. (2008) E2F in vivo binding specificity: comparison of consensus versus nonconsensus binding sites. *Genome Res.*, **18**, 1763–1777.
28. Xu,X., Bieda,M., Jin,V.X., Rabinovich,A., Oberley,M.J., Green,R. and Farnham,P.J. (2007) A comprehensive ChIP-chip analysis of E2F1, E2F4, and E2F6 in normal and tumor cells reveals interchangeable roles of E2F family members. *Genome Res.*, **17**, 1550–1561.
29. McCabe,K.M., Olson,S.B. and Moses,R.E. (2009) DNA interstrand crosslink repair in mammalian cells. *J. Cell Physiol.*, **220**, 569–573.
30. Wang,P., Lee,J.W., Yu,Y., Turner,K., Zou,Y., Jackson-Cook,C.K. and Povirk,L.F. (2002) Gene rearrangements induced by the DNA double-strand cleaving agent neocarzinostatin: conservative non-homologous reciprocal exchanges in an otherwise stable genome. *Nucleic Acids Res.*, **30**, 2639–2646.
31. Jeggo,P.A. and Lobrich,M. (2007) DNA double-strand breaks: their cellular and clinical impact? *Oncogene*, **26**, 7717–7719.
32. Pommier,Y., O'Connor,M.J. and de Bono,J. (2016) Laying a trap to kill cancer cells: PARP inhibitors and their mechanisms of action. *Sci. Transl. Med.*, **8**, 362ps317.
33. Haupt,Y., Rowan,S., Shaulian,E., Vousden,K.H. and Oren,M. (1995) Induction of apoptosis in HeLa cells by trans-activation-deficient p53. *Genes Dev.*, **9**, 2170–2183.
34. Hicks,J.K., Chute,C.L., Paulsen,M.T., Ragland,R.L., Howlett,N.G., Gueranger,Q., Glover,T.W. and Canman,C.E. (2010) Differential roles for DNA polymerases eta, zeta, and REV1 in lesion bypass of intrastrand versus interstrand DNA cross-links. *Mol. Cell. Biol.*, **30**, 1217–1230.
35. Garcia-Higuera,I., Taniguchi,T., Ganesan,S., Meyn,M.S., Timmers,C., Hejna,J., Grompe,M. and D'Andrea,A.D. (2001) Interaction of the Fanconi anemia proteins and BRCA1 in a common pathway. *Mol. Cell*, **7**, 249–262.
36. Liu,T., Ghosal,G., Yuan,J., Chen,J. and Huang,J. (2010) FAN1 acts with FANCI-FANCD2 to promote DNA interstrand cross-link repair. *Science*, **329**, 693–696.
37. Nijman,S.M., Huang,T.T., Dirac,A.M., Brummelkamp,T.R., Kerkhoven,R.M., D'Andrea,A.D. and Bernards,R. (2005) The deubiquitinating enzyme USP1 regulates the Fanconi anemia pathway. *Mol. Cell*, **17**, 331–339.
38. McCabe,N., Lord,C.J., Tutt,A.N., Martin,N.M., Smith,G.C. and Ashworth,A. (2005) BRCA2-deficient CAPAN-1 cells are extremely sensitive to the inhibition of Poly (ADP-Ribose) polymerase: an issue of potency. *Cancer Biol. Ther.*, **4**, 934–936.
39. Lord,C.J. and Ashworth,A. (2017) PARP inhibitors: Synthetic lethality in the clinic. *Science*, **355**, 1152–1158.
40. Ishida,S., Huang,E., Zuzan,H., Spang,R., Leone,G., West,M. and Nevins,J.R. (2001) Role for E2F in control of both DNA replication and mitotic functions as revealed from DNA microarray analysis. *Mol. Cell. Biol.*, **21**, 4684–4699.
41. Ren,B., Cam,H., Takahashi,Y., Volkert,T., Terragni,J., Young,R.A. and Dynlacht,B.D. (2002) E2F integrates cell cycle progression with DNA repair, replication, and G(2)/M checkpoints. *Genes Dev.*, **16**, 245–256.
42. Bindra,R.S. and Glazer,P.M. (2006) Basal repression of BRCA1 by multiple E2Fs and pocket proteins at adjacent E2F sites. *Cancer Biol. Ther.*, **5**, 1400–1407.
43. Tategu,M., Arauchi,T., Tanaka,R., Nakagawa,H. and Yoshida,K. (2007) Systems biology-based identification of crosstalk between E2F transcription factors and the Fanconi anemia pathway. *Gene Regul. Syst. Bio*, **1**, 1–8.
44. Hoskins,E.E., Gunawardena,R.W., Habash,K.B., Wise-Draper,T.M., Jansen,M., Knudsen,E.S. and Wells,S.I. (2008) Coordinate regulation

of Fanconi anemia gene expression occurs through the Rb/E2F pathway. *Oncogene*, **27**, 4798–4808.
45. Clauson,C., Scharer,O.D. and Niedernhofer,L. (2013) Advances in understanding the complex mechanisms of DNA interstrand cross-link repair. *Cold Spring Harb. Perspect. Biol.*, **5**, a012732.
46. Chen,Q., Van der Sluis,P.C., Boulware,D., Hazlehurst,L.A. and Dalton,W.S. (2005) The FA/BRCA pathway is involved in melphalan-induced DNA interstrand cross-link repair and accounts for melphalan resistance in multiple myeloma cells. *Blood*, **106**, 698–705.
47. Hazlehurst,L.A., Enkemann,S.A., Beam,C.A., Argilagos,R.F., Painter,J., Shain,K.H., Saporta,S., Boulware,D., Moscinski,L., Alsina,M *et al.* (2003) Genotypic and phenotypic comparisons of de novo and acquired melphalan resistance in an isogenic multiple myeloma cell line model. *Cancer Res.*, **63**, 7900–7906.
48. Slupianek,A., Schmutte,C., Tombline,G., Nieborowska-Skorska,M., Hoser,G., Nowicki,M.O., Pierce,A.J., Fishel,R. and Skorski,T. (2001) BCR/ABL regulates mammalian RecA homologs, resulting in drug resistance. *Mol. Cell*, **8**, 795–806.
49. Xu,Z.Y., Loignon,M., Han,F.Y., Panasci,L. and Aloyz,R. (2005) Xrcc3 induces cisplatin resistance by stimulation of Rad51-related recombinational repair, S-phase checkpoint activation, and reduced apoptosis. *J. Pharmacol. Exp. Ther.*, **314**, 495–505.
50. Chen,J., Zhu,F., Weaks,R.L., Biswas,A.K., Guo,R., Li,Y. and Johnson,D.G. (2011) E2F1 promotes the recruitment of DNA repair factors to sites of DNA double-strand breaks. *Cell Cycle*, **10**, 1287–1294.
51. Guo,R., Chen,J., Mitchell,D.L. and Johnson,D.G. (2011) GCN5 and E2F1 stimulate nucleotide excision repair by promoting H3K9 acetylation at sites of damage. *Nucleic Acids Res.*, **39**, 1390–1397.
52. Guo,R., Chen,J., Zhu,F., Biswas,A.K., Berton,T.R., Mitchell,D.L. and Johnson,D.G. (2010) E2F1 localizes to sites of UV-induced DNA damage to enhance nucleotide excision repair. *J. Biol. Chem.*, **285**, 19308–19315.
53. Barber,L.J., Youds,J.L., Ward,J.D., McIlwraith,M.J., O'Neil,N.J., Petalcorin,M.I., Martin,J.S., Collis,S.J., Cantor,S.B., Auclair,M *et al.* (2008) RTEL1 maintains genomic stability by suppressing homologous recombination. *Cell*, **135**, 261–271.
54. Moldovan,G.L., Dejsuphong,D., Petalcorin,M.I., Hofmann,K., Takeda,S., Boulton,S.J. and D'Andrea,A.D. (2012) Inhibition of homologous recombination by the PCNA-interacting protein PARI. *Mol. Cell*, **45**, 75–86.
55. Martin,R.W., Orelli,B.J., Yamazoe,M., Minn,A.J., Takeda,S. and Bishop,D.K. (2007) RAD51 up-regulation bypasses BRCA1 function and is a common feature of BRCA1-deficient breast tumors. *Cancer Res.*, **67**, 9658–9665.
56. Kim,J.M., Parmar,K., Huang,M., Weinstock,D.M., Ruit,C.A., Kutok,J.L. and D'Andrea,A.D. (2009) Inactivation of murine Usp1 results in genomic instability and a Fanconi anemia phenotype. *Dev. Cell*, **16**, 314–320.